# DESIGN AND ANALYSIS OF RECONFIGURABLE ANTENNAS FOR WIRELESS APPLICATIONS

A Thesis Submitted In Partial Fulfillment of the Requirements for the Degree of

# DOCTOR OF PHILOSOPHY

by

M. Ganesh

(Roll No. 2K20/PHDEC/509)

**Under the Supervision of** 

Dr. Yashna Sharma (Supervisor)

Prof. N. S. Raghava (Joint-Supervisor-I)

Dr. Thennarasan Sabapathy (Joint-Supervisor-II)



**Department of Electronics and Communication Engineering** 

## DELHI TECHNOLOGICAL UNIVERSITY

(Formerly Delhi College of Engineering)

Shahbad Daulatpur, Main Bawana Road, Delhi 110042, India

February, 2025



# **DELHI TECHNOLOGICAL UNIVERSITY**

(Formerly Delhi College of Engineering) Shahbad Daulatpur, Main Bawana Road, Delhi-42

## **CANDIDATE'S DECLARATION**

I, M.GANESH, hereby certify that the research work being presented in the thesis entitled " Design and Analysis of Reconfigurable Antenna for Wireless Applications" in partial fulfillment of the requirements for the award of the Degree of Doctor of Philosophy, submitted in the Department of Electronics and Communication Engineering, Delhi Technological University is an authenticated record of my own work carried out during the period from January 2021 to February 2025 under the supervision of Dr. Yashna Sharma, Prof N.S. Raghava and Dr. Thennarasan Sabapathy.

The matter presented in the thesis has not been submitted by me for the award of any other degree of this or any other institute.

Candidate's Signature

This is to certify that the student has incorporated all the corrections suggested by the examiners in the thesis and that the statement made by the candidate is correct to the best of our knowledge.

gastina

- Bu

**Signature of the Supervisor(s)** 

**Signature of External Examiner** 

Ashob Mittal



# **DELHI TECHNOLOGICAL UNIVERSITY**

(Formerly Delhi College of Engineering) Shahbad Daulatpur, Main Bawana Road, Delhi-42

# **CERTIFICATE BY THE SUPERVISOR(s)**

Certified that M Ganesh (2k20/PHDEC/509) has carried out their search work presented in this thesis entitled "Design and Analysis of Reconfigurable Antenna for Wireless Applications" for the award of Doctor of Philosophy from Department of Electronics and Communication Engineering, Delhi Technological University, Delhi, under my supervision. The thesis embodies results of original work, and studies are carried out by the student himself, and the contents of the thesis do not form the basis for the award of any other degree to the candidate or to anybody else from this or any other University/Institution.

garlina

Dr. Yashna Sharma Assistant Professor Delhi Technological University

Delhi-110042, India

Maragrand.

Prof. N. S. Raghava
Professor
Delhi Technological University
Delhi-110042, India

- Shu

Dr. Thennarasan Sabapathy Associate Professor Univerisiti Malaysia perlis Arau-02600, Malaysia

Date: 21-02-2025

#### **ABSTRACT**

In this thesis, frequency and compound reconfigurable antennas (frequency and pattern, frequency, pattern, and polarization) are designed and analyzed for sub-6 GHz 5G, Wi-Fi 6E, vehicular, and Internet of Things (IoT) applications. However, already existing reconfigurable antennas are limited to narrow bandwidth and large size and utilize more RF switches for their reconfiguration. Due to these, the complexity of wireless systems increases, and the performance may be degraded. Therefore, tomaintain better performance over a wide frequency range, a partial ground concept and fewer RF switches are utilized to achieve compound reconfiguration with a compact size. Initially, a compact-size hexagonal-shaped frequency reconfigurable antenna is investigated by implementing the switchable slot on the ground plane, operating at 3.8 GHz and 3.6 GHz for new C-band 5G networks. Further, a V-shaped slit frequency reconfigurable antenna is implemented by incorporating the PIN diode MADP000907-14020 P at a suitable position on this slit and operating its ON and OFF states, obtained dual-band, operating at 3.9 GHz and 6.37 GHz in the ON state of the PIN diode. In the OFF state of the PIN diode, a single band is obtained, operating at 5.5 GHz for Wi-Fi applications with compact size and wideband operation. For IoT close-range applications, along with frequency reconfiguration, a pattern reconfiguration is also required for better spectrum utilization with minimal interference. Therefore, a frequency and pattern reconfigurable antenna is investigated in further chapters based on the Yagi-Uda principle. The reported structure provides omnidirectional and directional patterns that operate at 5 GHz and 4.3 GHz, respectively, at three distant modes by connecting and disconnecting the two parasitic stubs on the ground plane through two PIN diodes. However, this structure is limited to frequency and pattern reconfiguration. To obtain three reconfigurations, namely frequency, pattern, and polarization in a single structure with a lesser number of PIN diodes for wireless and automotive applications operating in the sub-6 GHz (n77/n78 bands), a compound reconfigurable electronically switched parasitic monopole antenna is designed and analyzed. The design has two inverted L-shaped parasitic stubs and a half-hexagonal radiating element, both of which are coupled to a PIN diode for reconfiguration in frequency. Furthermore, comparable parasitic stubs are integrated into the ground plane via PIN diodes, allowing for pattern tilting and polarization reconfiguration. The antenna supports three polarization states, namely linear, left-hand circular, and right-hand circular polarization, and it achieves pattern tilting from boresight to end-fire at the target bands. The PIN diode operating configurations enable the realization of these polarization states. Multiband antennas are desired instead of implementing different radiating structures for each band in modern communication systems. Along with multiband, for long-range coverage, highgain antennas are

preferable. So, here, a structural symmetry of a half hexagonal-shaped radiating element and split ring resonators is proposed for multiband and pattern tilting capability. Further, a Frequency Selective Surfaces (FSS)-based reflector is kept below the radiating element, and a gain is improved to 50% compared to without a reflector. Also, pattern tilting is obtained independently of frequency in three directions from this structure.

A full-wave electromagnetic simulator such as ANSYS High-Frequency Structure Simulator (HFSS) predicts the reported reconfigurable antennas' performances, which are fabricated and measured by the required parameters. They are compared with other cutting-edge antennas proposed for similar applications to verify the concepts and design performances.

#### **ACKNOWLEDGEMENTS**

First and foremost, I would like to express my sincere gratitude to my supervisors Prof. N. S. Raghava, Dr. Thennarasan Sabapathy, and Dr. Yashna Sharma for their invaluable guidance, advice, and support throughout this research work. Without their support, I couldn't have accomplished the milestones where I stand present.

I would like to express my heartfelt gratitude to Prof. O.P. Verma, Head of the Department of Electronics and Communication Engineering, along with DRC members, faculty, and technical staff of the ECE department for their help and encouragement during this research study.

I gratefully acknowledge all my colleagues at the Microwave Computer-Aided Design Research Laboratory at Delhi Technological University.

I acknowledge Prof Binod Kumar Kanaujia, Director, NIT Jalandhar, and Prof Vandana Vikas Thakare, MITS, Gwalior, for their invaluable help and suggestions for this research work.

I would like to express my heartfelt thanks to all my family members, whose blessings and affection have inspired me.

Words cannot express my deep gratitude to my life partner, "K. Hari Priya," for her encouragement, motivation, understanding, cooperation, and positive support during every stage of this work. I might not be able to reach this stage without her. She is always there cheering me up and equally stood by me through the good and bad times.

M. Ganesh

# **DEDICATED TO MY BELOVED PARENTS**

# **M BHAGYAMMA**

&

**M CHENGAIAH** 

And

My Wife

K HARI PRIYA

# TABLE OF CONTENTS

	Title	Page No.	
	Certificate	iii	
	Abstract	iv	
	Acknowledgments	vi	
	Dedication	vii	
	List of Figures	xi	
	List of Tables	XV	
	List of Symbols and Abbreviations	xvi	
1	Introduction	1-	12
	1.1 Background and Motivation	1	
	1.2 Reconfigurable Antennas in Wireless Applications	3	
	1.2.1 Comparison of traditional and reconfigurable antennas	3	
	1.2.2 Applications of reconfigurable antennas	4	
	1.3 5G spectrum bands	5	
	1.4 Scope of research	7	
	1.5 Research Methodology	8	
	1.6 List of Publications	11	
	1.7 Thesis Organization	12	2
2	Background study and literature review of Reconfigurable Antenna	13	<b>3-4</b> 0
	Technologies		
	2.1 Introduction	13	3
	2.2 Types of Reconfigurable Antennas	13	3
	2.2.1 Frequency Reconfigurable Antennas	13	3
	2.2.2 Pattern Reconfigurable Antennas	17	7
	2.2.3 Polarization Reconfigurable Antennas	20	)
	2.2.4 Hybrid Reconfigurable Antennas	22	2
	2.3 Reconfiguration Techniques	25	5
	2.3.1 Details of reconfiguration through PIN diode	26	6
	2.3.2 Reconfiguration through RF MEMS	29	)
	2.3.3 Reconfigurable Antennas Based on Varactor Diodes	30	)
	2.3.4 Optical switches based reconfigurable antennas	32	2

	2.3.5 Reconfigurable Antennas Based on Structure Physical Change	33
	2.3.6 Reconfigurable Antennas Based on Smart Materials	34
	2.4 DC biasing analysis of MADP-000907-14020 PIN diode	37
	2.5 Design Challenges for Reconfigurable Antennas	48
	2.6 Summary	40
3	Design and analysis of frequency reconfigurable antennas for new C-band 5G	41-58
	networks and WLAN/Wi-Max applications	
	3.1 Introduction	41
	3.2 Design and analysis of hexagonal-shaped frequency reconfigurable antenna	42
	3.3 Simulation Results and Discussions of Hexagonal-shaped Frequency	46
	reconfigurable antenna	
	3.3.1 PIN diode ON state simulated results	47
	3.3.2 PIN Diode OFF state simulated results	48
	3.4 Design and analysis of V-shaped slit frequency reconfigurable antenna	50
	3.5 Simulated results and discussions of V-shaped slit frequency reconfigurable	52
	antenna	
	3.5.1 PIN diode ON state simulated results	52
	3.5.2 PIN diode OFF state simulated results	54
	3.6 Summary	58
4	Design and analysis of frequency and pattern reconfigurable antenna for IoT	59-67
	applications	
	4.1 Introduction	59
	4.2 Design and analysis of frequency and pattern reconfigurable antenna	60
	4.2.1 Parametric analysis on ground length	61
	4.3 Simulated Results and Discussions of frequency and pattern reconfigurable	63
	antenna	
	4.3.1 Mode 1 (when both diodes are in the OFF state)	63
	4.3.2 Mode 2 and Mode 3 (one diode is ON or another diode is OFF)	64
	4.4 Radiation pattern analysis on smart fixed vehicles	65
	4.5 Comparison of proposed frequency and pattern reconfigurable antennas with	66
	existing structures	
	4.6 Summary	67
5	Design and analysis of Compound/Hybrid reconfigurable antenna for Sub 6	68-86
	GHz wireless standards and Vehicular applications	
	5.1 Introduction	68

	3.2 Design Evaluation of Compound Reconfigurable Antenna	09
	5.2.1 Parametric study on parasitic stub length (p) to obtain the axial ratio	71
	(AR) below 3 dB at operating frequencies	
	5.2.2 Analysis of radiation pattern and polarization of the compound	71
	reconfigurable antenna	
	5.2.3 Analysis of  S <sub>11</sub>   in Ansys circuit using S2P files of PIN diodes	76
	5.3 Experimental validation of simulated results in three modes	76
	5.3.1 Operating state 1 (0000)	76
	5.3.2 Operating state 2 (0001) & Operating state 3 (0010)	77
	5.3.3 Operating state 4 (0100) & Operating state 5 (1000)	78
	5.3.4 Operating state 6 (0101) & Operating state 7 (1010)	80
	5.4 Comparison of the compound reconfigurable antenna with existing structures	85
	5.5 The main contribution of the proposed compound reconfigurable antenna	86
	5.6 Summary	86
6	Design and analysis of Multiband hybrid reconfigurable antenna (HRA) with	87-108
	enhanced gain for Wi-Fi-6E and 5G NR wireless Standards	
	6.1 Introduction	87
	6.2 Design and analysis of frequency and pattern reconfigurable antenna	87
	6.2.1 Selection of suitable PIN diode in contrast to artificial switch	91
	6.2.2 Biasing analysis of Selected suitable PIN diode	91
	6.2.3 Analysis of E-Field distribution on a radiating element in three modes	92
	6.3 Methodology of Gain Enhancement	94
	6.4 Experimental validation of simulated results in three modes	97
	6.5 Comparison of proposed gain enhanced HRA with existing structures	106
	6.6 The major contribution of the proposed gain enhanced hybrid reconfigurable	107
	antenna	
	6.7 Summary	108
7	Conclusion, Future Scope, and Social Impact	109-112
	7.1 Conclusion	109
	7.2 Future Scope	110
	7.2.1 Emerging Materials and Technologies	110
	7.2.2 Integration with AI and Machine learning for reconfigurable antenna	111
	design	
	7.3 Impact of Reconfigurable Antenna on Social Environment	112
	References	113-124

# **LIST OF FIGURES**

Fig. No	Figure Description	Page No	
1.1	Various shapes of the microstrip patch antenna	1	
1.2	Different feeding techniques for the microstrip patch antenna		
1.3	Applications of Reconfigurable antennas		
1.4	5G spectrum bands penetration Vs distance		
1.5	FCC Allotted frequency spectrum for New C-band 5G networks	6	
1.6	Proposed antenna designs research methodology flow Chart	9	
1.7	Flow chart for general reconfigurable antenna designs	10	
2.1	Different Types of Reconfigurable Antennas	14	
2.2	Frequency reconfigurability of an antenna through various modes	15	
2.3	Methods to achieve frequency reconfiguration	16	
2.4	Various designs of frequency reconfigurable antennas in existing open	17	
	literature		
2.5	Pattern reconfiguration for various states of PIN diode	18	
2.6	Different methods to achieve pattern reconfigurable antenna	19	
2.7	Various designs of pattern reconfigurable antennas in existing open literature	20	
2.8	A Polarization Reconfigurable Antenna for Satellite Application	21	
2.9	Methods to obtain the polarization in reconfigurable antenna		
2.10	Various designs of polarization reconfigurable antennas in existing open	22	
	literature		
2.11	Types of hybrid/compound reconfigurable antennas	23	
2.12	Various compound/hybrid reconfigurable antennas existing in the open	24	
	literature		
2.13	Techniques to achieve reconfiguration in reconfigurable antenna	25	
2.14	Equivalent model of PIN diode and its implementation in HFSS	27	
2.15	Compound reconfigurable antennas through PIN diodes	28	
2.16	The schematic view of RF MEMS and its equivalent lumped elements	29	
2.17	Reconfigurable antennas based on RF MEMS switch		
2.18	Equivalent circuit of varactor diode	30	
2.19	Reconfigurable antennas based on varactor diode	31	

2.20	Optical switches-based reconfigurable antennas			
2.21	Reconfigurable antennas based on physical structure changes			
2.22	Smart materials-based reconfigurable antennas			
2.23	PIN diode Biasing Circuit			
2.24	The implementation model of PIN diode biasing in ADS using S2P files			
2.25	Parametric variations of blocking capacitor and RF choke inductor			
3.1	Hexagonal-shaped radiating element	43		
3.2	Simple planar hexagonal-shaped monopole antenna	43		
3.3	Parametric analysis of proposed frequency reconfigurable antenna	44		
3.4	Schematic diagram of Proposed frequency reconfigurable antenna structure	45		
3.5	Equivalent circuit model of MADP000907-14020 P PIN diode	46		
3.6	Simulated performance characteristics of the proposed antenna when PIN diode ON state			
3.7	Simulated performance characteristics of the proposed antenna when PIN diode OFF state	48		
3.8	Proposed frequency reconfigurable antenna analysis using Ansys Circuit	49		
3.9	Proposed V-shaped slit frequency reconfigurable radiating structure schematic	51		
	diagram			
3.10	Parametric analysis on ground length of V-shaped silt reconfigurable antenna	52		
3.11	Simulated performance characteristics of the proposed V-shaped slit frequency	53		
	reconfigurable antenna when PIN diode ON state			
3.12	Simulated performance characteristics of the proposed V-shaped slit frequency reconfigurable antenna when PIN diode OFF state			
3.13	Simulated performance characteristics of the proposed V-shaped slit frequency	56		
	reconfigurable antenna when PIN diode ON state (Right side)			
4.1	Proposed frequency and pattern reconfigurable antenna and its geometrical	60		
	dimensions			
4.2	Parametric studies on ground length (lg) and parasitic stub length (d)	62		
4.3.	Radiation patterns of parasitic stub lengths (d=7, 9, 11 and 12 mm)	63		
4.4	Simulated Results in mode 1 (both diodes are in the OFF state)	64		
4.5	Simulated results in mode 2 (D1 is OFF and D2 is ON state)	65		
4. 6	Simulated results in mode 2 (D1 is ON and D2 is OFF state)	65		
4.7.	Communication between vehicles to other networks via IoT	66		

4.8.	Pattern analysis of the proposed structure on top of the intelligent vehicle		
5.1.	Step-by-step design evolution of proposed compound reconfigurable antenna		
5.2	Simulated (a) S <sub>11</sub> and (b) Axial Ratio (AR) variation with a length of a		
	parameter (p)		
5.3	The 3D polar plot radiation patterns for pattern tilting in various operating	72	
	states (i-xi)		
5.4	Simulated surface current distribution for OS4(0100) and OS6 (0101)	75	
5.5	Simulated circuit representation of OS7 (1010) in Ansys circuit		
5.6	The experimental and simulated results of the proposed structure in OS1 (0000)	77	
5.7	The experimental and simulated results of the proposed structure in OS2 (0001)	78	
	& OS3 (0010)		
5.8	The experimental and simulated results of the proposed structure in OS4	79	
	(0100)/ OS5 (1000) for linear polarization @ 3.7 GHz		
5.9	The experimented and simulated normalized LHCP/RHCP gain patterns in	80	
	OS4 (0100) / OS5(1000)		
5.10	The experimented and simulated results of the proposed structure in OS6	80-81	
	(0101) &OS7 (1010)		
5.11	The simulated and experimental axial ratios in OS4 (0100) and OS6 (0101)	81	
5.12.	Photograph of the fabricated compound reconfigurable antenna (CRA)	82	
5.13	Measurement setup of proposed CRA		
6.1	Proposed Hybrid Reconfigurable Antenna (HRA) with enhanced gain and its	88-89	
	geometrical dimensions.		
6.2	Different prototypes (a)-(d) for designing the proposed radiating element	89-90	
	antenna		
6.3	(a) Simulated reflection coefficient curves and (b) Comparison of PIN diode	91	
	models for the proposed HRA		
6.4	(a) Biasing arrangement of the PIN diode (b) $S_{11}(dB)$ and $S_{21}(dB)$ for the PIN	92	
	diode(c) Analysis of the biasing effect of the proposed structure in mode 2(a)		
6.5	The electric field distributions of HRA in all modes	93	
6.6	Gain enhancement techniques	94	
6.7	Design and analysis of the proposed unit cell (FSS)		
6.8	Performance characteristics of the proposed HRA in mode 3 with an FSS-based	96	
	reflector		
6.9	Measured and simulated $\left S_{11}\right $ dB and realized gain in (a) Mode 1 (b) Mode 2 (a	97-99	
	& b), (c) Mode 3		

6.10	Normalized patterns of the proposed structure at 6.5 GHz in Mode 2 (a and b)	
	and Mode 3	
6.11	Simulated 3-D radiation pattern of Mode 2 (a and b) and Mode 3 at 6.5 GHz	101
6.12	Normalized simulated and measured cross and co-polarization at three modes	101-103
	on a) XZ plane b) YZ plane	
6.13	A photograph of the fabricated HRA with FSS	105
6.14	Snapshot of S parameter measurement at mode 3	106

# **List of Tables**

Table No.	Table Description	Page No.	
1.1	Comparison of traditional and reconfigurable antennas	4	
3.1	The designed frequency reconfigurable antenna geometrical dimensions	45	
3.2	Summary of observations for the proposed frequency reconfigurable antenna structure		
3.3	Comparison of proposed frequency reconfigurable antenna structure parameters with Published work.	50	
3.4	The V-shaped slit frequency reconfigurable antenna structure dimensions	51	
3.5	Summary of observations for the proposed radiating dual and single band frequency reconfigurable antenna	57	
3.6	Comparison of proposed V-shaped slit frequency reconfigurable antenna structure parameters with published work	57	
4.1.	Geometrical dimensions of frequency and pattern reconfigurable antenna	61	
4.2.	Comparison of proposed frequency and pattern reconfigurable with existing structures		
5.1	CRA Geometrical Dimensions (mm)	70	
5.2	Operating States of Proposed CRA	70	
5.3	The performance characteristics of CRA in seven operating states	84	
5.4	Comparison of the compound reconfigurable antenna with the existing structures	85	
6.1	Geometrical dimensions of the proposed frequency and pattern reconfigurable antenna with enhanced gain structure	90	
6.2	HRA performance characteristics with and without FSS-based reflector	104	
6.3	Comparison of Proposed gain enhanced HRA with existing structures	107	

## ABBERVIATIONS AND SYMBOLS

#### Symbol/Abbreviations **Description** Relative permittivity of dielectric $\epsilon_r$ Wavelength λ Velocity of light c Loss tangent Tan $(\delta)$ Effective relative permittivity $\epsilon_{eff}$ h Substrate thickness dBi Decibel in isotropic FR-4 Flame Retardant-4 **HFSS** High-Frequency Structure Simulator 3D Three Dimensional 2D Two Dimensional **IEEE** Institute of Electrical and Electronics Engineers **GPS** Global Position System 5G Fifth Generation **WLAN** Wireless Local Area Networks RF Radio Frequency **CPW** Co Planar Waveguide RA Reconfigurable Antenna IoT Internet of Things **MEMS** Micro Electro Mechanical System **HRA** Hybrid Reconfigurable Antenna **DGS Defective Ground Structures FSS** Frequency Selective Surfaces **SIW** Substrate Integrated Waveguide DC Direct Current NR New Radio $S_{11}$ Reflection coefficient CP Circular Polarization LP Linear Polarization

Left Hand Circular Polarization

**LHCP** 

RHCP Right Hand Circular Polarization

CST Computer Simulation Technology

ADS Advanced Design Software

RL Return Loss

VSWR Voltage Standing Wave Ratio

WiMAX Worldwide interoperability for Microwave Access

Wi-Fi Wireless Fidelity

OS Operating State

AR Axial Ratio

CRA Compound Reconfigurable Antenna

FCC Federal Communication Commission

ISM Industrial, Scientific and Medical

PCB Printed Circuit Board

DMM Digital Multimeter

SMA Sub Miniature Version A

mm millimeter

#### **CHAPTER 1: INTRODUCTION**

## 1.1 Background and Motivation

Nowadays, modern wireless devices such as mobile phones, smartwatches, and different smart home devices are integral parts of human daily lives. These devices require antennas for wireless communication. The antenna is a structure capable of receiving and radiating electromagnetic waves. These antenna structures include dipole, monopole, bow-type, microstrip patch antennas, etc.,[1]. The microstrip patch antenna structure is widely used to implement antennas due to various features, such as low profile, lightweight, and easy fabrication. The shape of the patch antenna can be rectangular, circular, or hexagonal, as shown in Fig.1.1.

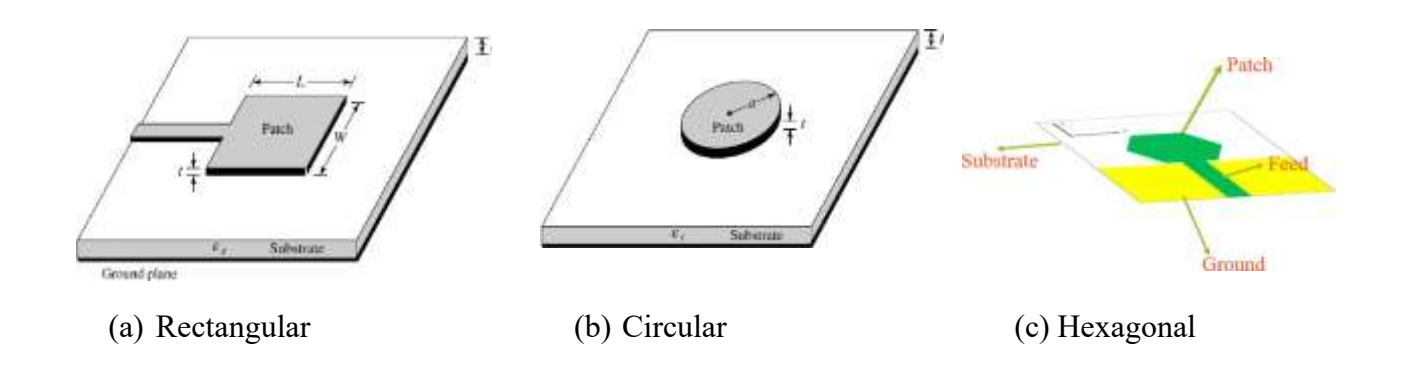


Fig.1.1. Various shapes of the microstrip patch antenna [1]

However, compared to rectangular and circular-shaped antennas, a hexagonal-shaped antenna provides better design flexibility, higher bandwidth, and excellent multiband capability in a compact size. These structures require feeds to radiate and receive electromagnetic waves. Basic feeding methods such as aperture coupling, proximity coupling, coaxial feeding, microstrip line feeding, and coplanar waveguide (CPW) feeding are used to feed the microstrip patch antennas [1]. The two most often used methods are coaxial and microstrip line feeding techniques because of their benefits, which include reduced spurious radiation and simple impedance matching. However, the coaxial feed needs multilayer fabrication, which makes the production process more difficult. Similarly, proximity and aperture-coupled feeding techniques are less commonly employed and the microstrip line feeding technique shown in Fig. 1.2 (a) is frequently used for reconfigurable antenna designs because of its simple design and easy fabrication.

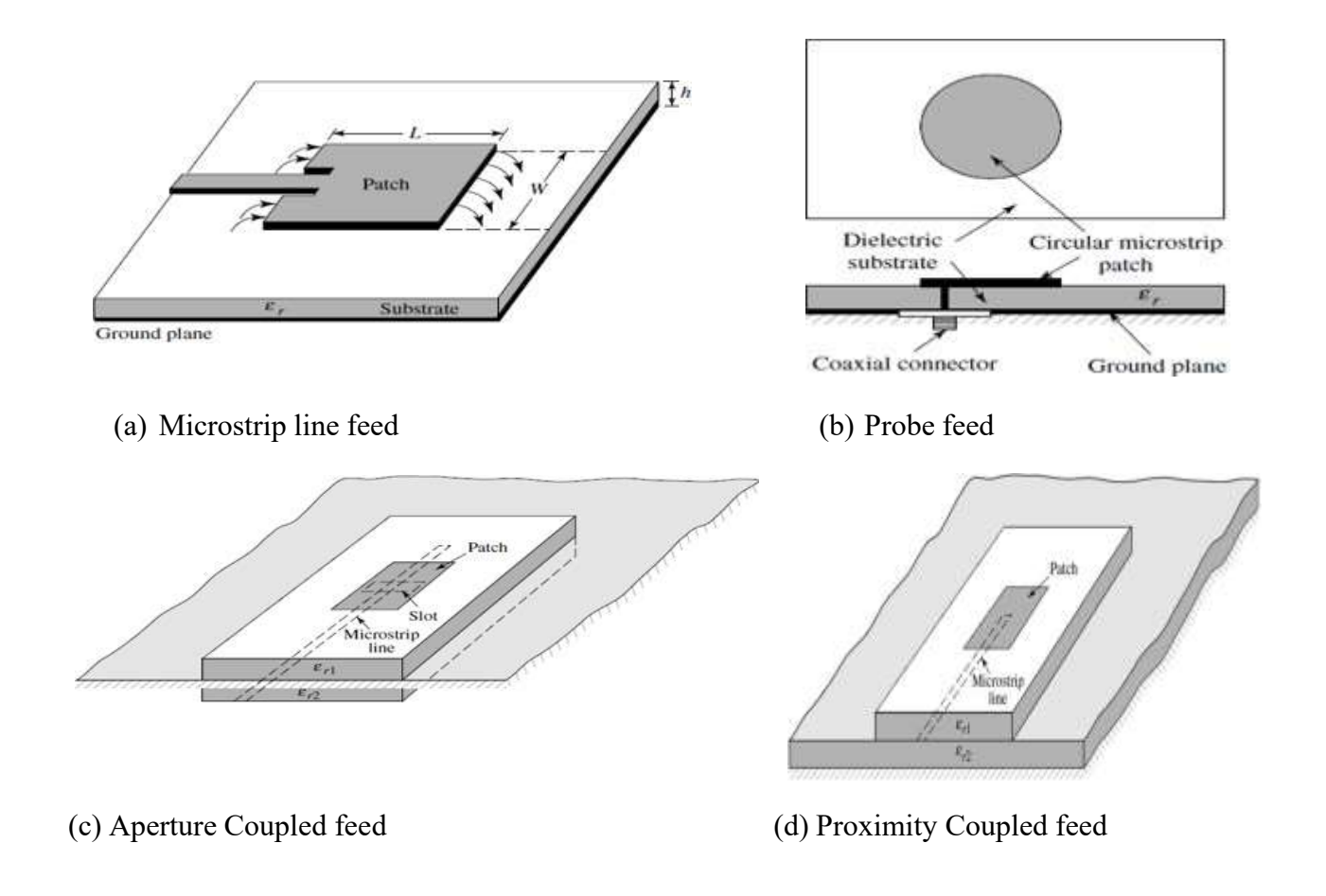


Fig. 1.2. Different feeding techniques for the microstrip patch antenna [1]

The traditional antennas in wireless communication systems operate at static frequencies and provide fixed patterns and polarization. Integrating these antennas in wireless systems to support various wireless standards increases the system complexity and difficulty in controlling the system performance and reduces the system's overall efficiency. The rapid evolution of wireless communication technologies calls for multifunctional, smart antennas capable of adapting to modern system requirements. As wireless services expand across different sectors, providing more services without adding complexity or increasing device size becomes difficult. The future communication trends are expected to reshape connectivity by introducing new technologies to meet massive data demands, high-speed connectivity, and seamless communications. Developing antennas with flexible and controllable properties is crucial to meet the needs of current and future wireless systems.

A promising solution to these challenges is the design of multifunctional antennas that can dynamically adapt the frequency, pattern, and polarization to various conditions. These antennas can address many of the issues posed by traditional fixed-performance antennas, adding functionality and improving system efficiency. Recent design advancements have introduced multiple approaches to antenna reconfigurability, including individual feeds for different elements, partial or complete physical movements, reconfigurable feeding networks, and impedance-matching circuits etc.,

However, these methods can affect antenna performance and compromise compactness due to the inclusion of mechanical movements, external feed circuits, and additional control mechanisms. Reconfiguring antenna performance using controllable RF and microwave circuits requires proper integration, further complicating the design. From this standpoint, a stand-alone reconfigurable antenna that does not rely on complex external feed systems offers a more practical and flexible solution. Such antennas hold significant potential for use as single or array elements, with their performance independent of external feeding networks. However, sophisticated antenna designs make it harder to achieve dependable reconfigurability. Therefore, a significant area of current study is the creation of innovative designs for high-performance, multifunctional reconfigurable antennas, reducing control complexity, minimizing losses, and improving system-level integrity are all achieved by simplifying design complexity.

This thesis aims to create low-profile, easily controllable single- and multi-reconfigurable antennas with reliable reconfiguration performance and simplified procedures.

# 1.2 Reconfigurable Antennas in Wireless Applications

#### 1.2.1 Comparison of traditional and reconfigurable antennas

Reconfigurable antennas play an important role in modern wireless systems as compared to traditional static-performance antennas in terms of multi-functionality, adaptability, and flexibility as discussed earlier. A more significant number of fixed-performance antennas in wireless systems to operate in various bands can easily be replaced by a single multifunctional reconfigurable antenna to support multiple bands without degrading its performance characteristics. Due to this size, the cost and complexity of wireless systems are reduced. The characteristics of a reconfigurable antenna compared to the traditional one are listed in Table 1.1.

 Table 1.1: Comparison of traditional and reconfigurable antennas

S. No	Characteristic	Traditional antenna	Reconfigurable antenna
1	Operating frequency	Static	Changes dynamically as required
2	Multiband or wideband	Less adaptable	Adaptable
3	Polarization	Fixed either linear,	Dynamically adjust the polarization
		circular, or	from linear to circular and vice versa
		elliptical	
4	Radiation pattern	Fixed	Adopt or steer the pattern in response
			to specific system requirements
5	Multi-functional capability	Inflexible	Flexible to frequency switching,
			beam steerable, and diverse
			polarization
6	Size for multiband operation	Large	Small or compact
7	Adaptability and flexibility	Limited	Limitless
	to environmental changes		
8	Reliability	Low	High
9	Spectrum utilization	Low	High
	efficiency		
10	Support for modern wireless	Moderate	Better
	standards		

# 1.2.2 Applications of reconfigurable antennas

Traditional antenna performance is effective in various applications. However, they are limited by their performance in dynamic environmental situations and adaptation to modern system requirements. Thus, reconfigurable antennas are proposed in this thesis. The major applications of these antennas are represented in Fig. 1.3.

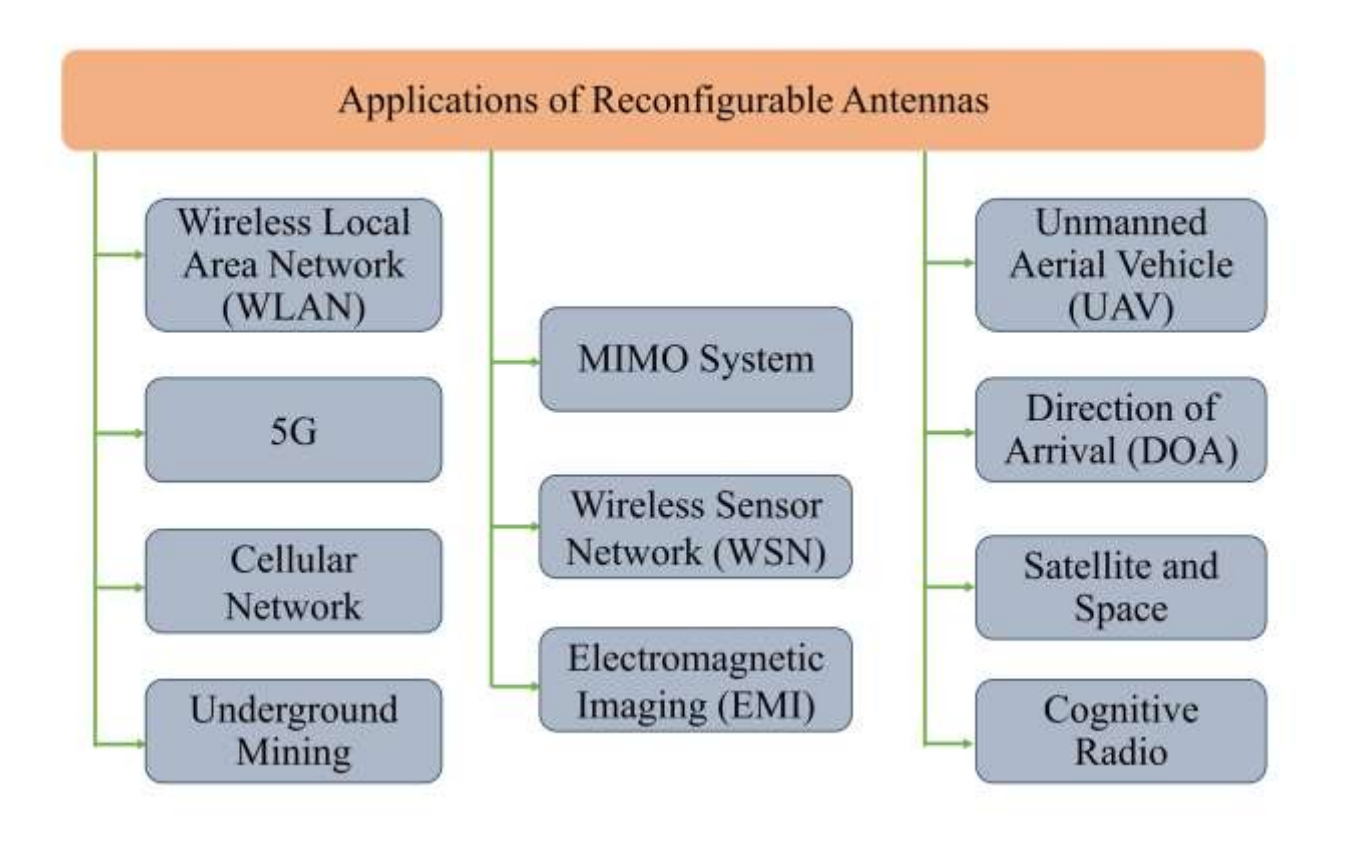


Fig 1.3. Applications of Reconfigurable antennas [2]

# 1.3 5G Spectrum Bands

In general, any type of antenna is designed for a particular operating frequency band. Nowadays, the requirement of data rate is increasing rapidly and for that purpose, higher bandwidth is necessary. The Federal Communications Commission (FCC) divided the primary 5G spectrum into three categories: a lower band (up to 1 GHz), a sub-6 GHz band as a mid-band 5G spectrum, and a mm-wave band as an upper band, as shown in Fig.1.4. The upper band spectrum operates in the frequency range of 24 GHz-52 GHz and offers high data rates with a larger capacity but is limited to a shorter range due to atmospheric attenuation. Sub-6 GHz/Mid-band frequencies (1 - 7 GHz) can travel longer distances without attenuation. Therefore, sub-6 GHz frequencies are primarily used across the world.

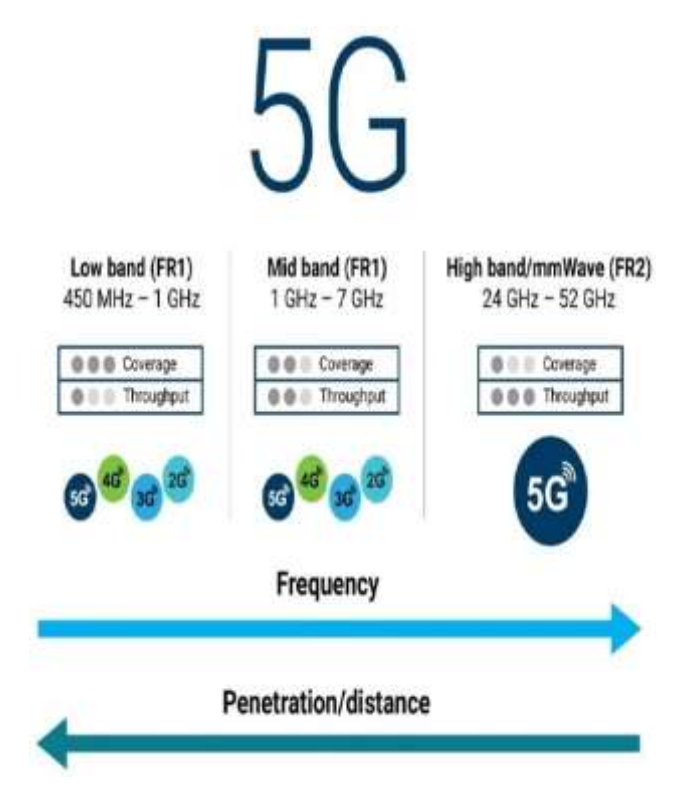


Fig. 1.4 5G spectrum bands penetration V<sub>s</sub> distance [3]

As shown in Fig. 1.4, as the frequency increases, the penetration of the RF signal decreases, and vice versa. At mm-wave frequencies, the RF signal suffers more due to atmospheric absorptions and various environmental conditions. To overcome this, antennas with high gain and higher directivity are preferable for effective wireless communications. In the year 2020, the FCC reassigned the existing c-band for 5G communications under the categories of mid band, as shown in Fig.1.5.

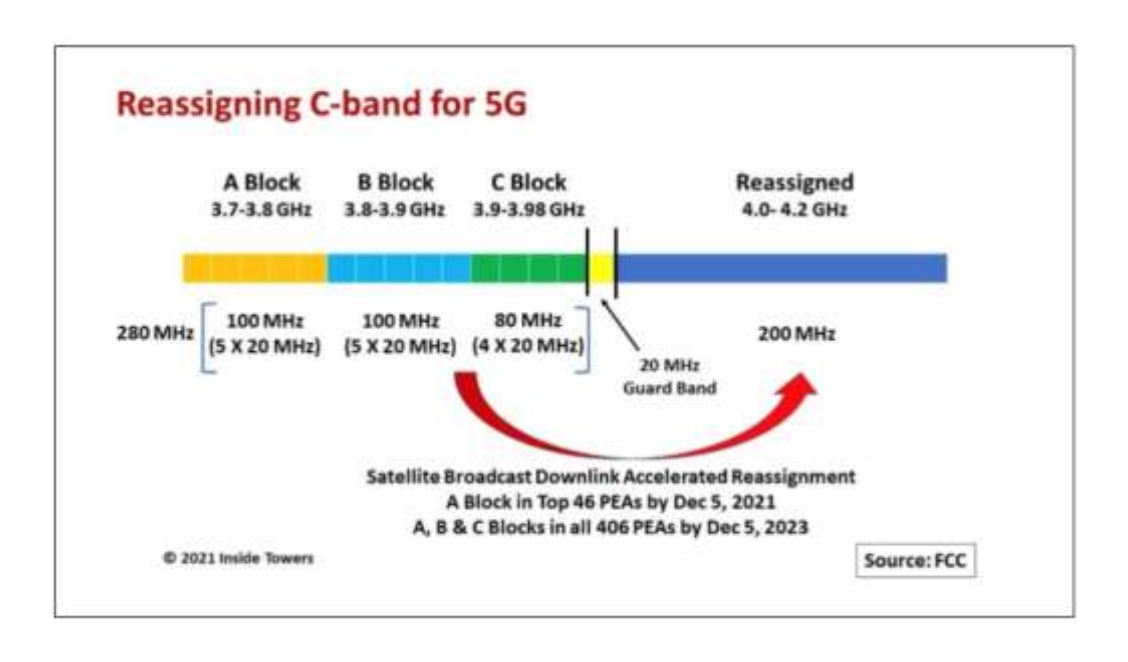


Fig.1.5 FCC Allotted frequency spectrum for New C-band 5G networks [3]

#### 1.4 Scope of Research

The present work revealed the various issues in existing reconfigurable antennas. Many RA concepts depend on more RF switches for compound reconfiguration and multiple feeding networks for polarization reconfigurability. This research focuses on the design and analysis of RA's with compact size, less complexity, and improved performance for sub-6 GHz vehicular, Wi-Fi 6E, and IoT wireless standards through partial ground plane concept, RA's with combined multiple reconfigurability functions, and high-gain RA through FSS-based reflectors through PIN diode RF switching technology aimingto enhance the spectrum utilization and avoid interference and multipath fading.

To accomplish the goals of this thesis, the following strategies are used:

- ➤ Identifying reconfigurable technologies and methodologies, evaluating the applicability and constraints of the current strategy, and putting forward new ideas to implement better, simpler reconfigurable antenna designs suited to modern wireless communication systems.
- ➤ Designing of frequency reconfigurable antennas: Design of single and dual-band frequency reconfigurable with wideband and compact size for new C-band 5G networks and WLAN /Wimax applications.
- ➤ Developing a frequency and pattern reconfigurable antenna: This involves the development of a frequency and pattern reconfigurable antenna for IoT close-range devices based on activating and deactivating parasitic stubs electronic, and beam tilting of the developed structure is analyzed on the static vehicle through Ansys SBR+ software.
- ➤ Compound/hybrid reconfigurability functions: An electronically switched parasitic stubs on the ground as well as on the radiating structure, a compound reconfigurable antenna is designed and analyzed for different wireless standards based on the Yagi-Uda concept and changing the effective resonant lengths through RF switches.
- Realizing multiband frequency and pattern reconfigurable antennas with enhanced gain through a frequency selective surface (FSS)-based reflector: A multiband hybrid reconfigurable antenna is investigated with the help of two PIN diodes. This design has split ring resonators placed symmetrically on half-hexagonal-shaped radiating elements to obtain the multiband. By keeping the reflector below the radiating element, a 50% gain is improved compared to without the reflector. High-gain reconfigurable antennas are useful for long-range coverage.
- ➤ Optimizing and testing the proposed reconfigurable antenna parameters, such as realized gain, reflection coefficient, and pattern, under various reconfigurable modes by changing the status (ON/OFF) of the PIN diode with a simple biasing circuit

The proposed structures in this research are implemented and analyzed using electromagnetic simulations such as ANSYS HFSS, Ansys circuit, SBR<sup>+</sup>, and ADS and validated simulated results through lab-based measurements. The study is limited to the design and analysis of RA's below sub-6 GHz frequency bands commonly used in Wi-Fi and IoT applications.

#### 1.5 Research Methodology

The research methodology of the proposed radiating structures in this thesis is shown in Fig. 1.6. Initially, basic radiating structures such as rectangular, circular and hexagonal-shaped microstrip patch antennas are studied to learn the basic concepts and mathematics behind the radiating structures. Further, a monopole concept is introduced for better performance of the antenna characteristics such as wide band, multiband, etc., this methodology and design concepts of reconfigurable antennae were initially evaluated with the help of a literature review.

To obtain better performance characteristics, parametric analysis is performed on the proposed radiating structures. From the simulations, if the required performance characteristics are achieved from the design, then it is fabricated using the prototype LPKF S60 PCB machine. After, the required circuit components and the SMA connector are soldered on the fabricated design at a suitable position in the soldering station. While doing soldering, more care has to be taken. Once the soldering is done, the voltage and current across the circuit component are measured using DMM, along with the DC power supply, breadboard, and wires, before measuring the scattering parameters. Then, the scattering parameters are measured using a Rohde & Schwarz ZVA-40 vector network analyzer. Using an anechoic chamber, radiation patterns are measured.

A few iterations of designed structures are fabricated and measured to obtain measured results similar to the simulated.

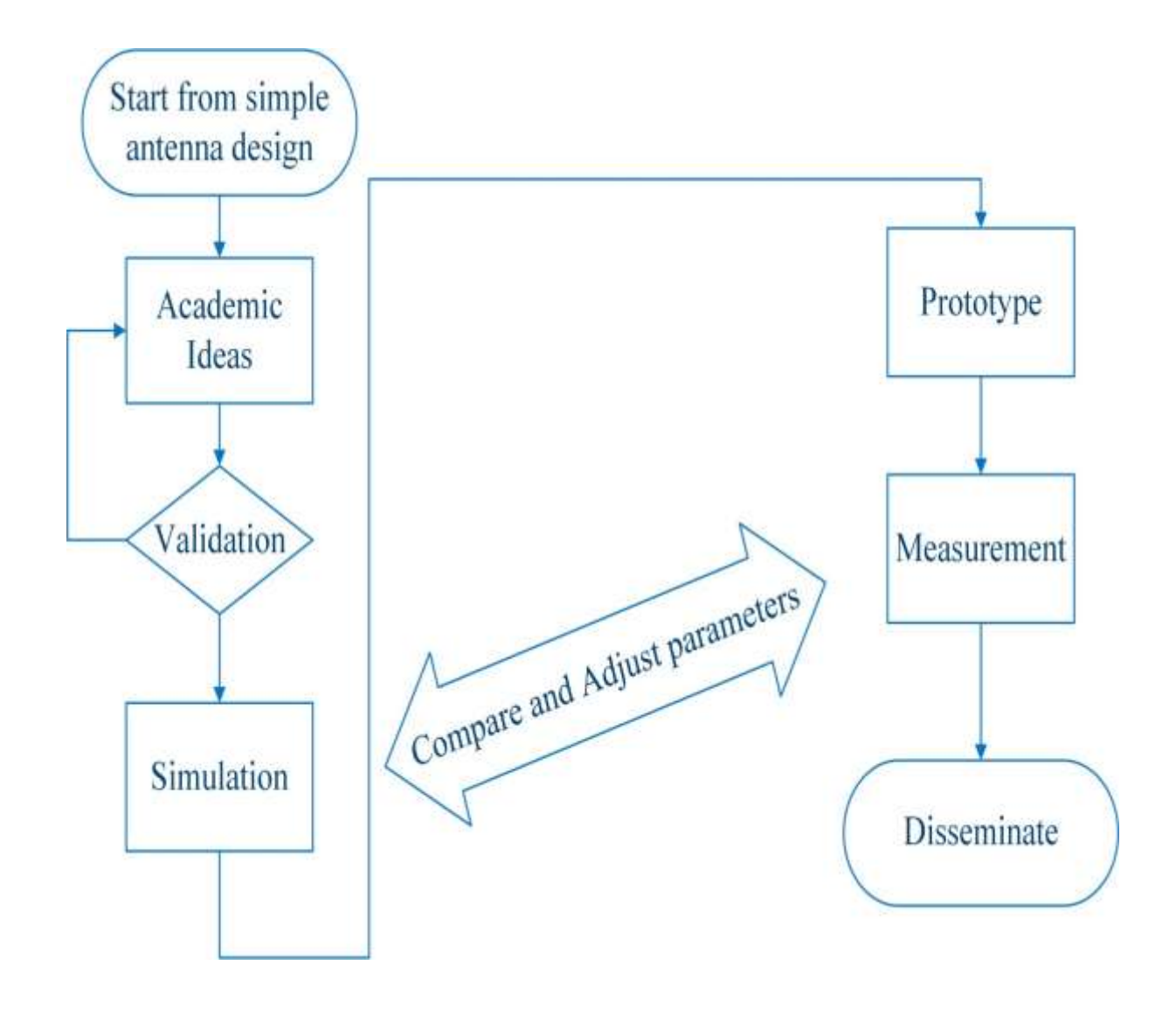


Fig.1.6 Proposed antenna designs research methodology flow chart

The general reconfigurable antenna design flow is shown in Fig 1.7. Initially, a suitable geometry of reconfigurable antenna is chosen based on the required application. The antenna geometries are evaluated at the required resonant frequency. Then, the designed antenna parameters are optimized through EM simulation software such as HFSS/CST to obtain the required performance characteristics from the designed structure. Finally, the design structures are fabricated, and the required parameters are measured and compared with the simulated results.

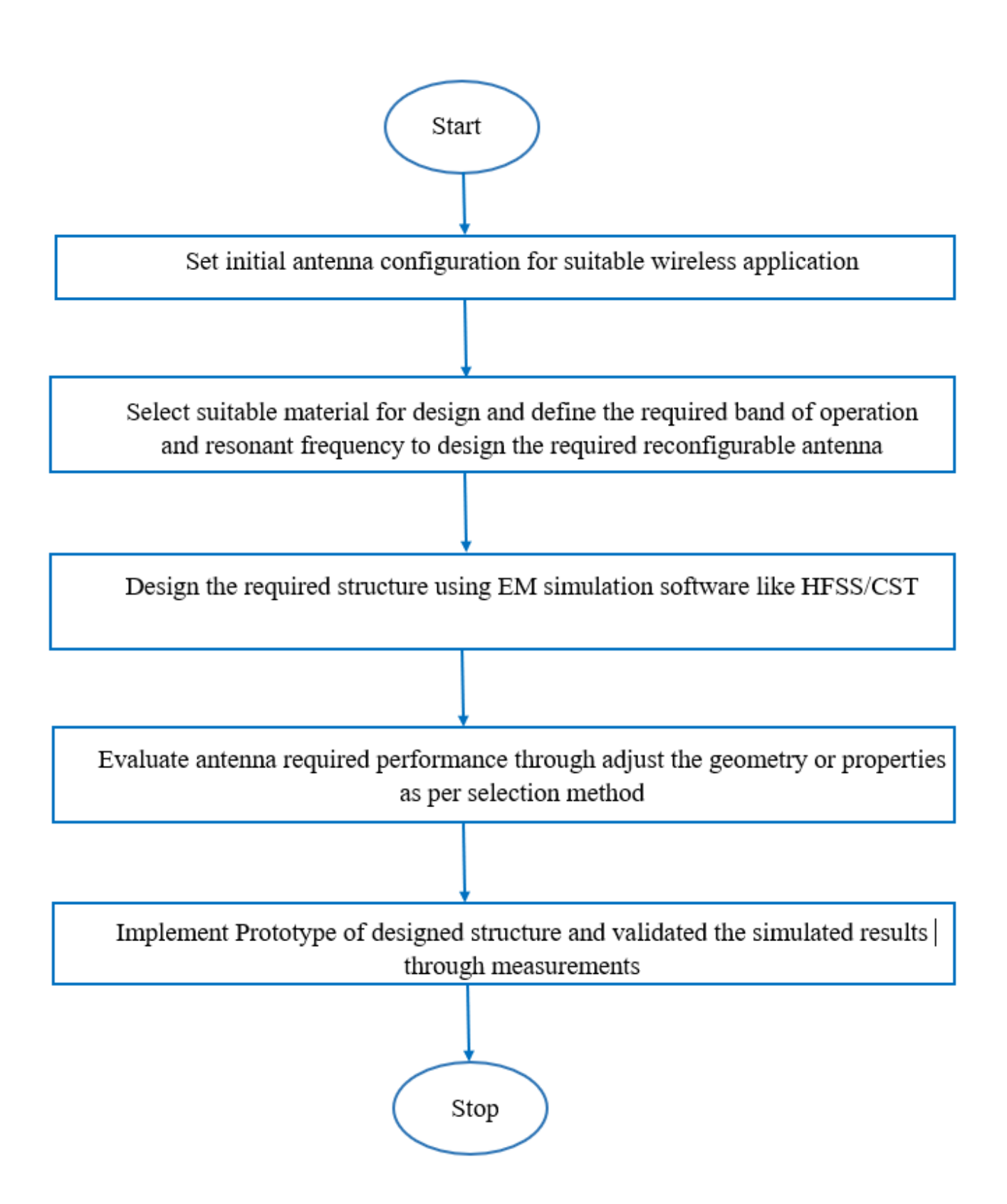


Fig.1.7 Flow chart for general reconfigurable antenna designs

#### 1.6 List of Publications

#### Journals:

- 1. M. Ganesh, N.S. Raghava, Thennarasan Sabapathy, Yashna Sharma, "A compound reconfigurable electronically switched parasitic monopole antenna for sub 6 GHz wireless and vehicular applications" AEU International Journal of Electronics and Communications, Volume 179,2024,155335, ISSN 1434-8411
- 2. M. Ganesh, N.S. Raghava, Thennarasan Sabapathy, Yashna Sharma, "A Gain Enhanced Multiband Frequency and Pattern Reconfigurable Antenna for Wi-Fi 6E and 5G New Radio Wireless Standards" International Journal of Communication Systems, October 2024. https://doi.org/10.1002/dac.6011.
- 3. M. Ganesh, N.S. Raghava, Thennarasan Sabapathy, Yashna Sharma, "An Electronically Beam Steerable Multiband Miniaturized Reconfigurable antenna for Sub 6 GHz 5G Wireless Standards. (Under review)

#### **Conferences:**

- 1. M. Ganesh, N. S. Raghava, and T. Sabapathy, "Design a hexagonal shape frequency reconfigurable antenna for new C-band 5G applications," 2022 IEEE International Conference on Electronics, Computing and Communication Technologies (CONECCT), Bangalore, India, 2022, pp. 1-5, doi: 10.1109/CONECCT55679.2022.9865714.
- 2. M. Ganesh, T. Sabapathy and R. Srinivasa Nallanthighal, "A Novel V-shaped slotted single, dual-band frequency reconfigurable antenna for C-band / 5G applications," 2022 IEEE Silchar Subsection Conference (SILCON), Silchar, India, 2022, pp. 1-6, doi: 10.1109/SILCON55242.2022.10028837.
- 3. M. Ganesh, N.S.Raghava, Yashna Sharma and T.Sabapathy "A Compact Frequency and Pattern Reconfigurable antenna for IoT Close range Devices" 2024 7<sup>th</sup> International Conference on Electronic Design (ICED) 2024 (Presented on 2-09-2024)

#### 1.7 Thesis Organization

This thesis discusses the research work in seven chapters as follows.

- > The first chapter provides the background and motivation of the research work and the importance of reconfigurable antennas in wireless applications.
- > The second chapter provides a brief overview of reconfigurable antenna technologies.
- > The third chapter discusses the frequency reconfigurable antenna for new c-band 5G applications.
- ➤ The fourth chapter explores a compact frequency and pattern reconfigurable antenna for closerange IoT applications based on the parasitic stubs on the ground plane. Further, the pattern tilting is analyzed on the innovative vehicle.
- ➤ In Chapter 5, a compound reconfigurable antenna analysis is performed by using a minimum number of PIN diodes with a simple biasing circuit for sub-6 GHz wireless and vehicular applications based on parasitic stubs on the radiating and the ground plane.
- A multiband antenna is implemented using a split-ring resonator, and an FSS-based reflector improves its performance characteristics for sub-6 GHz and Wi-Fi 6E applications, as discussed in Chapter 6.
- ➤ The conclusion of the whole thesis and further research scope on reconfigurable antennas are concluded in the last chapter.

#### **CHAPTER 2**

## Background study and literature review: Reconfigurable Antenna Technologies

#### 2.1 Introduction

This chapter briefly discusses the concept of reconfigurable antennas and their types. Besides discussing the reconfigurable antennas and their types, an overview of methods and technologies to achieve reconfiguration is also explored. Further a comprehensive review of reconfigurable antennas in terms of their design, analysis, and limitations is discussed to explore the new aspects and scope of research on them.

In 2014, the IEEE defined the reconfigurable antenna as an antenna that is 'capable of changing its performance characteristics (resonant frequency, radiation pattern, polarization, etc.) by mechanically or electrically changing its architecture.'

The basic concept behind the reconfigurable antenna is to modify the radiating fields on the aperture plane through electrical and optical switching techniques and physical structural changes. These require additional RF components. Without additional components, antenna reconfiguration can be achieved through innovative materials such as liquid crystals, graphene, etc., and unique shape-based designs such as origami shapes and fractal shapes [4].

## 2.2 Types of Reconfigurable Antennas

The reconfigurable antenna is mainly categorized into four types, namely frequency, pattern, polarization, and hybrid/ compound reconfigurable antenna, as shown in Fig.2.1. Further, the compound reconfigurable antenna is categorized into frequency and pattern, pattern, and polarization, frequency and polarization, frequency, pattern, and polarization [4].

## 2.2.1 Frequency Reconfigurable Antennas

The frequency reconfigurable antenna is defined as an antenna capable of changing the operating frequency dynamically through various modes of operation. Fig.2.2 shows the frequency reconfigurability of an antenna at two different frequencies [5].

The frequency reconfigurable antennas can replace multiple antennas that cover different frequency bands to reduce the system's complexity and size. The significant advantage of reconfigurable antennas, in which frequency is reconfigured, provides efficient use of the available spectrum dynamically with the rejection of noise in the unused frequency spectrum. The frequency reconfiguration can be achieved through various methodologies, as represented in Fig 2.3.

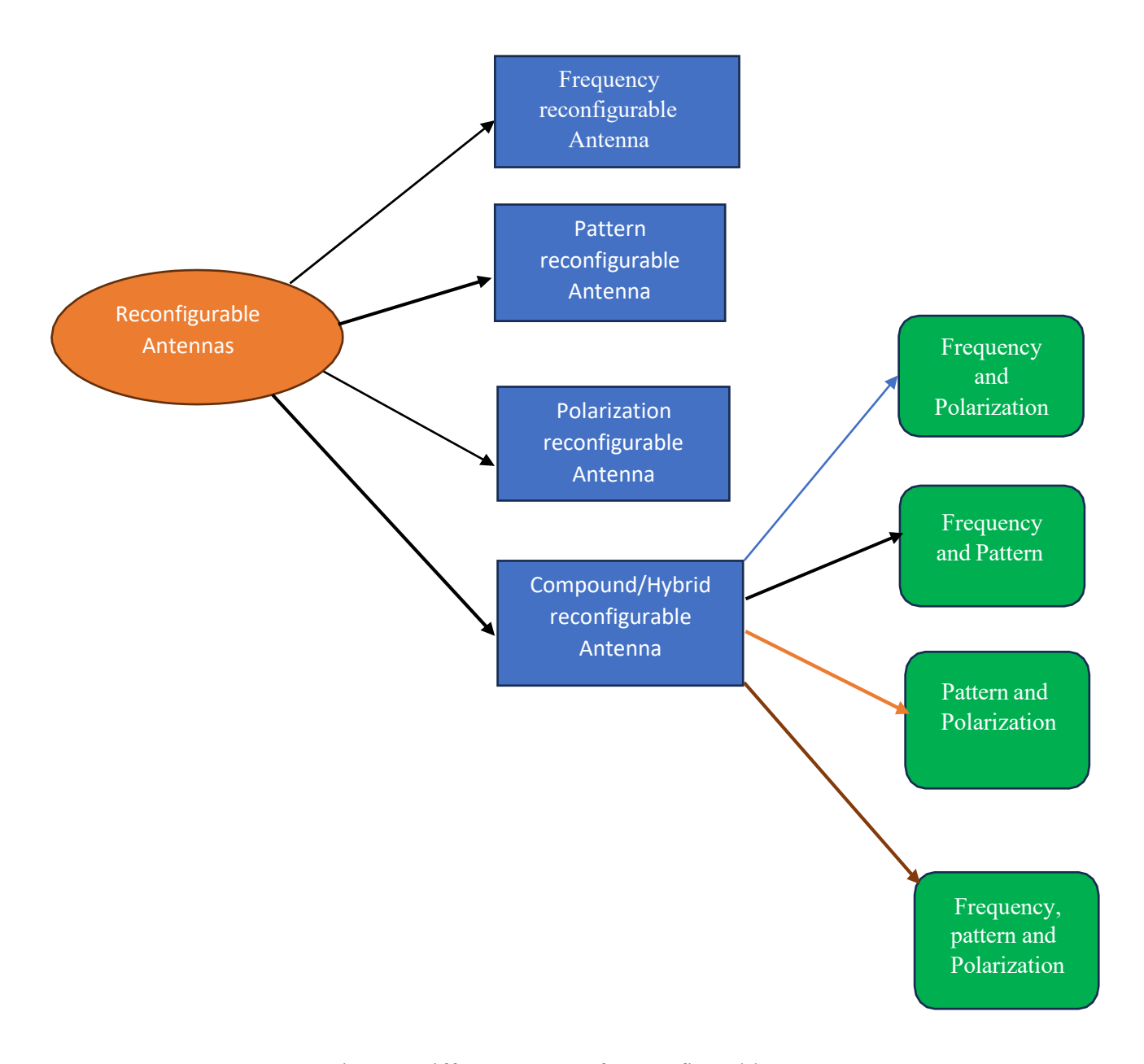


Fig. 2.1 Different Types of Reconfigurable Antennas [4], [6]

In ref [7], authors have reported an antenna with a lumped element switch to reconfigure the frequency at two triple band frequencies with a microstrip feed. A hexagonal-shaped antenna with a notch in the radiating structure is reported [8] for wireless local area networks (WLAN) applications, operating at two different bands of frequencies by ON/OFF of PIN diode switches.

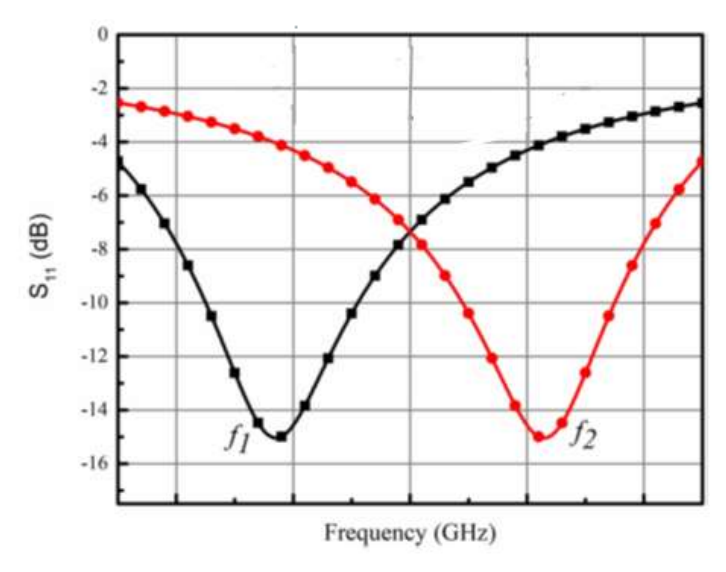


Fig. 2.2 Frequency reconfigurability of an antenna [5]

A hexagonal-shaped radiating structure is reported [9] with a coplanar waveguide feed for portable wireless applications operating at four distinct frequency bands with two PIN diodes based on changing surface current on the radiating structures. An antenna consisting of a co-planar waveguide-fed triangular monopole and two additional stubs attached to the radiating patch through a PIN diode has been reported in [10] to obtain the single-band, dual-band, and wide-band operations through redistributing the surface current on the additional stubs. In ref [11], a compact, flexible, and CPW-fed slotted circular patch antenna has been reported for different frequency bands. In ref [12], a slotted switchable reconfigurable antenna is discussed by utilizing the PIN diode compared to the performance of an antenna without slots. The slotted reconfigurable antenna provides a wider bandwidth than the without-slotted antenna. For the reconfigurability of an antenna in terms of frequency, a slotted microstrip patch radiating structure is the best candidate due to its wide tuning in frequency and convenience for switching between different frequency bands through RF switches across the slot.

A multiple-frequency band antenna with a reconfigurability function in frequency was reported in [13] by using the PIN diode as a switch in the compact antenna structure, in which seven multiple bands were obtained, and its performance was better in all seven bands by changing the effective resonant lengths through the PIN diode. When the antenna size increases, the resonance has the lowest operating frequency, and when the length of the antenna decreases, the resonant has a higher frequency. A compact, wide, multi-band frequency reconfigurable antenna was reported in [14] for multi-wireless standards such as C-band, WLAN, and 5G sub-6 GHz frequency bands. For Sub-6

GHz 5G (3.5 GHz) and WLAN (2.45 GHz) applications, a reconfigurable antenna is reported in [15] by proximity coupling feeding structure.

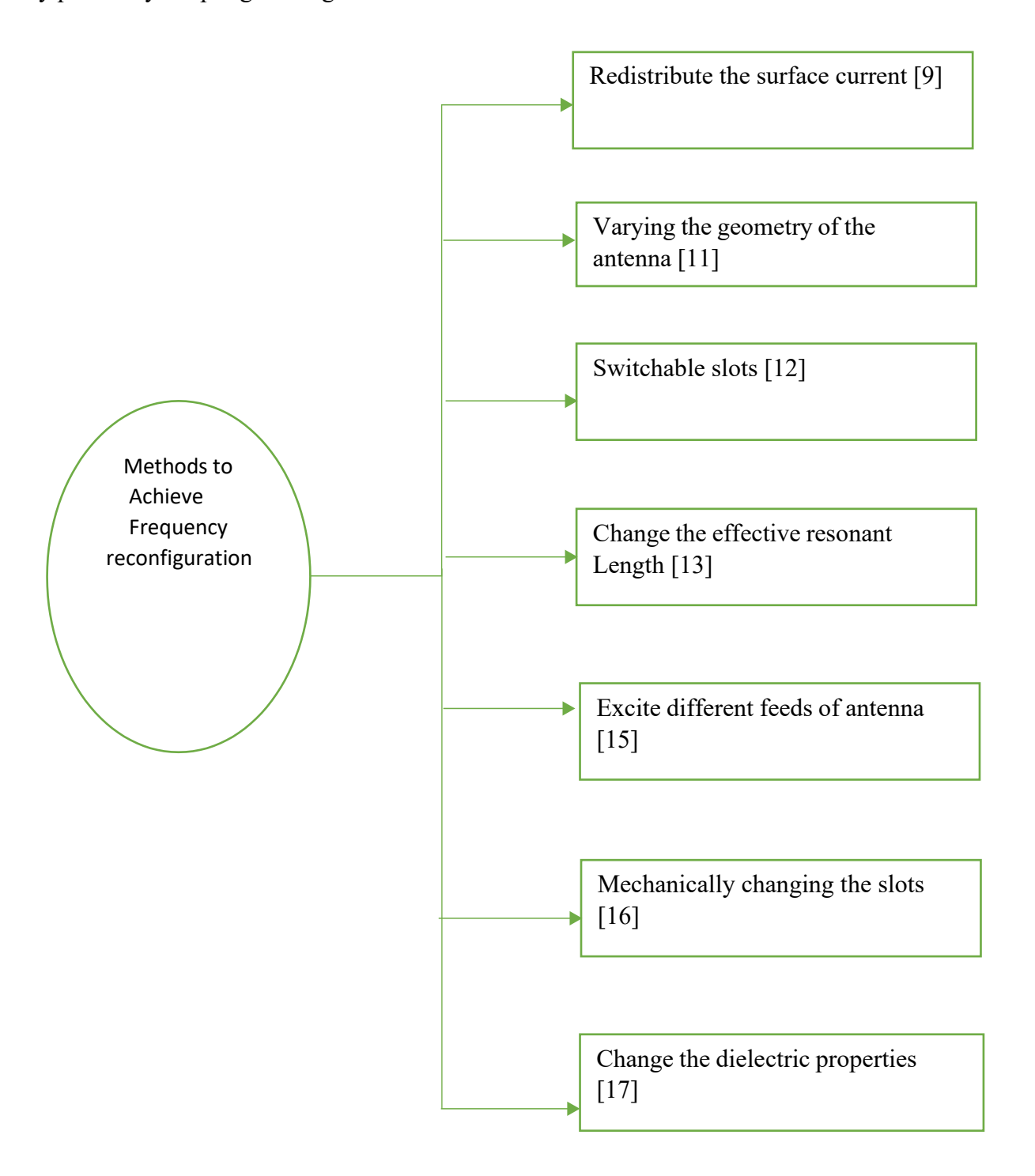
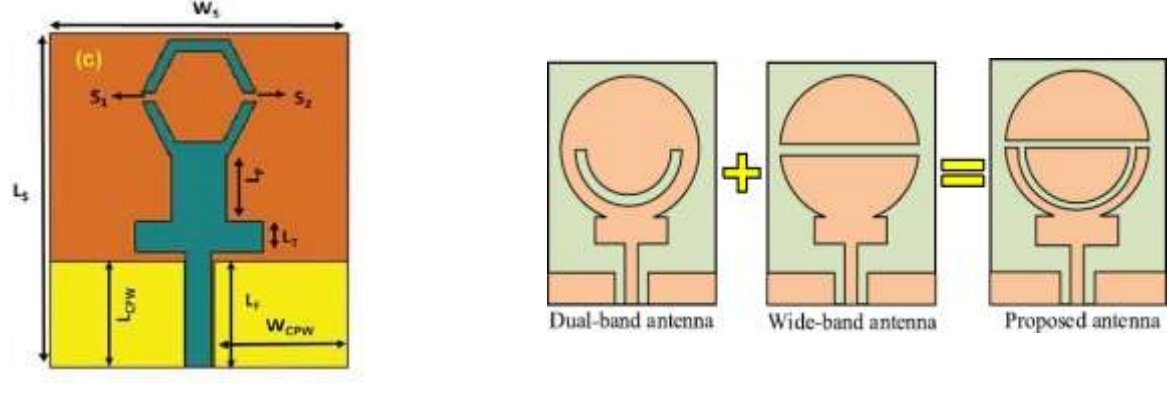
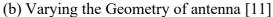


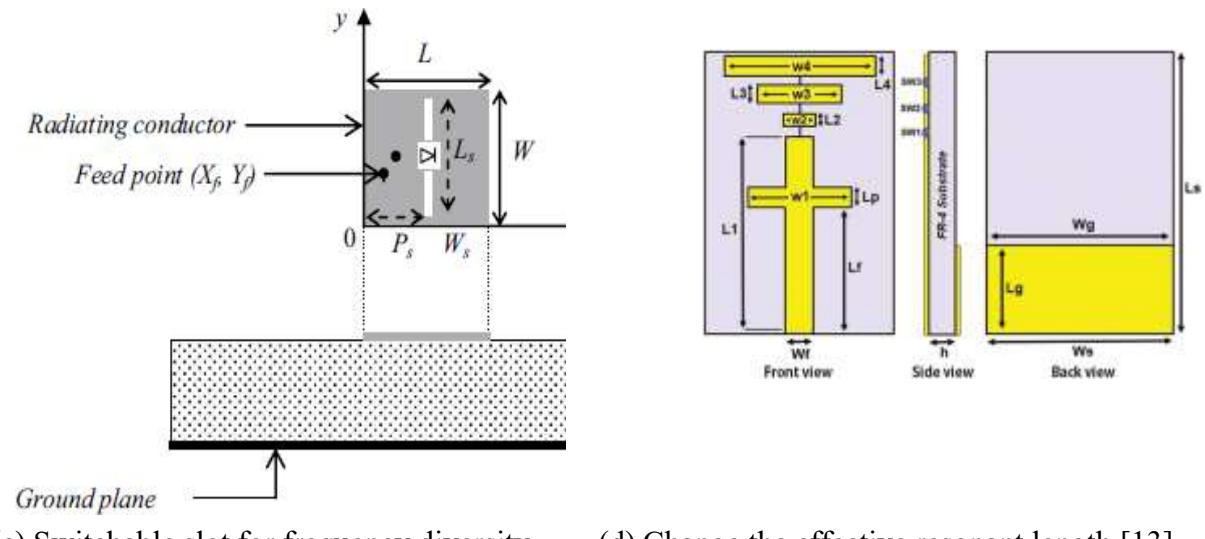
Fig 2.3. Methods to achieve frequency reconfiguration

The methods for frequency reconfiguration discussed up to this point require additional RF components. However, without additional components, the frequency reconfiguration can be achieved through mechanically changing slots as reported in [16]. By changing the dielectric properties of the substrate frequency reconfiguration is obtained in ref [17].



(a) Redistribute the surface current [9]





- (c) Switchable slot for frequency diversity [12]
- (d) Change the effective resonant length [13]

Fig. 2.4 Various designs of frequency reconfigurable antennas in existing open literature

## 2.2.2 Pattern Reconfigurable Antennas

In a pattern reconfigurable antenna, the radiation pattern direction of the antenna changes dynamically by modifying the aperture field on the radiating surface without changing the antenna's physical size. This property of the antenna can minimize the interference of the signal and improve the transmission by directing the maximum gain towards the right direction. The simple pattern reconfiguration independent of frequency by changing the status of the diode is shown in Fig. 2.5.

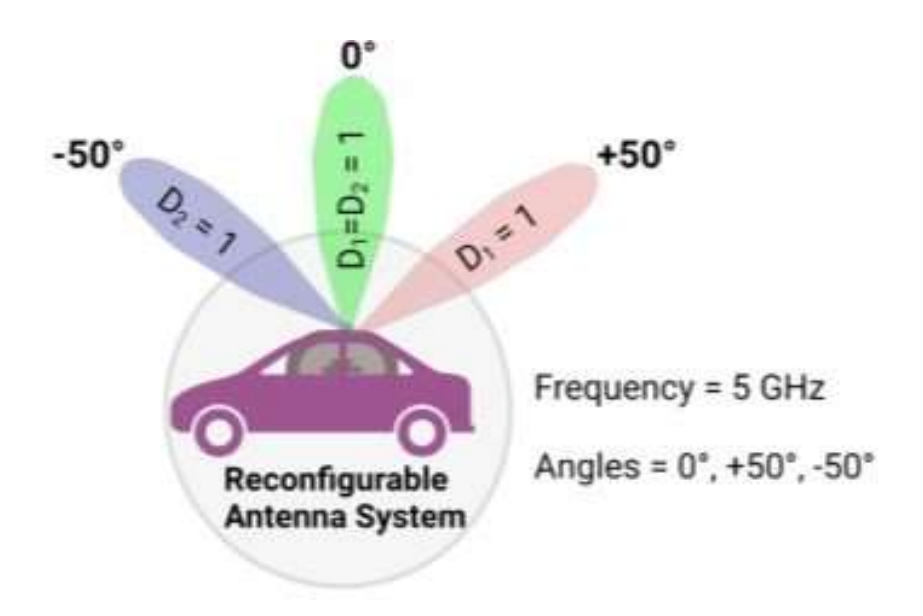


Fig.2.5 Pattern reconfiguration for various states of PIN diode [18]

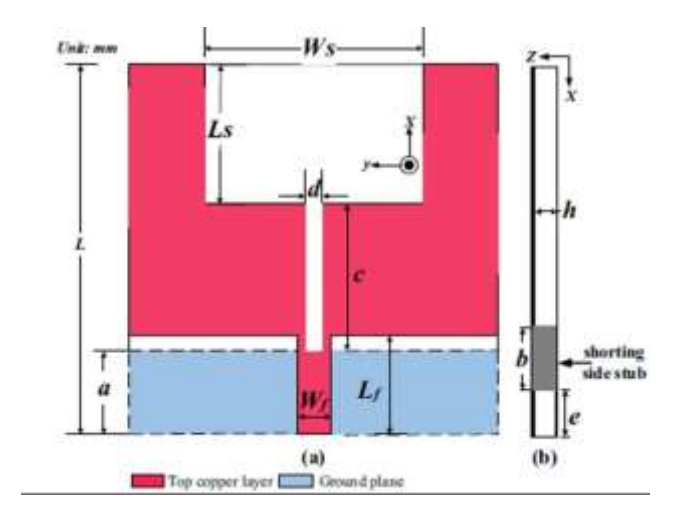
The various methods are shown in Fig. 2.6 to achieve the pattern reconfiguration. In [19], authors reported a comprehensive review on the reconfigurability of antenna structures in terms of radiation pattern reconfigurable for upcoming 5G new radio frequency bands.

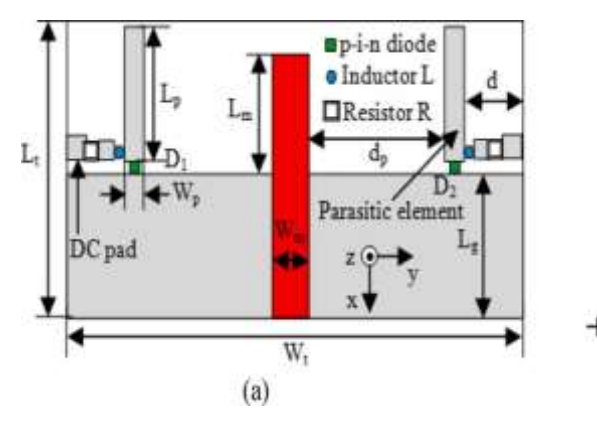
An omnidirectional to directional radiation pattern tilting is achieved through the shorting side stub from the slotted stepped monopole to the ground plane for the ISM band (2.45 GHz) in ref [20]. For sub 6 GHz IoT applications, a four-state pattern tilting reconfigurable antenna was reported in ref [21], based on the Yagi-Uda principle. It has two parasitic stubs on the ground plane, and these stubs act as a director or reflector. Pattern reconfigurable antenna for Wi-Fi applications based on electromagnetic complementary Huygens's principle is reported in [22], [23]. The top plane consists of a mushroom structure acting as an electric dipole, and the bottom plane consists of a slot-loaded shorted patch to improve the bandwidth acting as a slot-magnet dipole. By switching the feed excitation for different radiating elements, pattern reconfiguration is achieved from omnidirectional to directional in ref [24].

The reconfigurable antennas were reported in [25], [26] changes its mode of operation from monopole to Vivaldi, by switching the feed path through PIN diodes. The bias voltage of PIN diode controlled the radiation pattern. In, ref [27], a mushroom-shaped reflector is placed around the modified T-shaped split ring resonators to tilt the radiation patterns for sub-6 GHz applications. Some of the pattern reconfigurable antennas that existin the existing open literature based on different methods are mentioned in Fig. 2.6.

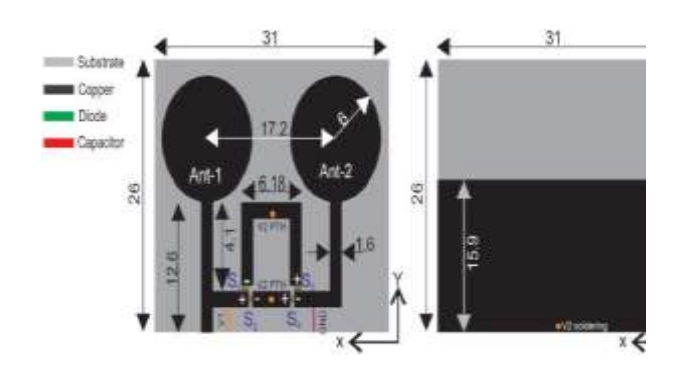


Fig.2.6 Different methods to achieve pattern reconfigurable antenna



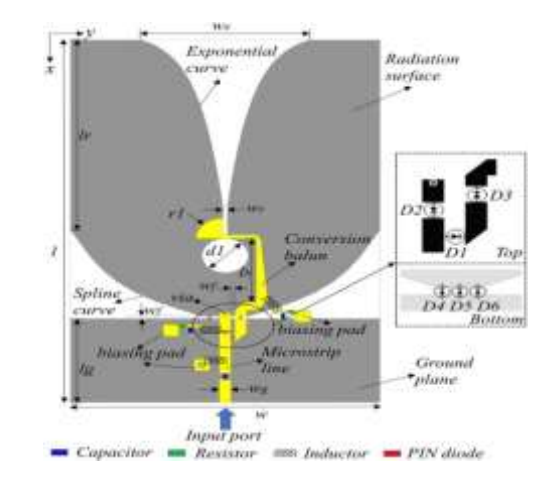


(a) Pattern reconfigurable antenna based on shorting side stub [20]



(c) Loading electronic switching elements to change the currents [24]

(b) Based on Yagi-Uda principle [21]



(d) Choose various feeding networks [25]

Fig 2.7. Various designs of pattern reconfigurable antennas in existing open literature

# 2.2.3 Polarization Reconfigurable Antennas

To reduce the multipath fading and interference the polarization reconfigurable antennas suitable. With the help of switching techniques these antennas have ability to flip from linear to circular polarization or vice versa. Further, the circular polarization flips from left hand circular polarization to right hand circular polarization. The basic methods to obtain the polarization reconfiguration in the antenna are implementing slots, slits, parasitic structures and truncated the corners on the main radiator with active elements. The application of polarization reconfigurable antennas in satellite communication is shown in Fig. 2.8.



Fig .2.8 A Polarization Reconfigurable Antenna for Satellite application [28]

The methods to achieve polarization reconfigurable are shown in Fig. 2.9. using asymmetrical U-shaped slots on the radiating elements a dual band circularly polarized reconfigurable antenna was proposed in [29]. The most popular method with single microstrip feed to obtained the polarization is truncated corners of the main radiator [30], [31]. In ref [32] circularly polarized reconfigurable was proposed based on the polarization conversion meta-surface by kept the below monopole radiator.

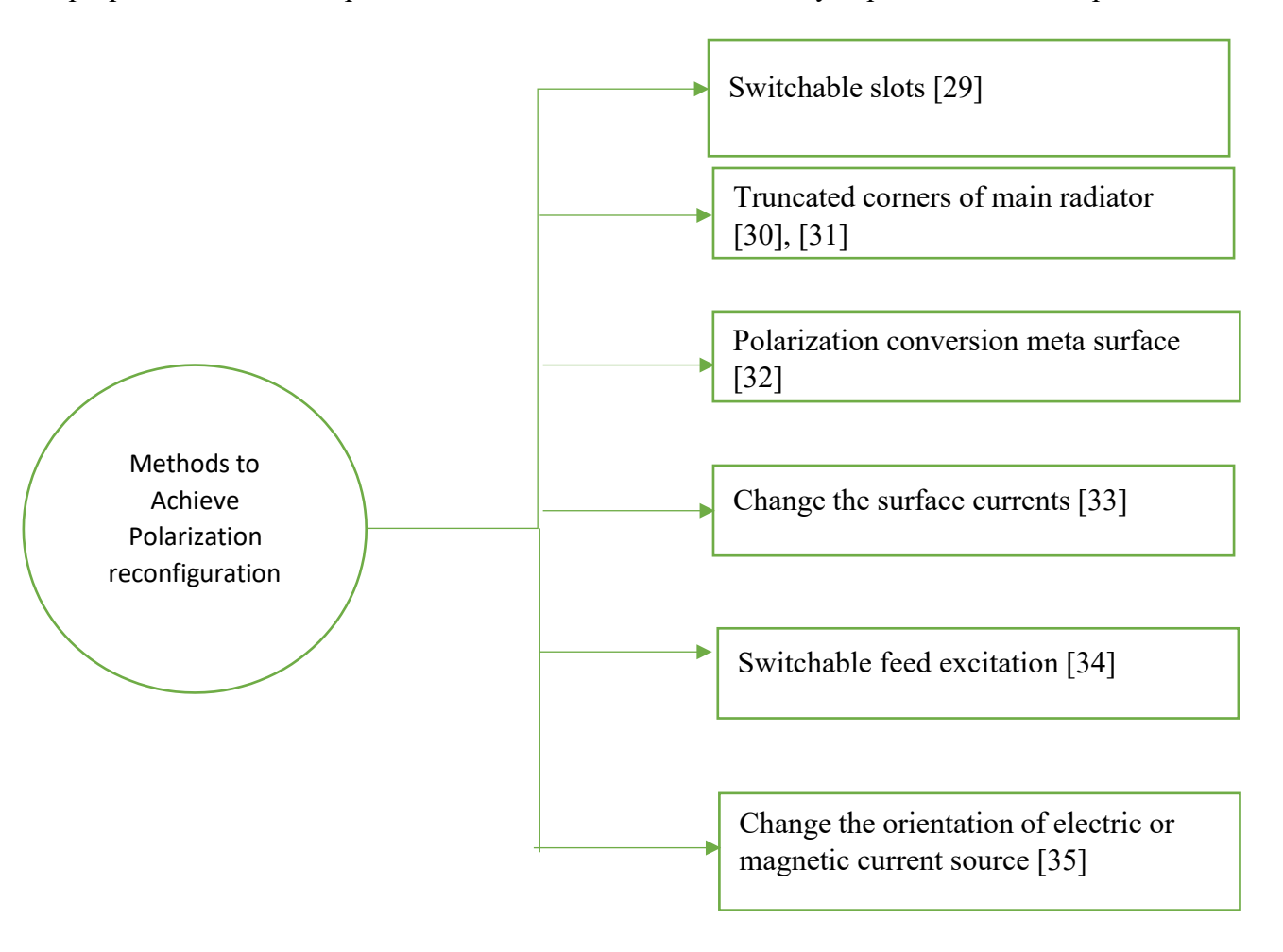


Fig.2.9. Methods to obtain the polarization in reconfigurable antenna

A circularly polarized monopole reconfigurable antenna was reported in ref [33] by creating the horizonal surface currents on the ground plane through rectangular strips. The various polarized reconfigurable antennas are shown in the Fig.2.10. Adopting meta-surfaces, switchable feeds [34] and reconfigurable external polarizers or phase shifters in the radiating structure changes the surface current through electric and magnetic current sources [35].

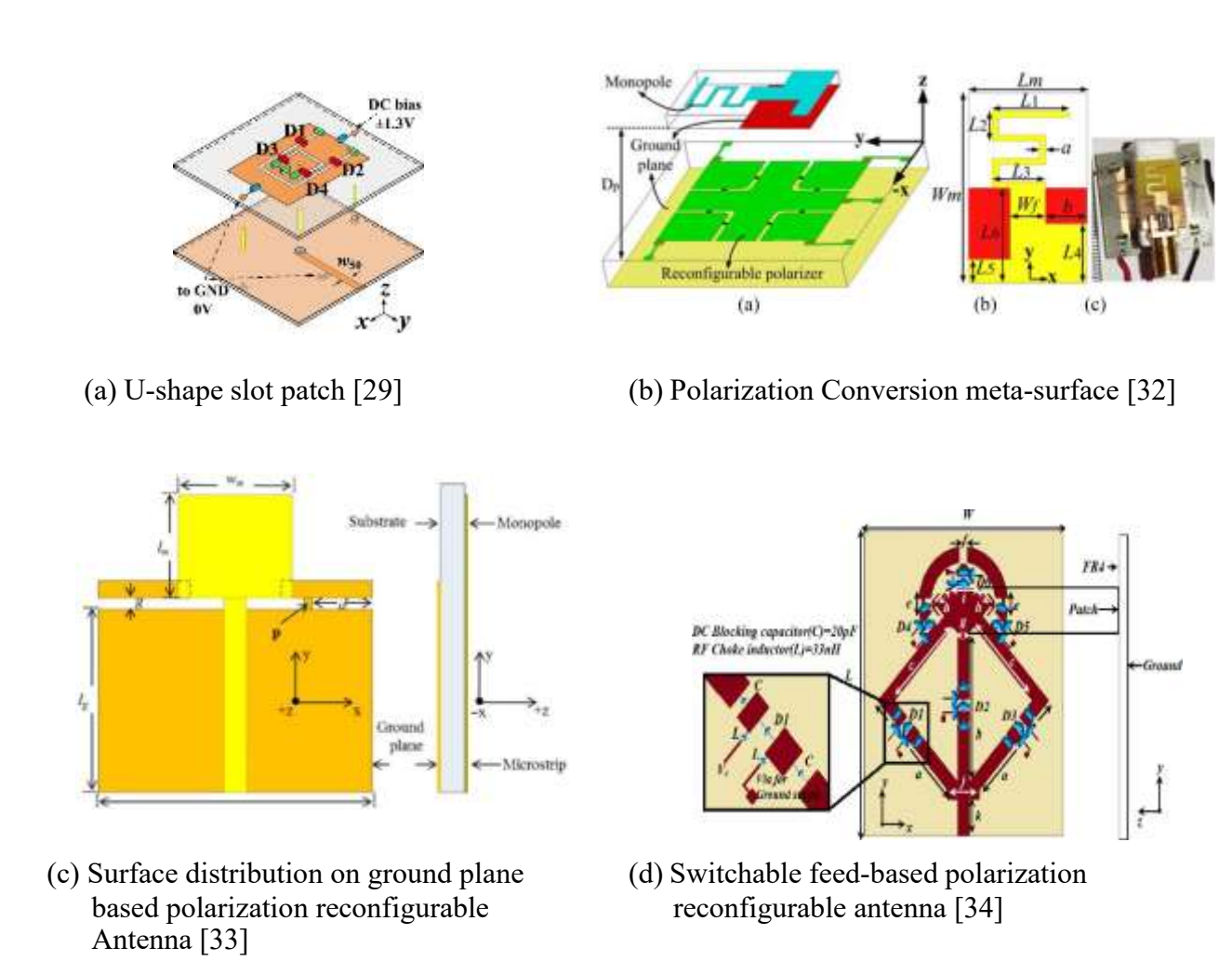


Fig 2.10. Various designs of polarization reconfigurable antennas in existing open literatures

# 2.2.4 Hybrid Reconfigurable Antennas

In this section, the combination of the above-discussed reconfigurable antennas is explored. The characteristics of an antenna such as frequency, pattern and polarization are depending each other. By reconfiguring one characteristic may affect the other characteristics of an antenna in such situations designing a compound reconfigurable antenna is a crucial task. However, the researchers are implementing new techniques to achieve the compound reconfiguration with minimal effects on antenna characteristics.

The various types of compound/ hybrid reconfigurable antennas are shown in the Fig 2.11.

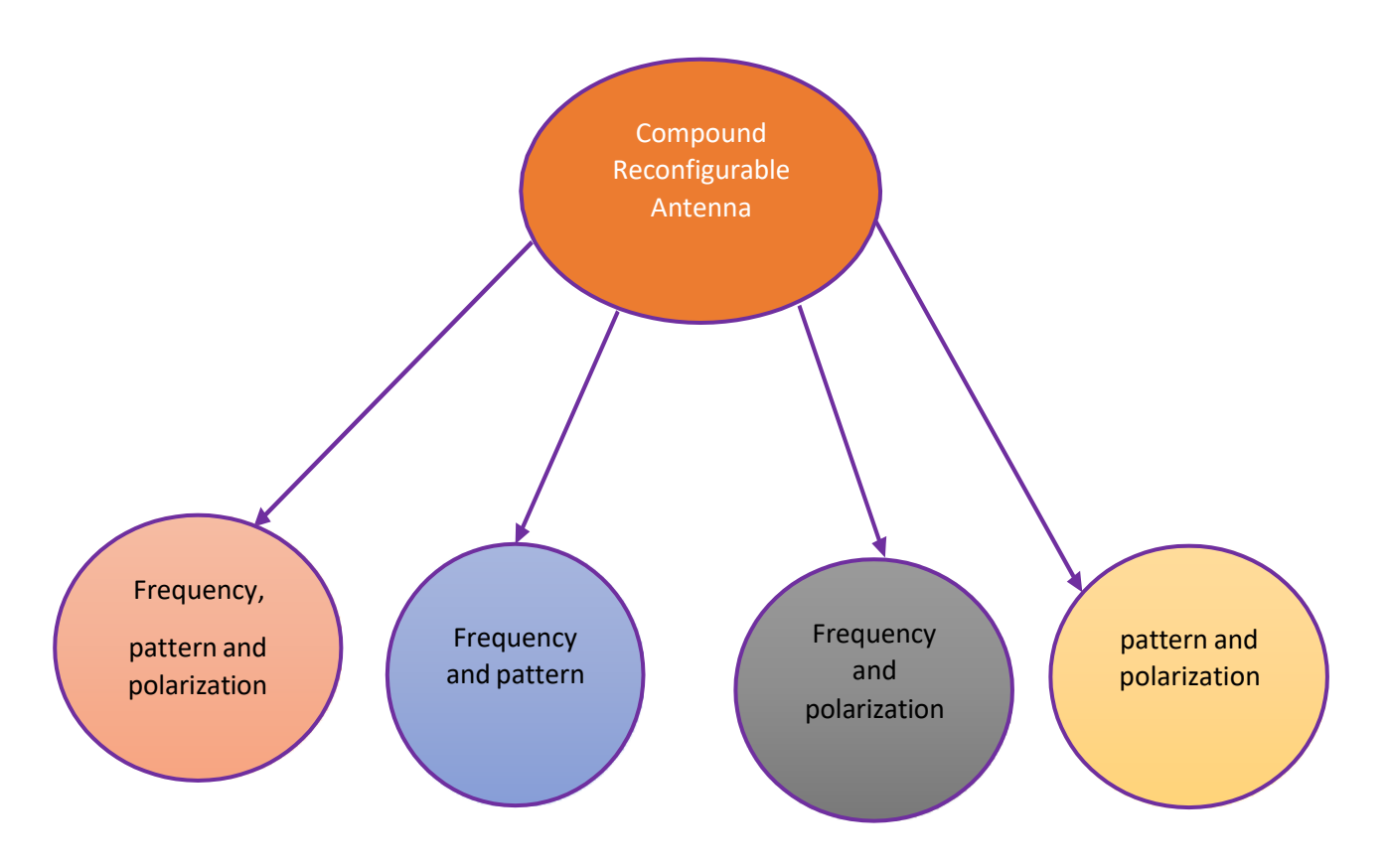


Fig 2.11. Types of hybrid/compound reconfigurable antennas

As discussed in previous sections, integrating several methods to achieve reconfiguration in terms of frequency, pattern and polarization in a single radiating structure is useful to designing compound reconfiguration. However, such design must be done carefully. Active elements such as varactors and PIN diodes are primarily used traditional method for frequency switching operations in antenna design. Concepts like slotting and slitting configurations of the antenna ground plane are used to achieve pattern reconfiguration, which corresponds to a change in the surface current distribution of the antenna radiating element, thereby using switchable directors at different sizes of the main antenna radiator provides features like steerability of radiation pattern. Polarization reconfigurable antenna can be achieved through switchable feed network or truncated corners of the main radiator. Fig 2.12 shows the different compound reconfigurableantennas. A simple frequency and pattern reconfigurable antenna were proposed in ref. [29]. For frequency reconfiguration, the resonant length and geometry of radiating structure is changed and toobtain the pattern tilting a Yagi-Uda principle is utilized independently. A single feed frequency and polarization reconfigurable antenna was proposed [30] for frequency reconfiguration, switchable slots are used and for polarization reconfiguration switchable truncated corners are used.

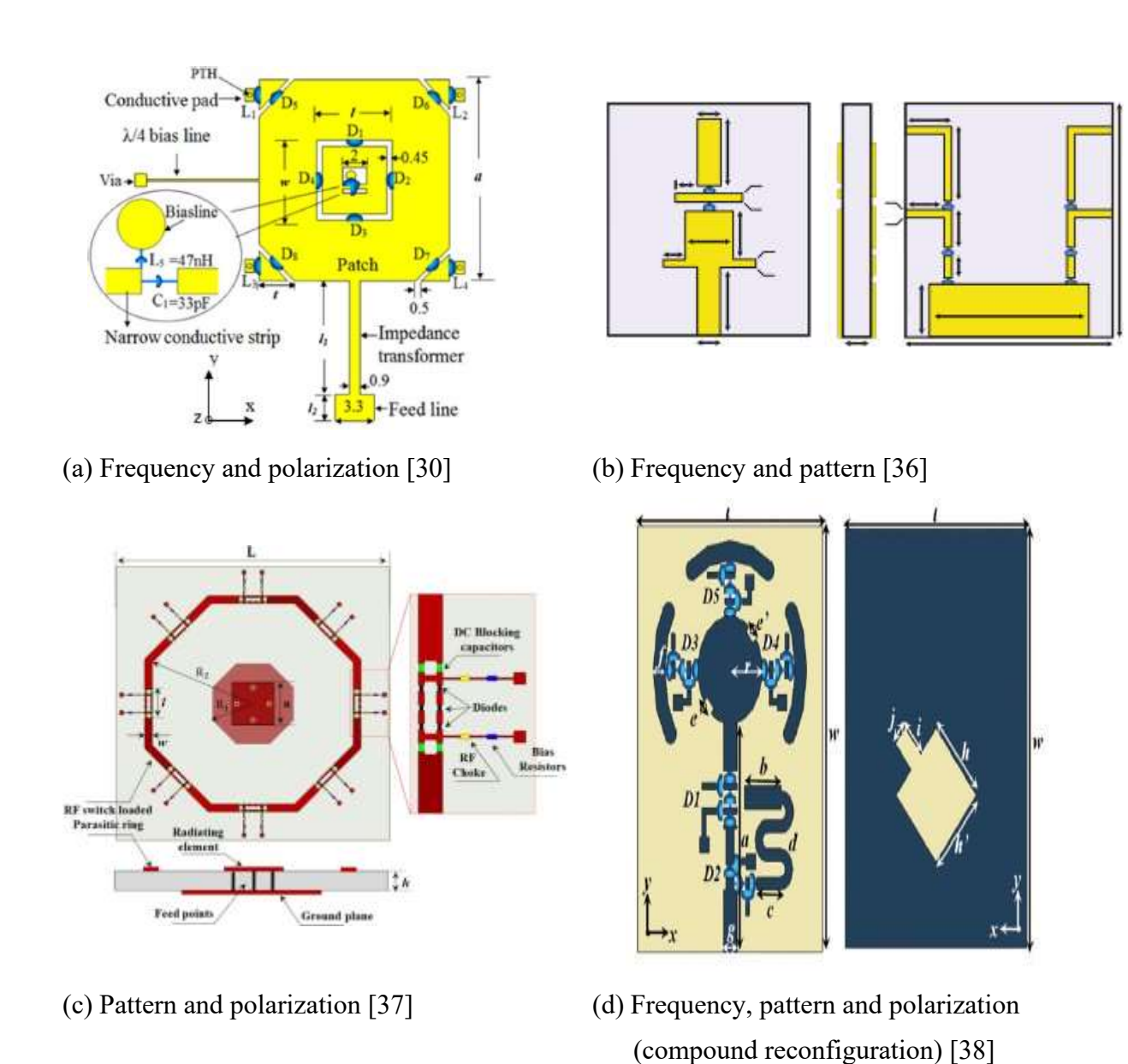


Fig.2.12 Various compound/hybrid reconfigurable antennas existing in open literature

A pattern and polarization reconfigurable antenna was reported in [37] by implementing the quad coaxial feed to the radiator to obtain the polarization and for pattern octangle shaped parasitic rings are connected through the RF switches. Parasitic stubs on either side of the main radiator on the ground plane are used forpattern tilting and frequency reconfigurability; different lengths of patches are used in ref [38] and did not achieve multiband operation with pattern tilting.

# 2.3 Reconfiguration Techniques

The reconfiguration techniques to achieve the required reconfiguration are mainly categorized into four types, as represented in Fig.2.13

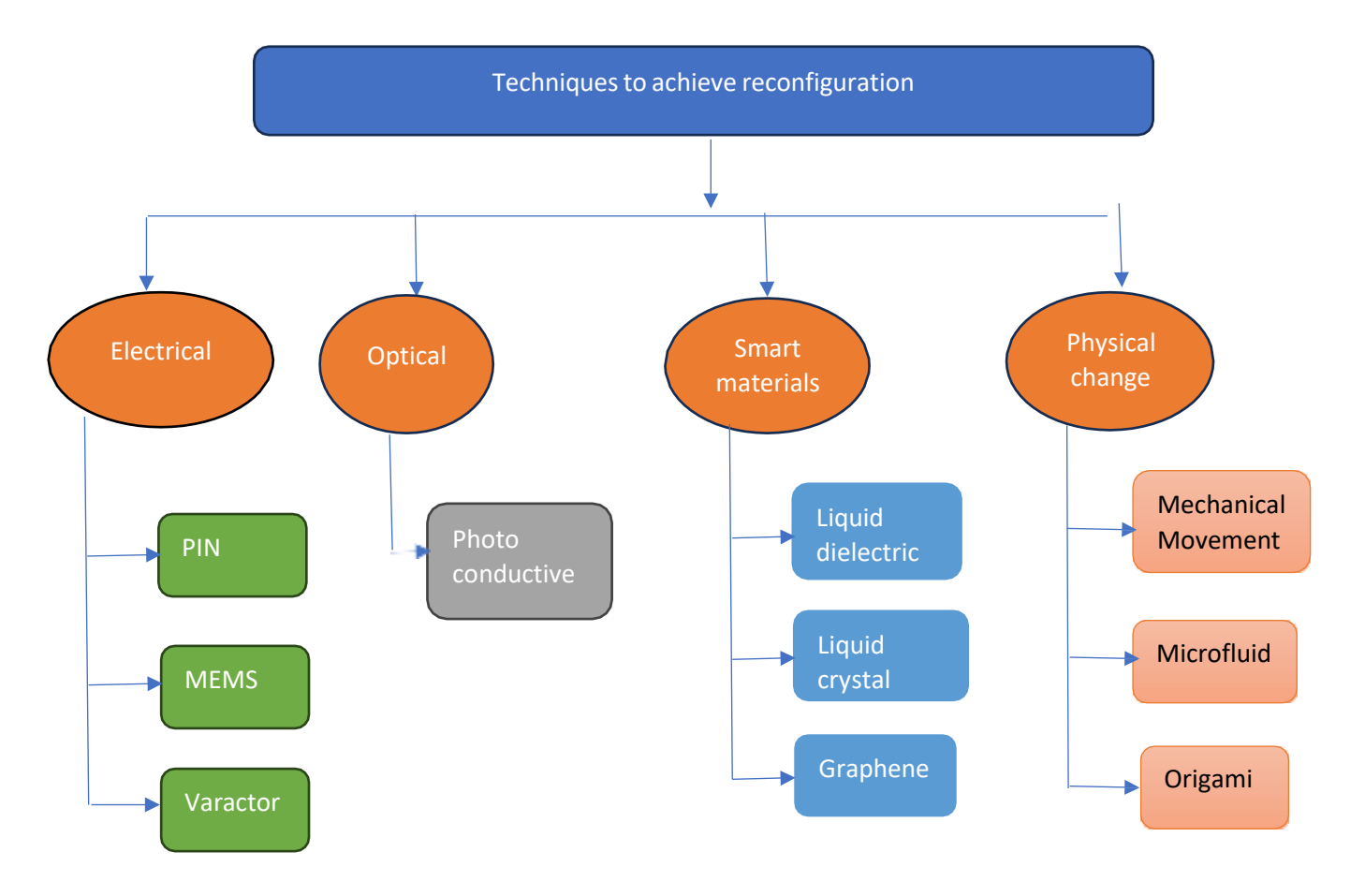


Fig.2.13. Techniques to achieve reconfiguration in reconfigurable antenna

Under the electrical switching techniques, the antenna reconfiguration is achieved by connecting and disconnecting various parts of the radiating element through PIN diodes, MEMS, for discrete switching and continuous switching through varactors. In optical switching, the reconfiguration is achieved by connecting and disconnecting the radiating elements through external light excitation, for external light, a photodiode can be used. The electrical and optical switching techniques require the bias circuit for their operation. In the next category, reconfiguration is achieved through innovative materials such as liquid crystals, dielectrics, and graphene. If the dielectric property is changed from these materials, it affects the antenna performance and achieves the desired reconfiguration. In this technique, biasing is not required for its operation, however, structure fabrication complexities can be increased.

In the physical structure change reconfiguration technique, the required performance is achieved by modifying an antenna's physical dimensions. For example, micromotor can modify the geometry of an antenna by moving its components

### 2.3.1 Details of reconfiguration through PIN diode

The PIN diodes are the most suitable RF switches for reconfiguration since they have a fast response and require low DC values for their excitation. A PIN diode at RF frequencies behaves as an open and closed circuit at respective insert positions, thus modifying the resonant behavior of the radiating element through capacitive and inductive effects.

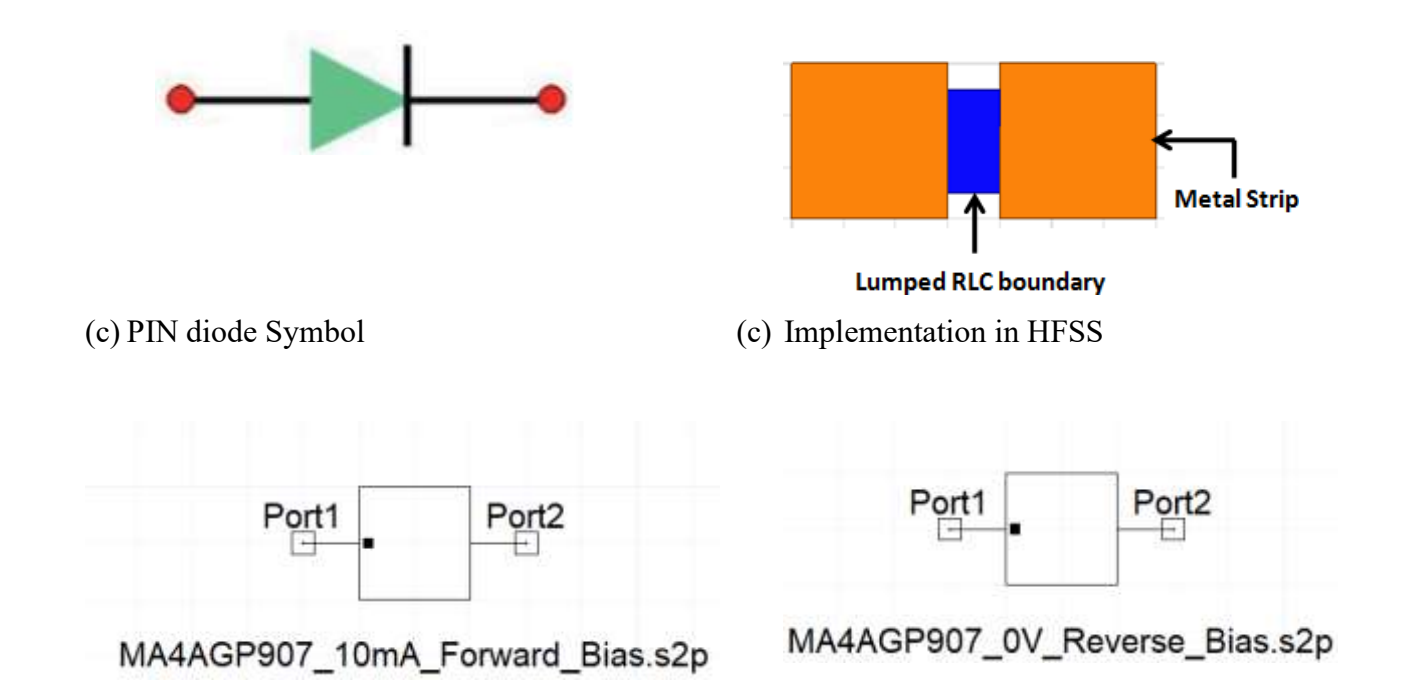
Basically, the impedance of the PIN diode at RF and UHF frequencies controlled by applying the DC excitation in forward bias and reverse bias. Its construction has heavily doped P type and N-type regions and a high resistivity intrinsic I-region is sandwiched between these two regions. When the diode is forward biased the charge carriers such as electrons from N-type region and holes from P-type region are injected into the intrinsic region and not recombine immediately after the injection in the I-region takes time referred as carrier life time, this results an average charge is stored which lower the forward effective resistance of I-region. Therefore, in forward bias the PIN diode is represented as an equivalent resistance value as shown in the Fig. 2.14 (a). In the reverse bias, the charge is not stored in the intrinsic region and the diode equivalent circuit represents as a capacitor parallel with the resistor, as shown in Fig 2.14 (b). The various models of PIN diode and equivalent lumped values are listed inthe ref [2].

The equivalent lumped circuit models are implemented in the simulations for respective PIN diodes. These values are not constant over the entire operating frequencies causes deviations from measured results. To overcome this, instead of lumped value direct S2P files from their data sheet are incorporated in the simulations to get better results. For example, in this thesis MADP-000907-14020 P PIN diode used for achieving the reconfiguration and its ON and OFF state S2P circuit representations [39] are shown in the Fig 2.14 (e &f) respectively.

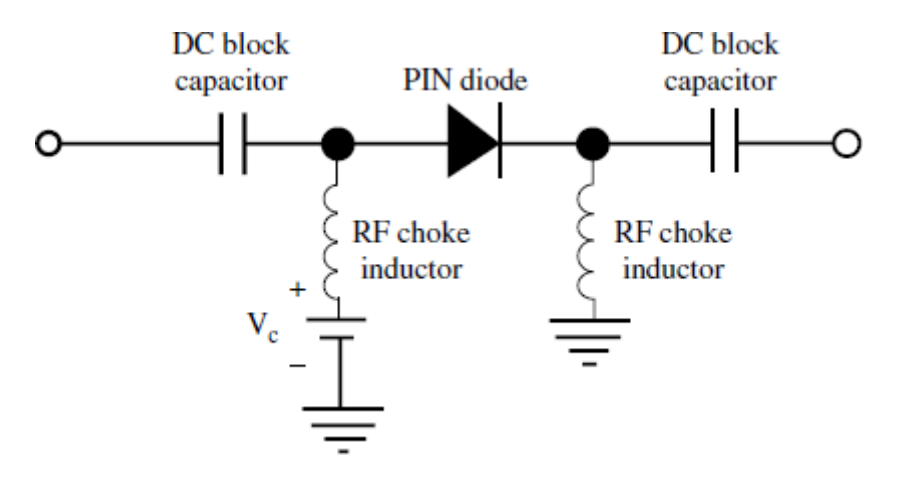


(a) ON state equivalent lumped element

(b) OFF state equivalent lumped element



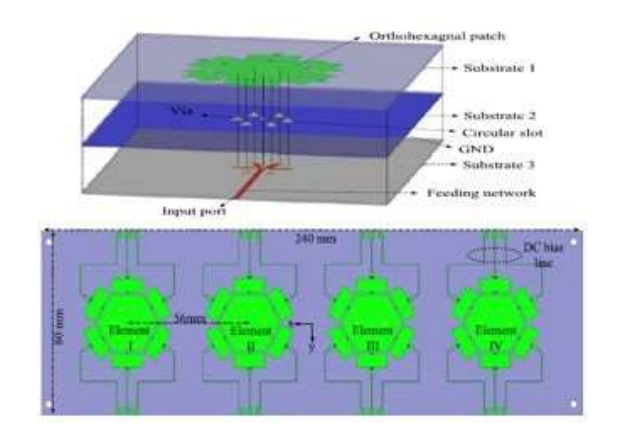
- (d) ON state S2P file symbol of PIN diode
- (e) OFF state S2P file symbol of PIN diode



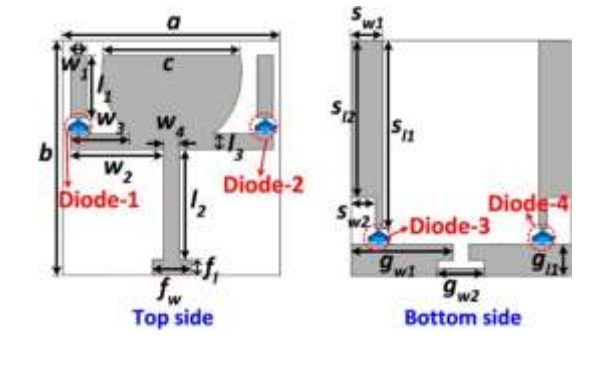
(f) A typical Biasing circuit of PIN diode [40]

Fig 2.14. Equivalent model of PIN diode and its implementation in HFSS

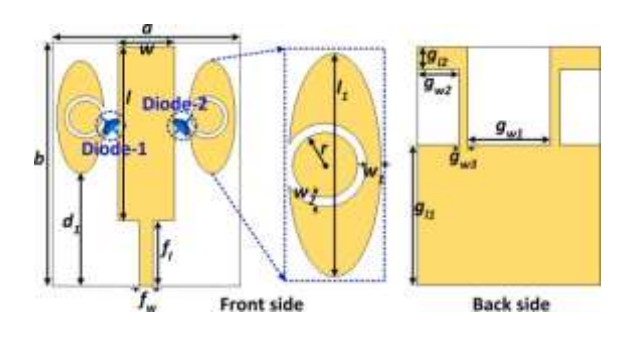
The recent reconfigurable antennas based on PIN diodes are represented in Fig.2.15.



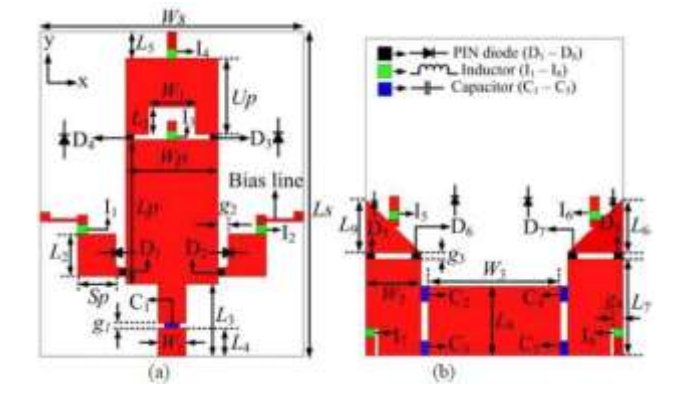
(a) Compound reconfigurable antenna array [41]



(b) Low-profile hybrid reconfigurable antenna [42]



(c) Pattern reconfigurable antenna [43]



(d) Monopole hybrid reconfigurable antenna [44]

Fig 2.15. Compound reconfigurable antennas through PIN diodes

A 1x4 compound reconfigurable antenna array was proposed in [41] by using PIN diodes through multilayer radiating elements. Based on Yagi-Uda principle a frequency and pattern reconfigurable was reported in [43]. In which, a simple rectangular shape antenna is acts as main radiator and two oval-shaped patches besides of main radiator acts as an either reflector or director based on the RF switch status. The structure is symmetry with respect to feed to maintain the parameters are stable. A simple compoundreconfigurable antenna with dual-band reconfigurable CP is reported in [44] with an AR bandwidth of 7.1% and 15.9 % at 3.6 GHz and 5.5 GHz, respectively by utilizing eight PIN diodes with pattern tilting in the range of  $\pm 30^{\circ}$ , but the structure has complex operating states with a lower peak gain andlow efficiency

### 2.3.2 Reconfiguration through RF MEMS

RF MEMS switches have superior characteristics over semiconductor-based switches and are also easily integrated into flexible and rigid substrates to meet the specific performance characteristics [45], [46], [47]. Therefore, MEMS switches can be utilized to design reconfigurable antennas, which can be attached and detached directly to the radiating structure, ground plane, and parasitic stubs. The schematic view of RF MEMS and its equivalent lumped elements are shown in Fig. 2.16.

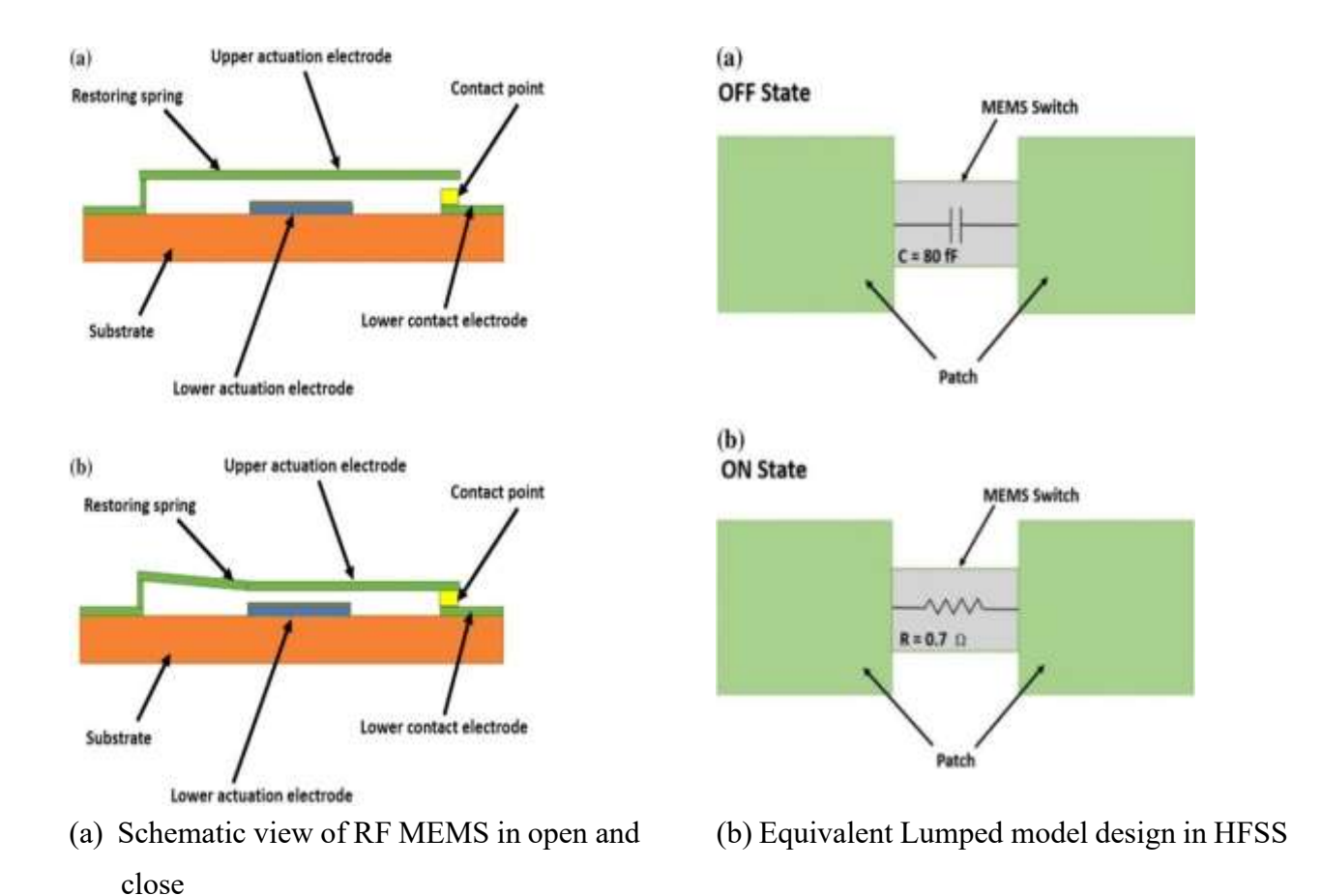
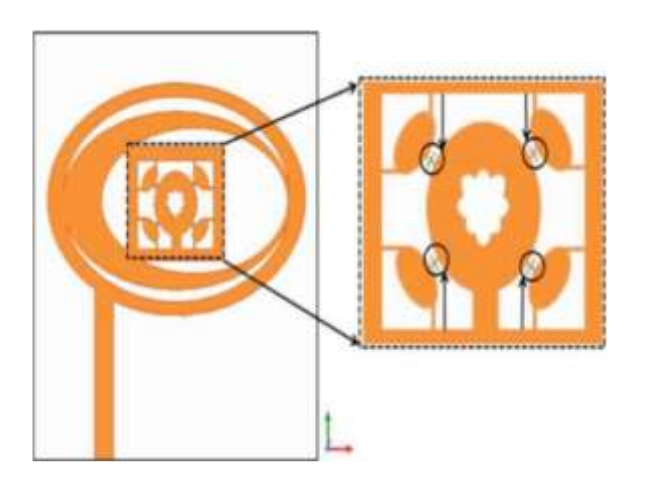
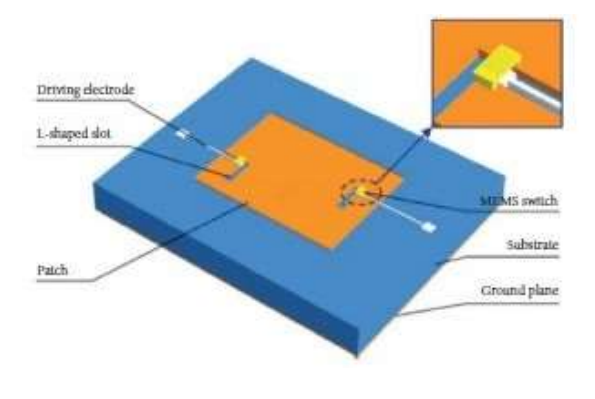


Fig. 2.16. The schematic view of RF MEMS and its equivalent lumped elements [45]

Ref [48] proposed a MEMS switch-based L-slot frequency reconfigurable U-band antenna capable of four tuning states. In which, by controlling the MEMS switch status in the L-shaped slot frequency reconfiguration is obtained by changing the effective resonant length. A shunt capacitive MEMS switches are incorporated into the elliptical-shaped radiating structure to obtain the frequency reconfiguration [49].





(a) Elliptical shaped frequency reconfigurable antenna [49]

(b) L-shaped slot frequency reconfigurable
Antenna [48]

Fig. 2.17. Reconfigurable antennas based on RF MEMS switch

Except for PIN diodes, which regulate the circuit's ON/OFF state, MEMS switches can be integrated with novel materials and rigid/flexible substrates. Additionally, while designing performance-reconfigurable antennas, the kind and positioning of MEMS switches are pretty important. However, MEMS switches' structural complexity and high-intensity field characteristics limit their application in the low-power consumption market.

### 2.3.3 Reconfigurable Antennas Based on Varactor Diodes.

Varactor diodes, as opposed to PIN diodes, can constantly modify the capacitance values through changes in their reverse bias voltages. A varactor diode or variable capacitor is an electrical device made from a typical PN junction that functions as a variable capacitor at different reverse bias voltages. Materials of the N and P types are stacked together to form the varactor's structure. The capacitance of the junction is reduced when the breadth of a varactor's depletion region increases nonlinearly with the square root of the applied reverse voltage. Figure 2.18 displays the varactor diode's lumped equivalent circuit.

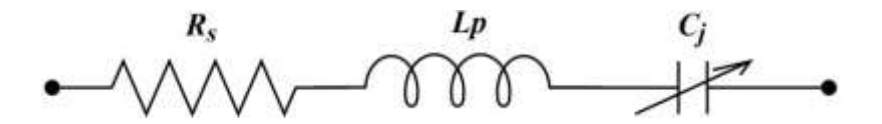
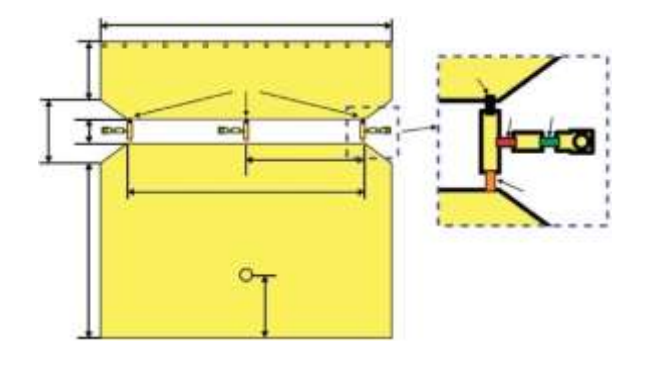


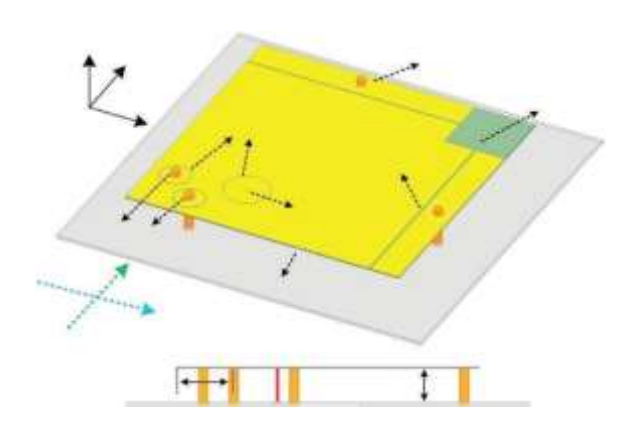
Fig 2.18. Equivalent circuit of varactor diode

Varactor diodes are typically modeled as lumped components in RLC series in antenna design [50], [51]. Reconfigurable antenna design is made possible by precisely tuning antennas by adjusting their capacitance value, which also changes the circuit current value [52]. Typical varactor diode-based

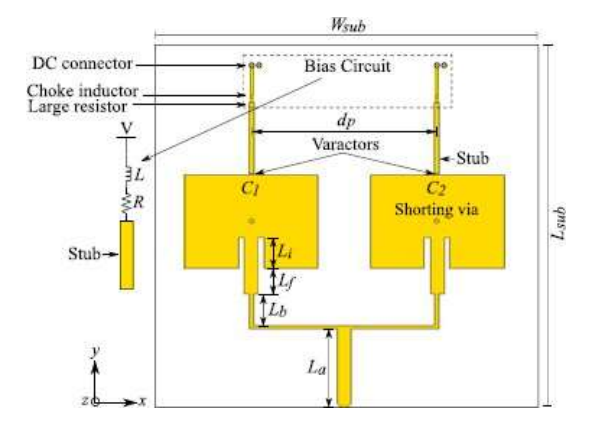
reconfigurable antennas are depicted in Figure 2.19. Varactor diode placement frequently requires careful consideration because of the changing capacitance.



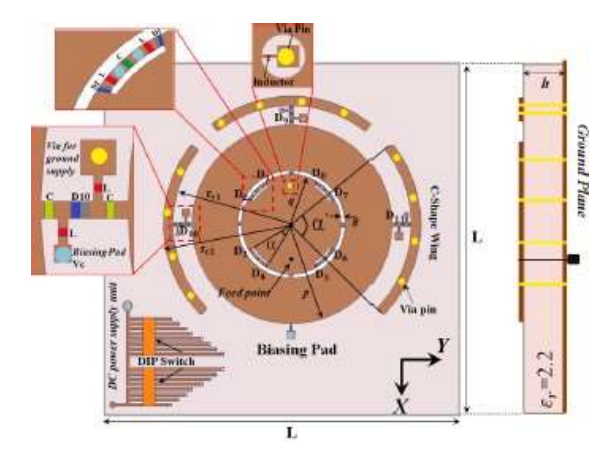
(a) Tuning range frequency reconfigurable antenna [53]



(b) Capacitance loaded polarization reconfigurable antenna [54]



(c) Frequency and pattern reconfigurable antenna [55]



(d) Compound reconfiguration through varactor diode [56]

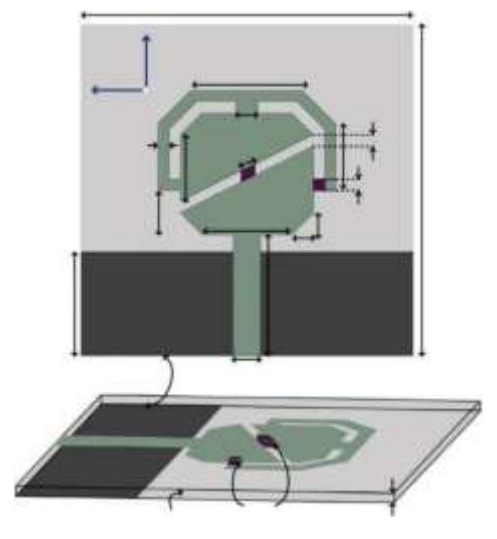
Fig 2.19 Reconfigurable antennas based on varactor diode

Three tuning range extension options for varactor-based frequency-reconfigurable planar patches were proposed in [53]. These strategies included reducing parasitic capacitance, using various radiation modes, and co-optimizing antenna dimensions and varactor attributes. A miniature circularly polarized capacitance-loaded patch antenna with a straightforward design and frequency reconfigurability was proposed in [54], as seen in Fig.2.18 (b). In contrast to the traditional half-wavelength patch antenna, it doesn't need a vast ground plane because of its cavity-like structure. Capacitive loading significantly reduces the antenna size, and adding two varactor diodes to adjust the quadrature radiation gap results in frequency reconfigurability. However, there is a trade-off regarding gain or bandwidth due to the smaller design. It's also important to note how many varactor diodes are used. Specifically, more varactor diodes will result in a more complex antenna structure,

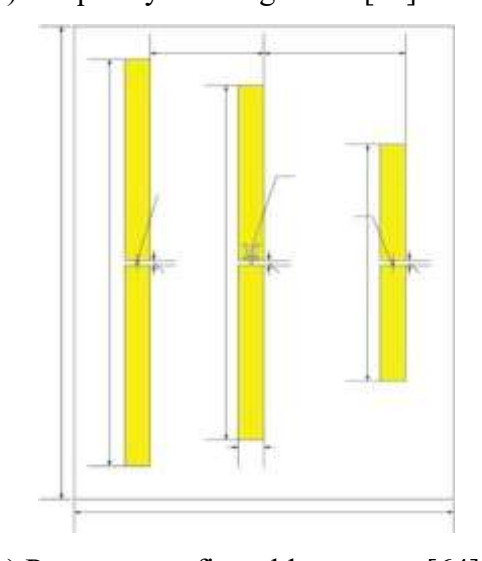
whereas fewer varactor diodes will cause increased cross-polarization. Ref [56] presents a compound reconfigurable antenna using varactor diodes for S-band applications. In which, the frequency reconfiguration is achieved by varying the capacitance of varactor diode with proper biasing voltages and to obtain the pattern and polarization an arc shaped and C-shaped parasitic stubs are connected to the main circle shaped radiator. Due to their ability to continually alter capacitance by varying their reverse bias voltages, varactor diodes are used mainly in designing frequency reconfigurable antennas. The benefits of varactor diodes, electronic components, and antenna design should be combined in other performance reconfigurations. Based on varactor diodes with proper biasing a frequency and pattern reconfigurable antenna was proposed in [57]. The structure consists of parasitic stubs for pattern tilting from 0° to 360° in steps of 25.7° and multilayer structures for frequency reconfiguration with a large number of varactor diodes. Miniaturization is achieved through the dispersion feature by applying the periodic slow wave structure [58], and the frequency is reconfigured from 4.87 to 5.52 GHz by varying the varactor diode bias voltage from 9 to 16 volts.

### 2.3.4 Optical switches based reconfigurable antennas

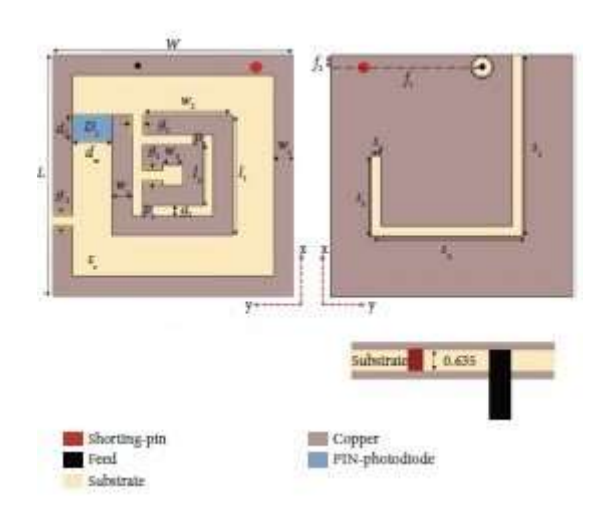
Light is used by optical switches, such as photodiodes, to regulate when the circuit is connected or disconnected. In contrast to other non-optical switches, it may be remotely controlled to alter the radiation components' circuit connect status, enabling antenna performance reconfiguration [59]. Additionally, they have the benefits of quick reaction times and no parasitic radiation, which won't interfere with the functioning of the antenna [60]. These reconfigurable antennas are typically used for specific application scenarios [61]. Several common reconfigurable antennas with photodiodes are depicted in Fig.2.20. Like PIN diodes, optical switches usually have two states: ON and OFF. The optical switches are modeled as an inductor connected in series with a parallel resistor and capacitor, and they are initially reverse-biased and in the OFF state. Nevertheless, the state can be changed to the ON state when the optical switches are exposed to infrared light, and the circuit model that corresponds to this is made up of resistors and inductors connected in series. In ref [62], specific operating frequency range. Using a split ring resonator, a frequency and pattern reconfigurable antenna was reported in [63] with coaxial feed obtained good impedance matching.



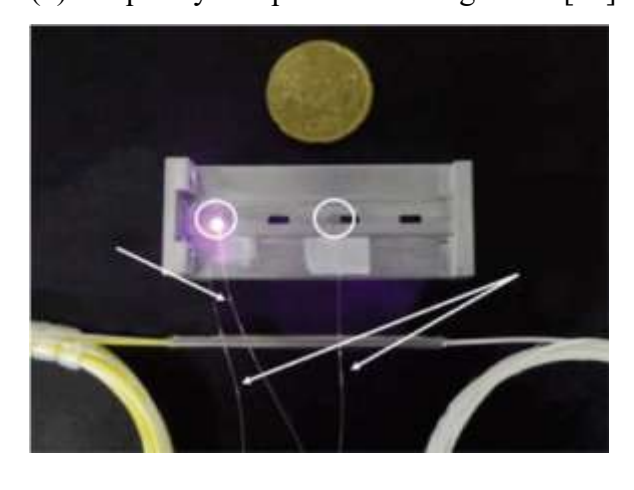
(a) Frequency reconfigurable [62]



(c) Pattern reconfigurable antenna [64]



(b) Frequency and pattern reconfigurable [63]



(d) Pattern and frequency reconfigurable antenna array [65]

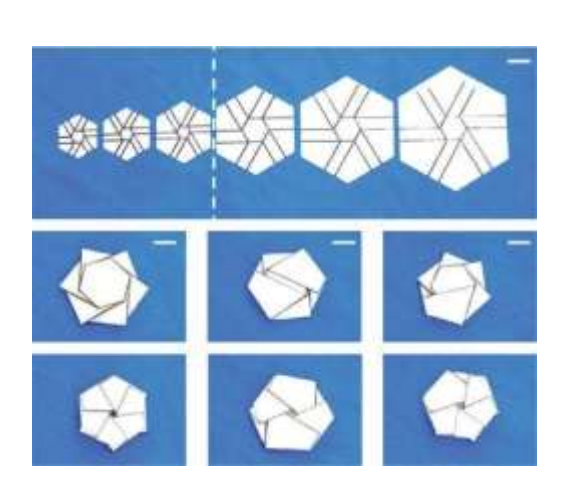
Fig. 2.20 Optical switches-based reconfigurable antennas

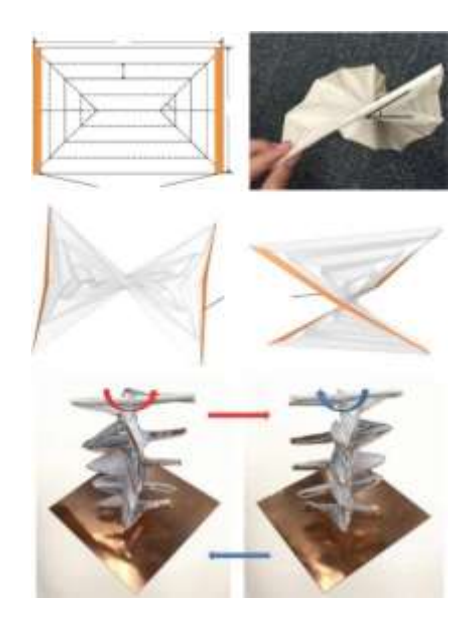
A Yagi-Uda principle-based pattern reconfigurable antenna was proposed in [64] using a photoconductive RF switch. Using light, a frequency and pattern reconfigurable slotted waveguide antenna array, changing the effective length, was reported in [65].

# 2.3.5 Reconfigurable Antennas Based on Structure Physical Change

Bias circuits and optical environments, like electrical switches, are unnecessary for structural changes. Based on structural physical changes, reconfigurable antennas may offer continuous tuning, reduced loss, and high-power handling capacity. Additionally, they typically depend on the antenna structure's or other components' physical movement, primarily the fold [66], rotation [67], and flow [68]. Origami antennas require folding paper sheets for the substrate and copper 3mm for the radiation conductor, in contrast to conventional antennas [69]. Origami's fascinating qualities of self-foldability,

multi-stability, and programmable curvature and collapse have led to widespread use in developing deployable and reconfigurable engineering systems in recent years. Firstly, antennas' effective height or length can be altered by folding and unfolding 3D origami geometry. Reconfigurable antennas based on mechanical movement with the advantages of agility and inexpensive cost have been developed by utilizing actuators or manual devices [70] [71] The reconfiguration is achieved by rotating or moving [72] the relative position of the antenna parts, such as the substrate, ground, and feed port radiation patch. Figure 2.21 shows serval typical reconfigurable antennas based on mechanical movement.





- (a) Hexagon twisted frequency reconfigurable antenna [73]
- (b) Polarization reconfigurable antenna [35]

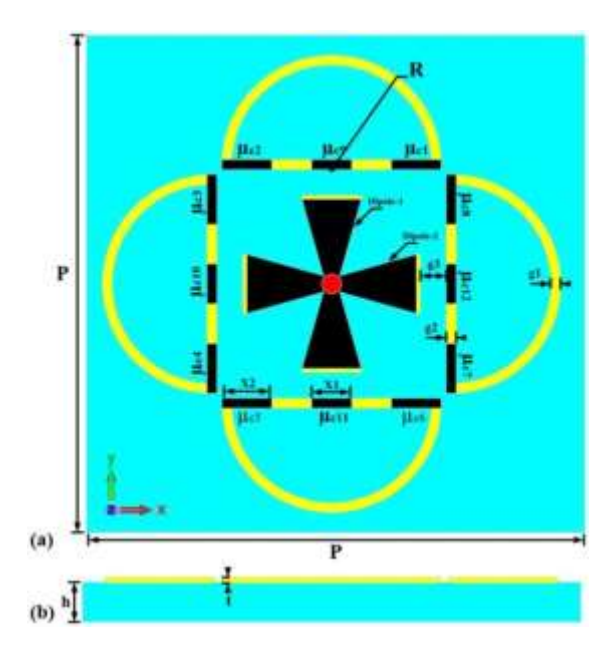
Fig.2.21 Reconfigurable antennas based on physical structure changes

A twisted hexagon-shaped frequency reconfigurable antenna was reported [73] based on an effective height change method, which obtained a better impedance match and was limited to the omnidirectional pattern. By changing the orientation of electric and magnetic current sources, a parasitic patch array polarized reconfigurable antenna with good circular polarization was reported in [35].

### 2.3.6 Reconfigurable Antennas Based on Smart Materials

Recently, the use of innovative materials has become a new trend in the design of reconfigurable antennas, such as liquid dielectrics, graphene, and SMAs, which can change the dielectric orgeometric properties of the antenna by changing their physical or chemical characteristics, thus achieving the desired reconfiguration of antenna performance. "Smart" materials use external factors like temperature and voltage to alter their physical size or characteristics. A common material for

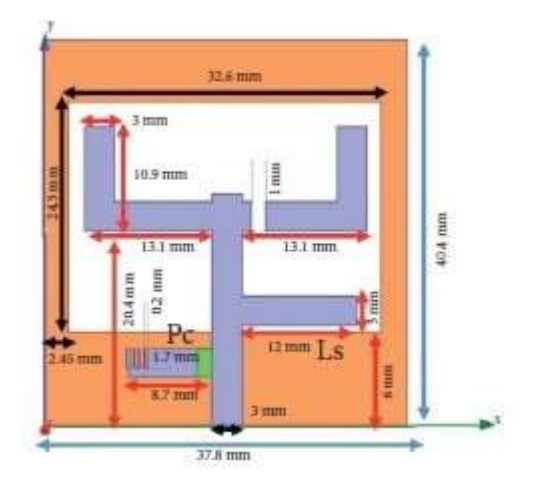
antenna substrates is liquid crystal, which can be thermally or physically altered to change its characteristics and enable frequency tunability. The radiating element can also be altered with specialized materials like liquid crystals for frequency and pattern reconfigurability. Smart materialbased reconfigurable antennas are a new type of antenna technology that uses cutting-edge material science to modify antenna performance. Flexible antenna designs are made possible using innovative materials, which allow for the reconstruction and modification of antenna characteristics, including size, shape, and dielectric constant by particular needs [74] [75]. Microfluidics are frequently utilized to reshape the antennas and accomplish antenna performance reconfiguration, such as the radiator or parasitic element of antennas [76] or to fill the channel [77]. A promising opportunity for creating a reconfigurable antenna is also presented by the liquid metal EGaIn alloy [78], a typical microfluidics material with numerous innovative features, including excellent conductivity, good fluidity, and nontoxicity. Furthermore, innovative materials may react to external stimuli, including light, magnetic, and electric fields. This enables the control of antennas' electromagnetic parameters, such as frequency, radiation pattern, and polarization. Reconfigurable antennas can be designed using a variety of innovative materials, such as phase-change material [79], liquid dielectric [80], [81], metallic micromesh [82], graphene [83], liquid crystals [84], and SMA [85], as illustrated in Fig.2.22. To effectively couple their resonances and lower the necessary magnetic biasing for reconfiguration, a frequency-reconfigurable antenna is constructed using the magnetic metamaterial integrated into the ferrite-embedded substrate. Reconfigurable antenna design versatility has increased with the quick development of cutting-edge materials like liquid dielectric, graphene, and shape memory alloy (SMA). These materials, like liquid crystals under voltage, can alter their permeability or permittivity in response to various external excitations. By implementing the channels in the substrate and filling with distilled water the permittivity of the substrate changes there after the E- field is changes in the antenna [86]. After studying different reconfiguration techniques, the importance of reconfigurable antennae is as follows. The citation [87] [88] lists the benefits and drawbacks of reconfiguration switching strategies. However, one of the most widely used methods "electrical reconfigurability" is implementing the previously stated categories of reconfigurability using electronic switches like PIN and varactor diodes. Over the past few years, academics have become interested in electrical reconfigurability because of its attractive characteristics, such as its low cost and simplicity of implementation. Varactors and PINs can enable reconfiguration at RF frequencies and change one or more antenna settings. Antennas have also been reconfigured using other reconfiguration methods. Photo-conductive switches, created when laser light strikes semiconductor material, are used in optical reconfiguration.

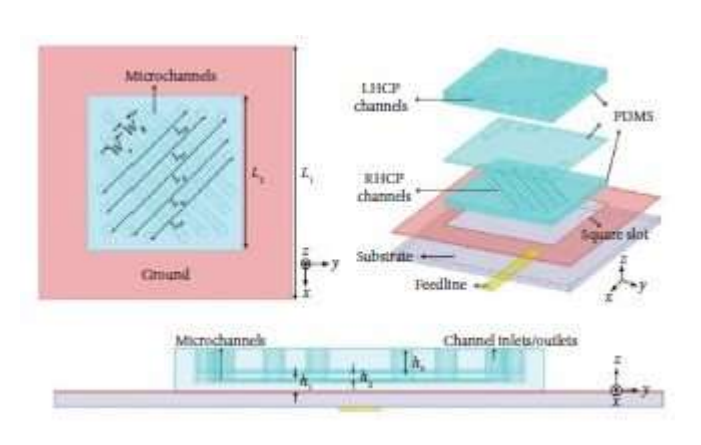


Channel 1 Channel 1 Channel 2 Channel 2 Channel 3 L, Monopole Microstrip Feed Line w (b) (a) Water filled channels Back cover  $L_{\varepsilon}$ L,

(a) Compound Reconfigurable Terahertz antenna Based on graphene [75]

(b) Frequency reconfigurable antenna based on water-filled channels [77]





(c) Polarization reconfigurable antenna [81]

(d) Frequency and polarization [86]

Fig.2.22 Smart materials-based reconfigurable antennas

Fast switching speeds can be achieved by embedding these switches, which do away with the necessity for metallic connections and biasing. However, sizeable optical power levels are used for laser light activation, particularly in highly resistive Si. Implementing physically or mechanically reconfigurable antennas involves manually modifying the antenna's construction to allow for reconfiguration. Instead of switching, this method uses motors, actuators, and other mechanical means to move components of the structure or alter its electrical characteristics. A typical example is a motor-based steerable reflector, like those found in radars. Although this mechanism is inexpensive, employing actuators and other tools necessitates high voltage, resulting in poor switching speed whiletaking up much space. A relatively recent method, smart antennas use materials like liquid metals,

water, and oil to implement reconfigurability. By pumping a fluid into a hollow beneath the design, one can modify the properties of the substrate, including electric permittivity and magnetic permeability, to adjust the parameters of an antenna. Although it can handle much power, this kind of reconfigurability has few uses because the materials employed are expensive, such as Galinstan, and some of them, like mercury, are known to be highly hazardous.

### 2.4 DC biasing analysis of MADP-000907-14020 PIN diode

The DC biasing of the PIN diode in a reconfigurable antenna is a crucial task. If proper biasing is not performed, the status of the diode is not changed, and the required reconfiguration property is not achieved successfully. A simple schematic of PIN diode biasing is shown in Fig.2.23 below.

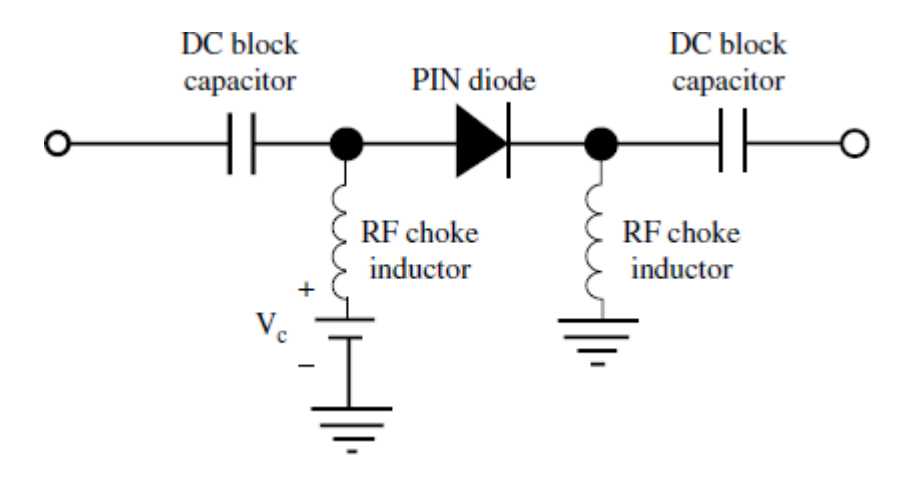


Fig. 2.23 PIN diode Biasing Circuit

The DC block capacitor blocks the DC value and allows the RF signal, and the RF choke inductor allows the DC value and blocks the RF signal. Proper values need to be choosen for biasing the PIN diode. Therefore, in this thesis, the MADP PIN diode from Macom company is used to design and analyze a reconfigurable antenna. The detailed analysis of the MADP PIN diode is evaluated in the ADS software, and the schematic is shown in Fig.2.24 below.

As per the datasheet of the PIN diode, the insertion, return, and isolation loss are validated by varying the DC blocking capacitor and RF choke inductor, as shown in Fig 2.25. After a thorough parametric study, the suitable values for proper biasing values are investigated as an RF choke inductor value of 100 nH and a DC blocking capacitor value of 1.2 nF, the return loss curve  $S_{11}(dB)$  and insertion curve  $S_{21}(dB)$  match the curves mentioned in the datasheet [39].

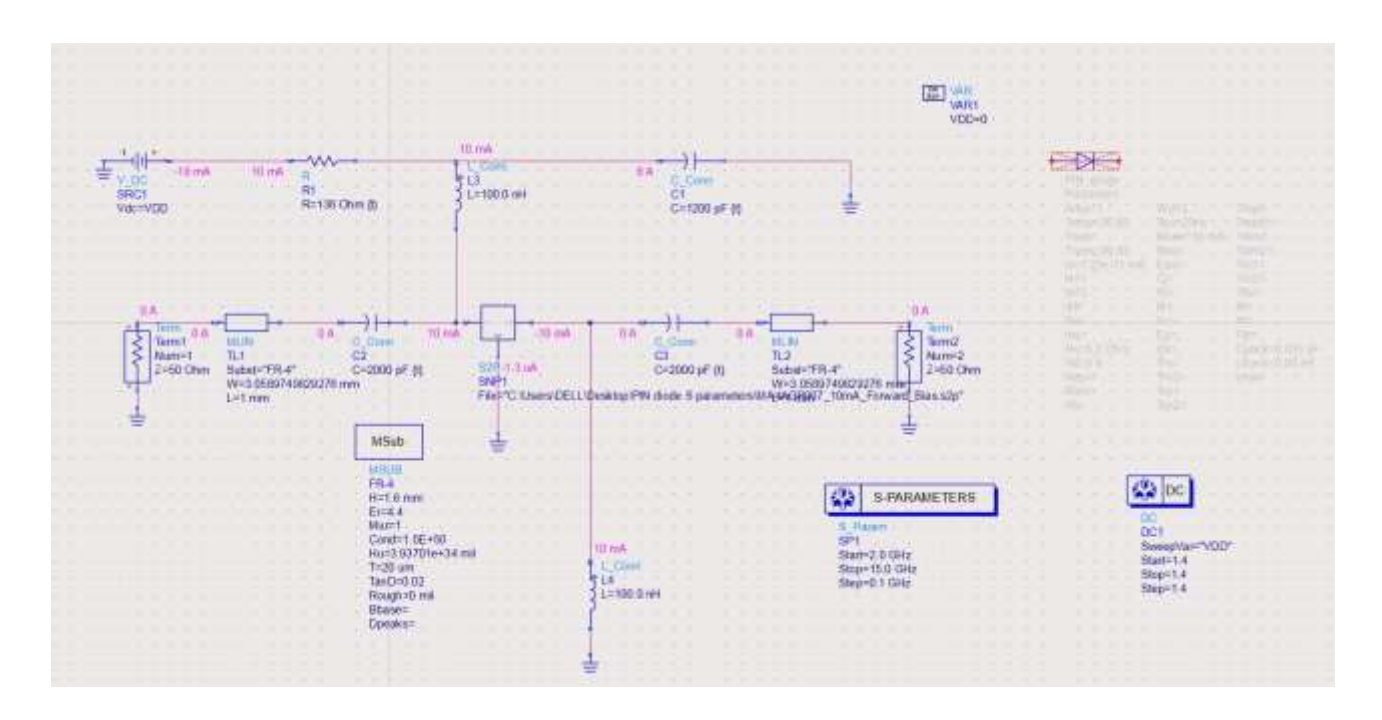


Fig.2.24. The implementation model of PIN diode biasing in ADS using S2P files

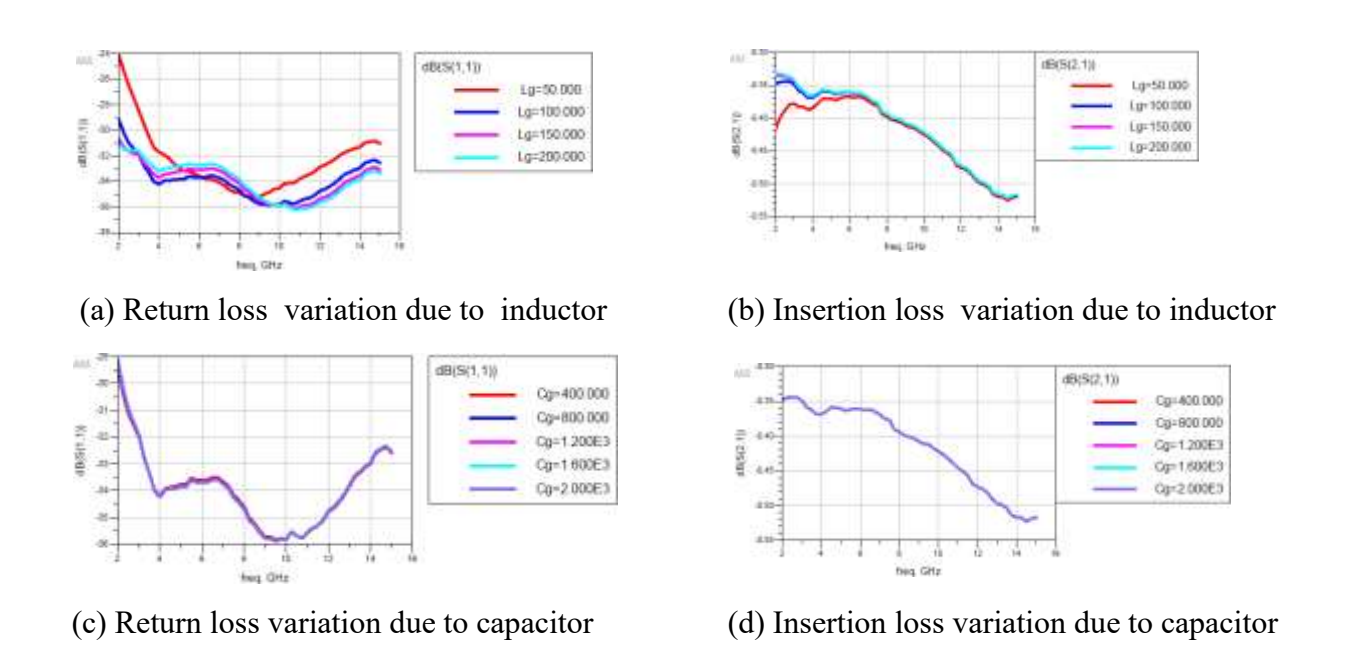


Fig.2.25 Parametric variations of blocking capacitor and RF choke inductor

### 2.5 Design Challenges for Reconfigurable Antennas

In modern wireless systems, the importance of reconfigurable antennas is increasing rapidly. However, a few design challenges need to be addressed.

➤ Design Complexity: For implementing more than one reconfigurable property, the complexity of the design increases due to a more significant number of RF components and radiating elements. This can lead to higher costs and unwanted losses

- ➤ Optimization of Parameters: Maintaining a balance between the antenna performance characteristics such as realized gain, impedance matching, and radiation stability is crucial for better performance. So, designers must consider suitable design processes to get the optimal results.
- > Selection of Suitable Material and Size: Most of the reconfigurable antenna's size and weight should be compact and small for smart modern wireless devices. This leads to a limit on material choices.
- > Switching Mechanism: The reconfiguration is achieved by connecting and disconnecting various radiation elements of the antenna via electrical and non-electrical switches. These introduce an additional challenge such as insertion loss, linearity, and power handling. These issues affect the overall performance of the antenna if not correctly managed.
- ➤ Environmental Adaptability: The performance characteristics of an antenna can decrease due to different environmental conditions, such as temperature, humidity, rain, snow, wind, mechanical vibration, proximity to objects, ground effects, antenna orientation, installation environment, etc. Since the antenna is tested in controlled environments such as anechoic chambers and in real-world scenarios, the performance of antennas can be affected due to multipath interference from other objects.
- ➤ Complexity in Fabrication and Prototyping: The microfabrication process and advanced innovative materials might be costly. The reconfigurable antennas can operate in different states or modes when changing the switches in different states or configurations, and each state or configuration needs validation. This raises the cost and duration of development.
- ➤ Control Algorithms and real-time adaptation: Advanced signal processing and adaptive algorithms are often required for real-time reconfiguration to maximize the antenna performance. This demands computational resources, which may not be readily available in all applications.
- ➤ Electromagnetic Interference (EMI) and Compatibility:

  With multiple configurations, the antenna may introduce additional EMI or be susceptible to surrounding EMI.

The strategies for addressing these challenges are as follows:

- Simplification Techniques
- ➤ Advanced simulation Tools
- > Innovative materials
- > Hybrid designs

### 2.6 Summary

This chapter thoroughly explains reconfigurable antennas, including how they are grouped, methods, and advancements made till date to achieve various reconfigurations. The second section involved a thorough analysis and discussion of specific frequencies, polarization, radiation patterns, and hybrid reconfigurable antennas documented in the literature. The performance of several agile localized elements has been compared, and the benefits and drawbacks of various reconfiguration strategies have also been covered.

The most common technique for modifying antenna characteristics is electrical reconfiguration, which uses active switches. On the other hand, despite their availability, optical switches are not as popular because of their complicated activation procedure and inherent loss. Although mechanical reconfiguration offers advantages, antennas of this type have limited flexibility and complex multipurpose adaptation. Applications in the terahertz frequency range are better suited for reconfiguration using active materials. Reconfigurable antennas with a single parameter perform exceptionally well. Multi-parameter reconfigurable antennas are becoming increasingly in demand as wireless communication technologies develop. These antennas provide compactness and adaptability for multipurpose communication systems by enabling the simultaneous reconfiguration of at least two of the three parameters.

#### **CHAPTER 3**

Design and analysis of frequency reconfigurable antennas for new C-band 5G networks and WLAN/Wi-Max applications

#### 3.1 Introduction

This thesis chapter aims to design and analyze frequency reconfigurable antennas with compact size and wideband operating at 3.8 GHz and 3.6 GHz for new C-band 5G networks and Wi-Max applications, respectively. It is achieved by implementing a hexagonal-shaped radiating element with a partial ground plane and a switchable slit on the ground plane. However, this design is limited to single-band operation. For better utilization of the frequency spectrum, further, a single and dual-band frequency reconfigurable antenna is designed by implementing a V-shaped slit on the radiating structure of the hexagonal-shaped microstrip antenna at a suitable position instead of the ground plane. This design achieves the dual-band based on the phase difference approach due to surface current modifications on the radiating structure. A MADP000907-14020 P PIN diode is placed at a suitable position on this slit and obtained dual-band, operating at 3.9 GHz and 6.37 GHz in the ON state of the PIN diode. In the OFF state of the PIN diode, a single band is obtained operating at 5.5 GHz for Wi-Fi applications with compact size and wideband operation. Compared to large and multiple bandsof an antenna, a frequency reconfigurable antenna is desired to perform effectively at the receiving end with a required frequency band by utilizing the frequency spectrum without disturbing other frequency bands.

The proposed radiating structures are designed and analyzed in the HFSS R.V23. Section 3.2 provides the design details and its mathematical analysis of the proposed radiating structures and simulated results with discussion are reported in section 3.3. Further, the single and dual-band frequency reconfigurable antenna design is reported in section 3.4, and its simulated results are discussed in section 3.5. Finally, a summary of proposed reconfigurable antennas is reported in the last section.

### 3.2 Design and analysis of hexagonal-shaped frequency reconfigurable antenna

With the rapid increase in data utilization of users, the Federal Communications Commission (FCC) recently allotted a new C-band for 5G networks in the year 2020, which will operate at a 3.7-3.98 GHz frequency band. The design of an antenna for these new communications has been accepted with admiringaccretion of interest. For the reconfigurability of the antenna in terms of frequency, a slotted microstrippatch radiating structure is the best candidate due to its wide tunning in frequency and convenience for switching between different frequency bands through RF switches across the slot [12]. Initially, a hexagonal-shaped monopole antenna is designed to operate at 3.8 GHz.

The resonant frequency (f<sub>r</sub>) of the circular shape of the radiator is calculated using the given eq. (3.1)

$$f_r = \frac{1.8412 \times C}{4\pi R_{eff} \sqrt{\varepsilon_r}} \tag{3.1}$$

Where C is the speed of light, and  $R_{eff}$  is the effective circular shape radiating element radius. The effective circular shape radiating element radius is evaluated using eq. (3.2)

$$R_{eff} = R_r \sqrt{1 + \frac{2h}{\pi \varepsilon_r R_r (ln(\frac{\pi R_r}{2h}) + 1.7726)}}$$
(3.2)

Where  $R_r$  is the radius of the circular-shaped microstrip patch antenna

Then, the side  $S_H$  of the hexagonal shape microstrip patch antenna value is calculated using eq. (3.3) utilizing the effective circular shape radiating element radius

$$\pi R_{eff}^2 = \frac{3\sqrt{3}}{2} S_H^2$$

$$S_H = \frac{\sqrt{2\pi} \times R_{eff}}{\sqrt{5.1962}}$$
(3.3)

For 3.8 GHz, the  $S_H$ =6.0652 mm i.e., side of hexagonal.

From the obtained side of a hexagon, its radius is calculated from [89].

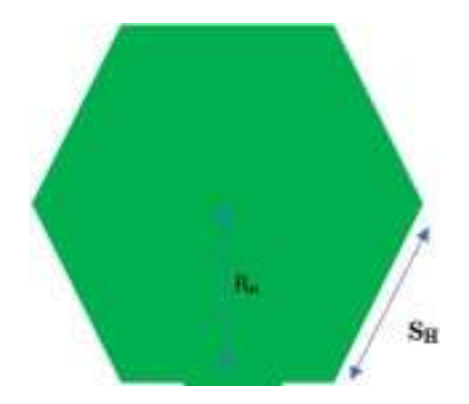


Fig.3.1 Hexagonal-shaped radiating element

With the hexagonal-shaped radiating element, a simple microstrip planar monopole antenna operating at 3.8 GHz is represented in Fig 3.2.

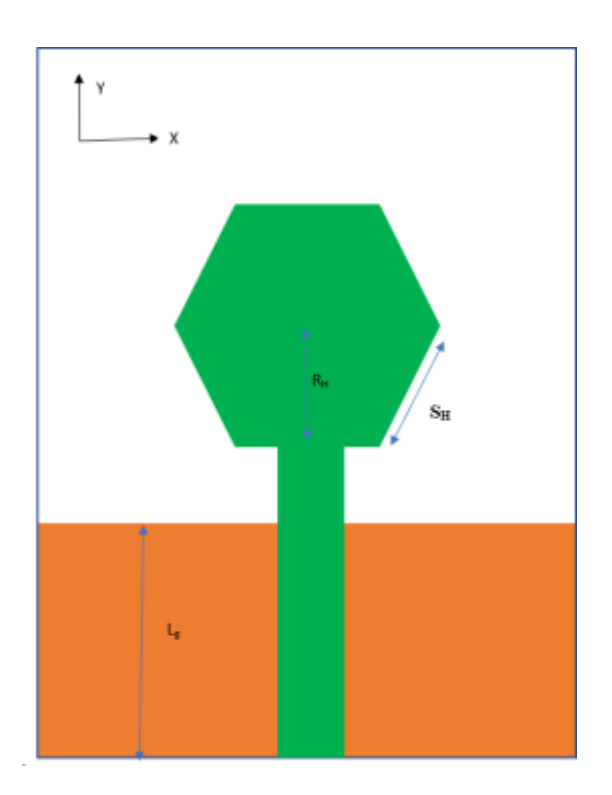


Fig 3.2 Simple planar hexagonal-shaped monopole antenna

In general, a microstrip antenna consists of the full ground plane, substrate, feed, and radiating element [1]. However, for obtaining wide bandwidth and operating as a monopole antenna, the groundplane and the feed length of the proposed structure are varied to obtain the operating frequency of 3.8GHz, as shown in Fig 3.3.

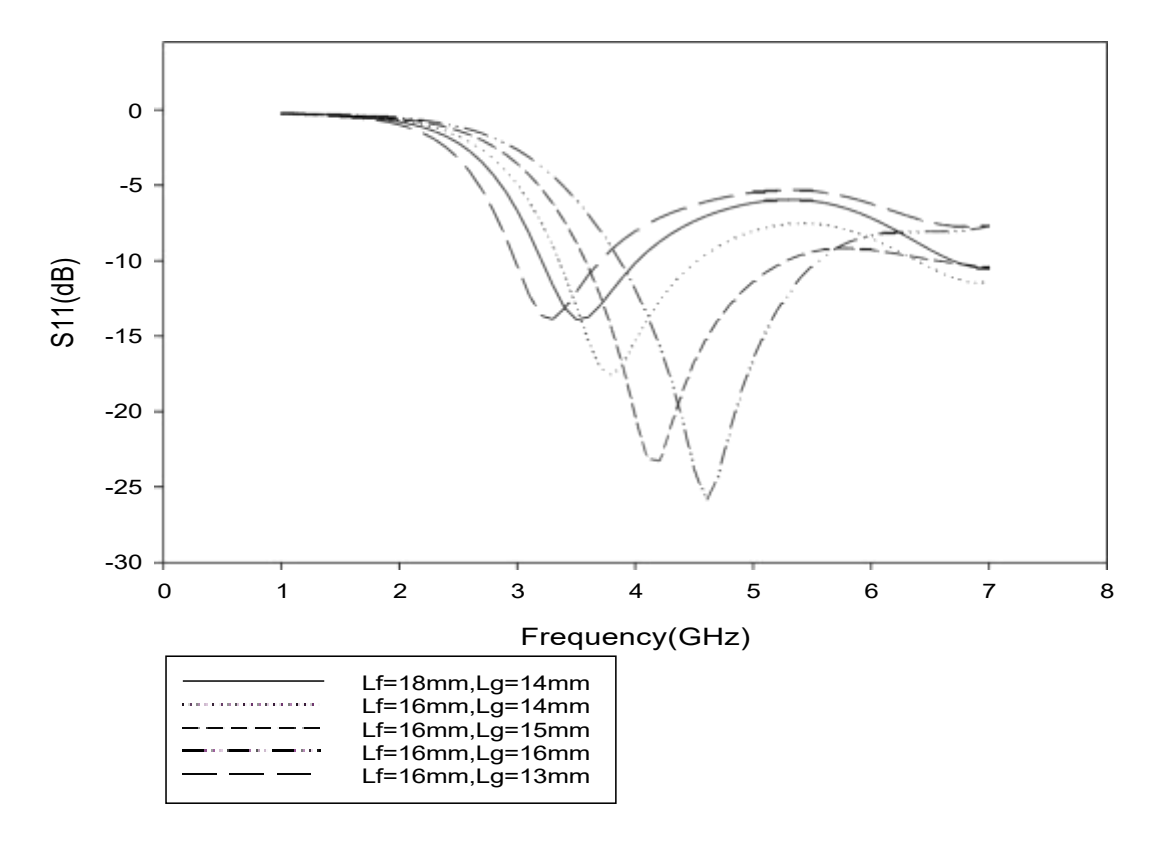


Fig 3.3 Parametric analysis of proposed frequency reconfigurable antenna

After varying ground length (Lg) and fed length (Lf), respectively, the better dip in the reflection coefficient is obtained for optimum values of Lg=14 mm and Lf=16 mm. However, for higher values of ground length better dip in reflection coefficient is obtained but not resonant required calculated frequency. Therefore, the values of Lg=14 mm and Lf=16 mm are considered in this proposed structure.

For introducing frequency reconfigurability in the proposed structure, a gap is created in the ground plane at a 12.5 mm position, and a PIN diode is adopted in this gap. The designed structure switches between two frequency bands by changing the PIN diode operating conditions, i.e., ON/OFF.

The PIN diode (MADP-000907-14020) from MACOM is utilized for switching purposes in this structure. A PIN diode at RF frequencies behaves as an open and closed circuit at respective insert positions, thus modifying the resonant behavior of the radiating element. The top and bottom views of the proposed frequency reconfigurable antenna are shown in Fig.3.4, and geometrical dimensions are tabulated in Table 3.1

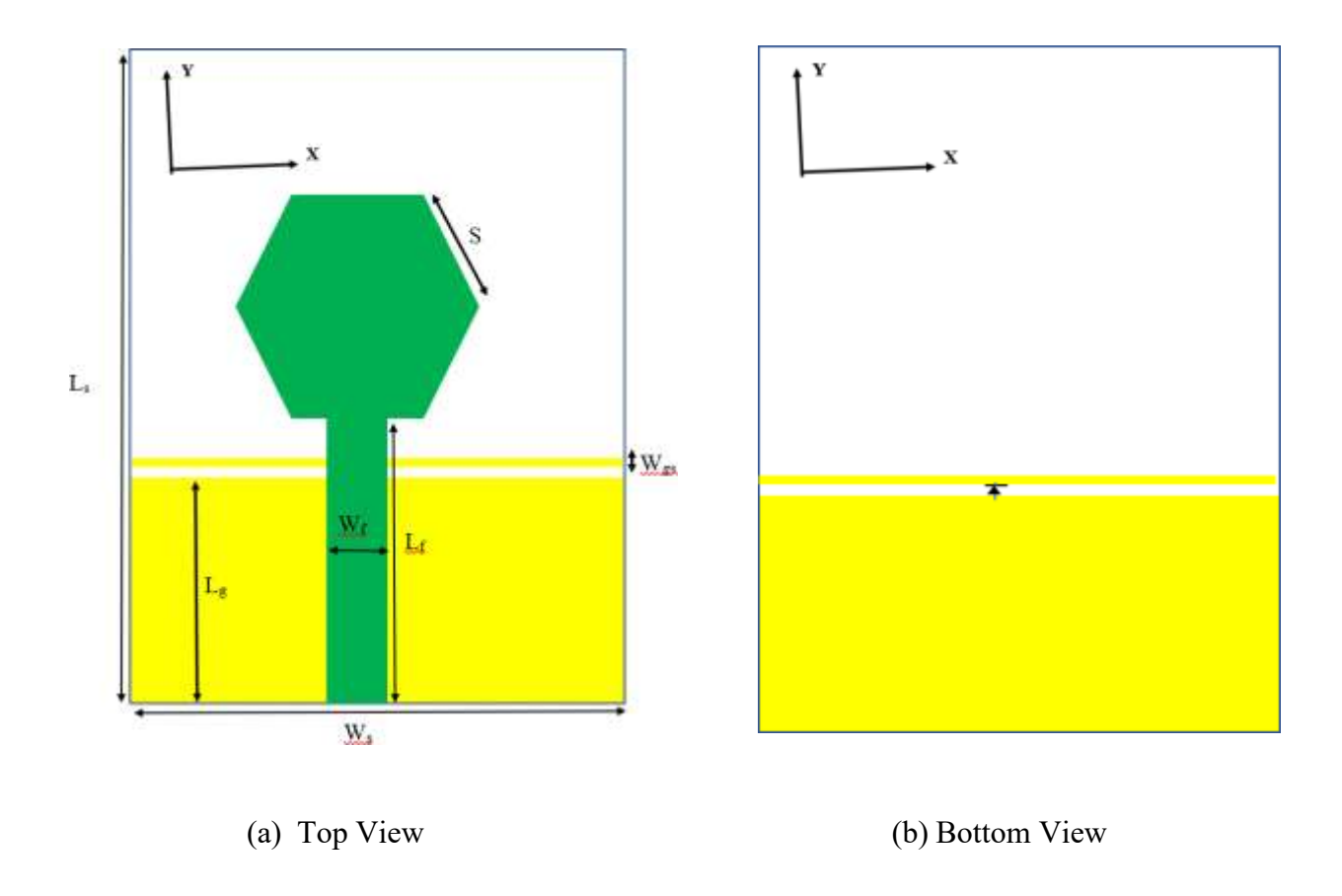


Fig 3.4. Schematic diagram of Proposed frequency reconfigurable antenna structure

 Table 3.1: The designed frequency reconfigurable antenna geometrical dimensions

Parameters	Values (mm)
Substrate width (Ws) and	38 mm x 36 mm
Length (Ls)	
Ground length (Lg)	12.5 mm
Ground strip width (Wgs)	0.5 mm
Feed width (Wf) and feed	3 mm x 16 mm
length (Lf)	
Hexagon Side(S)	6.065 mm
Switch Size	1 mm x 1 mm

The PIN diode equivalent circuit models are shown in Fig. 3.5 for both ON and OFF operating conditions.

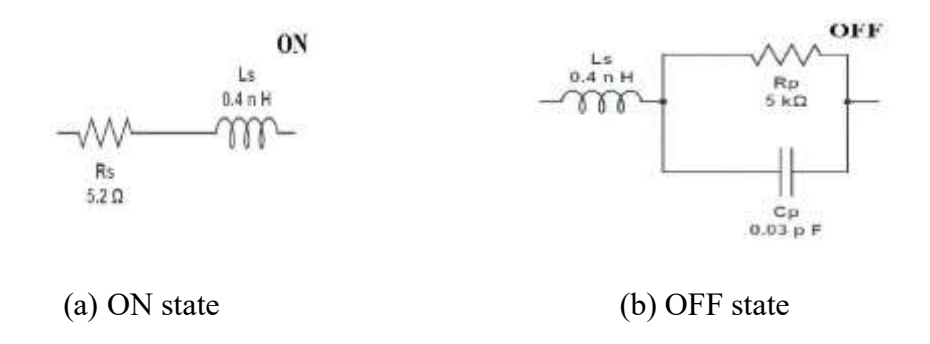


Fig. 3.5. Equivalent circuit model of MADP000907-14020 P PIN diode

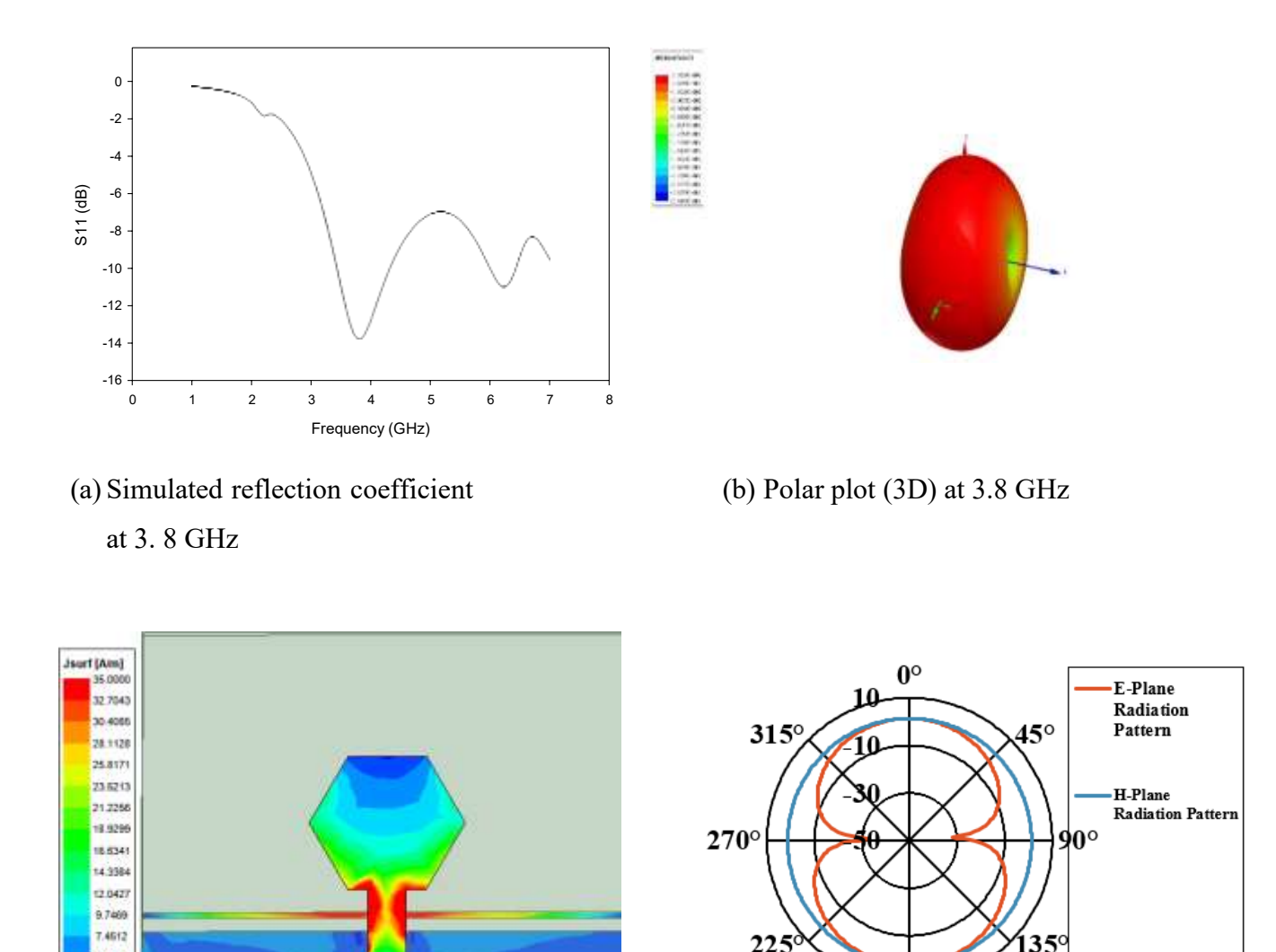
When the PIN diode is in ON condition, its equivalent circuit represents a series RL circuit with a low value of resistor Rs=5.2  $\Omega$  and inductor L=0.4 nH, and in OFF condition, represents a parallel combination of high resistor Rp=5 k $\Omega$  and low value of capacitance Cp=0.03 pF with the series combination of inductor L=0.4 nH.

#### 3.3 Simulation Results and Discussion

#### 3.3.1 PIN diode ON state simulated results

The antenna was designed and analyzed in terms of various antenna parameters using the Ansys - HFSS. When the PIN diode is ON, the designed structure of the return loss is depicted in Fig.3.6(a). The proposed antenna covers a 3.42 GHz to 4.2 GHz band with a minimum reflection coefficient of - 13.9213 dB at 3.8 GHz and a bandwidth of 930 MHz at - 10 dB. This bandwidth is suitable for 5 G networks.

The 3-D radiation polar plot is shown in Fig.3.6 (b) at a center frequency of 3.8 GHz, the designed antenna obtained a peak gain of 2.34 dBi. The surface current distribution is shown in 3.6 (c), in which the current flows into the upper strip in the ground plane, and the ground length in this case is 13.5 mm and Fig.3.6 (d) shows the E-Plane and H-Plane radiation patterns of proposed antenna at Phi=0<sup>o</sup> and Phi=90<sup>o</sup>. The E-plane is in the figure of eight patterns, and the H-plane is in the omnidirectional radiation pattern.



(c) Surface current distribution (d) Radiation patterns of E-plane and H-plane at 3.8 GHz

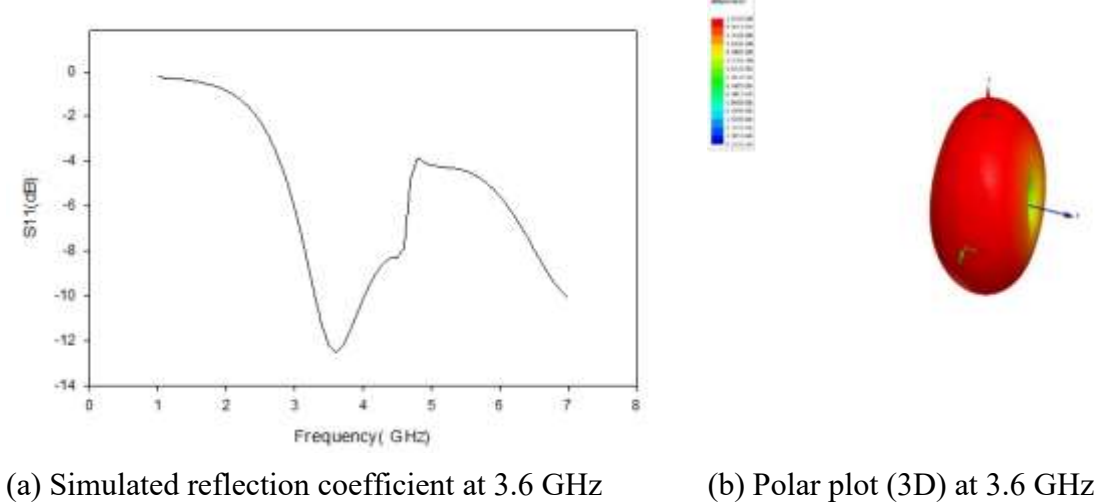
180°

Fig 3.6 Simulated performance characteristics of the proposed antenna when PIN diode ON state

#### 3.3.2 PIN Diode OFF state simulated results

5.1555 2.8507 0.5640

When the PIN diode is OFF, the designed structure return loss is depicted in Fig.3.7 (a). The antenna covers a 3.24 GHz to 4 GHz band with a minimum reflection coefficient of -12.638 dB at a center frequency of 3.6 GHz and a bandwidth of 760 MHz at -10 dB. Here, the frequency is decreased since the strip in the ground plane provides the capacitance effect, and its surface current distribution is represented in Fig.3.7 (c). At a frequency of 3.6 GHz, the designed structure obtained a peak gain of 2.2458 dBi at theta=180°. Fig.3.7 (b) shows a 3-D polar plot with an omnidirectional pattern. The E-plane and H-plane radiation pattern is depicted in Fig.3.7 (d).



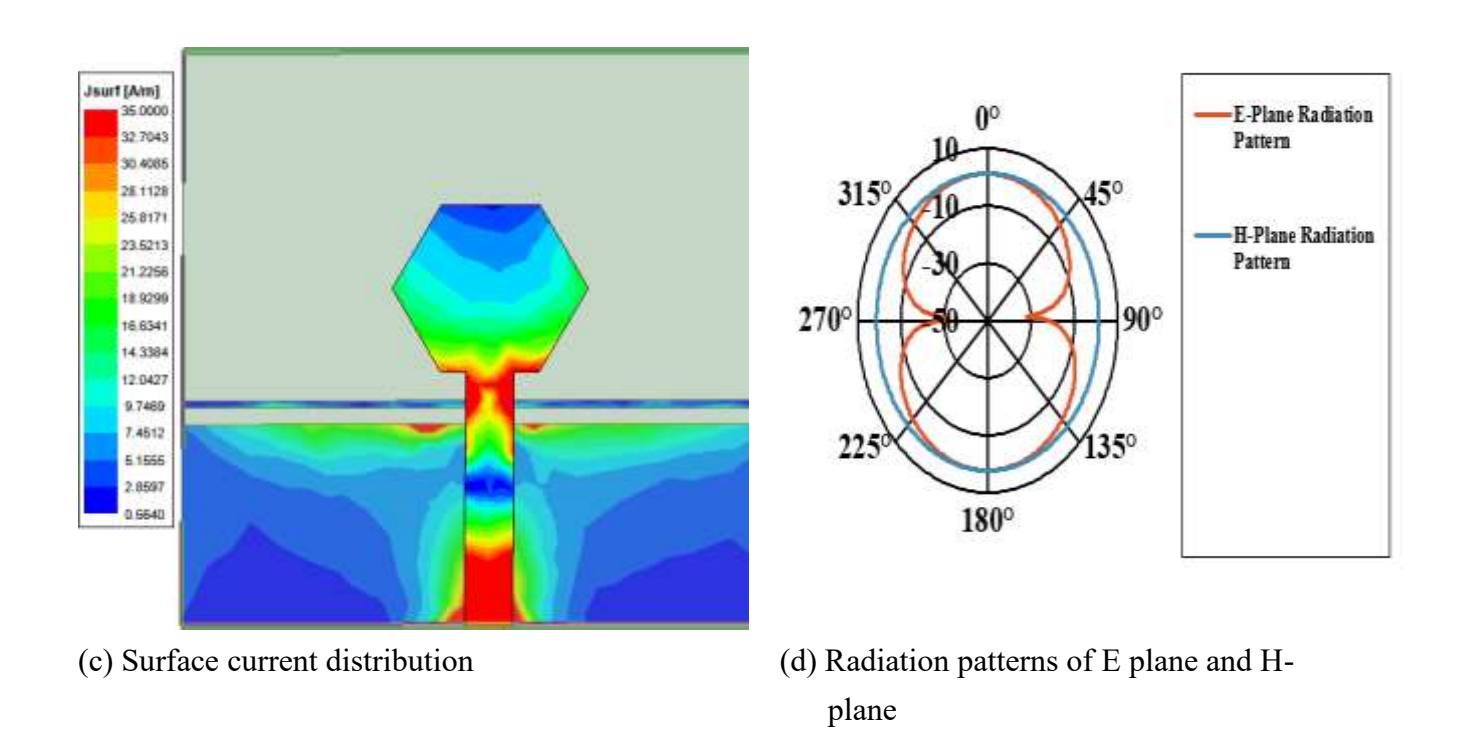
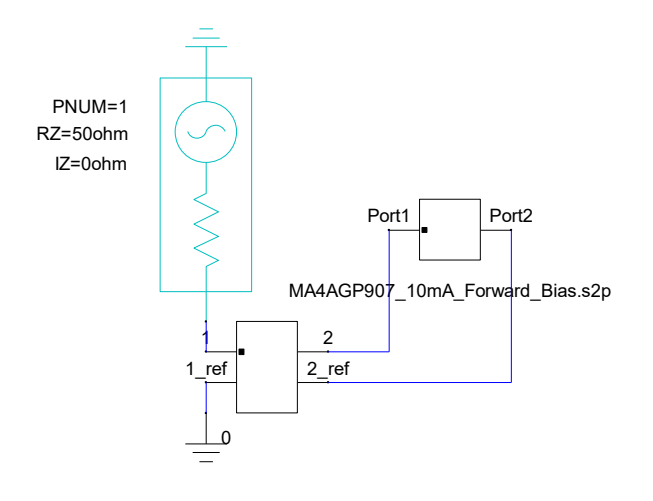
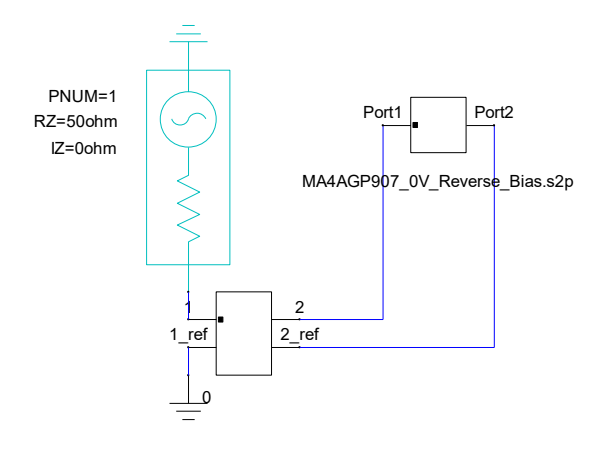


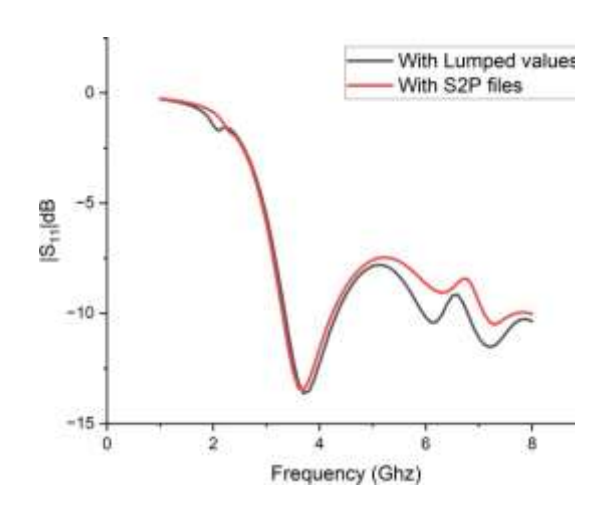
Fig 3.7 Simulated performance characteristics of the proposed antenna when PIN diode OFF state

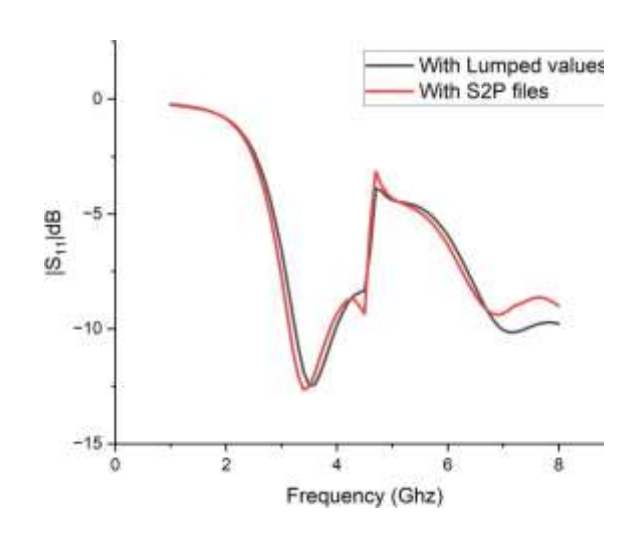




(a) Simulated Ansys circuit for PIN diode ON state

(b) Simulated Ansys circuit for PIN diode OFF state





(c) Reflection coefficient when PIN diode ON

(d) Reflection coefficient when PIN diode OFF

Fig 3.8 Proposed frequency reconfigurable antenna analysis using Ansys Circuit

Instead, lumped values of the PIN diode the s2p files provided by the MACOM company is used in the Fig.3.8 for analysis of frequency reconfigurable antenna in both PIN diode ON and OFF conditions. The reflection coefficient with lumped elements and s2p files is shown in the Fig 3.8 (c and d) respectively. There is no much difference in the reflection coefficient curves.

The summary of observations of the proposed frequency reconfigurable antenna is tabulated in Table 3.2

**Table 3.2**: Summary of observations for the proposed frequency reconfigurable antenna structure

Diode	Resonant	Bandwidth	Gain (dBi)
Status	Frequency (in GHz)		
ON	3.8	930 MHz	2.34
OFF	3.6	760 MHz	2.24

**Table 3.3:** Comparison of proposed frequency reconfigurable antenna structure parameters with published work.

Ref	Antenna	Number of	No of	Band	Gain [dBi]
No.	size(mm <sup>2</sup> )	Switches	operating	Width	
			bands	(MHz)	
[90]	45x50	2	1	800	2.2
[91]	40x30	4	2	400/500	2.24/2.76
Proposed	38x36	1	2	930/760	2.34/2.24

# 3.4 Design and analysis of V-shaped slit frequency reconfigurable antenna

In the previous section, the proposed structure provides only a single band of frequency reconfigurable antenna. However, emerging wireless communications systems require dual and multiband in operating mode of reconfiguration for transmitting one or two bands and receiving with another one or two bands. Therefore, this section discusses a dual and single band frequency reconfigurable antenna. For that purpose, a V-shaped slot is implemented on the upper part of the hexagonal shape patch radiator. A PIN diode is adopted left part of the V-shaped slot with a size of 1mm x 1mm. Dual and single frequency bands are obtained by altering the PIN diode ON and OFF operating states. The geometry and its dimensions are mentioned in Fig 3.9 and Table 3.4 respectively.

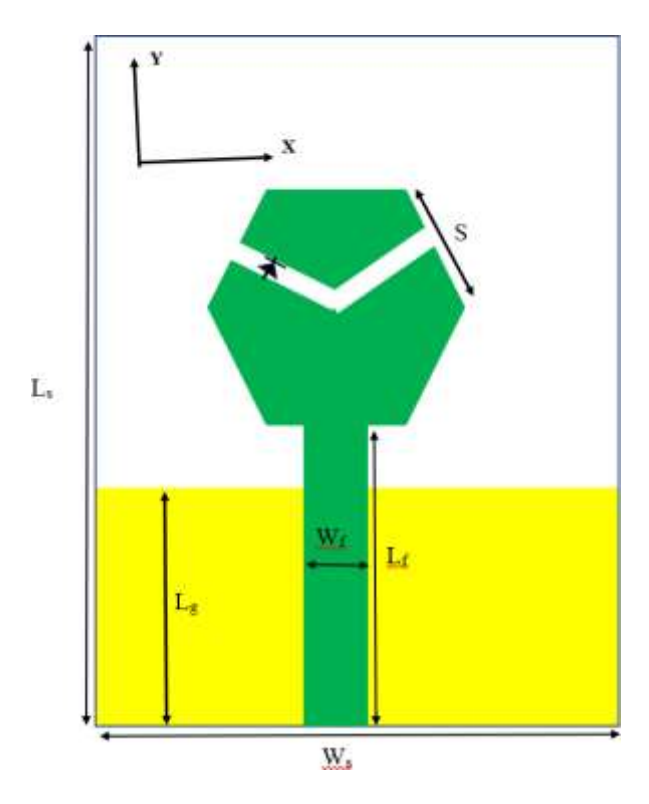


Fig.3.9: Proposed V-shaped slit frequency reconfigurable radiating structure schematic diagram

Table 3.4: The V-shaped slit frequency reconfigurable antenna structure dimensions

Parameters	Values (mm)
Substrate width (W <sub>s</sub> ) and	28 mm x 30 mm
Length (L <sub>s</sub> )	
Ground length (Lg)	15 mm
Slot gap width	1 mm
Feed width (W <sub>f</sub> ) and feed	3 mm x16 mm
length (L <sub>f</sub> )	
Hexagon Side (S)	6.065 mm
Switch Size	1 mm x 1 mm

As discussed in the frequency reconfigurable antenna, the impedance is not matching correctly, so the return loss is low, as shown in Fig 3.6 (a) and Fig.3.7(a), respectively. For better impedance matching in dual-band and single-band frequency reconfigurable antenna, the substrate's dimensions and the ground plane are varied. The parametric analysis of the ground length is represented in Fig 3.10. The ground length of 15 mm provides a wide band and better return loss, and a ground length of 30 mm provides the worst return loss.

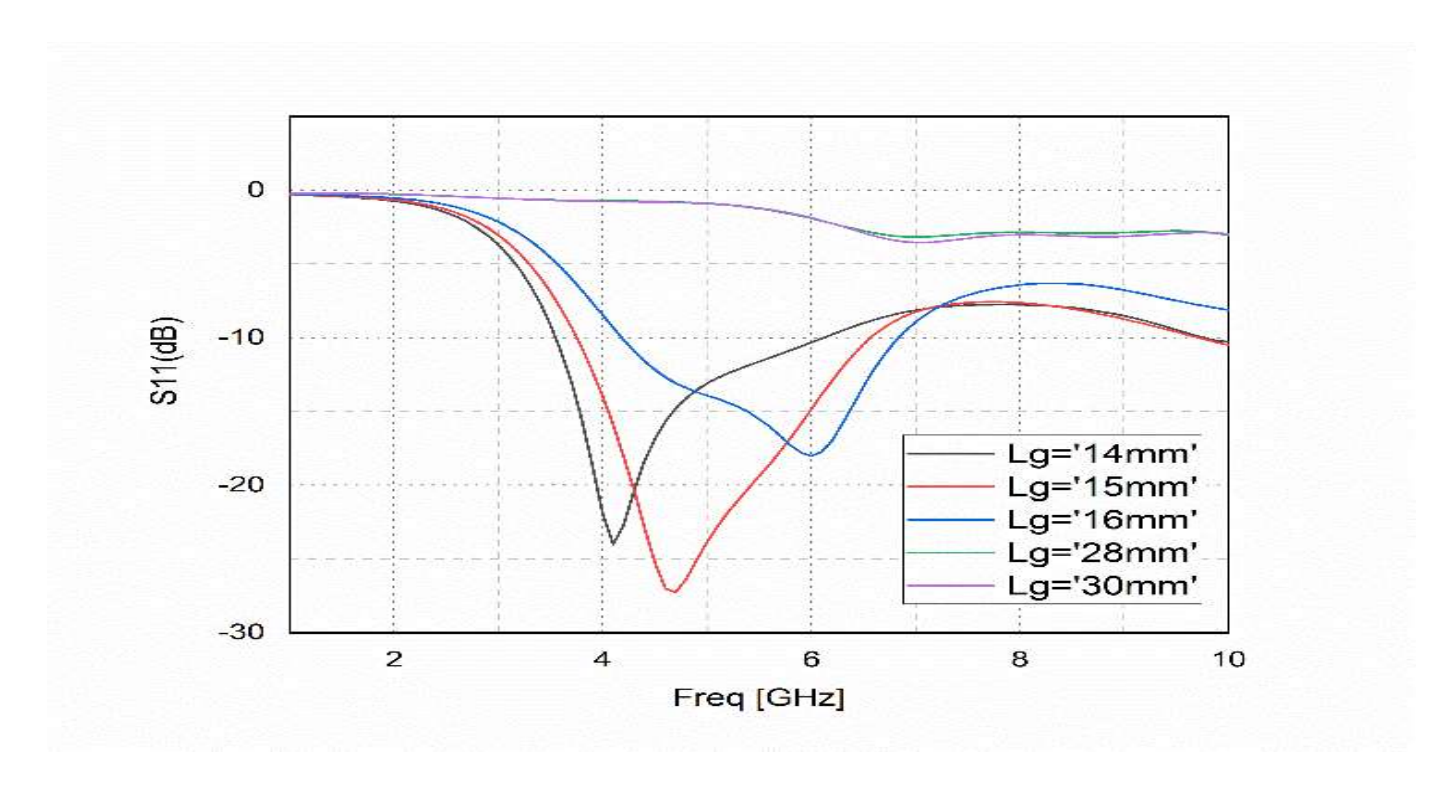
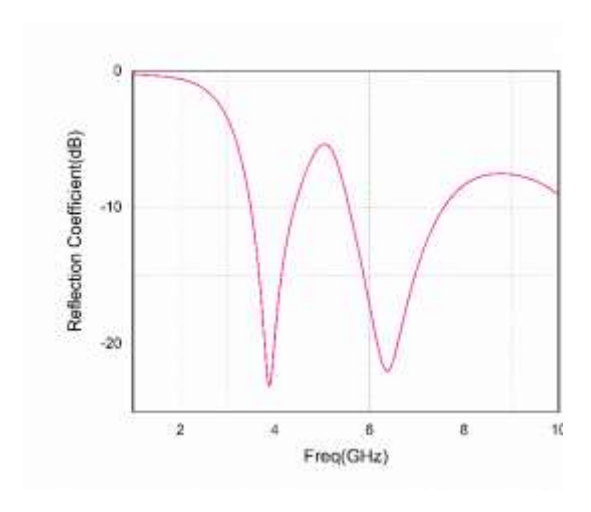


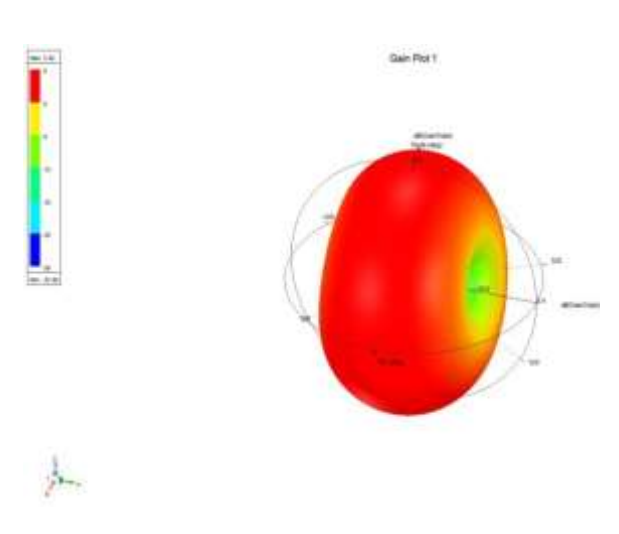
Fig 3.10 Parametric analysis on ground length of V-shaped silt reconfigurable antenna

# 3.5 Simulated results and discussions of V-shaped slit frequency reconfigurable antenna

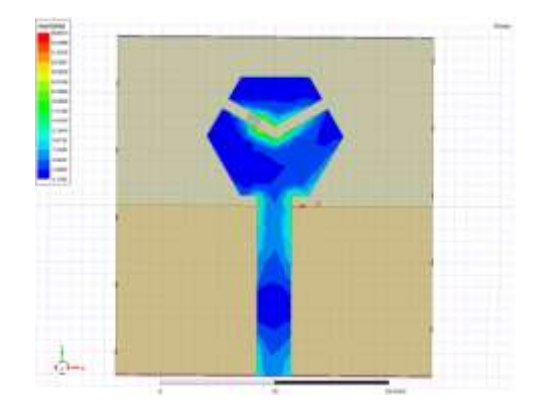
### 3.5.1 PIN diode ON state simulated results

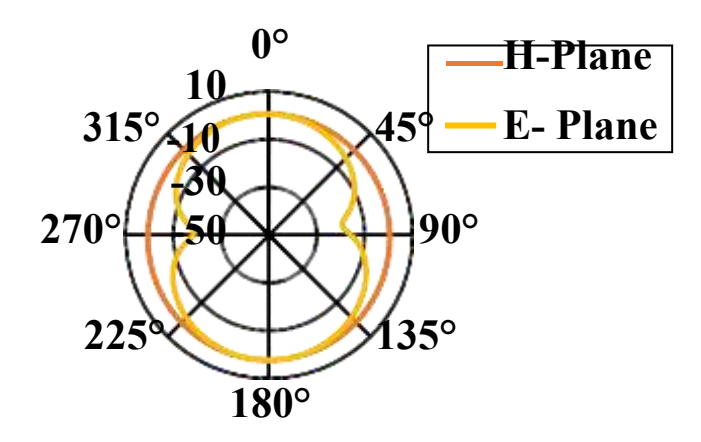
When PIN diode is in ON state, the proposed radiating structure performs dual-band operation in which the lowest operating frequency is at 3.9 GHz with a return loss of -23.18 dB and simulated -10 dB bandwidth of 1 GHz (4.465-3.4975 GHz) and another band is centered around 6.37 GHz with a return loss of -21.80 dB and simulated -10 dB bandwidth of 2 GHz (7.5925-5.59 GHz) respectively is shown in Fig.3.11 (a). The Simulated 3D polar plot, gain versus frequency, are shown in Fig.3.11 (b) and Fig.3.11 (e), respectively. From Fig 3.11 (e), the gain at centered frequency 3.9 GHz is 2.413 dBi, and the gain at 6.37 GHz is 2.519 dBi, respectively.



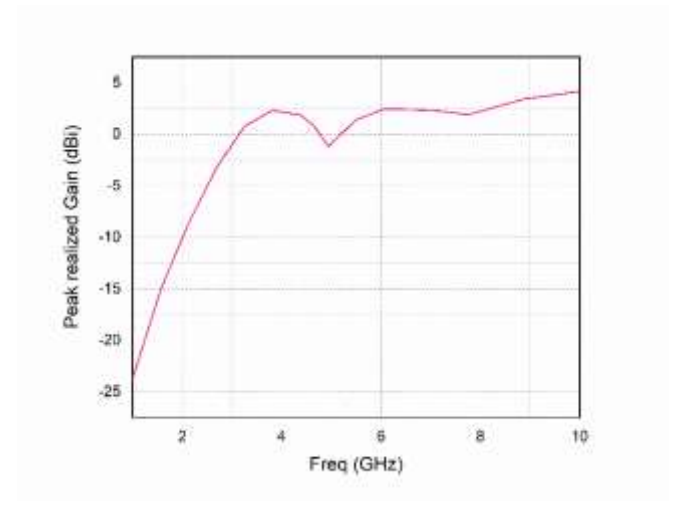


- (a) The simulated reflection coefficient for the diode is in the ON state
- (b) Polar plot (3D) for the diode is in the ON state





- (c) Electric Filed distribution for the diode is in the ON state
- (d) Simulated radiation patterns YZ-plane and XZ-plane for diode is in ON state



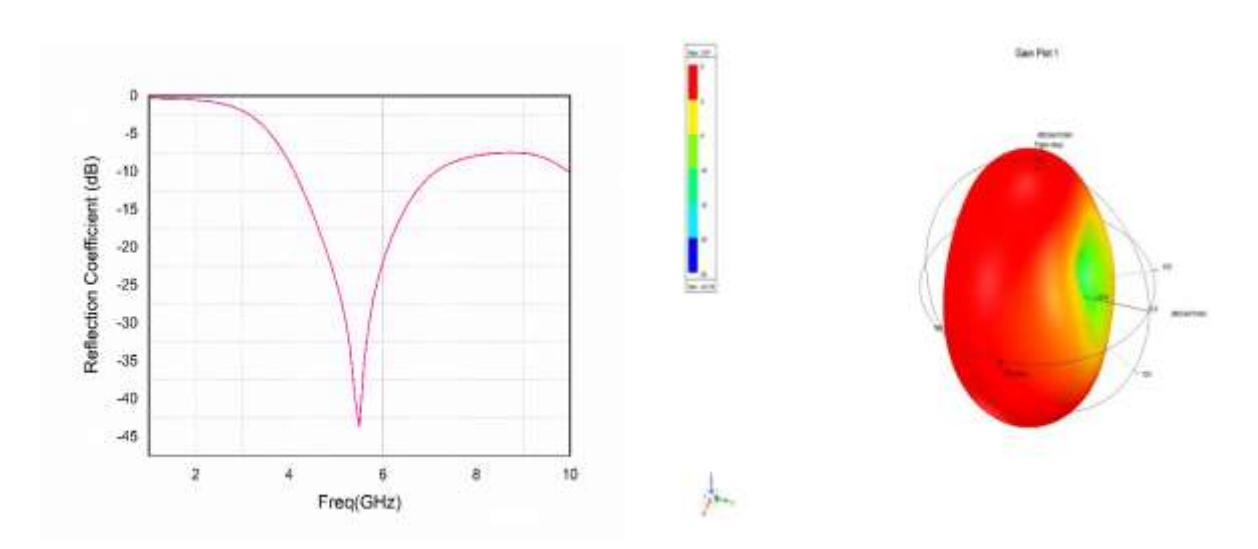
(e) Gain Versus frequency Plot for the diode is in the ON state

Fig 3.11 Simulated performance characteristics of the proposed V-shaped slit frequency reconfigurable antenna when PIN diode ON state

The surface current distribution indicates the resonant frequency of the proposed structure in detail. The PIN diode ON state surface current distribution is represented in Fig 3.11 (c), in which the radiating element is left side current distributes more area than the right side of the radiating element so that the proposed structure resonates dual band based on the phase difference approach. E-plane  $(YZ, \phi=90^{\circ})$  and H-plane  $(XZ, \phi=0^{\circ})$  simulated radiation patterns are depicted in Fig 3.11 (d). The E-plane radiation patterns are almost all bidirectional shapes, and the H-plane patterns are omnidirectional, respectively.

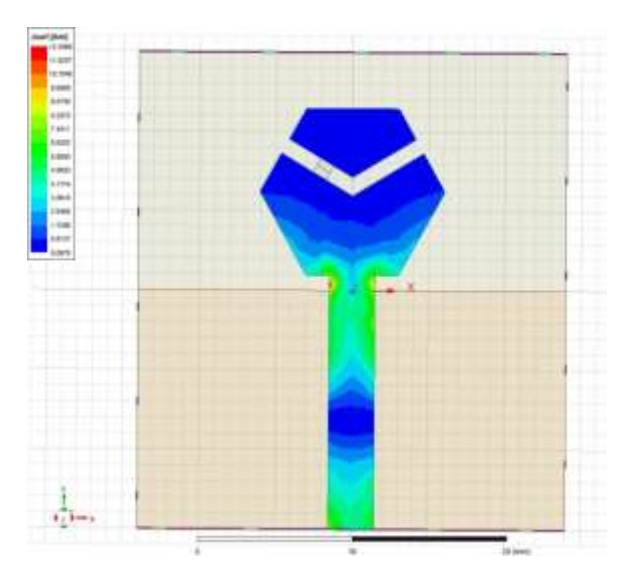
# 3.5.2 PIN diode OFF state simulated results

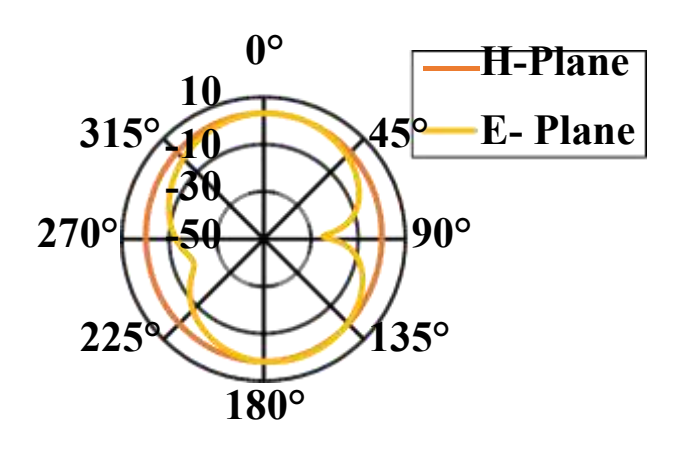
When the PIN diode is operating in the OFF state, the proposed radiating structures perform single band resonating at 5.5 GHz with a return loss of -40.213 dB and simulated -10 dB bandwidth of 3.11 GHz (7.14 -4.03 GHz) as shown in Fig 3.12 (a) and its 3D polar plot is represented in Fig 3.12 (b). The PIN diode ON state surface current distribution is depicted in Fig 3.12 (c), in which the radiating element below the V-shaped slit current distributes more area as compared to the upper portion of the radiating element so that the proposed structure resonating at a single band since there is no phase difference between the left and right sides of the radiating element. The E-plane (YZ,  $\phi$ =90°) and H-plane (XZ,  $\phi$ =0°) simulated radiation patterns are depicted in Fig 3.12 (d). The E-plane radiation patterns are almost all bidirectional shapes, and the H-plane patterns are omnidirectional, respectively.



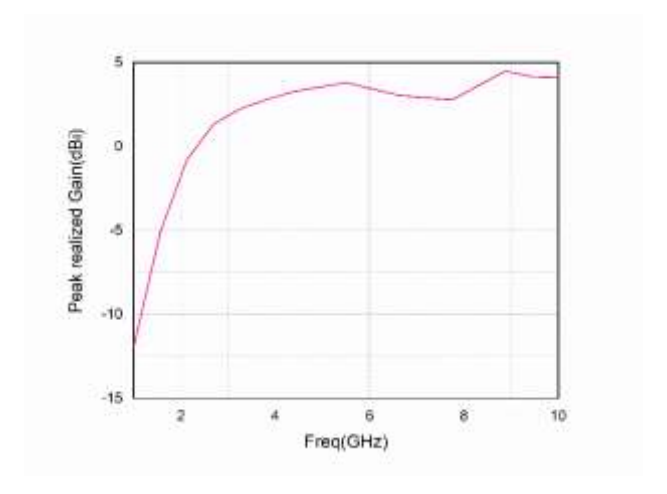
(a) The simulated reflection coefficient for the diode is in OFF state

(b) Polar plot (3D) for the diode is in OFF state





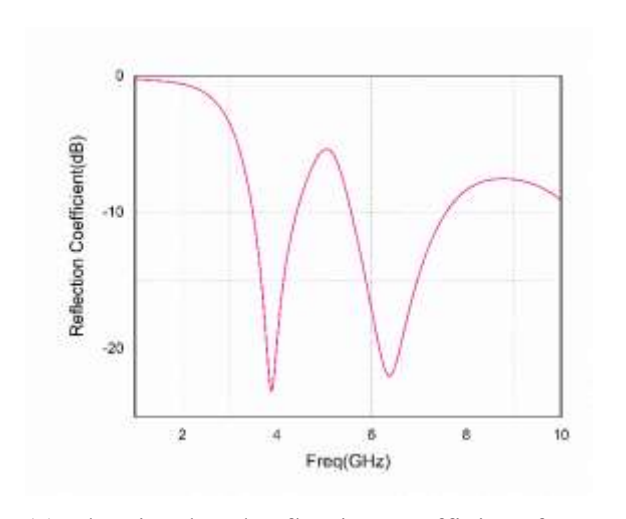
- (c) Electric Filed distribution for the diode is in OFF state
- (d) Simulated radiation patterns YZ-plane and XZ-plane for diode is in OFF state



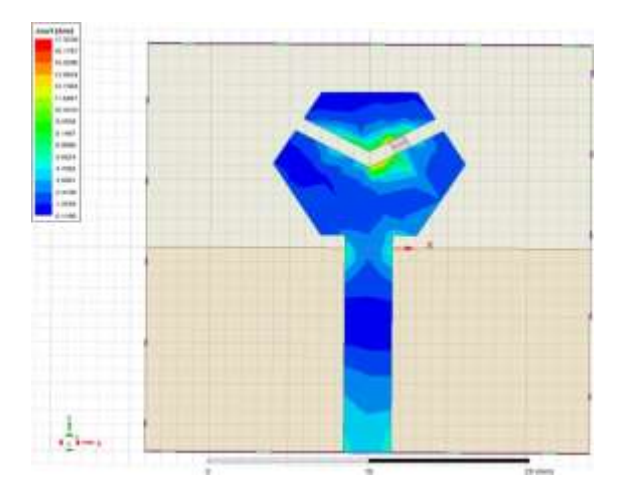
(e) Gain Versus frequency Plot for the diode is in the OFF state

Fig.3.12 Simulated performance characteristics of the proposed V-shaped slit frequency reconfigurable antenna when PIN diode OFF state

Further, the position of the diode is shifted symmetrically to the right side in a V-shape slot, and all parameters of the proposed radiating structure are shown in Fig.3.13 no significant changes are observed from this structure as compared to the proposed radiating structure with the diode position is the left side of V-Shape slit.

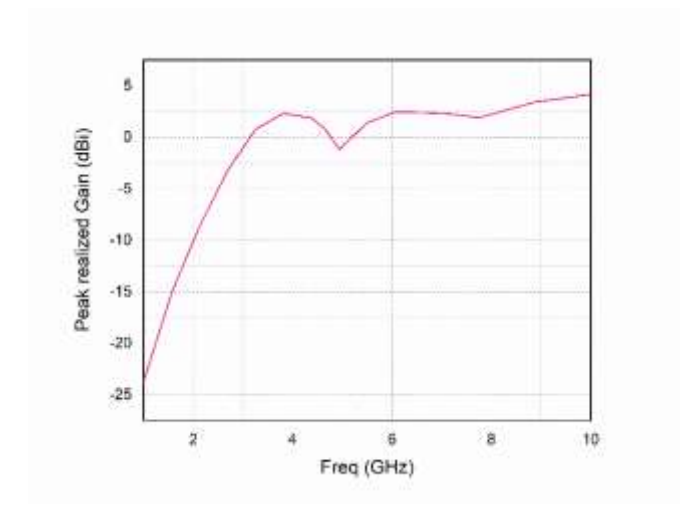


- (a) The simulated reflection coefficient for the diode is in the ON state (Right side)
- (b) Polar plot (3D) for the diode is in ON state (Right side)



315° 10 45° — H-Plane 270° 50 90° 225° 135°

- (c) Electric Filed distribution for the diode is in ON state (Right side)
- (d) Simulated radiation patterns YZ-plane and XZ-plane for diode is in ON state (Right side)



(e) Gain Versus frequency Plot for diode is in ON state (Right side)

Fig 3.13 Simulated performance characteristics of the proposed V-shaped slit frequency reconfigurable antenna when PIN diode ON state (Right side)

Similarly, The PIN diode is OFF condition in the position of the right side in a V-shaped slot, providing almost all the same results. The summary of the proposed radiating structure performance parameters is given in Table 3.5.

**Table 3.5:** Summary of observations for the proposed radiating dual and single band frequency reconfigurable antenna

Operating Mode	Switch Status	Frequency Band (GHz)	Bandwidth (MHz)	Gain (dBi)
Single band	OFF	5.5	3110	3.87
Dual-band	ON	3.9, 6.37	970, 2000	2.45, 2.51

Finally, the novelty in the proposed radiating structure compared to the already published works is tabulated in Table 3.6. From this, the proposed radiating structure provides optimum gain and bandwidth at both dual and single-band operations.

**Table 3.6:** Comparison of proposed V-shaped slit frequency reconfigurable antenna structure parameters with published work.

Ref No.	Dimensions	No. of	Operating	Bandwidth	Gain(dBi)
	(mm <sup>3</sup> )	diodes	Frequencies	(MHz)	
			(GHz)		
[7]	53x35x1.6	1	2.45,3.5,5.2	147-1820	1.7-3.4
[92]	113x113x1.6	2	1.32,1.66,2.54	134-370	NA
[93]	40x35x1.6	1	2.45,3.5,5.2	330-1250	1.48-3.26
[94]	39x37x1.6	1	2.4,5.4,3	550-1220	1.27-2.34
Prop.	30x28x1.6	1	5.5,3.9,6.37	970-3110	2.45-3.87

#### 3.6 Summary

A simple hexagonal-shaped frequency reconfigurable patch antenna with a switchable ground plane is discussed initially. It resonates at two frequencies 3.6 GHz for Wi-max and 3.8 GHz for new C-band 5G networks. The switching between two different frequencies was obtained by adopting a PIN diode in the ground plane. The designed antenna provides a peak gain of 2.34 dBi with a bandwidth of 930 MHz when the PIN diode is in the ON state. When the diode is in OFF condition, the designed antenna offers a peak gain of 2.24 dBi with a bandwidth of 760 MHz. These bandwidths are sufficient to support 5 G networks. However, it is limited to a single band of operation in each state of the PIN diode.

Further, a slotted hexagonal shape radiating structure with a single, dual-band frequency reconfigurable antenna is investigated for 5G and WLAN applications. A PIN diode is integrated into the left side of a V-shaped slit for obtaining the frequency switching. The structure provides a band (5.52 GHz) when the diode is in the OFF operating state with a bandwidth of 3.11 GHz and a gain of 3.866 dBi, respectively. When the diode is in an ON operating state, it provides a dual frequency band (3.9 GHz, 6.37 GHz) with a bandwidth of 1 GHz at a center frequency of 3.9 GHz and a bandwidth of 2 GHz at a center frequency of 6.37 GHz. Further, the diode is integrated on the right side of the V-shaped slot, and similar results are observed as the radiating structure with the diode integrated on the left side. The antenna has been designed for 3.9 GHz (5G), 5.5 GHz (WLAN), and 6.37 GHz (C-band) wireless applications. The presented radiating structure has a compact size, low cost, improved bandwidth, and gains over already published radiating structure.

#### **CHAPTER 4**

#### Design and analysis of frequency and pattern reconfigurable antenna for IoT applications

#### 4.1 Introduction

The previous chapter, discussed frequency reconfigurable antenna for new C-band 5G networks and Wi-Fi/Wi-Max and WLAN wireless applications. However, modern wireless systems such as IoT require compound reconfigurable antennas for effective communication between smart devices. Therefore, in this chapter a simple hexagonal-shaped monopole antenna is designed on RT duroid instead of FR-4 since it provides good performance at higher frequencies as well as different environmental conditions. To achieve the pattern and frequency reconfiguration, two parasitic stubs are added in the ground plane along the central radiator of the monopole antenna through PIN diodes. By operating these PIN diodes in three modes, the proposed structure provides omnidirectional and directional patterns that operate at 5 GHz and 4.3 GHz, respectively. Section 4.2 provides the details of the design and its mathematical analysis of the proposed radiating structures, and simulated results with discussion are reported in section 4.3. Finally, summary of proposed reconfigurable antennas is reported in last section.

#### 4.2 Design and analysis of frequency and pattern reconfigurable antenna

The frequency and pattern reconfigurable antennas are implemented and analyzed in the Ansys HFSS R22. The geometrical dimensions are listed in Table 4.1, and the structure is shown in Fig. 4.1, respectively. Initially radiating element is chosen as hexagonal shaped, and its dimensions are calculated based on the mathematical formulae mentioned in the ref [95] at an operating frequency of 3.8 GHz with a relative permittivity of 2.94. Then two parasitic stubs are added in the ground plane through two MADP-000907-14020 PIN diodes, for pattern tilting. The distance Cp from the center of the radiating element is chosen at approximately  $\frac{\lambda}{4}$  such that it does not affect the performance

characteristics of the proposed structure. Where is the operating wavelength evaluated at the lowest frequency of 4.3 GHz. The feed length and width are calculated using the well-known transmission line equations.

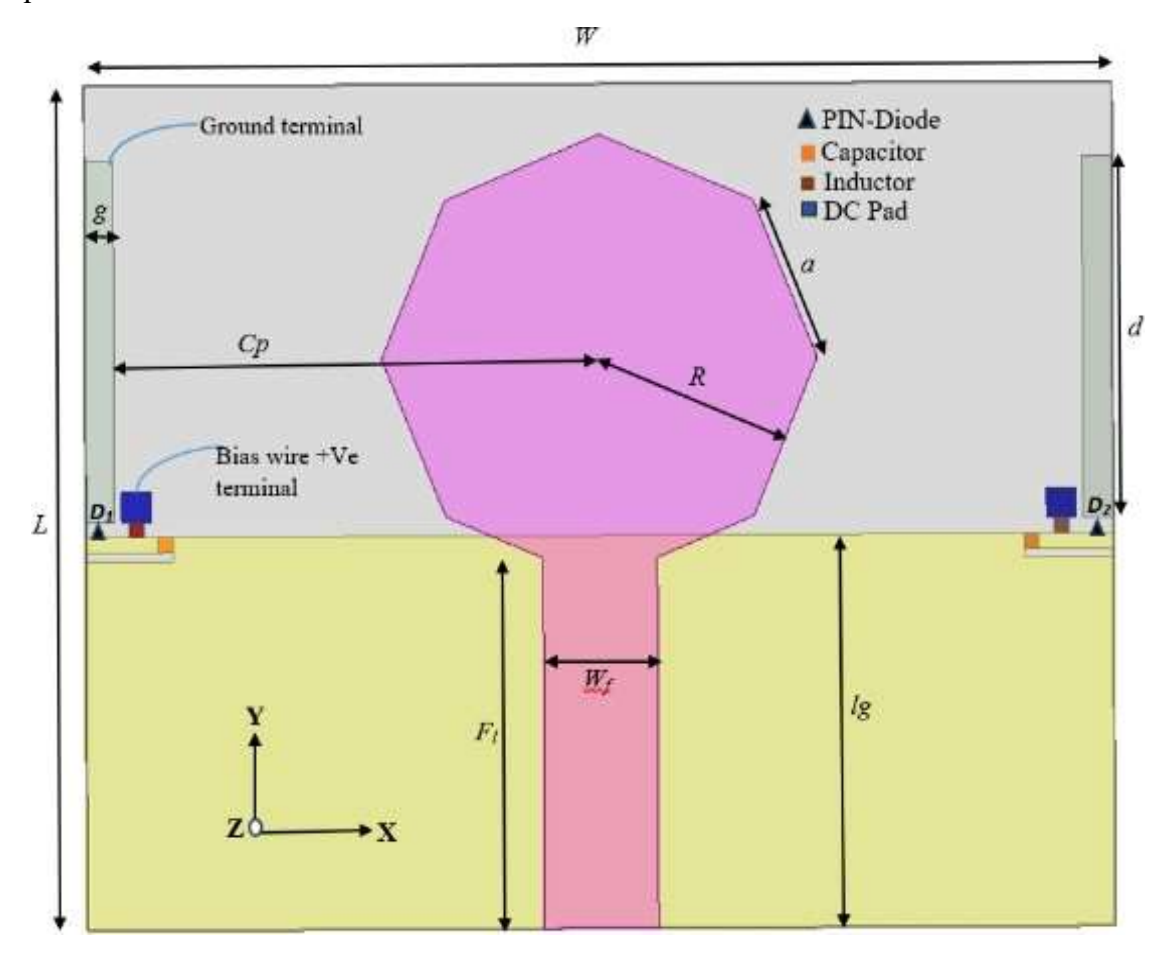


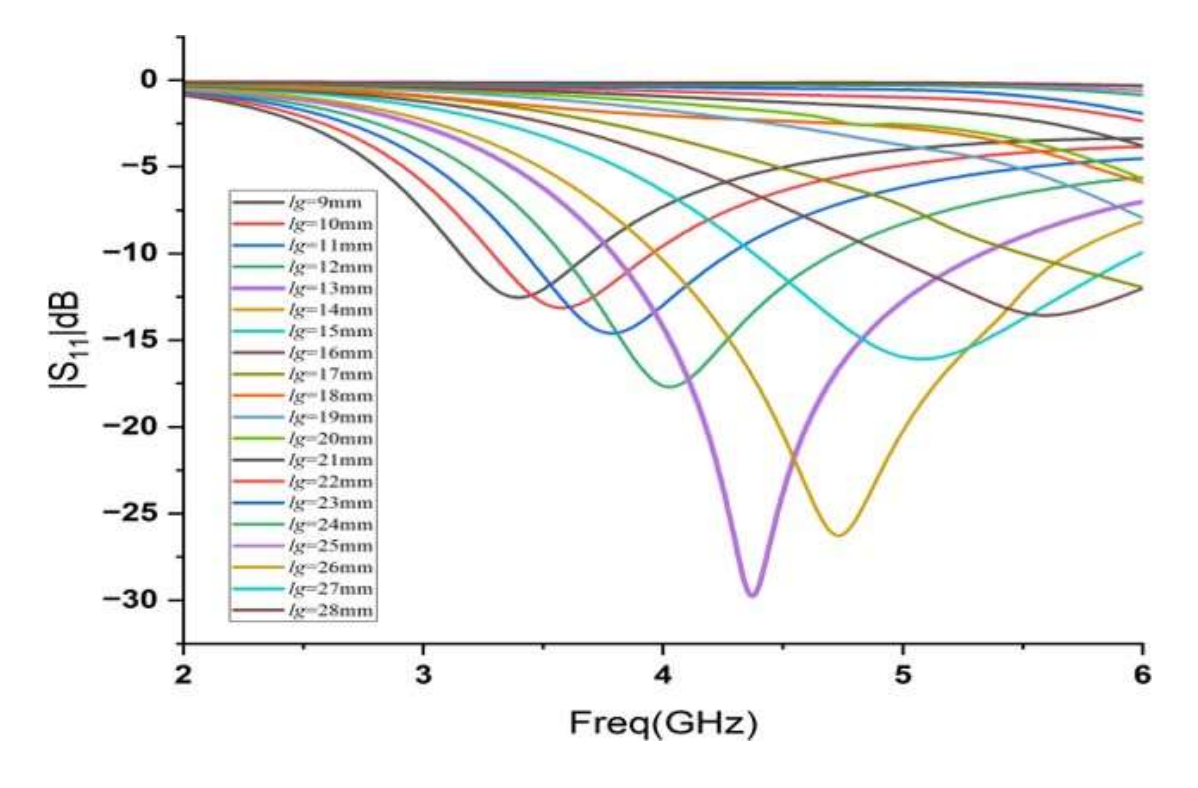
Fig.4.1. Proposed frequency and pattern reconfigurable antenna and its geometrical dimensions

Table 4.1. Geometrical dimensions of frequency and pattern reconfigurable antenna

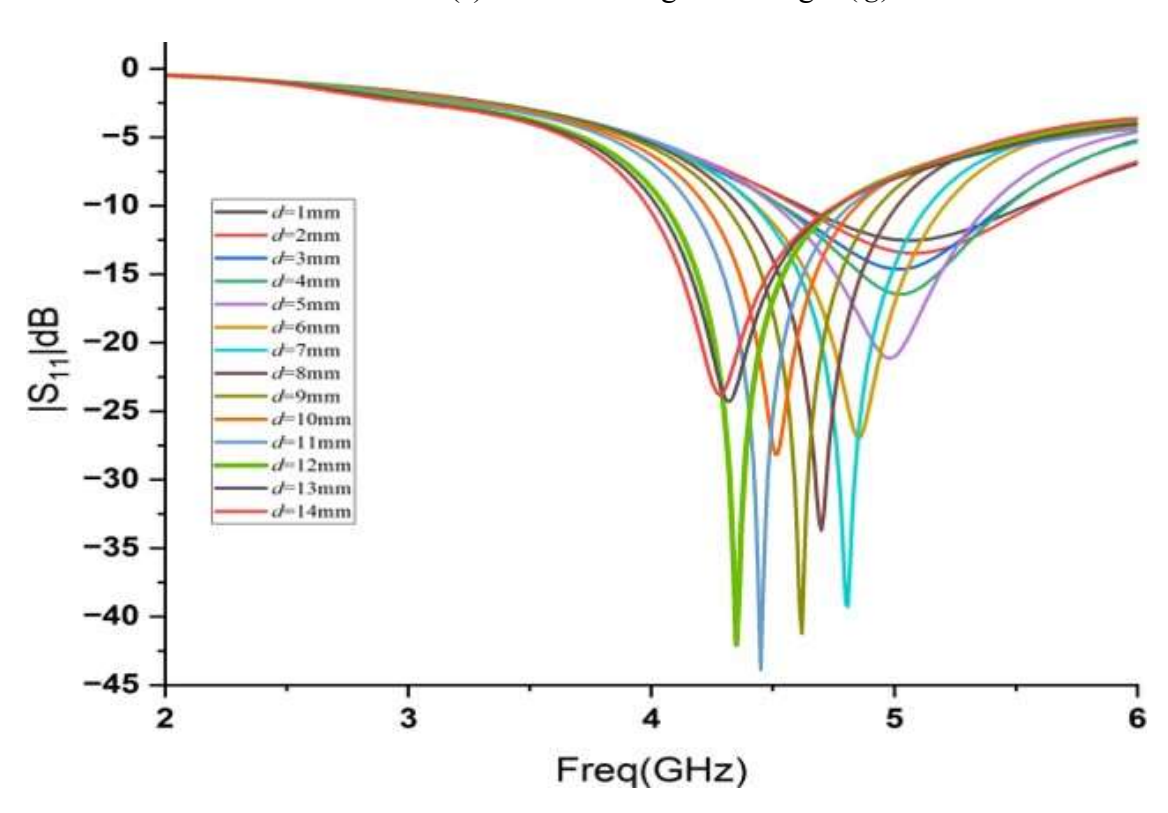
Parameter	Value	Parameter	Value
	(mm)		(mm)
L	28	$W_{\mathrm{f}}$	3.89
W	35	R	6.426
g	1	a	7.42
Ср	16.5	lg	13
F <sub>1</sub>	11.73	d	12

#### 4.2.1 Parametric analysis on ground length

Further, to understand the antenna working mechanism, parametric studies are carried out on parameters lg (ground length) and d (length of the parasitic stub), and their respective graphs are shown in Fig.4.2. For lg = 9 mm, it is resonating at 3.8 GHz, which matches the parameters evaluated for a hexagonal-shaped radiating element based on the mathematical calculations [11], but has not achieved a good dip in reflection coefficient. Further, the maximum dip and greater bandwidth are achieved at lg = 13 mm compared to the other values, therefore, in this structure, the ground length is fixed at 13 mm. After that, the parasitic stub length is changed from 1 mm to 14 mm, and a better dip in the reflection coefficient is achieved at parasitic stub lengths of 7, 9, 11, and 12 mm, respectively. However, at 7 mm and 9 mm, it provides omnidirectional with a lower gain, as shown in Fig.4.3 (a and b). At 11 mm, it provides directionality with less gain than d = 12 mm, as shown in Fig.4.3 (c). Therefore, d = 12 mm is finalized as the parasitic stub length in this structure. The concept of the Yagi-Uda principle is used, and the parasitic stubs act as reflectors.



(a) Variation of ground length (*lg*)



(b) Variation of parasitic stub length (d)

Fig.4.2. Parametric studies on ground length (lg) and parasitic stub length (d)

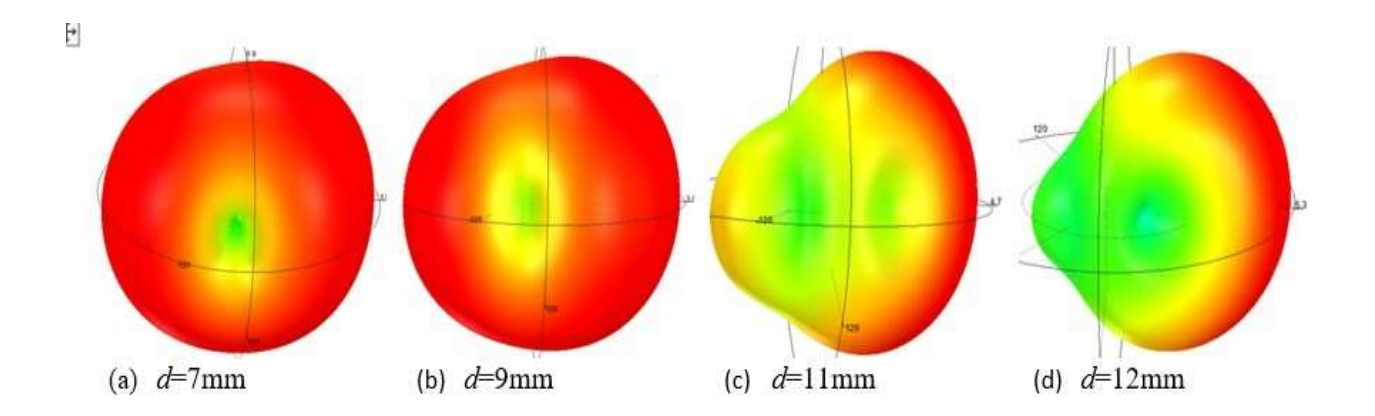


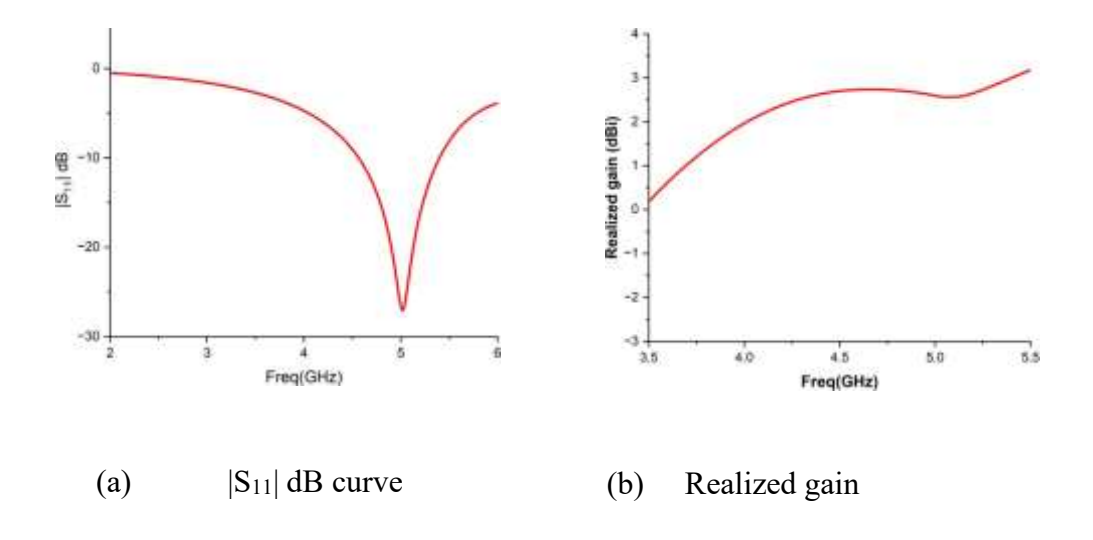
Fig.4.3. Radiation patterns of parasitic stub lengths (d=7, 9, 11 and 12 mm)

#### 4.3 Simulated Results and Discussions of frequency and pattern reconfigurable antenna

The proposed structure operates in 3 modes, namely mode 1, when both diodes are in the OFF state, and modes 2 and 3, in which either one diode is ON or another diode is OFF.

#### 4.3.1 Mode 1 (when both diodes are in the OFF state)

The reflection coefficient  $|S_{11}|$  dB is shown in Fig. 4.4 (a). In this mode, the proposed structure provides a 5 GHz resonant frequency with a bandwidth of 830 MHz. The realized gain is 2.55 dBi, and the radiation efficiency is 90%. The E-filed distribution is shown in Fig. 4.4 (d), and one can quickly identify that the maximum field is accumulated to the main radiating element only and no field in parasitic stubs. Therefore, the radiation pattern is omnidirectional, as shown in Fig. 4.4 (c).



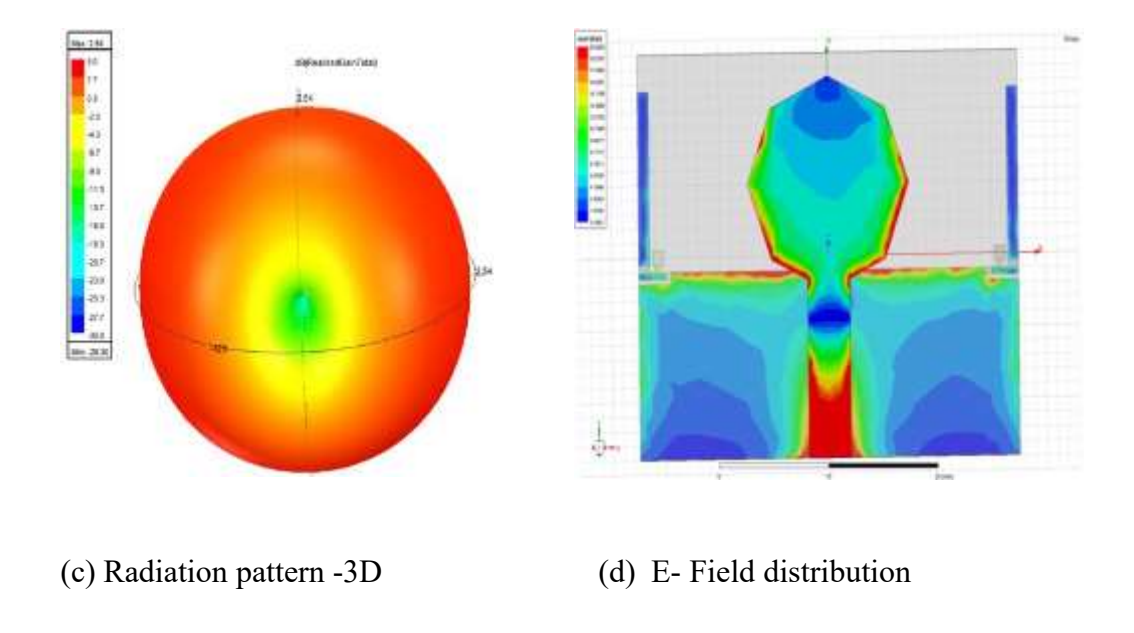


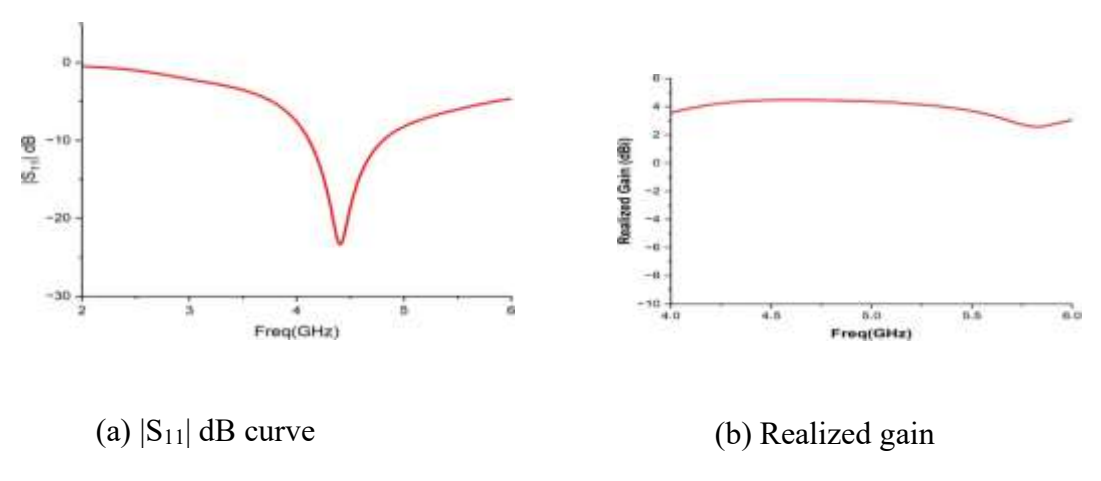
Fig. 4.4 Simulated Results in mode 1 (both diodes are in the OFF state)

This characteristic of the reconfigurable antenna is more suitable for general IoT close-range devices.

#### 4.3.2 Mode 2 and Mode 3 (one diode is ON or another diode is OFF)

In mode 2, the diode  $D_1$  is OFF, and  $D_2$  is ON. The proposed structure is resonant at 4.3 GHz with a bandwidth of 1090 MHz, as shown in Fig.4.5 (a), and the respective realized gain is shown in Fig. 4.5(b). The radiation efficiency is 85%, and the realized gain is 4.55 dBi. The 3-D radiation pattern and E-field distribution are shown in Fig. 4.5 (c and d), respectively. One can quickly identify that the parasitic stub is acting as a reflector; due to this, the beam is tilting towards the negative X-axis. In mode 3, the diode  $D_1$  is ON and  $D_2$  is OFF. The proposed structure provides the same resonant

frequency, but the radiation pattern tilts the positive X-axis since the left-side parasitic stub acts as a reflector in this mode Fig. 4.6 (a and b) shows the radiation pattern and E-field distribution. The performance characteristics of the proposed structure are listed in Table 4.3. When both diodes are OFF, it is resonant at 5 GHz with an omnidirectional pattern, and if one of the diodes is ON, another one is OFF. It is resonant at 4.2 GHz with a directional pattern concerning the activated parasitic stub.



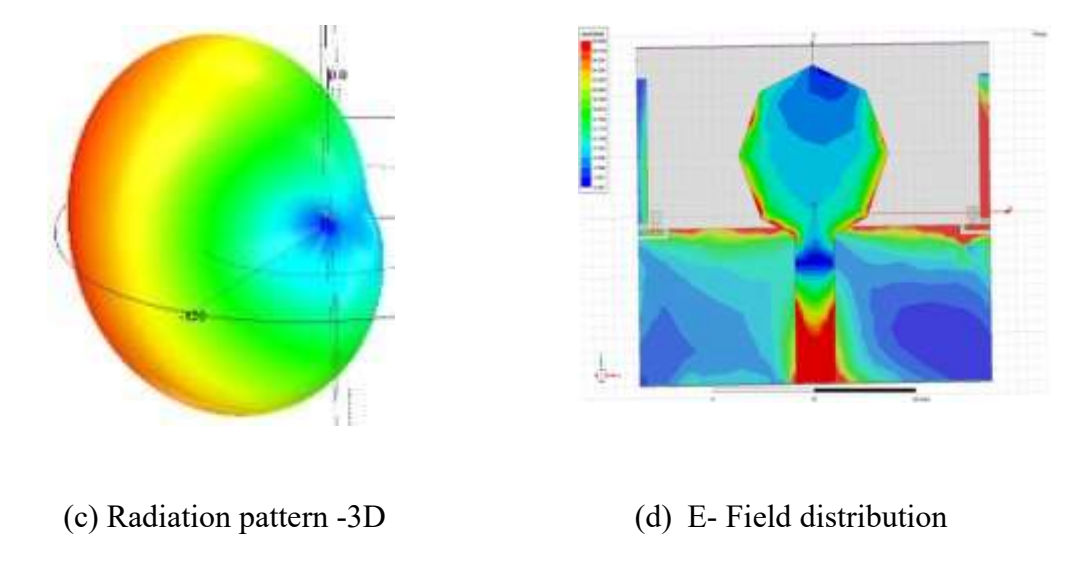


Fig. 4.5. Simulated results in mode 2 ( $D_1$  is OFF and  $D_2$  is ON state)

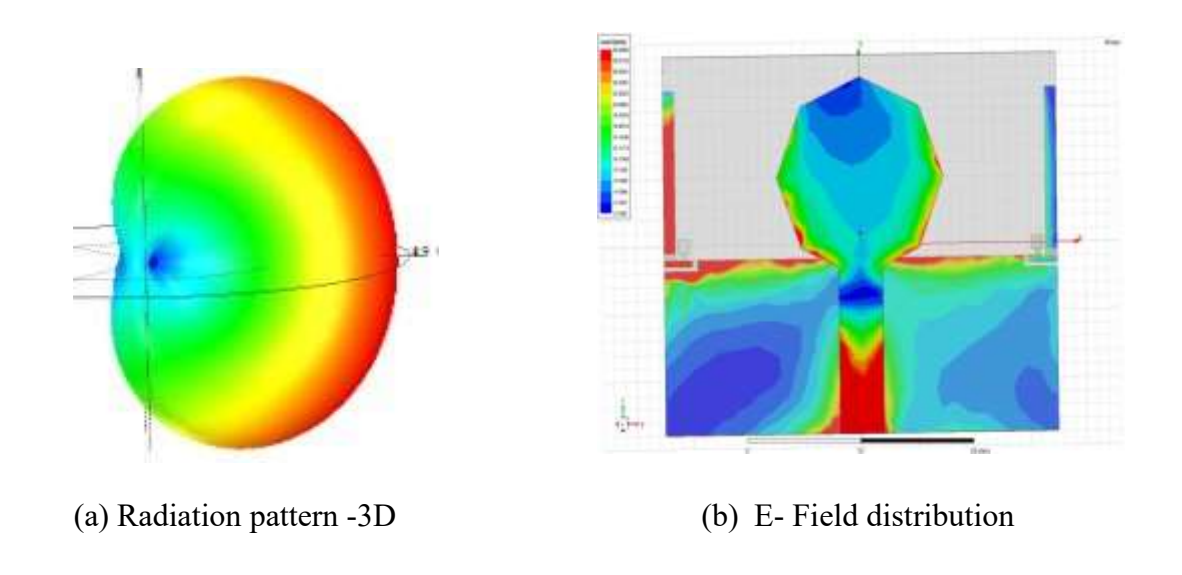


Fig.4. 6. Simulated results in mode 2 (D<sub>1</sub> is ON and D<sub>2</sub> is OFF state)

These characteristics of an antenna make them suitable for intelligent vehicles to communicate with each other.

#### 4.4 Radiation Pattern analysis on Smart fixed vehicles

Pattern analysis is performed on the static vehicle to explore whether the proposed structure suits the IoT platform to interconnect vehicles with other IoT-enabled devices.

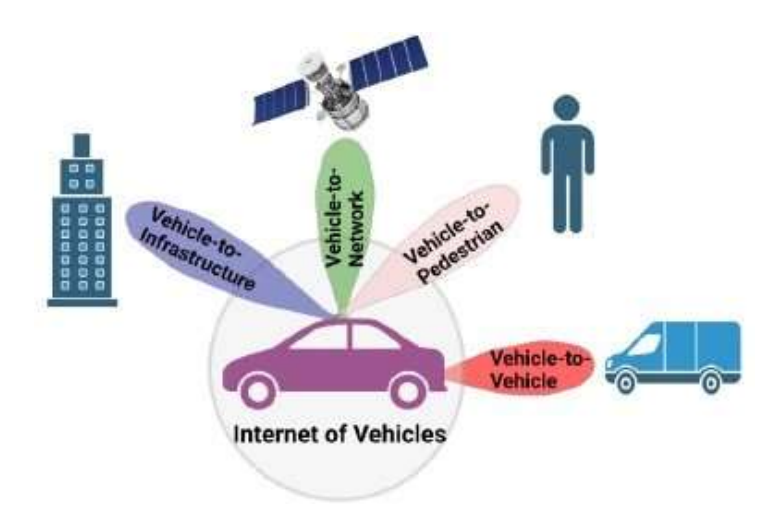


Fig. 4.7. Communication between vehicles to other networks via IoT [18]

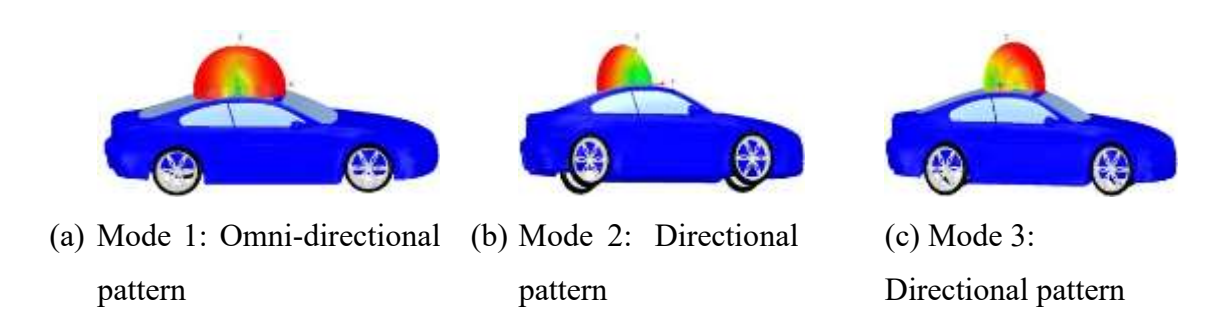


Fig. 4.8. Pattern analysis of the proposed structure on top of the intelligent vehicle

In Fig.4.8(a), the antenna is placed on top of the antenna, and when both diodes are in the off state, it provides an omnidirectional pattern. Similarly, when  $D_1$  is OFF and  $D_2$  is ON, the pattern tilts to the negative X direction, and the opposite scenario happens to mode 3, as shown in Fig. 4.8 (b and c), respectively.

# 4.5 Comparison of Proposed frequency and pattern reconfigurable antennas with existing structures

To explore the contribution of this design compared to existing designs listed in Table 4.2, As refs [42] and [96] are small in size and have achieved frequency and pattern but have not achieved an omnidirectional pattern, the antenna gain is also low. A high gain with omnidirectional patterns is achieved in refs [97] and [98] but is limited to pattern tilting with larger dimensions. However, the proposed structure provides frequency and pattern reconfigurability with a smaller size and omnidirectional pattern.

**Table 4.2.** Comparison of proposed frequency and pattern reconfigurable with existing structures

Ref No	Size (mm³)	Operatio n frequenc y (GHz)	No. of diodes	Reconfigura ble property	Omni/dire ctional patterns achieved (yes/No)	Realized gain (dBi)	Radiation efficiency (%)
[21]	59x32x0.8	3.5	2	P	Yes	2.13-4.93	62-82
[42]	14x15x0.787	3.55	4	F/P	No	1.23-2.39	NG
[97]	70x38	2.4	3	P	Yes	4	80
[96]	23x31	3.8	2	F/P	No	2-3	NG
Propos ed	35x28x1.52	5, 4.3	2	F/P	Yes	2.54-4.55	80-90

F/P: Frequency and pattern, P: Pattern only, NG: Not Given

#### 4.6 Summary

This chapter reports a frequency- and pattern-reconfigurable antenna using two PIN diodes for IoT close-range devices. The proposed structure provides omnidirectional and directional patterns that operate at 5 GHz and 4.3 GHz, respectively, at three distant modes by connecting and disconnecting the two parasitic stubs on the ground plane through two PIN diodes. The proposed structure could be used for IoT close-range applications with this performance. However, it limits to three modes of operation and depends on the ground length.

#### **CHAPTER 5**

Design and analysis of Compound/Hybrid reconfigurable antenna for Sub 6 GHz wireless standards and Vehicular applications

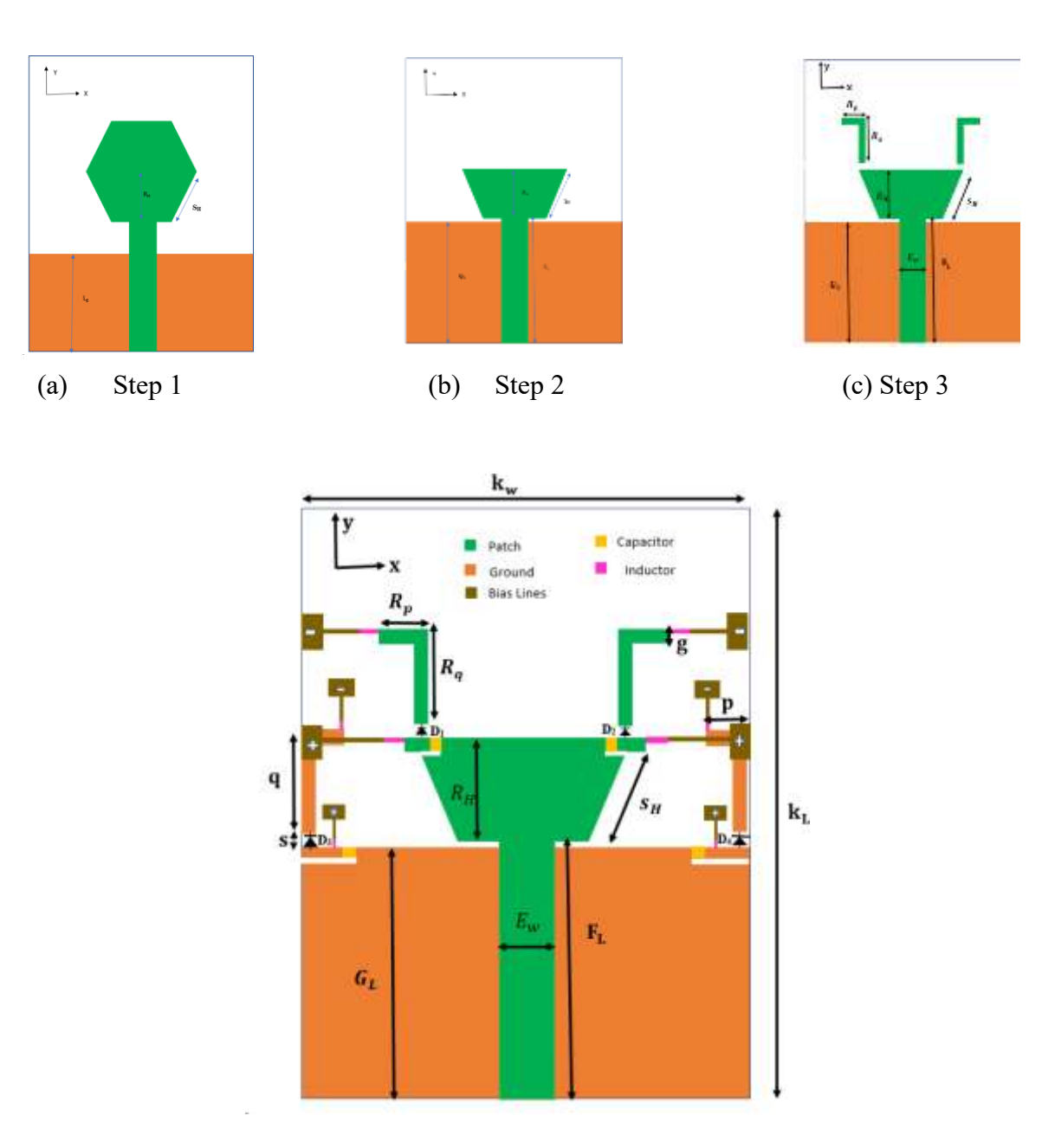
#### 5.1 Introduction

This thesis chapter aims to design and analyze compound reconfigurable antenna with compact size and wideband operation for Sub 6 GHz wireless standards and vehicular applications. It is achieved by implementing a half-hexagonal-shaped radiating element and two inverted L-shaped parasitic stubs. These stubs are connected to two PIN diodes, allowing for control over frequency. An additional pair of PIN diodes incorporates analogous parasitic stubs into the ground plane to facilitate pattern tilting and polarization. Switching these PIN diodes across seven Operating States (OS) allows the antenna structure to resonate in a single band, spanning 4.5-5.8 GHz (sub-6 GHz higher band), with an omnidirectional pattern specific to OS1. In OS2 and OS3, the antenna resonates in a single band within the range of 4.1–5.7 GHz, featuring beam tilting with linear polarization. In OS4 and OS5, the structure has two bands: one covers 3.3–4.2 GHz (5G-n77 band) with linear polarization, and the other covers 5.1–6.1 GHz (5G WLAN band) with right-hand circular polarization (RHCP) in OS5 and lefthand circular polarization (LHCP) in OS4 with an axial ratio bandwidth of 14.5%, including pattern tilting within the range of  $\pm$  34°. Finally, the OS6 and OS7 structures introduce dual bands of 3.3–3.8 GHz (5G-n78 band) and 4.8-5.8 GHz (sub-6 GHz higher band). Both bands feature LHCP/RHCP with an axial ratio bandwidth of 8.57% for the lower resonant band and 7.4% for the higher resonant band. Additionally, it incorporates radiation pattern reconfiguration capabilities. The structure is printed on an FR-4 substrate and measures various associated parameters.

Section 5.2 details the design and its mathematical analysis of the proposed radiating structures, and simulated and measured results of various operating states are discussed in section 5.3. Finally, a summary of proposed reconfigurable antennas is reported in the last section.

#### 5.2 Design Evaluation of Compound Reconfigurable Antenna

The step-by-step design evaluation of a compound reconfigurable antenna is presented in Fig. 5.1. The patch, ground, and parasitic stubs are printed on the 1.6-mm-thick FR-4 material with a relative permittivity ( $\varepsilon_r$ ) of 4.4. Initially, a hexagonal-shaped monopole antenna is designed to operate at 3.8 GHz [95], as shown in Fig.5.1 (a). As step 2 in Fig.5.1(b) shows, the ground length is altered to improve impedance matching, and half of the hexagonal is removed for frequency reconfigurability. Further, two inverted parasitic stubs are connected to a half-hexagonal-shaped radiating element through two PIN diodes for the frequency reconfigurable capability of the proposed structure.



(d) Proposed compound reconfigurable antenna (CRA)

Fig.5.1. Step-by-step design evolution of proposed compound reconfigurable antenna

The stub lengths are selected so that the radiating structure's overall length of the radiating element is nearly a quarter of the wavelength of the lowest working frequency. The antenna's lowest operating frequency,  $f_{Lo} = 3.5$  GHz, can be calculated by the following equation [99]:

$$f_{LO} = \frac{c}{4L\sqrt{\varepsilon_{eff}}} \tag{5.1}$$

where c is the speed of light, L is the overall length of the monopole, and this value is considered as  $L=R_H+R_p+R_q$ , in this structure and the effective permittivity  $\varepsilon_{eff}$  is given by,

$$\varepsilon_{eff} = \frac{\varepsilon_r + 1}{2} + \frac{\varepsilon_r - 1}{2} \left( 1 + 12 \left( \frac{w}{h} \right) \right)^{-0.5} \tag{5.2}$$

Where w is the width of the monopole, and h is the substrate thickness.

Finally, by adding inverted L-shaped parasitic stubs in the ground plane [43] through two more PIN diodes, different senses of polarization and pattern tilting are obtained, as shown in Fig. 5.1(d).

**Table 5. 1:** CRA Geometrical Dimensions (mm)

Parameter	Value (mm)	Parameter	Value (mm)
$k_L$	36	SH	6.065
$k_{\scriptscriptstyle W}$	30	$R_H$	5.252
$F_L$	16	g	1
$E_{W}$	3	q	6.25
$G_L$	15.5	p	3
S	0.75	$R_p$	3

Table 5.2: Operating States of proposed CRA

Operating State	Diode Status					
(OS)	$D_1$	$D_2$	<b>D</b> 3	$D_4$		
OS1	0	0	0	0		
OS2	0	0	0	1		
OS3	0	0	1	0		
OS4	0	1	0	0		
OS5	1	0	0	0		
OS6	0	1	0	1		
OS7	1	0	1	0		

The length of the stub is chosen so that the overall length of the radiating element is almost a quarter wavelength of the lowest operating frequency. The overall structure is simple and compact in size. In Table 5.2, seven operating states are listed. From this table, 0 indicates the diode is in an OFF state, and 1 indicates the diode is in an ON state.

## 5.2.1 Parametric study on parasitic stub length (p) to obtain the axial ratio (AR) below 3 dB at operating frequencies

Ground parasitic stubs are optimised to achieve the desired level of  $S_{11}$  (less than -10 dB) and axial ratio (less than 3 dB) within the desired frequency bands. In order to attain a balanced outcome between these two properties, a trade-off is made in selecting the optimal value for parameter p. For this purpose, the values of p are varied from 1 mm to 5 mm, and the respective reflection coefficient (S11) and axial ratio (dB) curves are shown in Fig. 3. (a and b), respectively. As shown in Fig. 3, at p = 3 mm, the antenna resonance impedance bandwidth perfectly matches the 3 dB AR resonance bandwidth, while the remaining p values do not match. Therefore, in this structure, p = 3 mm will be finalized.

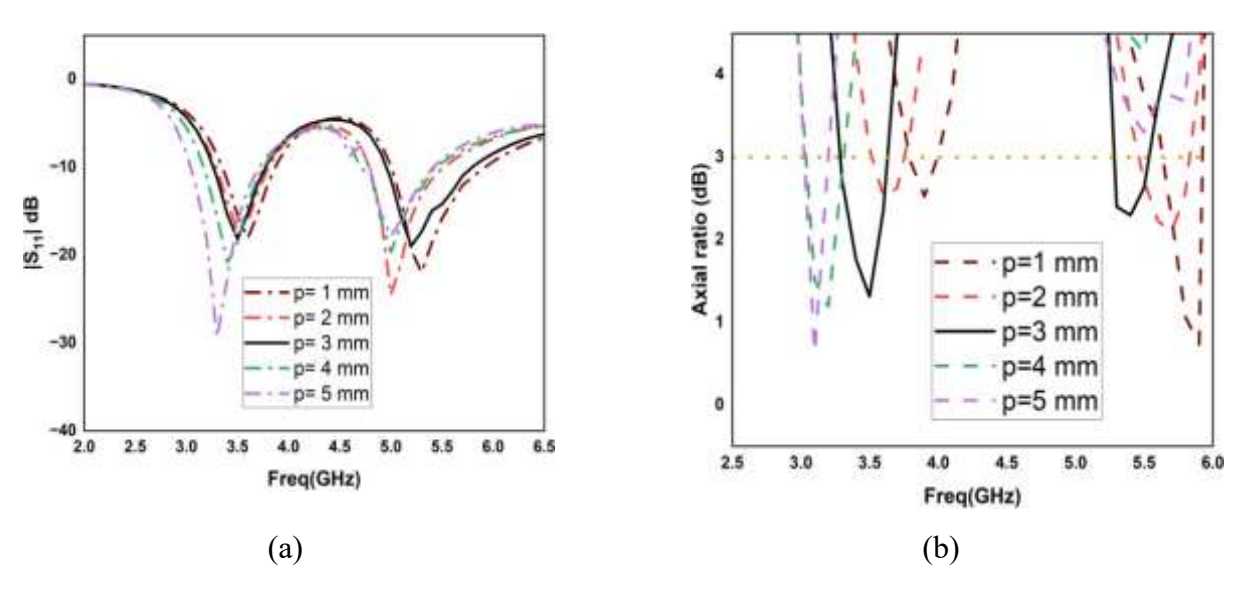
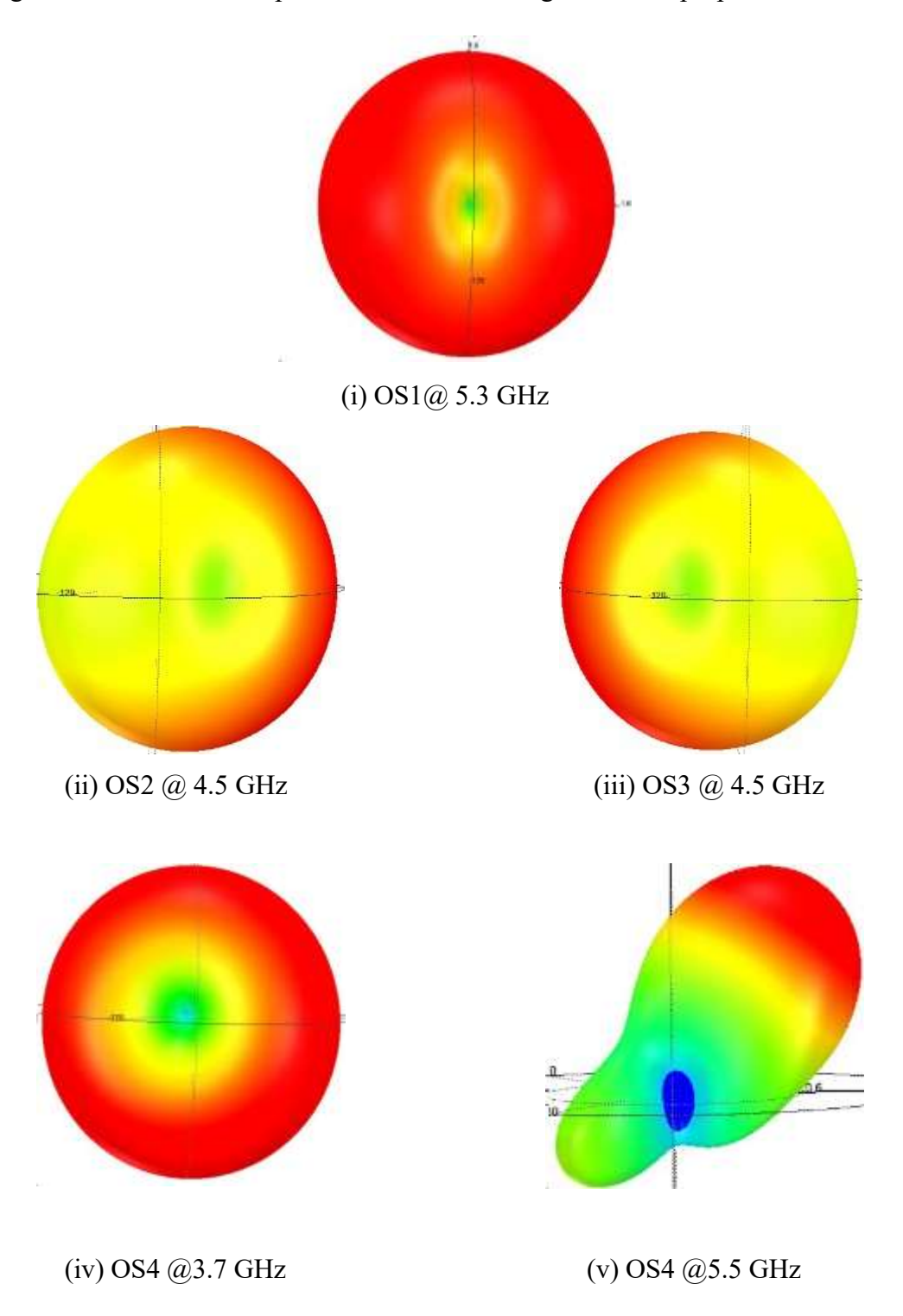


Fig. 5.2. Simulated (a) S<sub>11</sub> and (b) Axial Ratio (AR) variation with a length of a parameter (p)

### 5.2.2 Analysis of radiation pattern and polarization of the compound reconfigurable antenna

Different pattern diversity properties, such as omnidirectional and directional patterns, are necessary for 5G wireless standards and automotive applications [100]. In the proposed structure, the two inverted L-shaped parasitic stubs in the ground plane add more radiating cavities, and thus, by adjusting the phase difference between these two cavities, beam switching can be achieved [43]. In OS1, only the main radiator is excited, and it is centrally symmetric; therefore, the radiation pattern is omnidirectional, as shown in Fig. 5.3(i). In OS 3 (Fig. 5.3 (iii)), when the right-hand parasitic stub is connected but the left-handed parasitic stub is disconnected in the ground plane, the pattern tilts

towards the -x direction since the connected respective stub is acting as a reflector and the other one is acting as a director. In a similarly way, in OS 2 (Fig. 5.3 (ii)), when the left-hand parasitic stub is connected but the right-handed parasitic stub is disconnected in the ground plane, the pattern tilts towards the x direction, i.e., it pushes the pattern in the opposite direction. Similarly, in the remaining operating states, tilted radiation patterns are shown in Fig. 5.3 of the proposed structure.



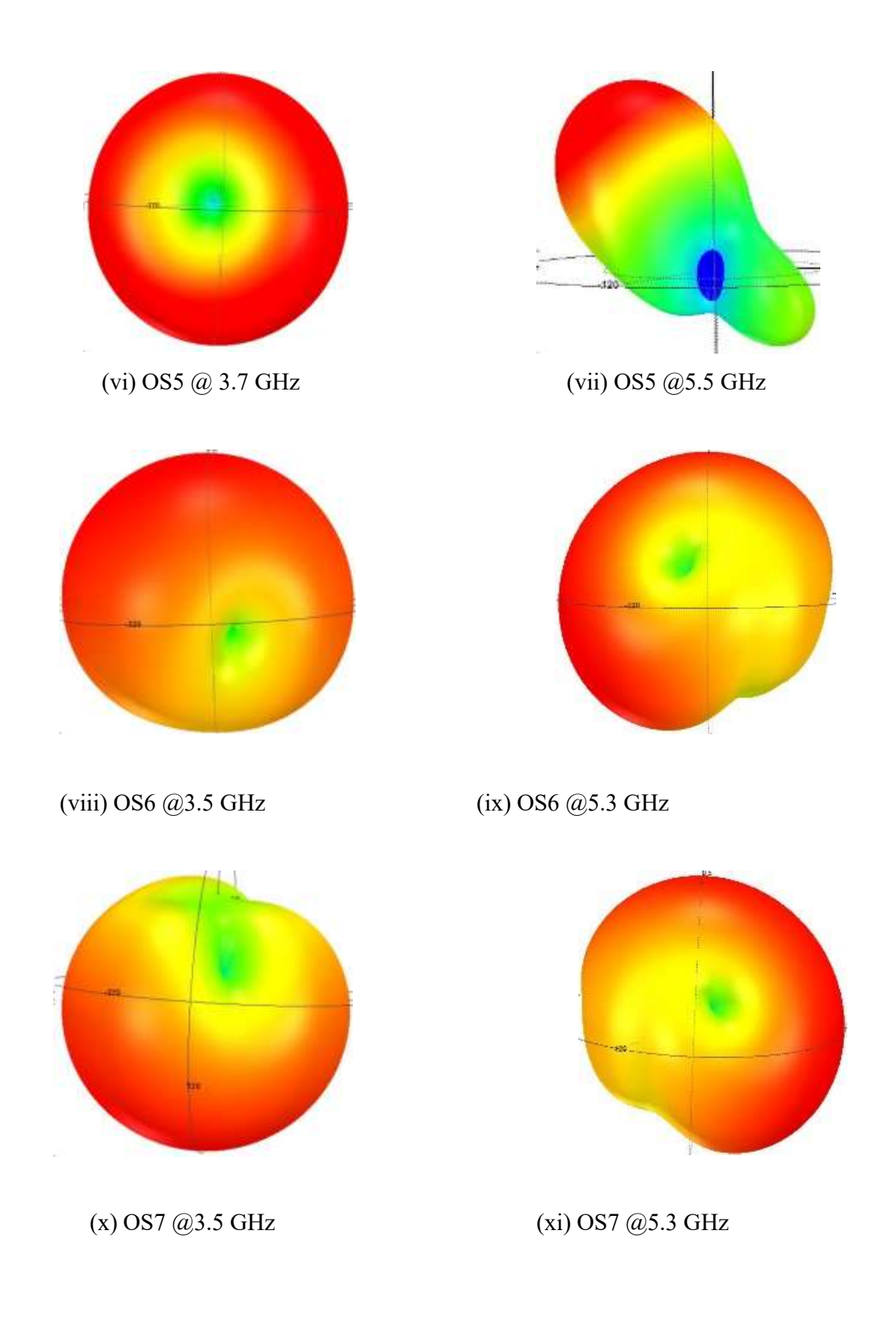


Fig 5.3. The 3D polar plot radiation patterns for pattern tilting in various operating states (i-xi)

For the polarization capability of the proposed CRA, the surface currents are analysed in OS4 (0100) and OS6 (0101), respectively, as shown in Fig. 5.4. The surface current distribution on an antenna determines the orientation of the electric field, and thus the polarization of the radiated electromagnetic wave could be observed. Linear polarization is achieved when the surface current flows along a straight line or in a linear direction. Meanwhile, circular polarization occurs when the surface current rotates in a circular pattern as it propagates.

In, Fig. 5.4 (a), the surface current distribution at the center frequency of 3.7 GHz (lower band) in OS4 (0100) is represented. At this frequency, the right-hand radiating patch parasitic stub is responsible for polarization since the diode  $D_2$  is ON and the remaining diodes are OFF. The maximum surface current direction at phi =  $45^{\circ}$  is +y (vertically up), and at phi =  $135^{\circ}$ , it is -y (vertically down). This frequency has no +x or -x (horizontal) movement of the maximum surface current. Generally, for circular polarization, both horizontal and vertical movements of surface currents are required [33]. Therefore, the proposed structure at this frequency provides linear polarization. The surface current distribution at 5.5 GHz in OS4 (0100) is shown in Fig. 5.4 (b). The responsible portion of this frequency is a half-hexagonal-shaped radiating element.

The maximum surface current direction is at phi =  $45^{\circ}$  in the -x direction, at phi =  $135^{\circ}$  in the +y direction, at phi =  $225^{\circ}$  in the +x direction, and at phi =  $315^{\circ}$  in the -y direction, respectively. Therefore, the surface currents rotate clockwise, i.e., LHCP is obtained in the +z direction. Fig. 5.4 (a) shows the surface current distribution of OS 6 (0101) at a center frequency of 3.5 GHz. One can easily observe that in OS 4 (0100), at the lower band, CP is not generated, but in OS 6 (0101), CP is generated due to the ground plane's right-side parasitic stub. This stub is responsible for generating the horizontal component, which in turn generates CP. Therefore, the right-side parasitic stubs on the ground plane and radiating plane are the primary targets for the analysis of surface currents.

At phi =  $45^{\circ}$ , the maximum surface current is moving in the -x direction in the ground plane, and at phi =  $135^{\circ}$ , the surface currents in the ground plane cancel each other due to out-of-phase movements. The maximum surface current direction is correct, radiating the parasitic stub towards the -y direction. In contrast, the surface currents at phi =  $225^{\circ}$  and phi =  $315^{\circ}$  are opposite concerning those at phi =  $45^{\circ}$  and  $135^{\circ}$ , respectively. Therefore, the surface currents rotate in an anti-clockwise direction, i.e., RHCP is obtained in the +z direction, as shown in Fig. 5.4 (c). For 5.3 GHz, i.e., the upper band in OS4 (0101), the more responsible part for analyzing polarization is the half-hexagonal shape d radiating element. At phi =  $45^{\circ}$ , the maximum surface current is moving in the -x direction in the half-hexagonal-shaped radiating element, and at phi =  $135^{\circ}$ , the surface currents are moving in the positive y direction.

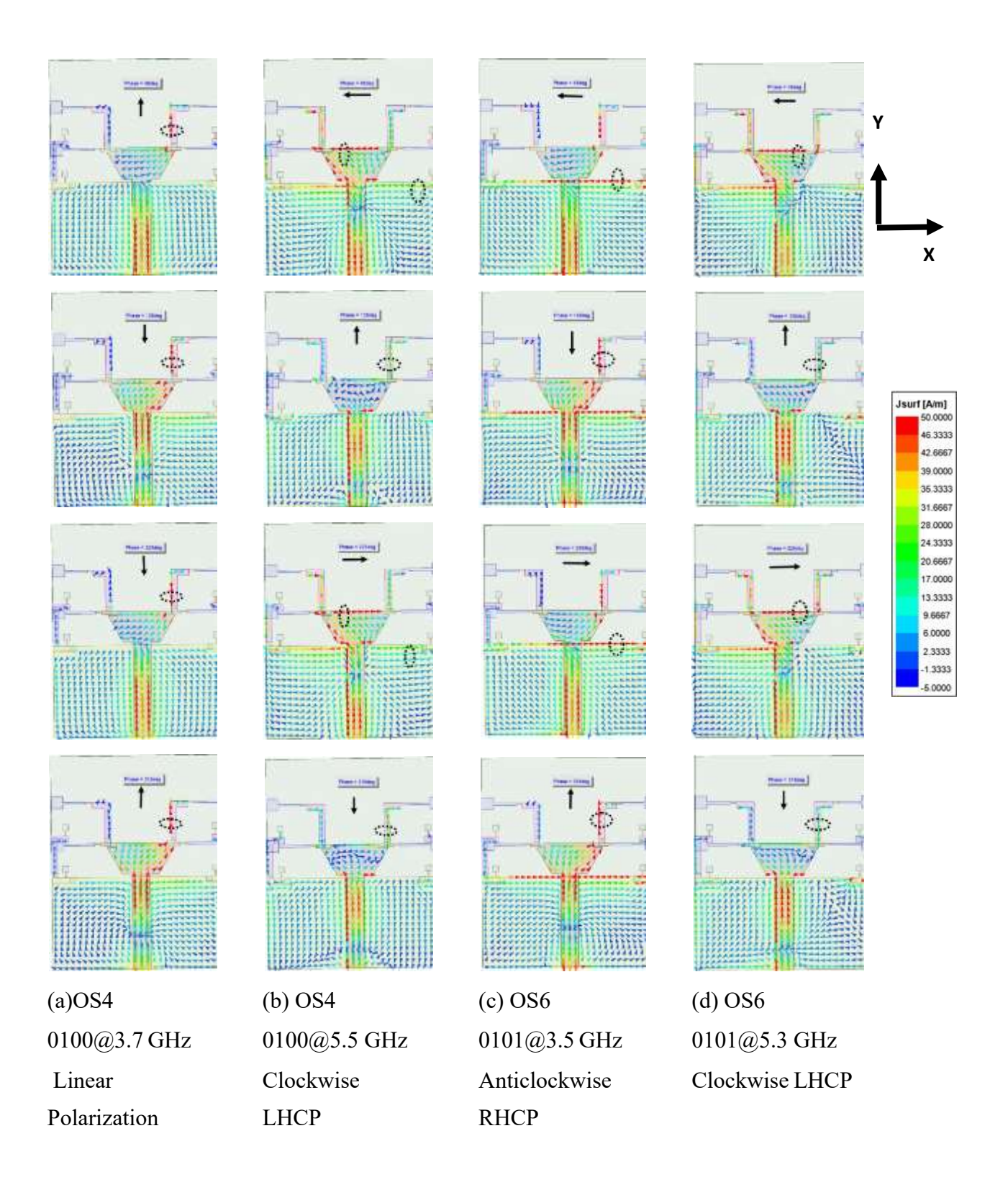


Fig. 5.4 Simulated surface current distribution for OS4(0100) and OS6 (0101)

Therefore, the surface currents are rotating clockwise, i.e., LHCP is obtained in the +z direction, as shown in Fig. 5(d). Due to the symmetry of this structure, one can quickly identify the polarization status in OS 5 (1000) and OS7 (1010).

#### 5.2.3 Analysis of |S<sub>11</sub>| in Ansys circuit using S2P files of PIN diodes

Initially, the antenna is designed and simulated in Ansys HFSS, considering the PIN diode equivalent model as a lumped RLC value. After that, the proposed design is imported into the Ansys circuit and uses s2p files of the PIN diode containing the scattering parameters provided by the manufacturer instead of lumped RLC values to simulate  $|S_{11}|$  dBs in all operating states, including with the RF choke inductor, DC blocking capacitor, and biasing lines. The following subsections show that almost all the simulated  $|S_{11}|$  dBs in Ansys HFSS and Ansys circuits in all operating states match the measured values. Fig. 5.5 displays the circuit simulation diagram for OS 7 (1010).

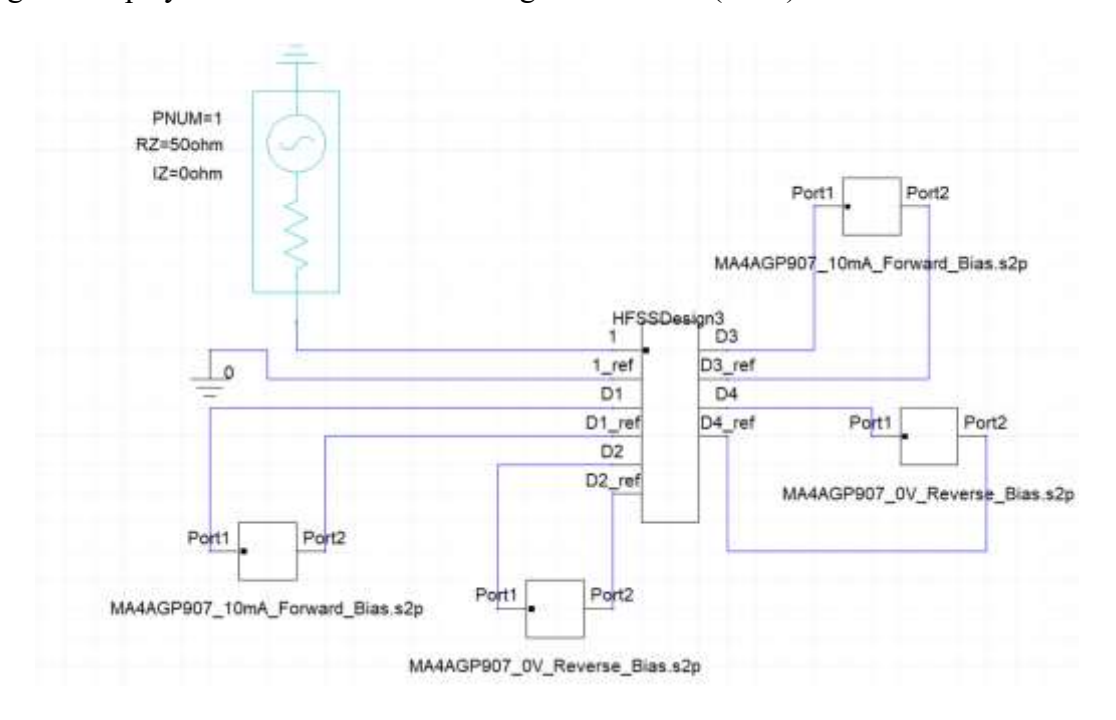


Fig. 5.5. Simulated circuit representation of OS7 (1010) in Ansys circuit

#### 5.3 Experimental validation of simulated results in three modes

#### **5.3.1 Operating state 1 (0000)**

In this operating state, all diodes are off, and the proposed structure resonance at 5.3 GHz (the maximum surface current accumulates in the half-hexagonal-shaped radiating patch) with a measured impedance bandwidth below -10 dB of 18.86% (4.8–5.8 GHz). The experimented and simulated reflection coefficient  $|S_{11}|$  dB in OS1 of the proposed CRA is shown in Fig. 5.6 (a). At the same time, the radiation efficiency and peak realized gain are 85.2% and 1.55 dBi, respectively, as shown in Fig. 5.6 (b).

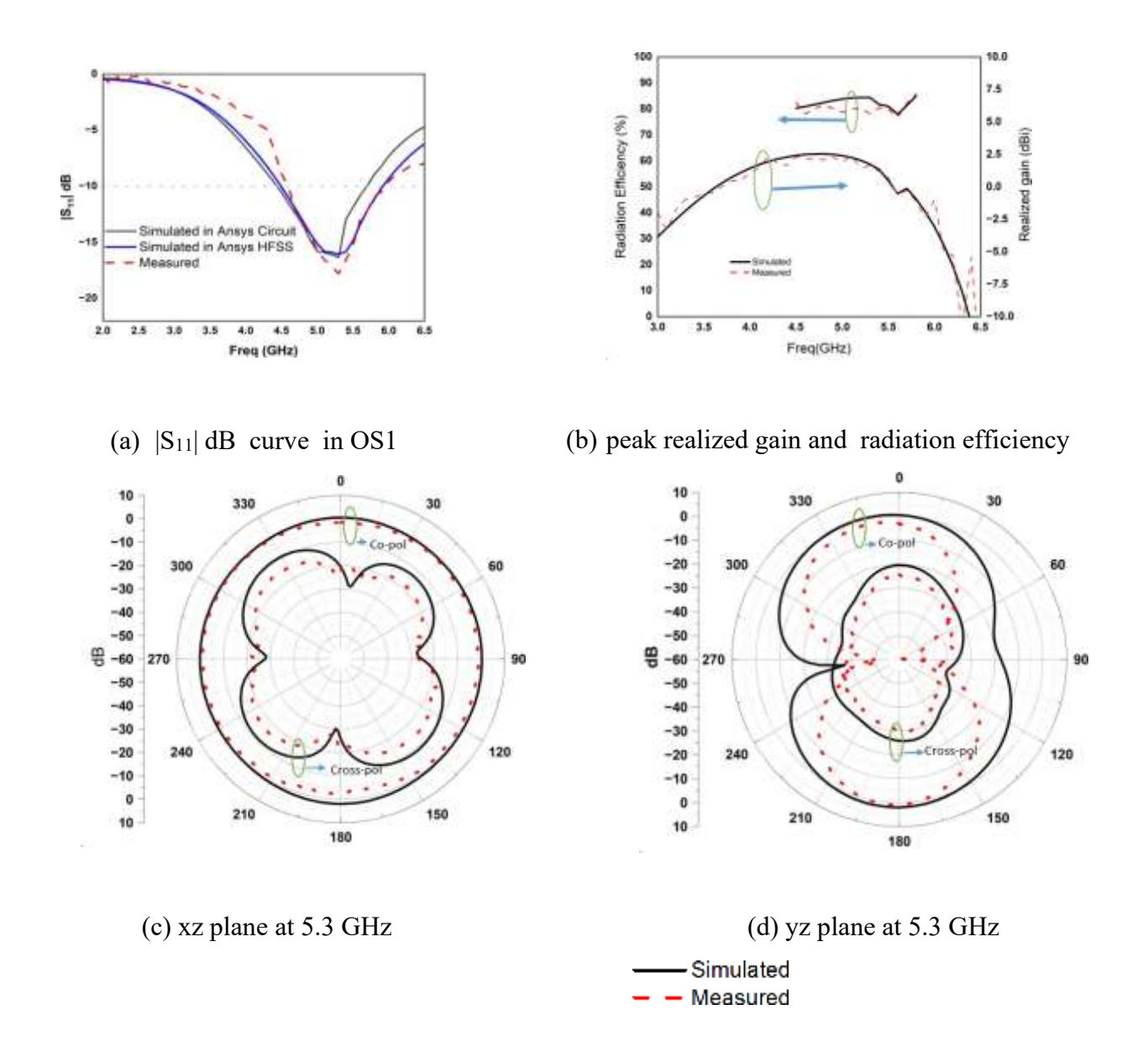


Fig. 5.6. The experimental and simulated results of the proposed structure in OS1 (0000)

Moreover, Fig. 5.6 (c and d) shows the experimented and measured co- and cross-polarization radiation patterns in the xz and yz planes, respectively. The cross-pol value is as low as -12 dB in the H plane and -30 dB in the E plane. The experimental results are similar to the simulated results, with minor variations due to the soldering of other components on the radiating structure.

#### **5.3.2** Operating state 2 (0001) & Operating state 3 (0010)

In this operating state, if any one of the diodes, either D<sub>3</sub> or D<sub>4</sub>, is ON in the ground plane and the remaining diodes are OFF, the proposed structure resonates at 4.5 GHz with a measured -10 dB impedance bandwidth of 35.5% (4.1 - 5.7 GHz), as shown in Fig. 5.7 (a). while the radiation efficiency in this operating state is approximately 85%, and the realized gain is 3.57 dBi, as shown in

Fig. 5.7 (b). The measured cross-polarization level is below -30 dB in the xz plane at 4.5 GHz (0001/0010), as shown in Fig. 5.7 (c and d), respectively. When D<sub>4</sub> (0001) is on, and the remaining diodes are off, the respective parasitic stub works as a reflector; that is, it pushes the radiation pattern in the reverse direction (towards the -x- direction), as shown in Fig. 5.7 (c). Similarly, when D<sub>3</sub> (0010) is ON, and the remaining diodes are OFF, the respective parasitic stub works as a reflector; that is, it pushes the radiation pattern in the reverse direction (towards +x-direction), as shown in Fig. 5.7 (d). In OS 2 and 3, the pattern tilts independent of the frequency.

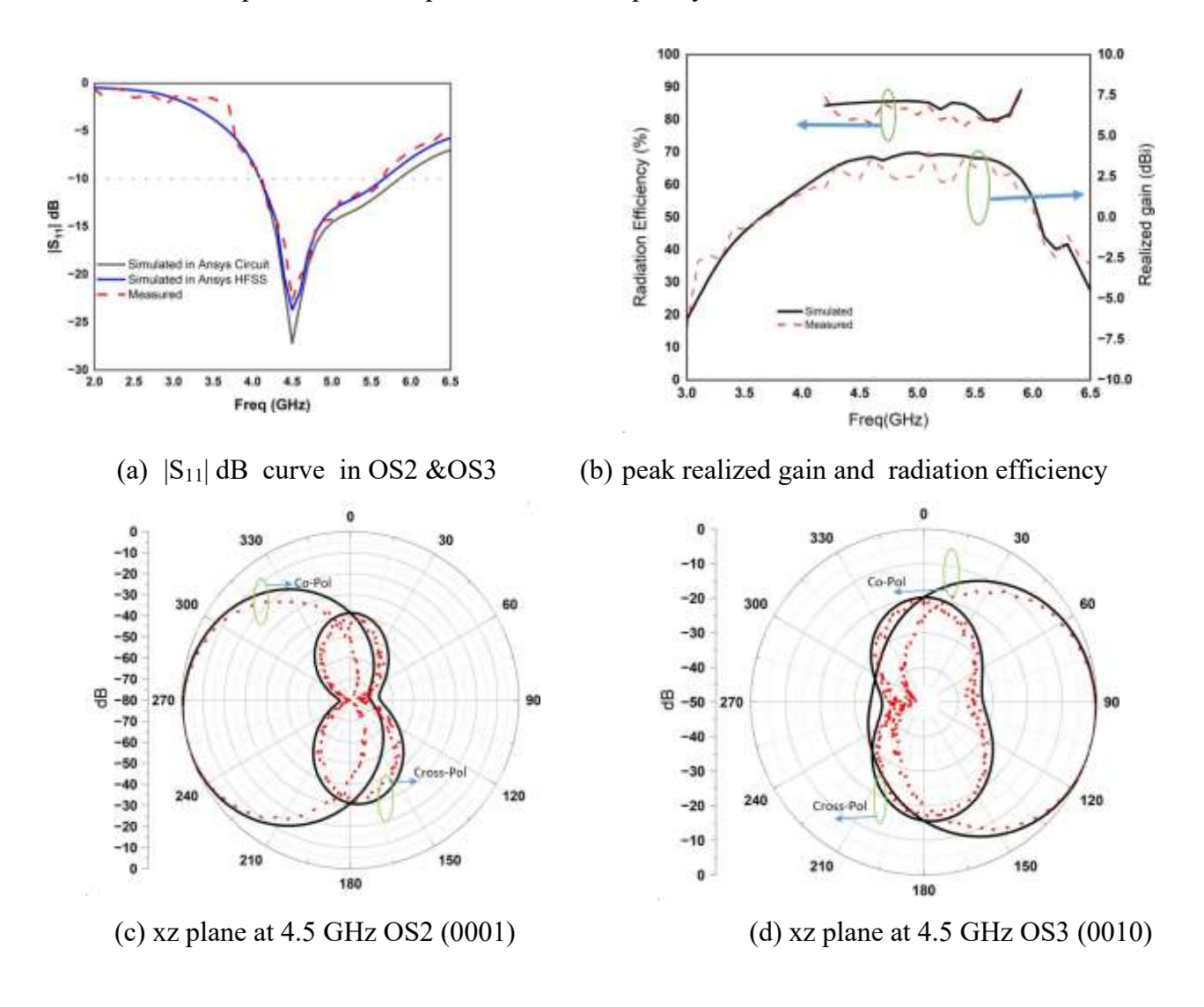


Fig.5.7. The experimental and simulated results of the proposed structure in OS2 (0001) & OS3 (0010)

#### **5.3.3** Operating state 4 (0100) & Operating state 5 (1000)

Due to an asymmetrical current flowing in the radiating structure, parasitic stubs in the OS 4 & OS 5 dual band are obtained. The lower band is obtained mainly due to the left/right radiating parasitic stub (1000/0100), and the higher band is due to the half-hexagonal-shaped radiating element. Specifically, in the indoor wireless system, an omnidirectional pattern is required for the control link at a lower

frequency band, and at a higher band for data transmission, a directional pattern is required. So, in this operating state, the proposed structure provides the required characteristics suitable for indoor 5G wireless standards. The experimental and simulated reflection coefficient |S<sub>11</sub>| dB curves are shown in Fig. 5.8 (a). The measured impedance bandwidth at the lower band is 24.3% (3.3–4.2 GHz) and 18.18% (5.1–6.1 GHz) at the higher band, respectively. The radiation efficiency and realized gain are 84% and 1.89 dBi at 3.7 GHz and 82% and 2.21 dBi at 5.5 GHz, respectively, as shown in Fig. 5.8 (b). Moreover, the simulated and measured co- and cross-polarization levels at 3.7 GHz are below -30 dB in the xz plane and -50 dB in the yz plane, respectively, as shown in Figs. 5.8 (c and d), respectively. Fig. 5.9 presents the simulated and measured normalized LHCP and RHCP gain plots in OS4 (0100) & OS5 (1000) at 5.5 GHz, respectively. At this frequency, the structure provides LHCP in a clockwise direction, as shown in the surface current distribution shown in Fig. 5.4 (b). Due to the symmetry of the proposed structure, OS 5 (1000) provides RHCP at 5.5 GHz since the surface current direction is anticlockwise.

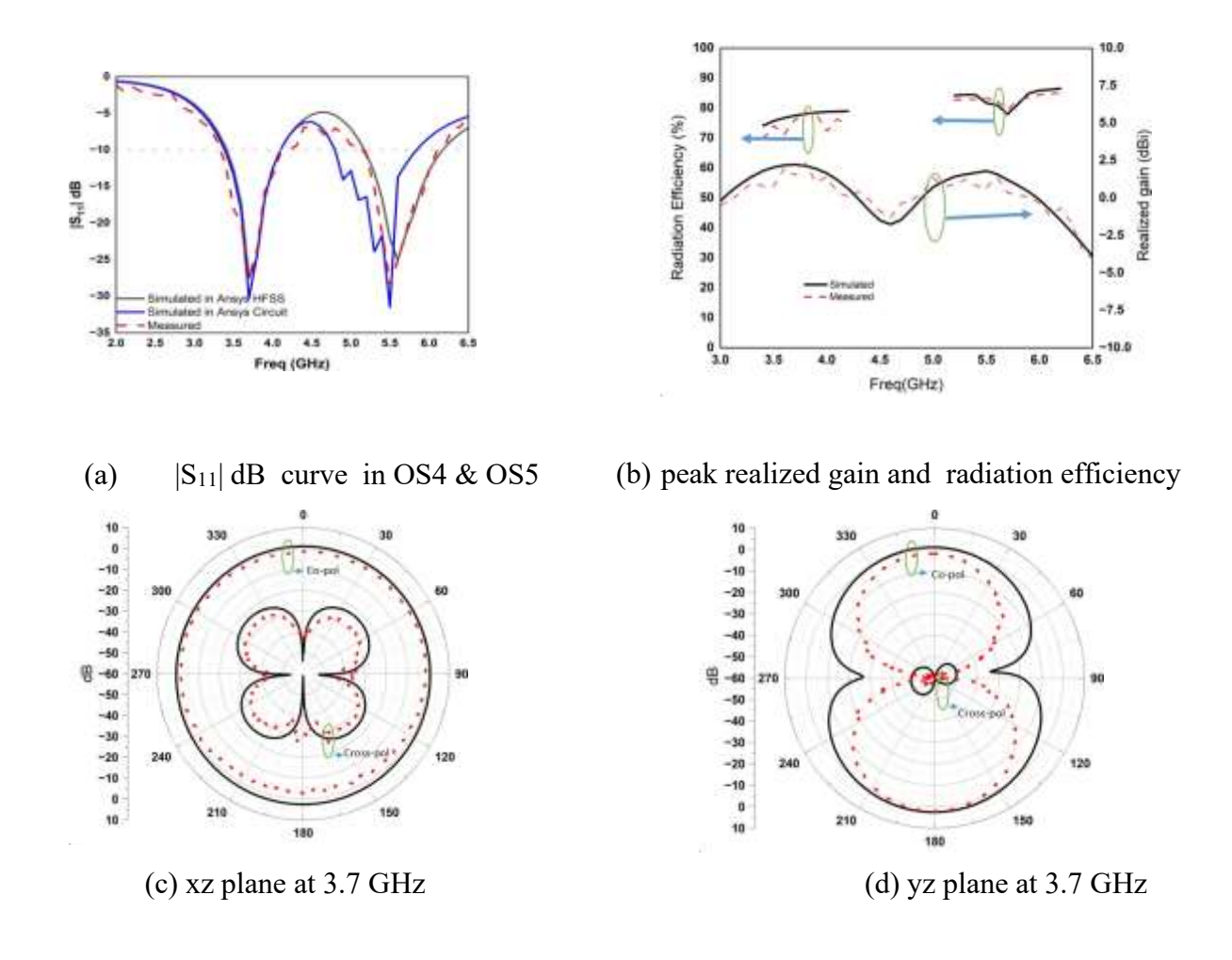


Fig.5.8. The experimental and simulated results of the proposed structure in OS4 (0100)/ OS5(1000) for linear polarization @ 3.7 GHz

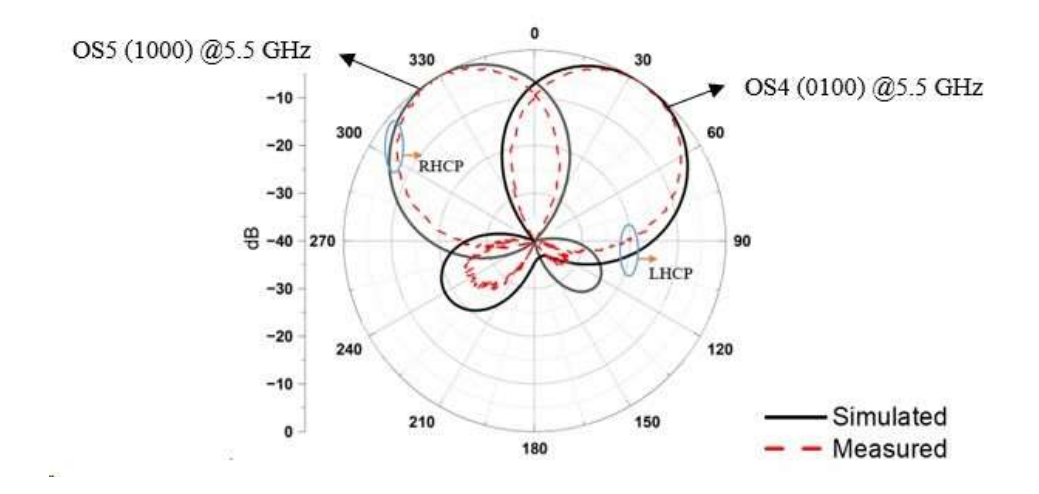
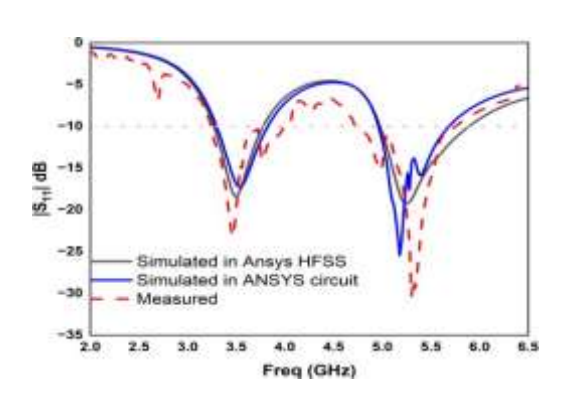
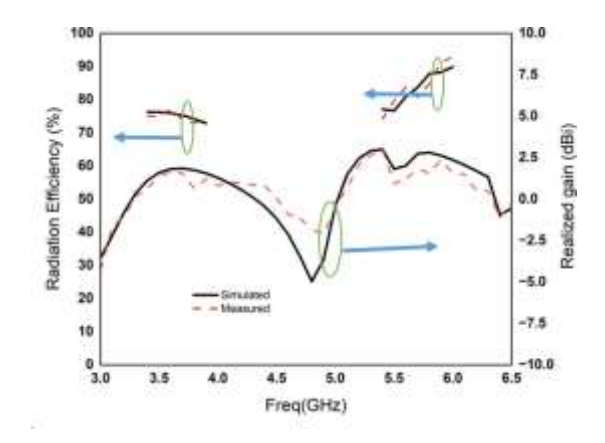


Fig.5.9. The experimented and simulated normalized LHCP/RHCP gain patterns in OS4 (0100)/ OS5(1000)

#### **5.3.4** Operating state 6 (0101) & Operating state 7 (1010)

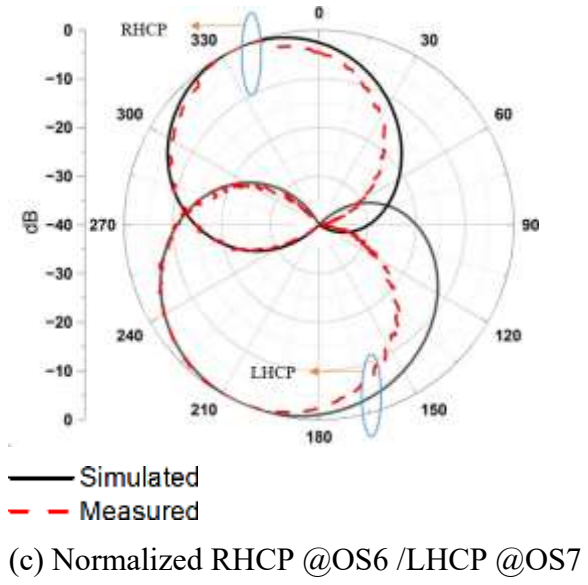
Fig. 5.10 (a) shows the experimental and simulated reflection coefficient |S<sub>11</sub>| dB. The measured impedance bandwidth at the lower band is 20% (3.3–4 GHz) and at the upper band is 18.86% (4.8–5.8 GHz), while the radiation efficiency is 78% and 80%, respectively. Moreover, the realized gain at 3.5 GHz is 1.49 dBi and at 5.3 GHz is 1.8 dBi, respectively, as shown in Fig. 5.10 (b), respectively. The radiation efficiency and realized gain are reduced compared to the previous operating state due to the increased number of diodes in the ON state.

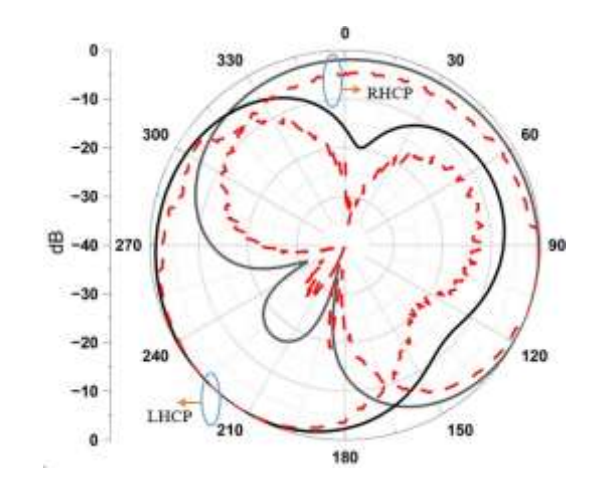




(a)  $|S_{11}|$  dB curve in OS6 & OS7

(b) peak realized gain and radiation efficiency





- (c) Normalized RHCP @OS6 /LHCP @OS7 realized gain patterns @ 3.5 GHz
- (d) Normalized LHCP @OS6/RHCP @ OS 7 realized gain patterns @ 5.3 GHz

Fig. 5.10. The experimented and simulated results of the proposed structure in OS6 (0101) & OS7 (1010)

The experiment and simulated normalized LHCP and RHCP gains for OS6 (0101) at 3.5 GHz and 5.3 GHz are shown in Fig.5.10 (c & d), respectively, and they mirror each other. Dual bands with different senses of polarization are useful in satellite communication applications.

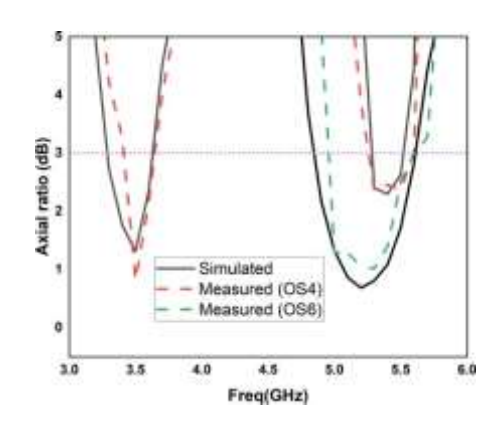


Fig. 5.11. The simulated and experimental axial ratios in OS4 (0100) and OS6 (0101)

Further, the axial ratios of OS4 (0100) and OS6 (0101) are shown in Fig. 5.11. In OS4 (0100), the measured 3dB axial ratio bandwidth is 14.5% (4.9–5.7 GHz) with respect to the center frequency of 5.5 GHz, which includes LHCP. Similarly, in OS6 (0101), the 3dB axial ratio bandwidth is 8.57% (3.3–3.6 GHz) with a center frequency of 3.5 GHz, including RHCP mode, and 7.54% (5.2–5.6 GHz) with a center frequency of 5.3 GHz, including LHCP mode.

When the biasing conditions of PIN diodes are reversed, an opposite sense of polarization is obtained; for example, OS5 (1000) obtained the RHCP at 5.5 GHz.

The fabricated compound reconfigurable antenna with top and bottom views is shown in Fig. 5.12, along with the biasing wires. The LPKF S-63 PCB machine fabricates the proposed structure on FR-4 substrate. After that, the diodes, capacitors, inductors, and SMA connectors are soldered. The S-parameters are measured using R&ZNB 40 VNA for different operating states, as shown in Fig. 5.13 (a). For the diode ON condition, a current of 10 mA and a voltage of 1.3 volts are required, as per the data sheet [38]. Therefore, the same value is provided using the DC power supply and current measured using DMM, as shown in Fig. 5.13 (b), and for the OFF condition, it provided zero volts from the DC power supply. Fig. 5.13 (c) illustrates the pattern measurement setup.

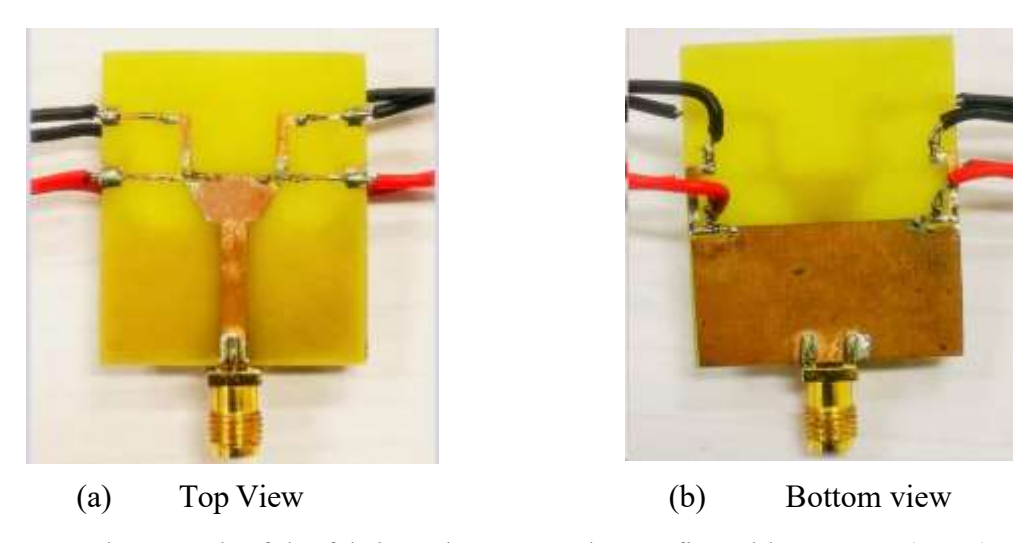
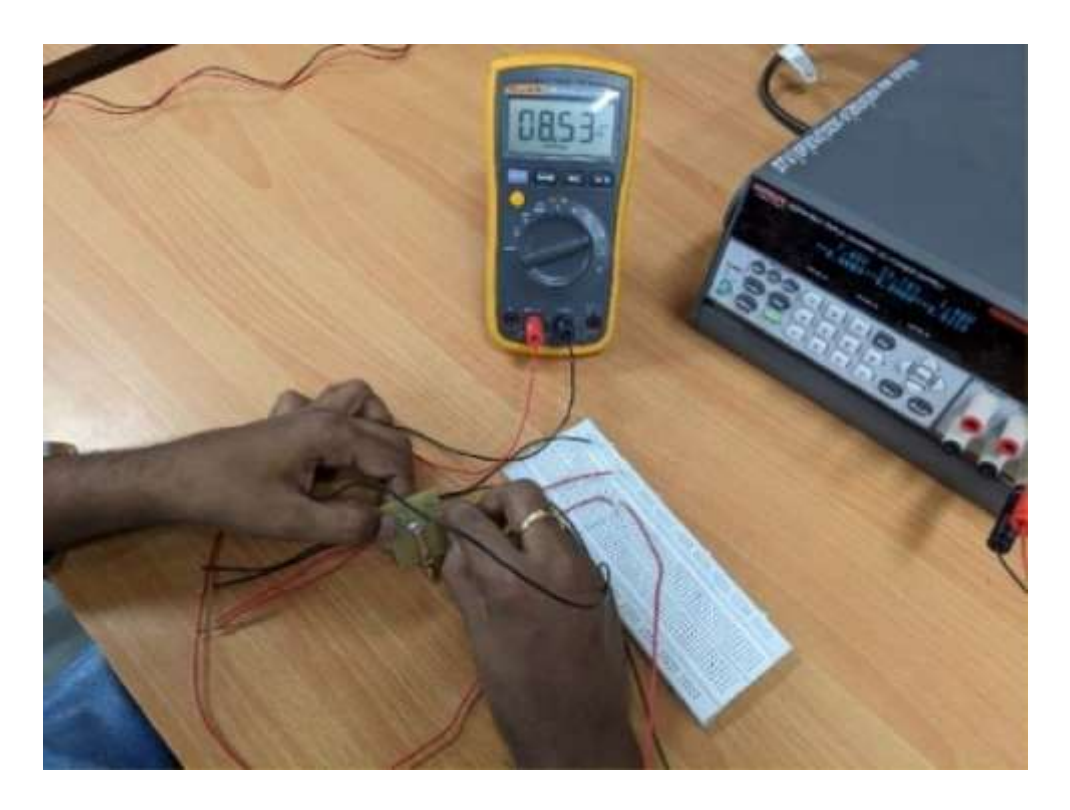


Fig. 5.12. Photograph of the fabricated compound reconfigurable antenna (CRA)



(a) S-parameter measurement



(b) ON state current measurement



(c) Pattern measurement

Fig 5.13. Measurement setup of proposed CRA

Table 5.3 encapsulates the performance characteristics of the proposed structure. The proposed structure in OS 1 (0000) provides an omnidirectional pattern with linear polarization at a centre frequency of 5.3 GHz. In OS 6 (0101), its resonant dual band one at 3.5 GHz and the other at 5.3 GHz. At 5.3 GHz, it provides a pattern tilting towards the left with left hand circular polarization. In OS7 (1010), it resonant dual band, one at 3.5 GHz and the other at 5.3 GHz. At 5.3 GHz, it provides a

pattern tilting towards the right with right hand circular polarization. Therefore, from the above analysis, in operating states (OS 1,6 & 7), the frequency is the same i.e., 5.3 GHz, but the pattern and polarization are changing. In OS2 (0001), it provides a right tilted pattern with linear polarization and in OS 4 (0100) providing a right tilted pattern but frequency and polarization are changing, i.e., the pattern is the same but frequency and polarization are changing. In OS 4 & 5, the structure provides a dual band and a different sense of polarization with good radiation pattern characteristics. These types of characteristics of an antenna are more useful in vehicular communication.

**Table 5.3**: The performance characteristics of CRA in seven operating states

Operating	Diode Status		Resonant	Frequency Range	Pattern Mode	Polarization		
State	$D_1$	$D_2$	<i>D</i> <sub>3</sub>	$D_4$	Frequenc			Status
					у			
					(GHz)			
OS1	0	0	0	0	5.3	4.5-5.8GHz (Sub	Omnidirectional	LP
						6 GHz higher		
						band)		
OS2	0	0	0	1	4.5	4.1-5.7GHz	Right end-fire	LP
	0	0	1	0		(Satellite	Left end-fire	LP
OS3						Communication		
						Band)		
OS4	0	1	0	0	3.7, 5.5	3.3-4.2GHz (5G-	Omnidirectional,	LP@3.7GHz
						N77 band) and	Right tilted	LHCP@5.5G
OS5						5.1-6.1GHz (5G		Hz
	1	0	0	0		WLAN band)	Omnidirectional,	LP@3.7GHz
							Left tilted	RHCP@5.5G
								Hz
OS6	0	1	0	1	3.5, 5.3	3.3-3.8 GHz (5G-	Left tilted	RHCP
						N78 band) and		@3.5GHz
OS7						4.8-5.8 GHz (Sub		LHCP
						6 GHz higher		@5.3GHz
	1	0	1	0		band)	Right tilted	LHCP
								@3.5GHz
								RHCP
								@5.3GHz

#### 5.4 Comparison of the compound reconfigurable antenna with existing structures

A comparison of existing compound reconfigurable antennas with the proposed design is tabulated in Table 5.4. The proposed structure, which has few PIN diodes, is low-cost and provides a simple working principle. It also provides CP at dual bands and achieves all polarization states with pattern capability. The work reported in [101] used a low number of diodes but did not achieve all three polarization states or have pattern-tilting capability.

**Table 5.4:** Comparison of the compound reconfigurable antenna with the existing structures

Ref	Antenna Size	N	N	ND	ARBW	A	Achieved	Pattern	Efficiency	Peak
No.	(mm <sup>3</sup> )	R	o		(%)	C	all three states'	Tilting	(%)	Realized
						D	Polarization	Achieve		Gain
							(LP/LHCP/	d		(dBi)
							RHCP)			
[24]	31x26X1.6	1	2	4	NA	×	×	<b>✓</b>	Not Given	3.6
[31]	90x70x3	2	4	4	3.8	✓	✓	×	Not Given	6.98
[34]	50x60x1.6	2	5	6	3.5	×	✓	<b>✓</b>	82-85	1.92
[38]	40x50x1.6	2	4	5	5.2- 6.4	X	✓	<b>✓</b>	80-83	8.9
[44]	28x34.5x1.6	2	2	8	7.1-15.9	✓	×	<b>√</b>	53	0.85-1.02
[100]	35x50x0.508	1	3	2	NA	×	×	<b>✓</b>	84.3	4
[101]	37.8x40.4x1.6	2	2	4	5.7-16.6	✓	×	×	76.2-85.5	0.65-1.92
[102]	38x40x0.787	4	4	5	NA	×	×	<b>√</b>	73-91	2.42-3.5
[103]	66x44x1.575	3	4	48	3.5	×	✓	<b>✓</b>	39.9-58.7	4
This	30x36x1.6	5	7	4	7.54-14.5	<b>√</b>	✓	<b>√</b>	78-88	1.2-3.57
work										

NR: No. of resonant frequencies, NO: No. of Opearting states ND: No. of Diodes ACD: Achieved CP at dual bands, ARBW: Axial ratio bandwidth.

The tilting pattern is obtained in [104] However, CP at dual bands or three polarization states is not received, and the number of resonant frequencies is also lower. Other detailed information is provided in Table 5.3 to highlight the main contribution of the proposed design.

#### 5.5 The main contribution of proposed compound reconfigurable antenna

- A single radiation structure can achieve all types of reconfigurable properties with a minimum number of diodes.
- A single planner antenna can achieve compound reconfiguration without the need for complex structures, like electromagnetic band gap, frequency selective surfaces, antenna array [38], [41], and patristic pixel layer [105].
- > Capable of tilting beam patterns from omnidirectional to directional radiation patterns, including sense of polarization capability.
- ➤ It provides a broad band bandwidth to cover the entire 5G-N78 band spectrum (3.3 3.8 GHz), along with pattern and polarization capability and excellent radiation characteristics.
- Achieves dual-band, dual-sense circularly polarized characteristics covering the 5G-n78 band and the WLAN band.
- Achieved dual-band dual-sense orthogonal circular polarization and linear polarization with compact size as compared to [31].

#### 5.6 Summary

A compound monopole reconfigurable antenna for sub-6 GHz (N77/N78 bands) and 5G WLAN bands is reported. At these bands, the structure provides a pattern tilting from boresight to end-fire as well as three states of polarization namely LP, LHCP and RHCP. They are obtained from various operating states of the PIN diode, where this antenna characteristic is useful in vehicular communication and 5G wireless standards. In OS 4 and 5, this structure provides a dual-band with LP and LHCP/RHCP with an axial ratio of 14.5%. Meanwhile, in OS 6 and 7, a dual-band with dual sense polarization is obtained, with an axial ratio of 8.57 % at the lower band and 7.54 % at the higher band, with a pattern tilting capability. Where this type of antenna'scharacteristics are found helpful in satellite communications, it can also be observed that the proposedantenna is capable of reconfiguring the radiation pattern at a standard center frequency of 5.3 GHz (indoor WLAN applications) in three directions, namely omnidirectional, left end-fire, and right end-fire, respectively.

#### **CHAPTER 6**

Design and analysis of Multiband hybrid reconfigurable antenna (HRA) with enhanced gain for Wi-Fi-6E and 5G NR wireless Standards

#### 6.1 Introduction

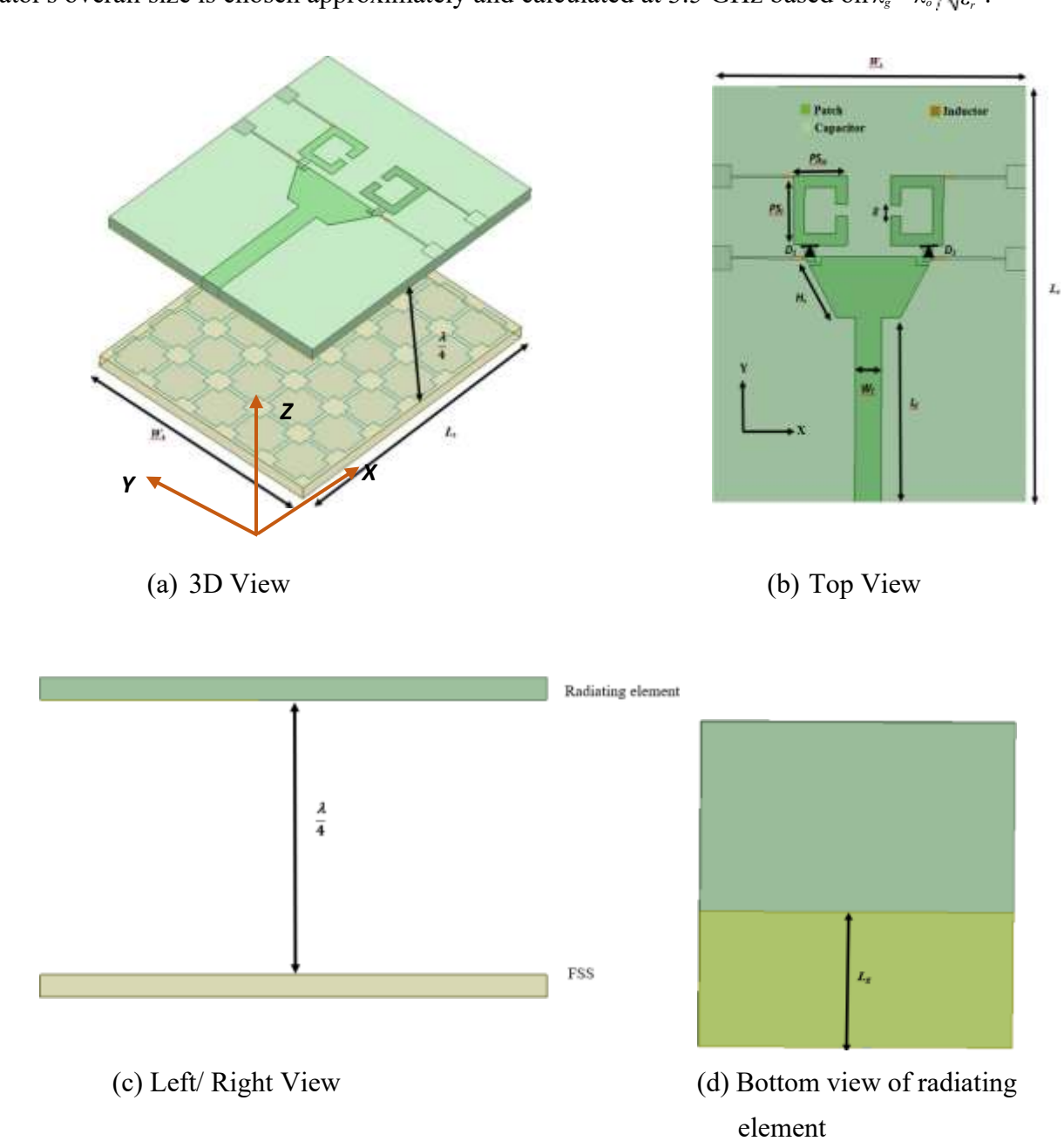
This thesis chapter aims to design and analyze multiband frequency and pattern reconfigurable antenna with enhanced gain for Wi-Fi 6E and 5G new radio wireless standards. It is achieved by implementing a half-hexagonal radiating element along with a partial ground plane and a switchable split ring resonator on the ground plane for multiband operation. An FSS-based reflector is placed below the radiating element to enhance gain. A MADP000907-14020 P PIN diode is placed at a suitable position on the half-radiating element to connect and disconnect the two rectangular symmetrical split ring resonators. The structure works in three modes, and in each mode, it selects various frequencies with a tilting radiation pattern. In mode 1, the antenna resonates at dual bands of 5.3 and 6.5 GHz with a bandwidth of 1.8 GHz and 1 GHz and a radiation pattern in the maximum direction of 180 ° and 265 °, respectively. In mode 2, the antenna resonates with multiband (3.3 GHz, 5.1 GHz, and 6.5 GHz) and independently controls radiation pattern shifts without affecting each other with a bandwidth of 0.5 GHz, 1 GHz, and 1 GHz, respectively. Finally, in mode 3, the antenna resonates in dual bands of 3.5 GHz and 6.5 GHz with a bandwidth of 0.9 GHz and 0.5 GHz, respectively. In all three modes, the realized gain is enhanced by the FSS-based reflector by nearly 2-4 dBi without affecting the other performance characteristics of the proposed HRA.

The proposed radiating structures are designed and analyzed in the HFSS R.V23. Section 6.2 provides the details of the design and analysis of the proposed radiating structures and methodology for gain enhancement discussed in section 6.3. Further, the simulated and measured results in three modes of the proposed antenna are reported in section 6.4, and its simulated results are discussed in section 6.5. Finally, a summary of proposed reconfigurable antennas is reported in the last section.

#### 6.2 Design and analysis of frequency and pattern reconfigurable antenna

The proposed hybrid reconfigurable antenna geometry and design parameters are shown in Fig.6.1. The, step-by-step design process of the proposed radiating element is shown in Fig.6.2. Their respective reflection coefficient results are provided in Fig. 6.3. In the first step, a simple hexagonal shape [95] is designed, as shown in Fig.6.2 (a). The antenna resonates at 5.1 GHz (Wi-Fi) applications, and this frequency is considered the midband in the proposed structure. To introduce frequency

reconfigurability, the top half of the hexagonal-shaped radiating element [106] is truncated, as shown in Fig. 6.2 (b). This modification helps the antenna resonate at 6.5 GHz for Wi-Fi 6E (5.925 - 7.125 GHz) applications, which is considered the upper resonating frequency of the proposedstructure. Finally, two symmetrical rectangular-shaped single split ring resonators are connected through the PIN diodes to achieve a multiband [107], as shown in Fig.6.2 (c). The biasing network isintroduced in step 4. The effectiveness of DC biasing is validated in simulation to ensure the OFF condition contributes minimally to the antenna's performance compared to the ideal OFF condition implemented in step 3. Fig.6. 3 (a) indicates that the proposed antenna (both diodes OFF condition)  $|S_{11}|$  dB curve matches Ant. 3. (without diodes)  $|S_{11}|$  dB curve. Here, the rectangular single-split resonator's overall size is chosen approximately and calculated at 3.5 GHz based on  $\lambda_g = \lambda_o / \sqrt{\epsilon_r}$ .



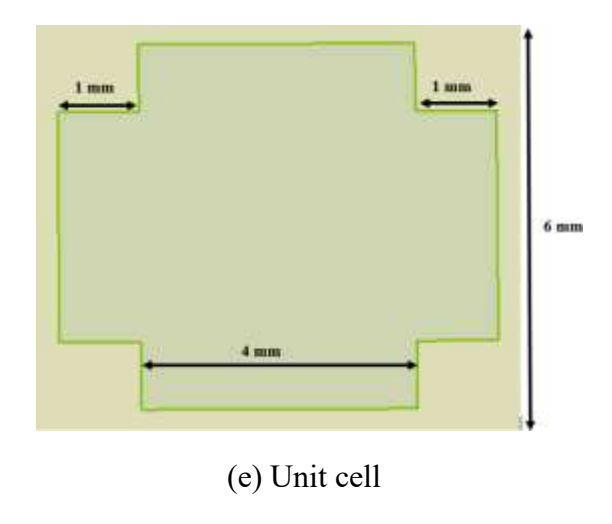
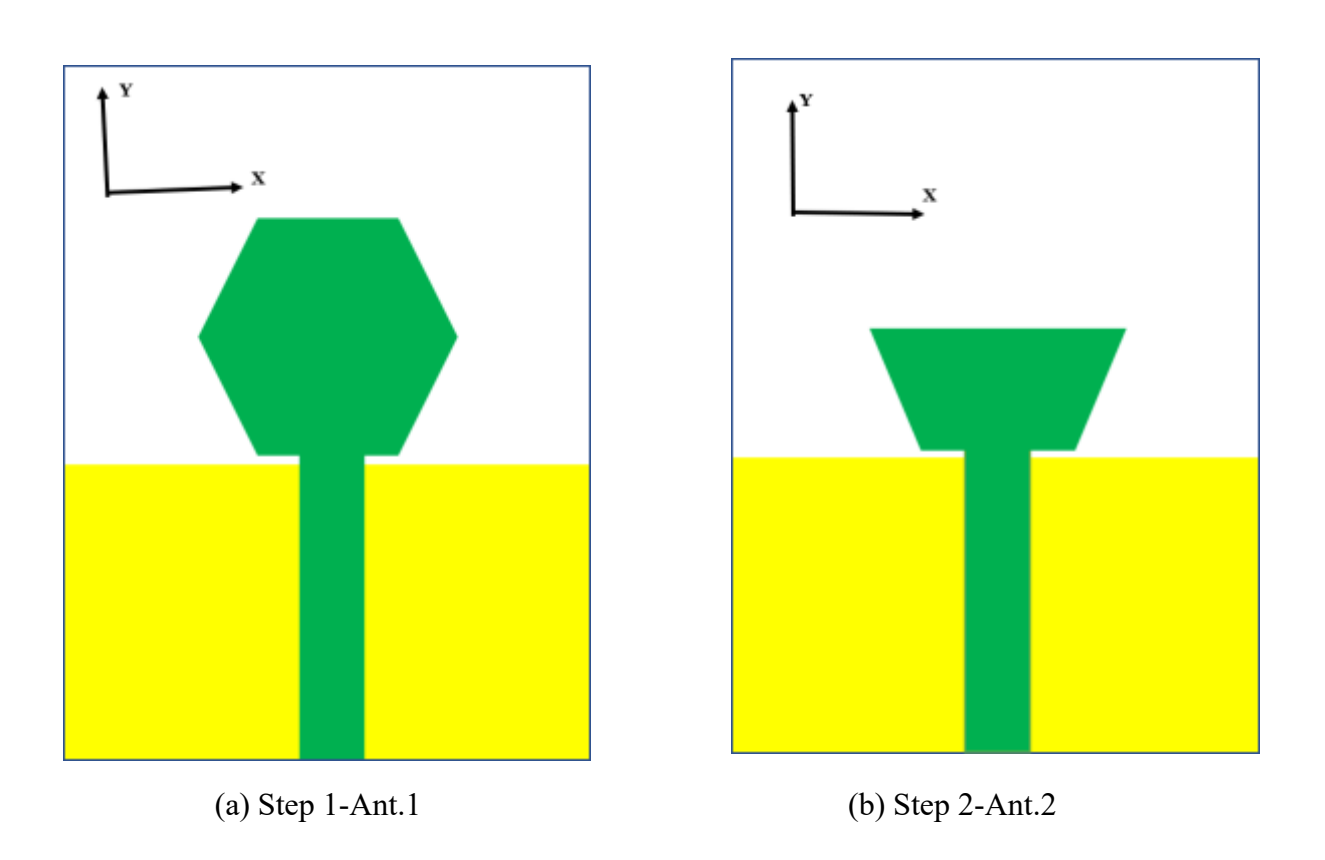


Fig.6.1 Proposed Hybrid Reconfigurable Antenna (HRA) with enhanced gain and its geometrical dimensions.



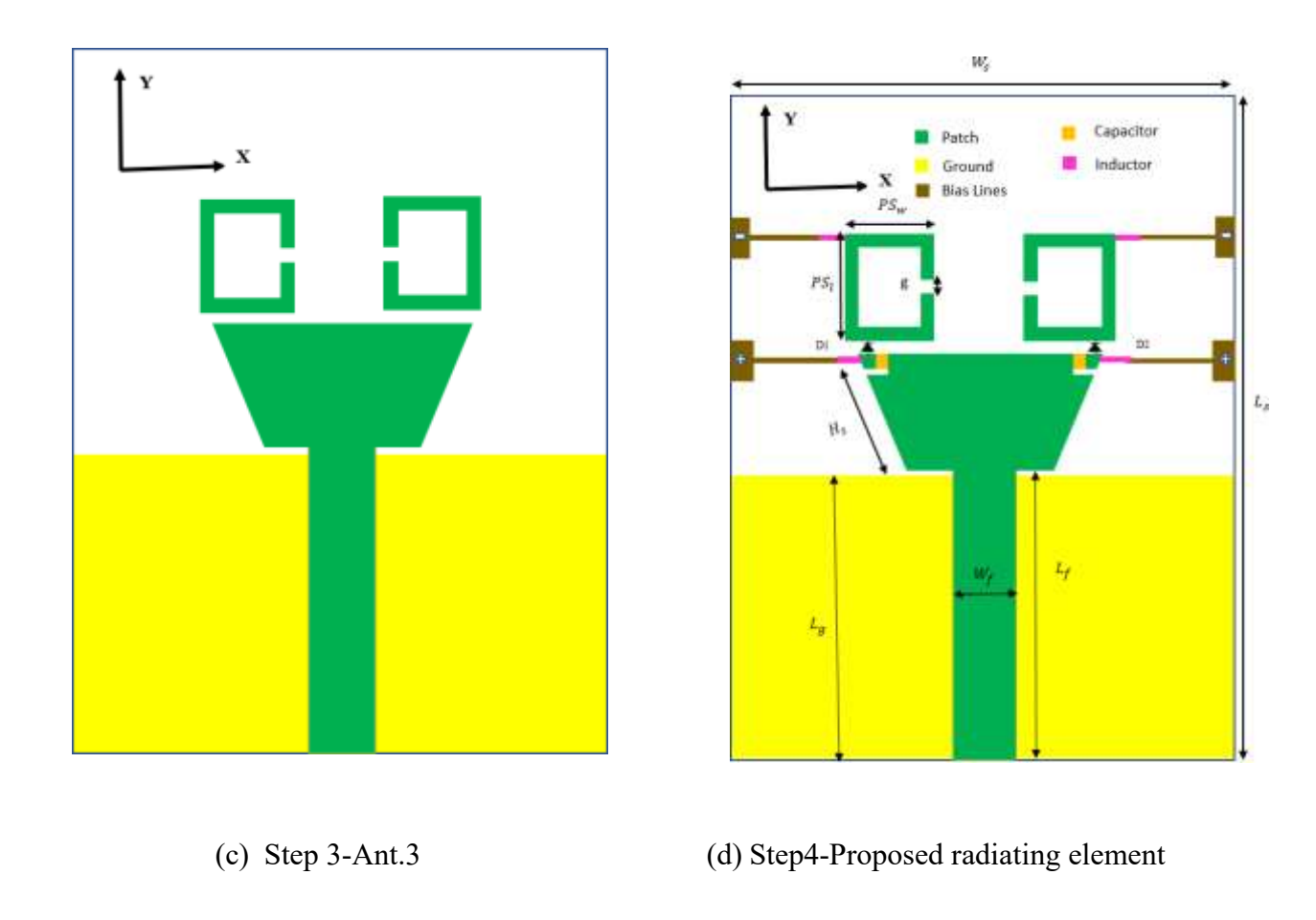


Fig. 6.2. Different prototypes (a)–(d) for designing the proposed radiating element antenna

**Table 6.1** Geometrical dimensions of the proposed frequency and pattern reconfigurable antenna with enhanced gain structure

Parameter	Value (mm)	Parameter	Value(mm)
$W_s$	30	g	1
$L_s$	36	$W_f$	3
$L_g$	15.5	$L_f$	16
$H_s$	6.065	$PS_w$	5
$PS_l$	6		

#### 6.2.1 Selection of suitable PIN diode in contrast to artificial switch

The switch selection is carefully selected after the antenna is optimized for frequency and radiation pattern reconfiguration using an artificial switch (stripline) in the simulation. The artificial switches are assumed to be ON when the strip line is copper and OFF when the material is changed to vacuum. Then, an intensive analysis is performed to select a suitable PIN diode for reconfigurability compared to the artificial switch, as shown in Fig.6.3 (b). The switches are located at a gap of 1 mm between the half-hexagonal-shaped radiating element and rectangular-shaped single split ring resonators. The simulated structure resonates at 5.4 GHz and 6.9 GHz with no diodes placed. Two different diodes were adopted in the simulation, namely BAR63-02L and MADP-000907-14020P. The lumped equivalent values for the BAR63-02L PIN diode model are  $R_{ON}$ =1  $\Omega$  and  $C_{OFF}$ =0.3 pF. For the MADP-000907-14020P PIN diode model,  $R_{ON}$ =5.2  $\Omega$ ,  $R_{OFF}$ =5 k $\Omega$ , and  $C_{OFF}$ =0.03 pF with package inductance of 0.4 nH. The simulated |S<sub>11</sub>|dB of MADP-000907-14020P offers better matching towards the artificial switch than the BAR63-02-L model, as shown in Fig.6.3 (b). Therefore, in this chapter, the MADP-000907-14020P PIN diode model is chosen. The diode exhibits an exceptionally low RC product (0.1 ps) and 2-3 ns switching speed. This rapid switching between modes ensures optimal signal quality and coverage, especially in environments with higher user mobility.

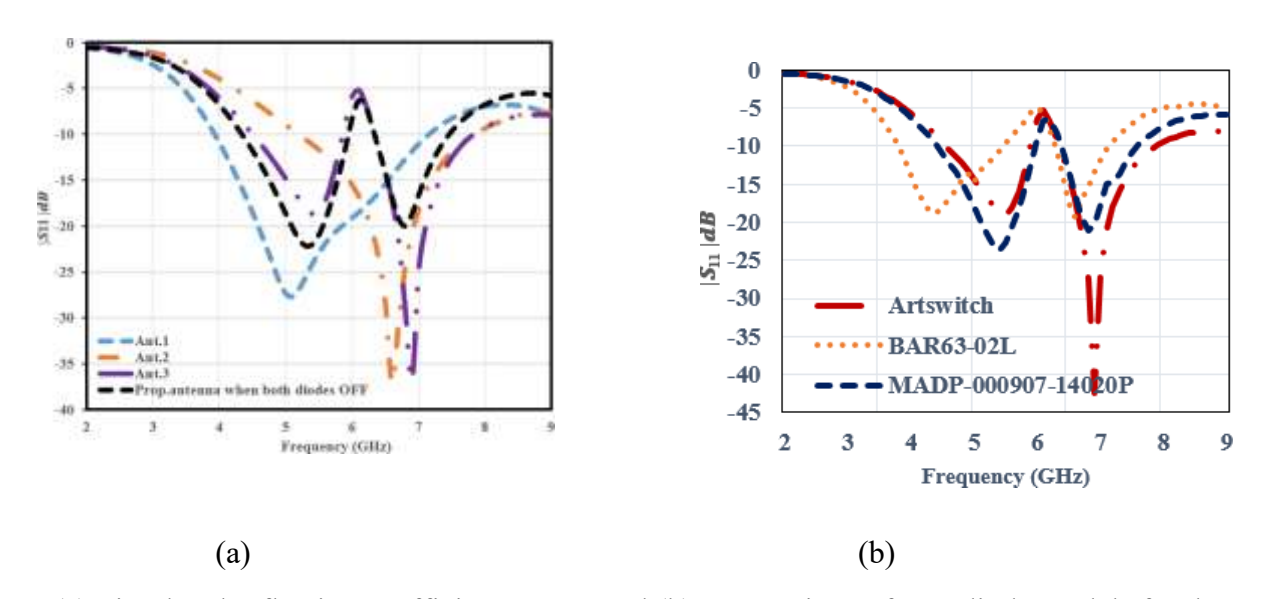


Fig.6.3. (a) Simulated reflection coefficient curves and (b) Comparison of PIN diode models for the proposed HRA

#### 6.2.2 Biasing analysis of selected suitable PIN diode

The biasing arrangement of the PIN diode utilized in the proposed structure is shown in Fig.6.4 (a), and it is implemented and analyzed in ADS software to assess the effect of the biasing circuit on the

proposed structure. They are engraved on the radiating structure to avoid the impact of the RF signal from DC biasing. For an RF choke inductor value of 100 nH and a DC blocking capacitor value of 1.2 nF, the return loss curve  $S_{11}(dB)$  and isolation curve  $S_{21}(dB)$ , as shown in Fig. 6.4 (b), match the curves mentioned in the datasheet [39]. The respective diode is biased for the ON state with a current of 10 mA. Due to biasing elements, the overall performance of the antenna is slightly affected in terms of return loss dip value and bandwidth, as shown in Fig. 6.4 (c).

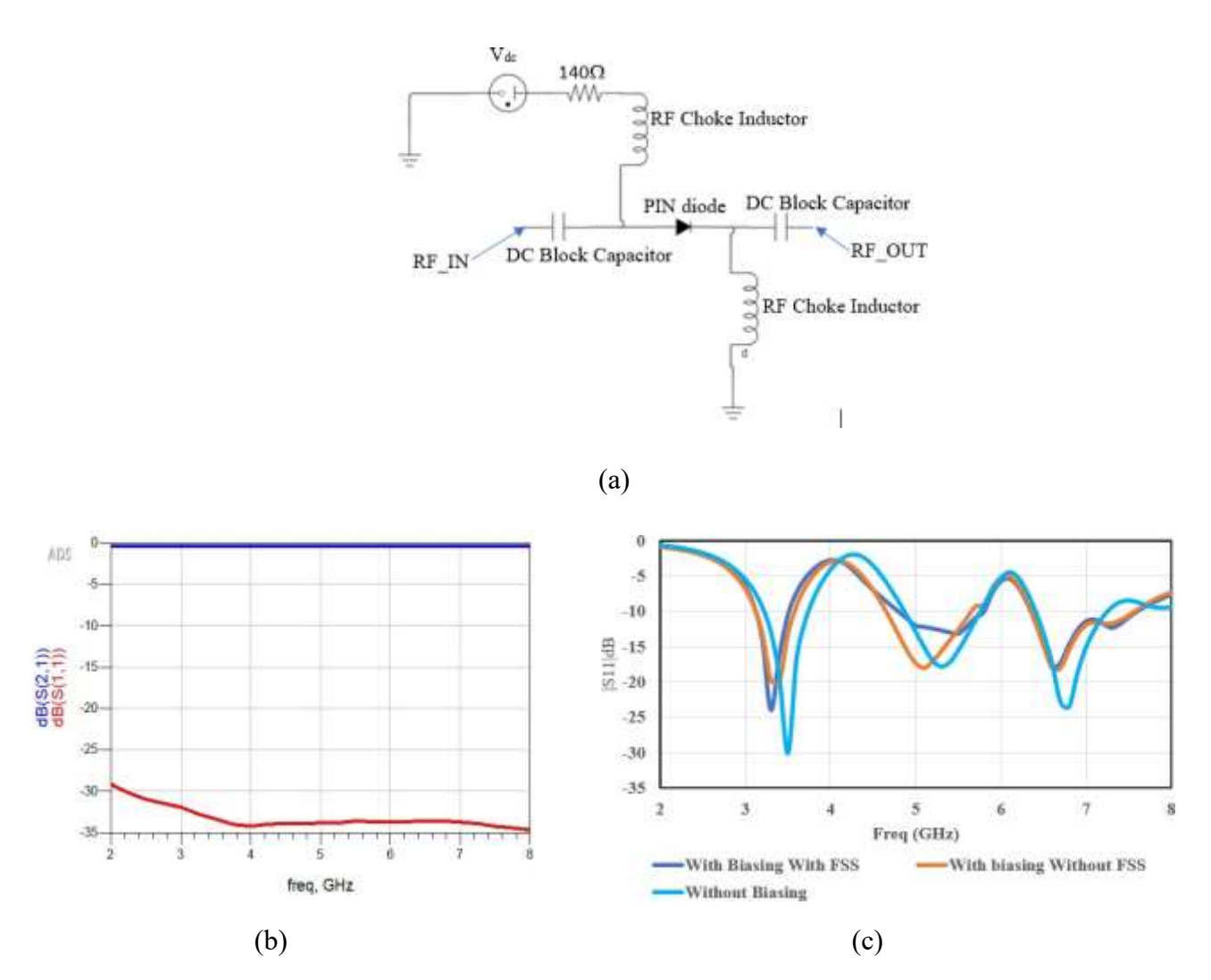


Fig. 6.4. (a) Biasing arrangement of the PIN diode (b) S<sub>11</sub>(dB) and S<sub>21</sub> (dB) for the PIN diode (c)Analysis of biasing effect of the proposed structure in mode 2(a)

# 6.2.3 Analysis of E-Field distribution on a radiating element in three modes

The electric field distributions of HRA in all modes are shown in Fig. 6.5. In each mode, these fields provide information regarding resonant frequencies and pattern tilting.

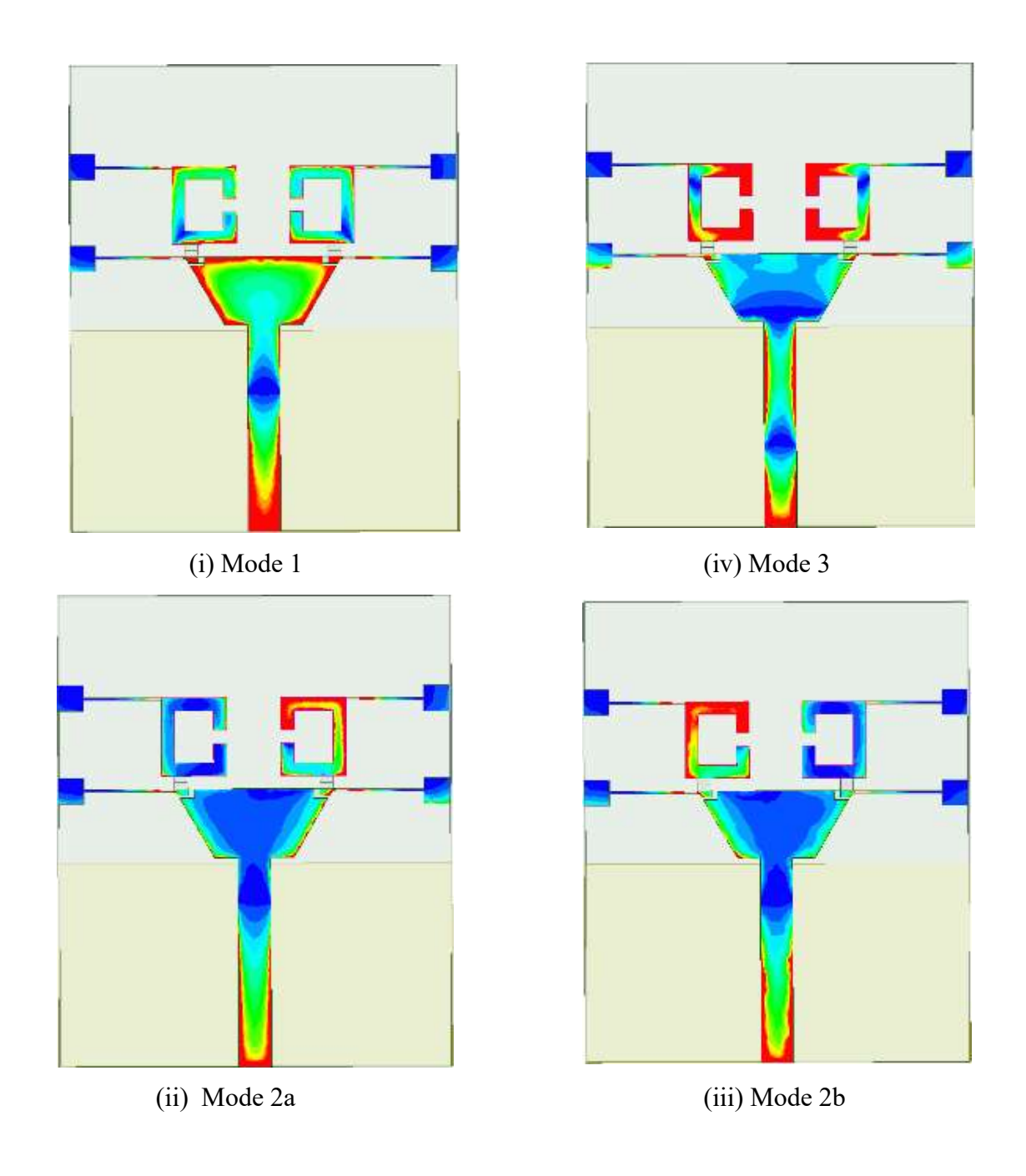


Fig 6.5. The electric field distributions of HRA in all modes

In mode 1, the maximum field is distributed on the half-hexagon-radiating patch and less on the split-ring resonators, as shown in Fig. 6.5 (i). In mode 2, the field distribution is strong in the respective ON split ring resonators as shown in Fig. 6.5 (ii & iii), respectively. Patterns titling towards  $\pm$  13° are observed, which is shown in Fig. 6.9. Similarly, in mode 3, the field distribution mainly focuses on the split ring resonators, and a pattern is observed similar to mode 1, but with different resonant frequencies are observed due to electrical length variation as shown in Fig. 6.8 (a) and (e) respectively.

### 6.3 Methodology of Gain Enhancement

Due to the need for higher frequency bands where the spectrum is suited for massive volumes of data transfer, antenna gain has become increasingly important for current and future communication systems. Since the signal is dispersed rather than in waveform when the frequency is raised to the millimeter wave range, antennas with high gains are more advantageous for establishing communication. To enhance the gain of a reconfigurable microstrip patch antenna, the basic methods explored in the open literature are the basic antenna array concept, loading the shorting pins on the ground plane or the radiating plane and coupling the parasitic patches along with the main radiator and advanced techniques are Electromagnetic band gap structure and metamaterials/ Meta surfaces as shown in the Fig 6.6. Metamaterial is commonly used in antennas to improve performance, such as gain improvement or bandwidth, because of its powerful and versatile properties [108].

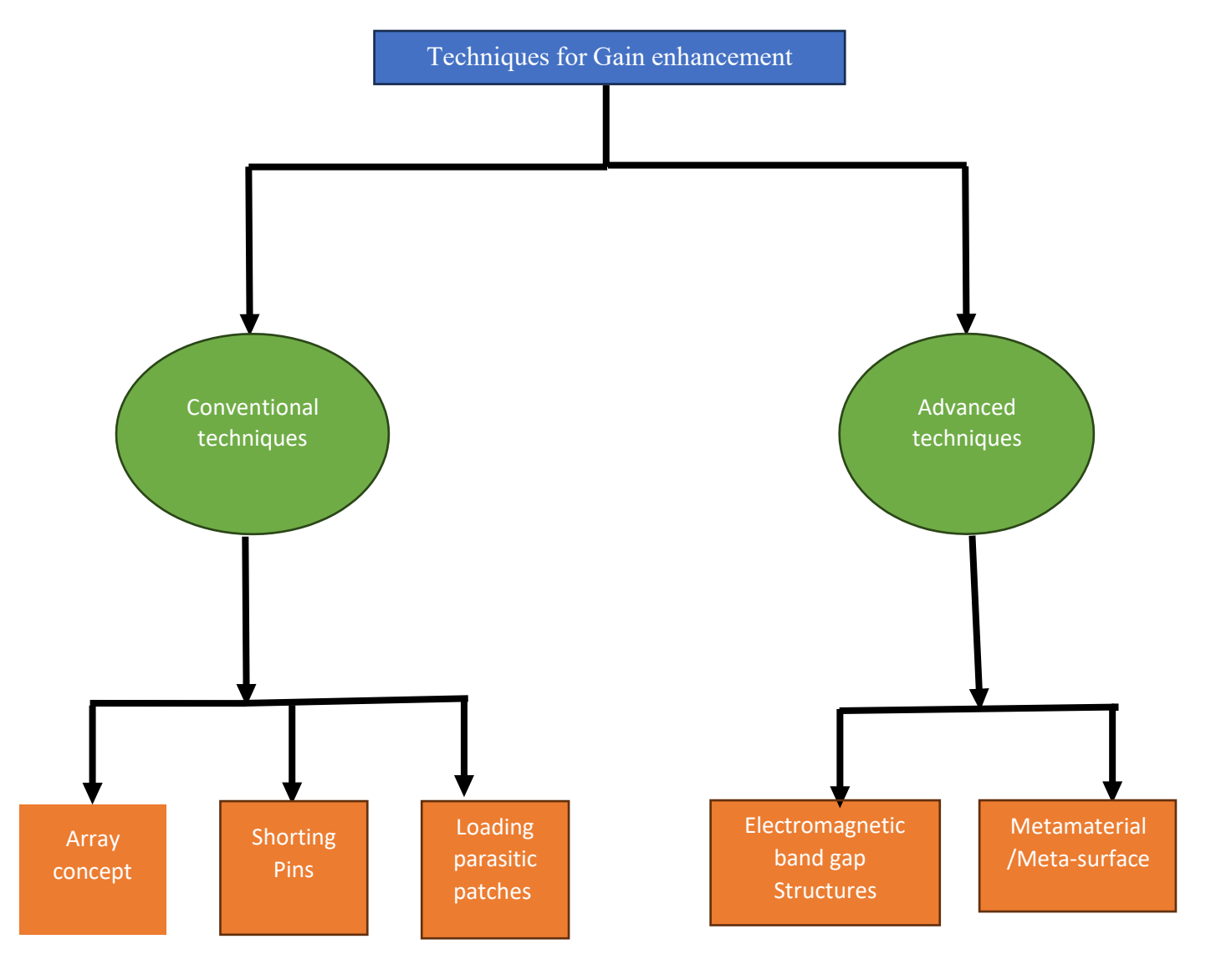
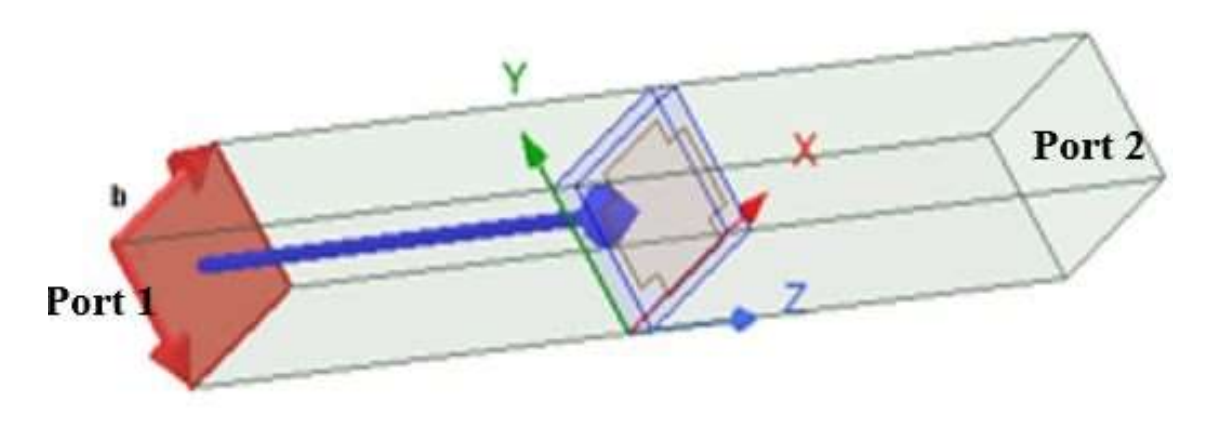
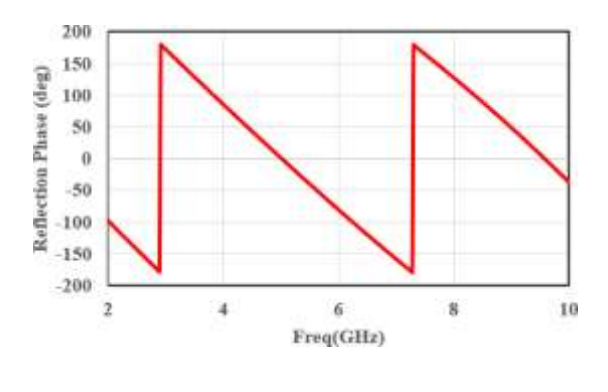


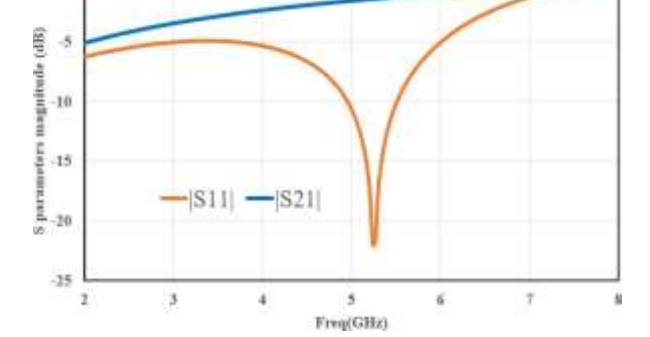
Fig 6.6 Gain enhancement techniques [109]

In this chapter, to enhance the gain of the proposed hybrid reconfigurable antenna, the FSS-based reflector is placed at a distance of approximately  $\frac{\lambda}{4}$  Where  $\lambda$  is the free space wavelength at the lowest operating frequency of 3.3 GHz. A rectangular shape with four corners slit unit cell is printed on one side of the FR-4 substrate with a thickness of 1.6 mm and a relative permittivity of 4.4, and on the other side, copper is etched to implement FSS, as shown in Fig.6.1(b) The unit cell is excited by employing the master-slave boundary conditions and by the Cloquet ports, as shown in Fig.6.7(a). The simulated reflection phase (deg) and s-parameter magnitudes (dB) are represented in Fig. 6.7 (b and c), respectively. The simulated characteristics show that the designed FSS works as a reflector at a center frequency of 5.3 GHz, where the reflection phase is  $0^{0}$ , and the magnitude of the S<sub>11</sub> and S<sub>21</sub> are -25 dB and nearly 0 dB, respectively. The FSS-based reflector consists of 5 x 6 unit cells and is placed below the radiating element. The distance between the FSS and radiating element is chosen at approximately four, as shown in Fig.6.1(b), and the unit cell's length is carefully selected from at approximately  $\frac{\lambda}{10}$  at an operating frequency of 5.3 GHz to avoid issues related to mutual coupling between the elements and electromagnetic interference.



(a) Floquet port excitation of unit cell



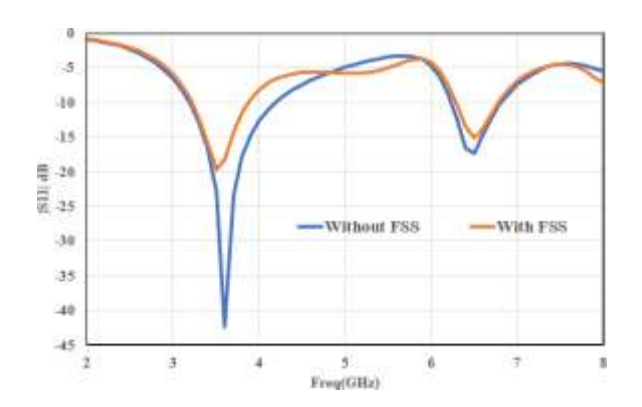


(b) Reflection Phase (deg)

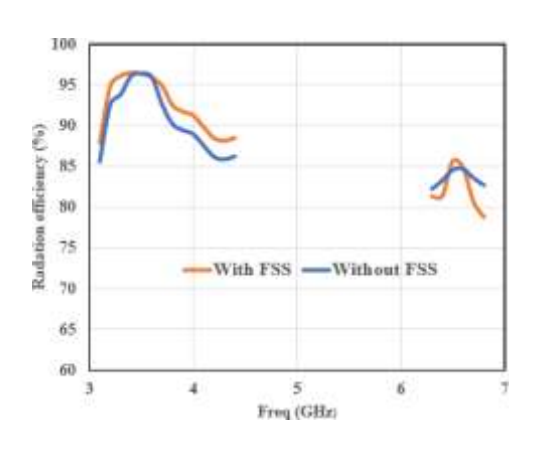
(c) Magnitude of S-parameters for unit cell

Fig. 6.7. Design and analysis of the proposed unit cell (FSS)

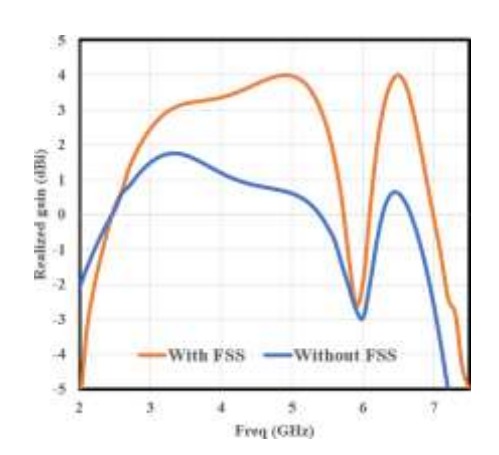
The simulated reflection coefficient, radiation efficiency, and realized gain of mode 3 with and without FSS are shown in Fig. 6.8 It can be easily observed that there is a 2-3% increment in radiation efficiency and a narrower beamwidth with FSS, as shown in Fig. 6.8 (a and b), respectively. However, the realized gain rapidly increases from 1.68 dBi to 3.15 dBi at 3.5 GHz and from 0.6 dBi to 3.76 dBi at 6.5 GHz, which is almost double at 3.5 GHz and six times more at 6.5 GHz than that of the proposed hybrid reconfigurable antenna without FSS, as shown in Fig. 6.8 (c). The radiation efficiency of an antenna can decrease due to different environmental conditions, such as temperature, humidity, etc. Since the antenna is tested in controlled environments such as anechoic chambers and in real-world scenarios, the performance of antennas can be affected due to multipath interference from other objects. Further, additional experimental validations are necessary, such as mechanical, thermal, humidity, and corrosion testing for physical durability, EMC, PIM, and power handling tests for electrical performance, and long-term aging and environmental interference tests for reliability and robustness.



(a) Reflection coefficient with and without FSS



(b) Radiation efficiency with and without FSS

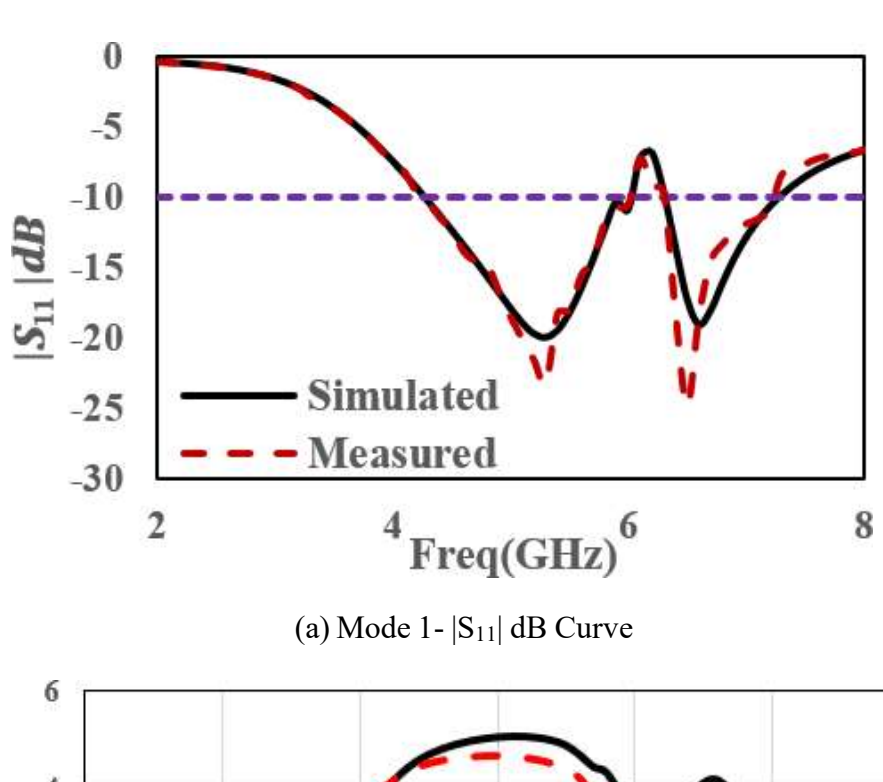


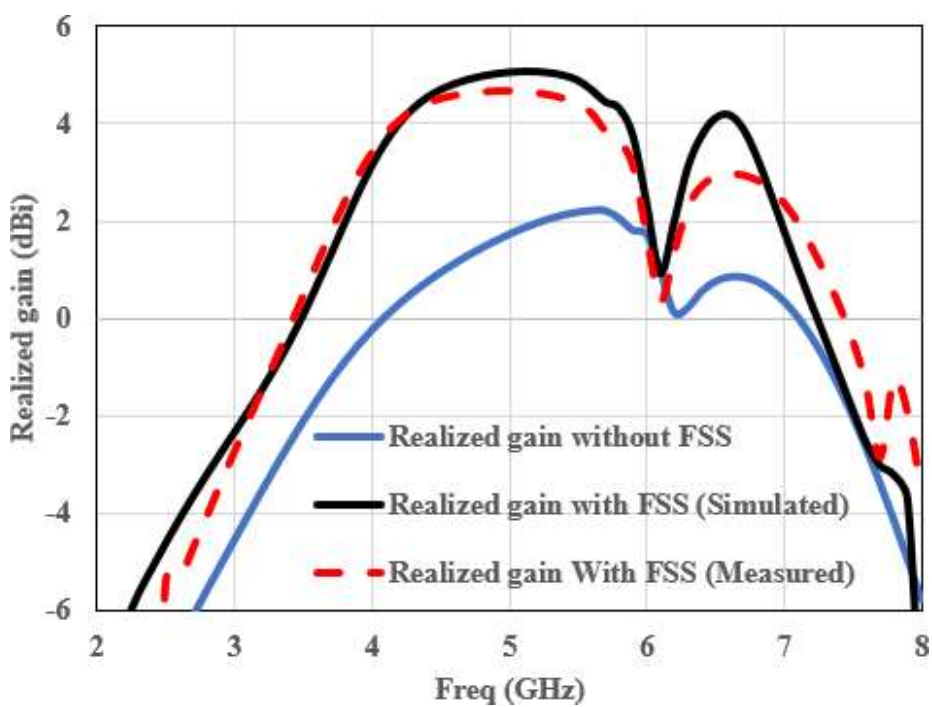
(c) Realized gain with and without FSS

Fig. 6.8 Performance characteristics of the proposed HRA in mode 3 with an FSS-based reflector

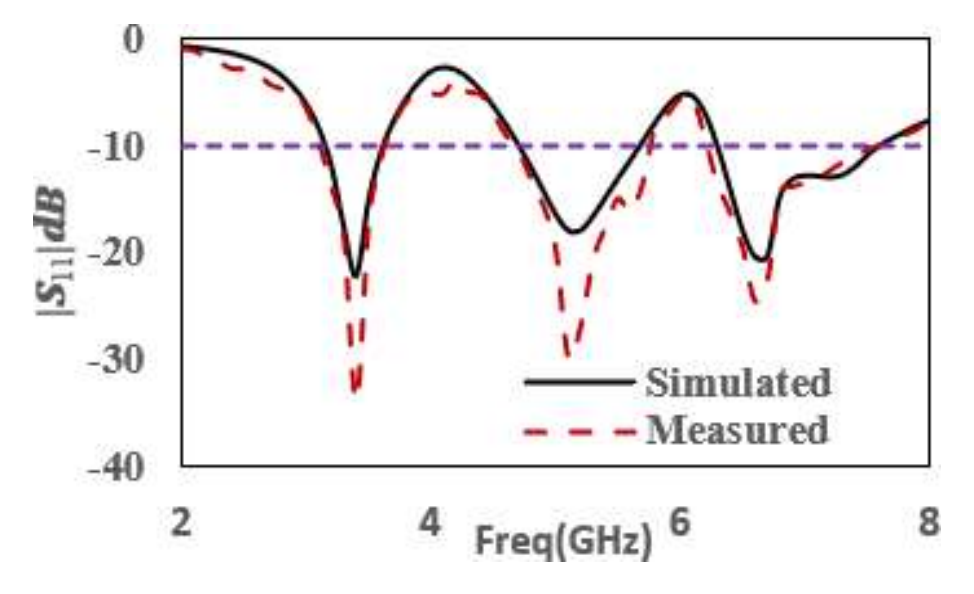
# 6.4 Experimental validation of simulated results in three modes

The proposed antenna operates in three modes. In Mode 1, both diodes are OFF; in Mode 2, either one of the diodes is in the ON state (Mode 2a:  $D_1$  is OFF and  $D_2$  is ON; Mode 2b:  $D_1$  is ON and  $D_2$  is OFF), and in mode 3, both diodes are in the ON state.

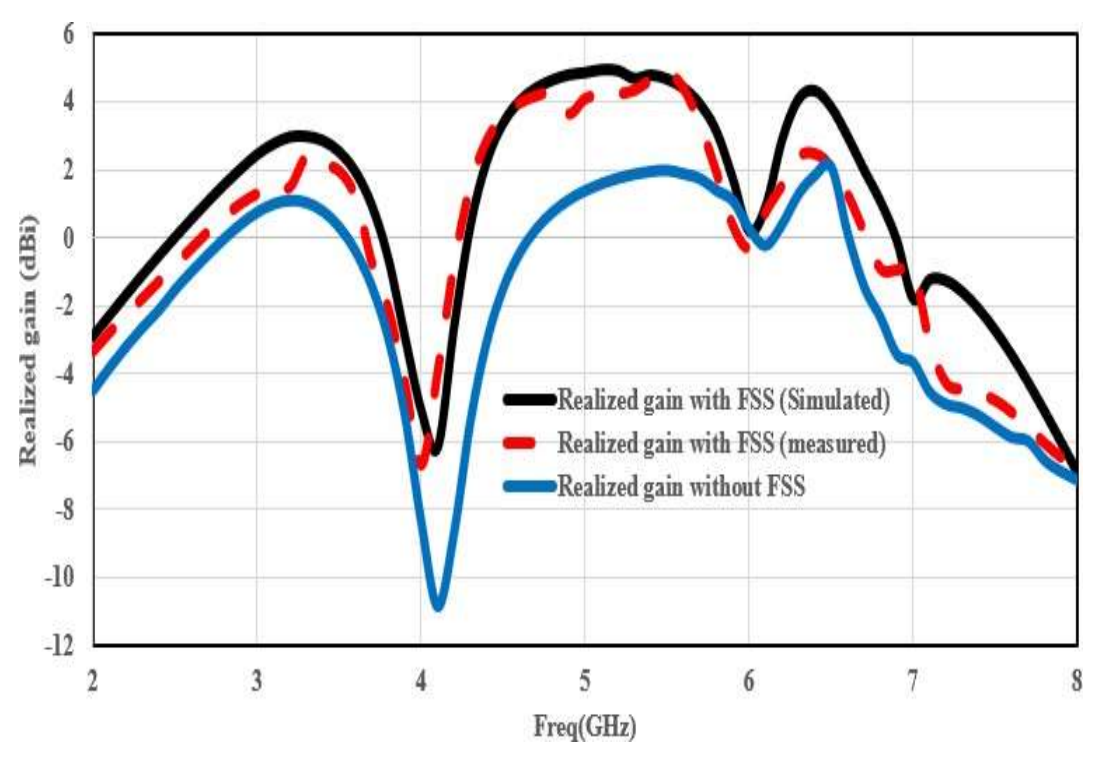




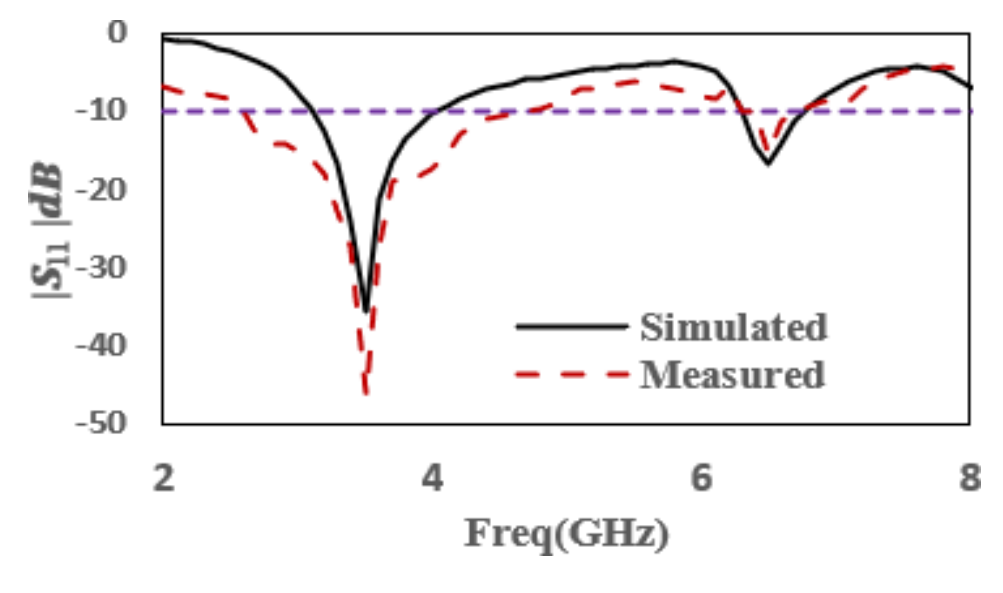
(b) Mode 1- Realized gain



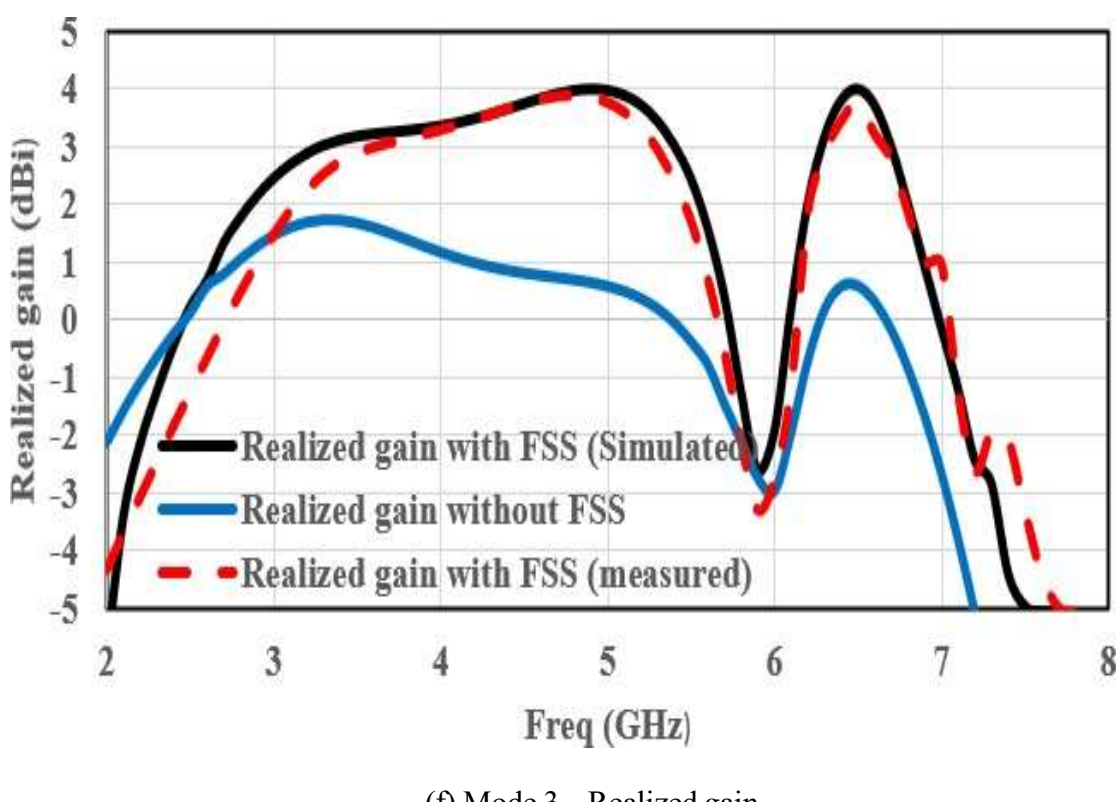
(c) Mode 2 (a & b) -  $|S_{11}|$  dB Curve



(d) Mode 2 (a & b) – Realized gain



(e) Mode 3 - |S<sub>11</sub>| dB Curve



(f) Mode 3 – Realized gain

Fig. 6.9. Measured and simulated |S<sub>11</sub>| dB and realized gain in (a) Mode 1 (b) Mode 2 (a & b),

# (c) Mode 3

Fig. 6.9 shows the simulated and measured  $|S_{11}|$  and realized gain plots with and without FSS in all three modes. The measured results are consistent with the simulation results. In Mode 1, the proposed antenna resonates in two bands, one at 5.3 GHz (4.3 GHz–6.1 GHz) with a 1.8 GHz bandwidth and another

resonating at 6.5 GHz (6.3 GHz–7.3 GHz) with a 1 GHz bandwidth, which covers the Wi-Fi 6E band as shown in Fig. 6.9 (a). The radiation efficiency and peak realized gain at 5.3 and 6.5 GHz are 91%, 87%, 1.68 dBi, and 0.6 dBi, respectively, without FSS. With FSS, the realized gain increased to 3.15 dBi at 3.5 GHz and 3.76 dBi at 6.5 GHz, respectively, as shown in Fig. 6.9 (b). However, the radiation pattern and Sparameters are not affected much more by the FSS-based reflector.

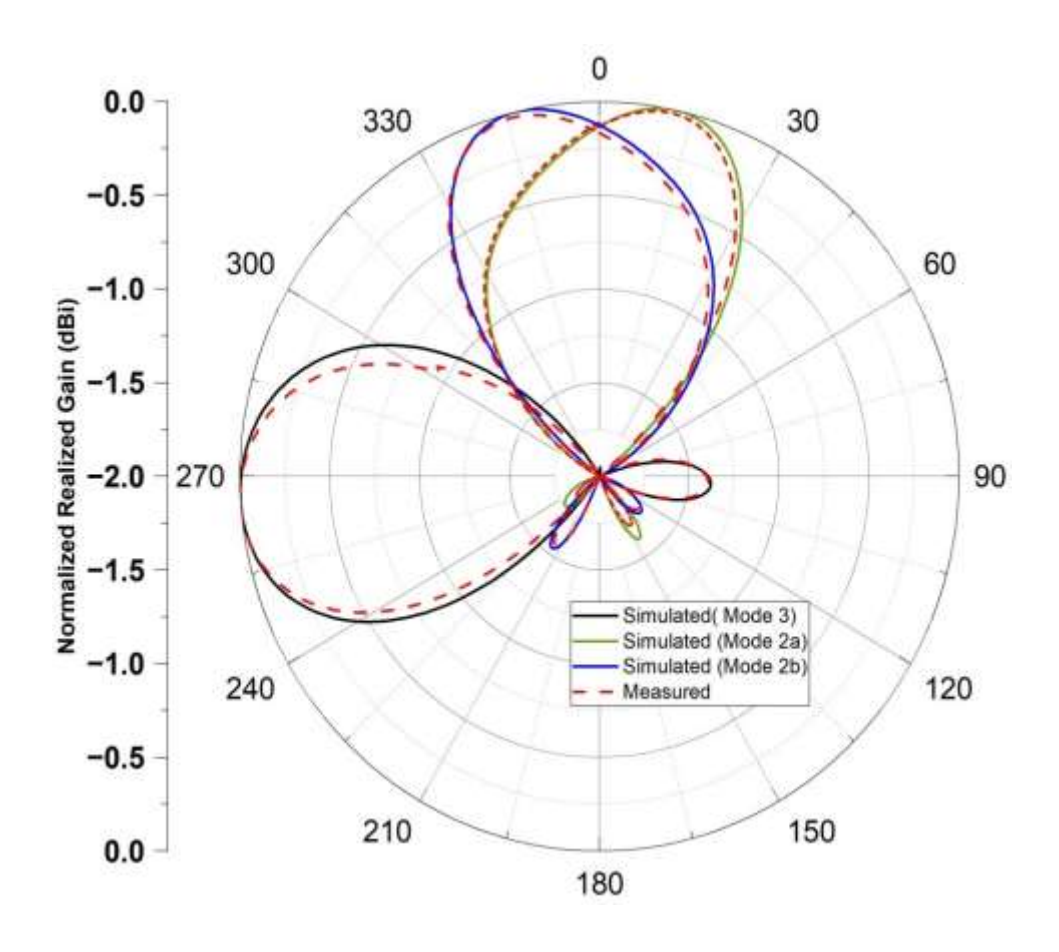


Fig. 6.10. Normalized patterns of the proposed structure at 6.5 GHz in Mode 2 (a and b) and Mode 3

In mode 2 (a and b), the proposed antenna resonates in three bands (multiband), one at 3.3 GHz (3.1 GHz–3.6 GHz) with a 0.5 GHz bandwidth, another at 5.1 GHz (4.6 GHz–5.6 GHz) with a bandwidth of 1 GHz, and the next band at 6.5 GHz (6.3 GHz–7.3 GHz) with a 1 GHz bandwidth, respectively, as shown in Fig. 6.9 (c). In addition, pattern tilting of  $\pm 8^{\circ}$  at 3.3 GHz,  $\pm 8^{\circ}$  at 5.1 GHz, and  $\pm 13^{\circ}$  at 6.5 GHz is attained due to the phase difference between the left and right side rectangular split ring resonators. The phase difference occurred since  $D_1$  was OFF and  $D_2$  was on (Mode 2a), i.e., the right side SRR acts as an inductor and the left side provides a capacitance effect, so that the pattern tilted

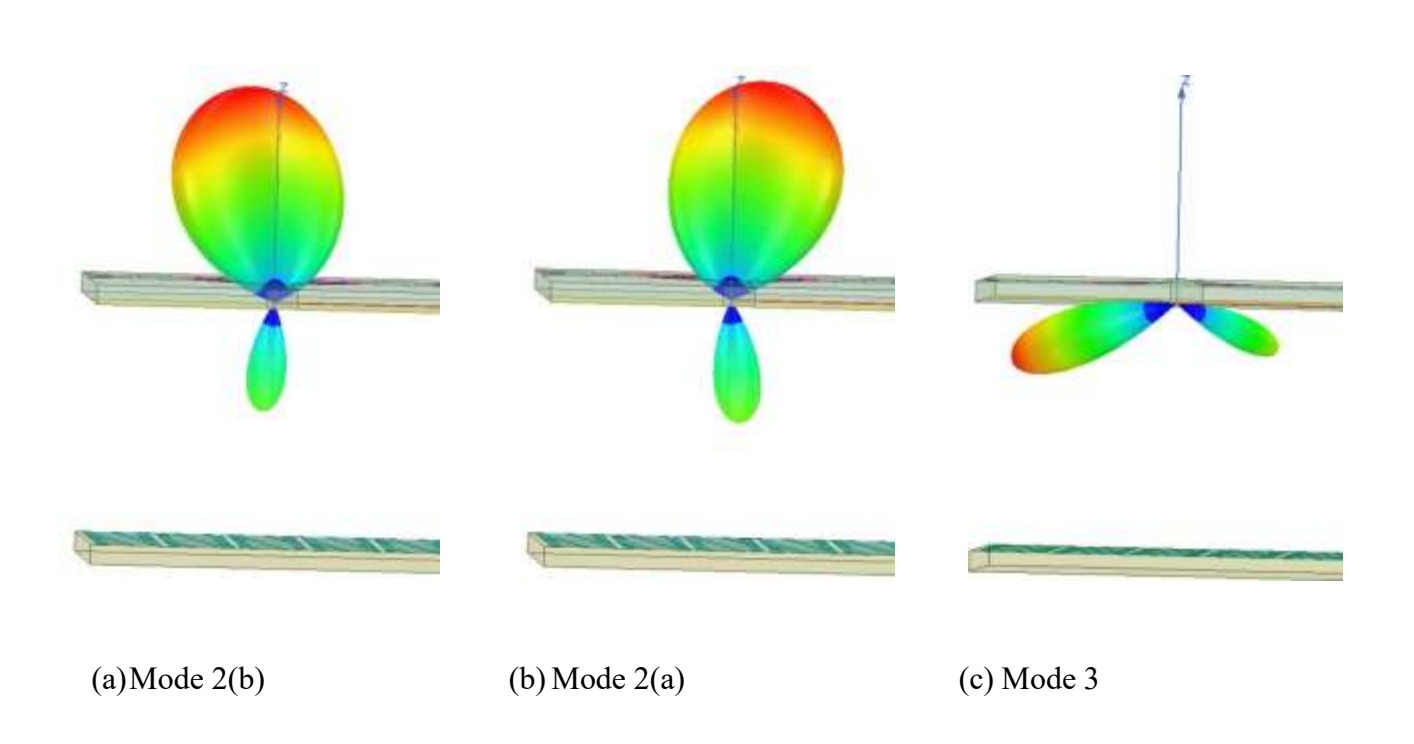
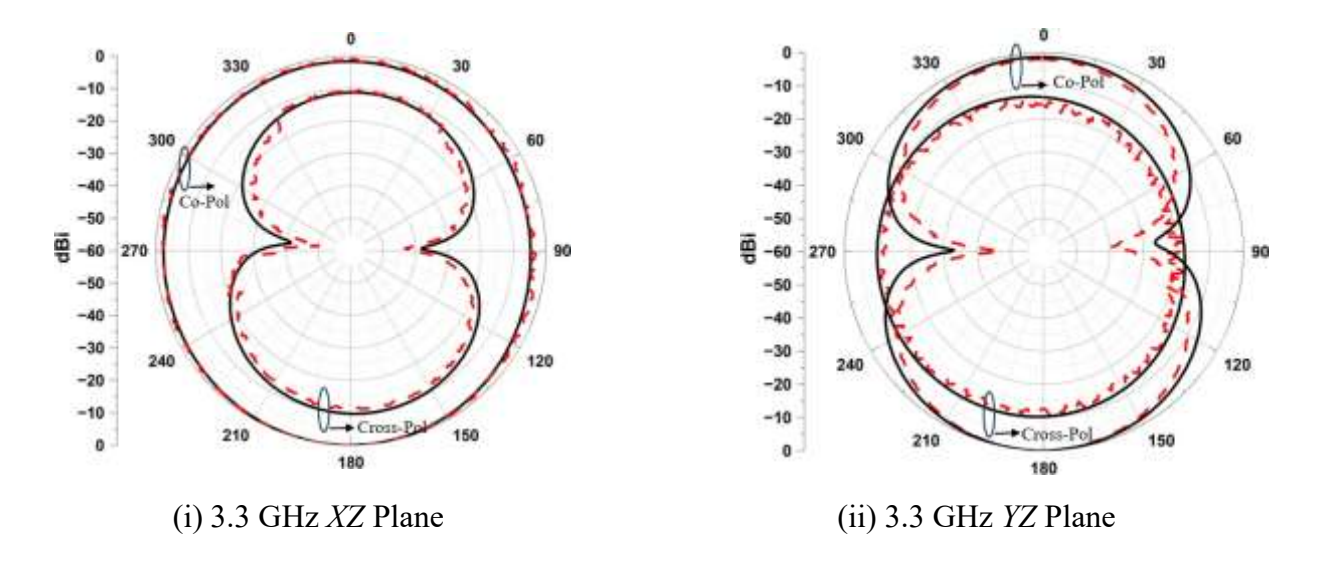
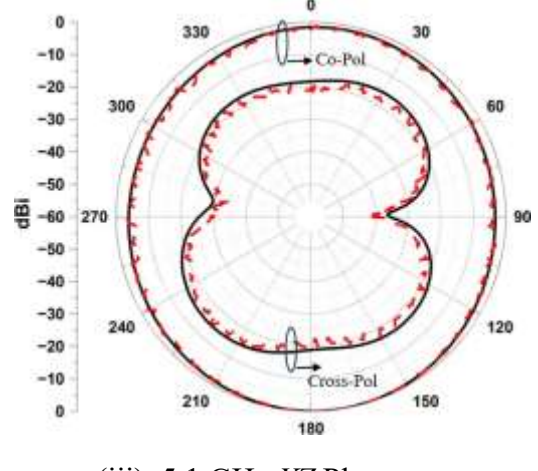


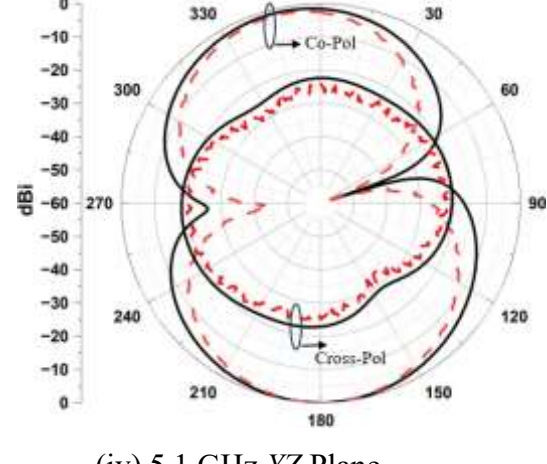
Fig. 6.11. Simulated 3-D radiation pattern of Mode 2 (a and b) and Mode 3 at 6.5 GHz

Similarly, in mode 2 (b), the pattern tilted towards the left side, as shown in Fig. 6.11 (a). The radiation efficiency and peak realized gain are 89%, 88%, 92%, and 0.985 dBi, 1.09 dBi, and 2.08 dBi, respectively, without FSS. With the FSS-based reflector, the realized gain is increased to 3 dBi, 5.05 dBi, and 4.1 dBi, respectively, as shown in Fig. 6.11 (d). The, use of FSS enhanced gain, therefore the antenna beam tilted in the uni-direction. If a broader beam width is required, then FSS can be removed.

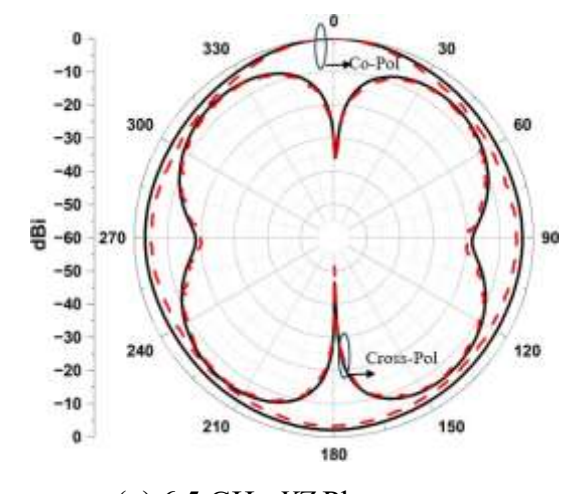




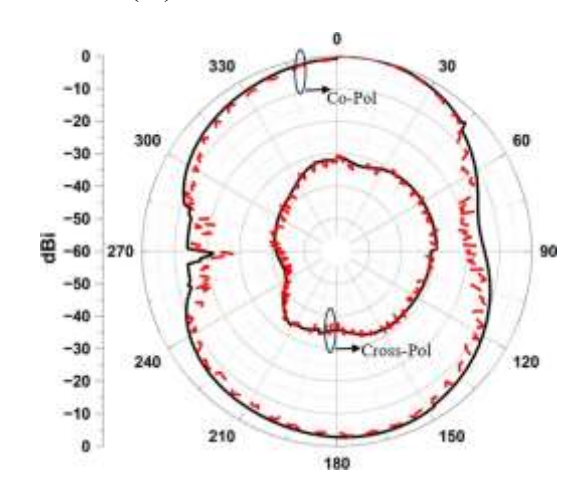
(iii) 5.1 GHz XZ Plane



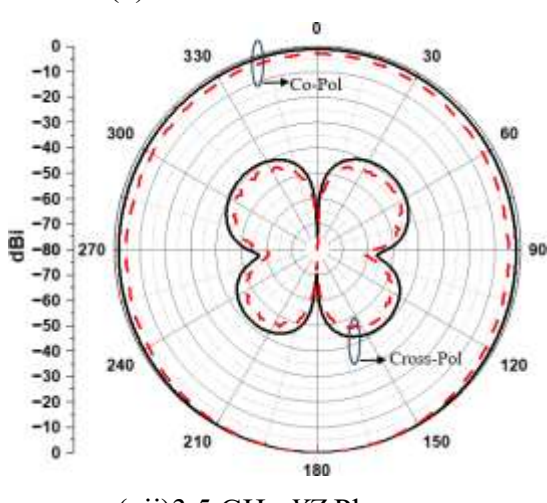
(iv) 5.1 GHz YZ Plane



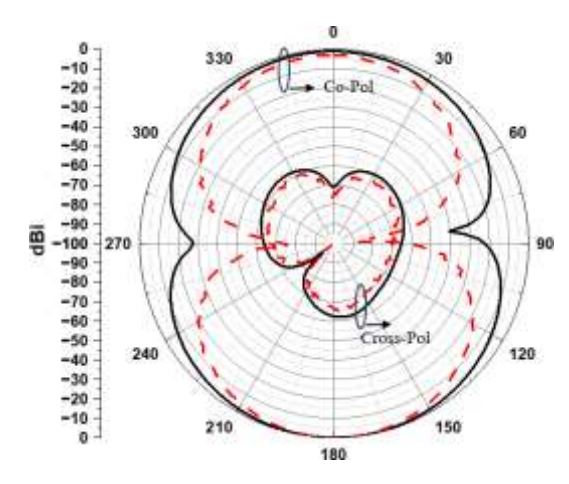
(v) 6.5 GHz XZ Plane



(vi) 6.5 GHz YZ Plane



(vii)3.5 GHz XZ Plane



(viii)3.5 GHz YZ Plane

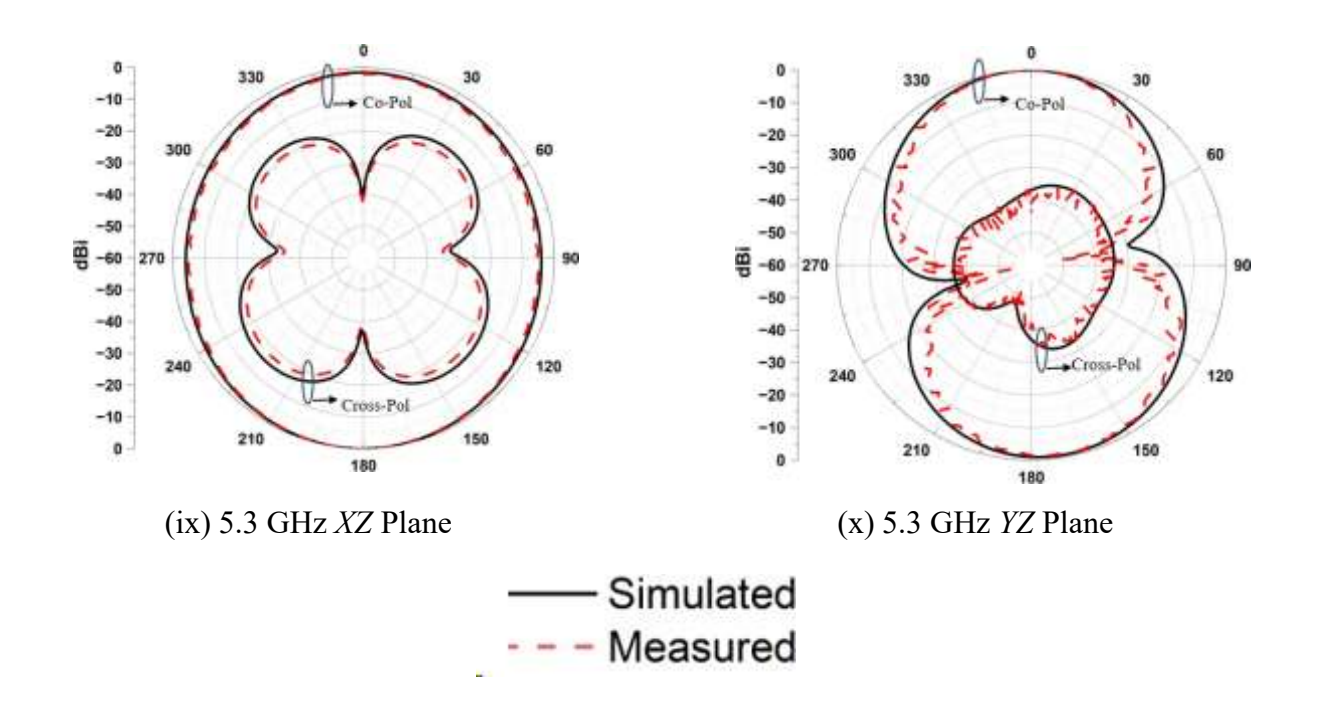


Fig.6.12. Normalized simulated and measured cross and co-polarization at three modes on a) XZ plane
b) YZ plane

Due to the symmetrical structure, the resonant frequency is the same as when  $D_1$  is ON and  $D_2$  is OFF (Mode 2b), but the pattern is tilted towards the left side, as shown in Fig.6.10 at 6.5 GHz.

In Mode 3, the proposed antenna resonates at 3.5 GHz (3.1–4 GHz) with a 0.9 GHz band width, which covers the 5G N78 Band. It is also resonant at 6.5 GHz (6.3 – 6.7 GHz) with a 0.5 GHz bandwidth, as shown in Fig. 6.9 (e). These bandwidths support higher data in 4G LTE systems and 5Gsystems with advanced modulation schemes such as QAM and OFDM. For example, in a 4G LTE system, a 0.01 GHz bandwidth is sufficient to handle several hundred Mbps of data. Scaling this up toa 0.9-GHz bandwidth supports data rates in the Gbps range. Similarly, the bandwidth of 0.5 GHz is also capable of supporting high data rates but has slightly less capacity compared to the 0.9 GHz bandwidth. At 6.5 GHz, the beam is tilting towards 265°, as shown in Fig. 6.11 (c). The peak realizedgain with and without FSS is shown in Fig. 6.9 (f). The radiation efficiency is listed in Table 6.2.

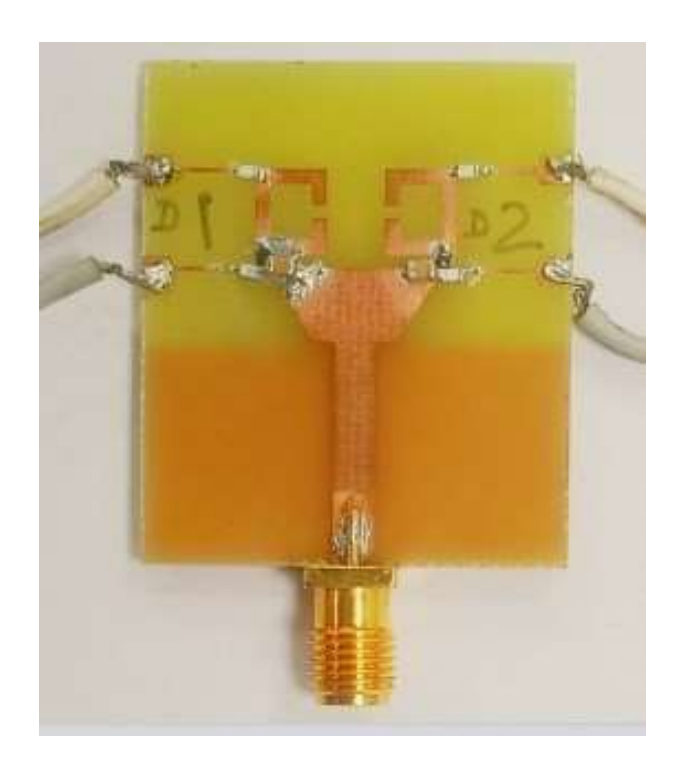
The important characteristics of HRA are summarized in Table 6.2 in all modes. One can observe that in mode 2(a and b) the resonant frequency is the same, but the pattern is tilting as shown in Fig.6.11. Additionally, for radiation pattern reconfiguration, it can be observed that at a common operation frequency of 6.5 GHz, the maximum tilt angle can be steered towards 265° (at Modes 1 and 3) and  $\pm$  13° (at Modes 2a and 2b) as shown in Fig.6.10. It shows that the proposed structure enables the pattern reconfigurable functionality independently with minimal effects at 6.5 GHz. Also, this structure

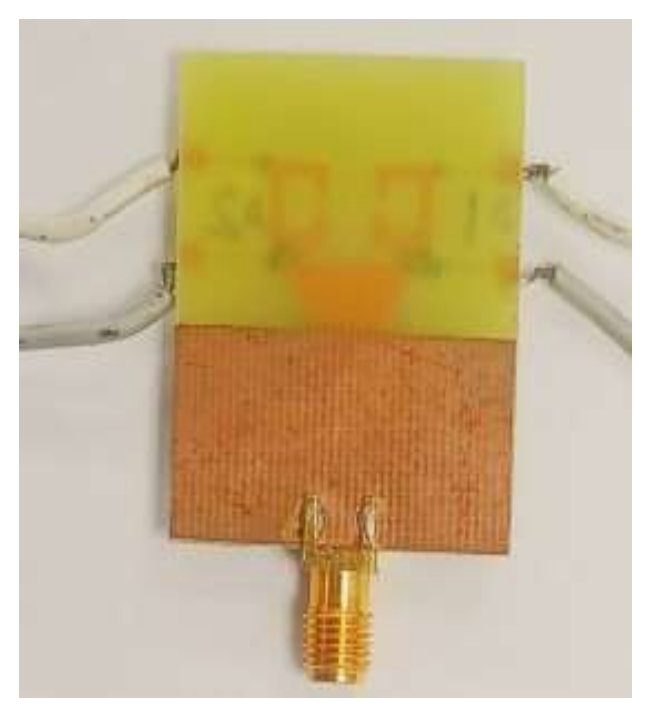
provides a simulated efficiency greater than 85% in all three modes reported in Table 6.2. The realized gain is enhanced by 2-4 dBi with an FSS-based reflector without altering the other performance characteristics of the proposed HRA. The cross-polarization levels are below the co-polarization levels for the XZ as well as the YZ planes of the proposed hybrid reconfigurable antenna in all three modes, as shown in Fig. 6.12 at various operating frequencies. The maximum isolation is obtained at mode 1 with a value of -50 dB, and the minimum difference is obtained at mode 3 with a value of -20 dB. A high level of isolation is needed to ensure independent signal paths and maximize the channel capacity in various wireless communication systems.

The fabricate photo copy fabricated enhanced gain hybrid reconfigurable antenna is shown in Fig.6.13. The LPKF S-63 PCB machine fabricates the proposed structure on FR-4 substrate. After that, the diodes, capacitors, inductors, and SMA connectors are soldered. The S-parameters are measured using R&ZNB 40 VNA for different operating states, as shown in Fig. 6.14. For, the diode ON condition, a current of 10 mA and a voltage of 1.4 volts are required, as per the data sheet[39]. Therefore, the same value is to be provided using the DC power supply. The manufacturing cost of this proposed structure is low due to the utilization of the FR-4 substrate. However, using thick dielectric material with a lower dielectric constant can improve the radiation efficiency of the antenna, but the minimum size, weight, and power cost pose significant challenges. Additionally, the increased material cost associated with specialized dielectric substrates can impact the overall system's affordability. Therefore, in most industries, the FR4 substrate is preferred due to its low cost and enhanced performance by innovative design techniques.

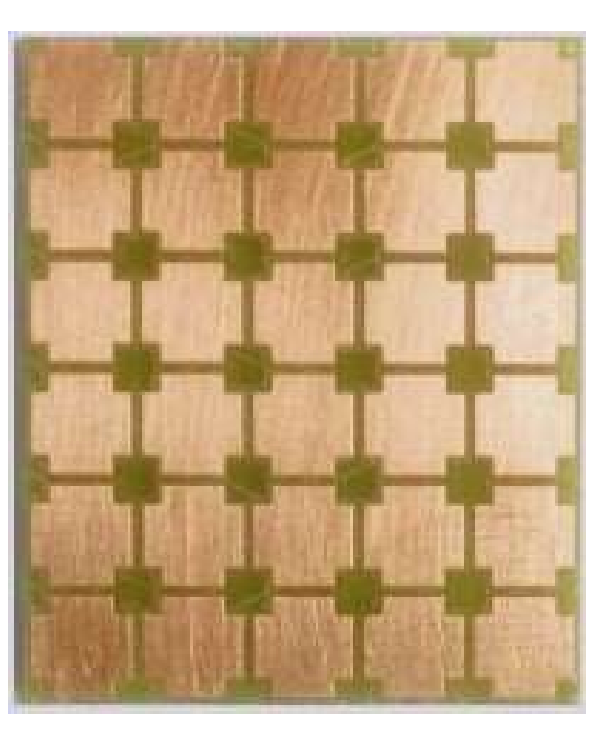
**TABLE 6.2** HRA performance characteristics with and without FSS based reflector

Modes	Resonant	Realized Gain	Realized Gain	Beam	Radiation
	frequencies	without FSS	with FSS	DirectionPhi=	Efficiency
	(GHz)	(dBi)	(dBi)	0° cut	(%)
Mode 1	5.3, 6.5	2.04,0.84	5.05 ,4.13	180°,265°	91%, 87%
Mode 2a	3.3, 5.1, 6.5	0.985,1.09,2.08	3.0,5.05,4.1	173°,172°,13°	89%, 88%,
					92%
Mode 2b	3.3, 5.1, 6.5	1.03,1.09,1.98	2.95,4.90,4.29	188°,187°,337°	90% 88%,
					89 %
Mode 3	3.5, 6.5	1.68,0.6	3.15,3.76	180°,265°	96%, 85%





(a) Top view of radiating structure



(c) FSS

(b) Bottom view of radiating structure



(d) Proposed hybrid reconfigurable antenna

Fig.6.13. A photograph of the fabricated HRA with FSS

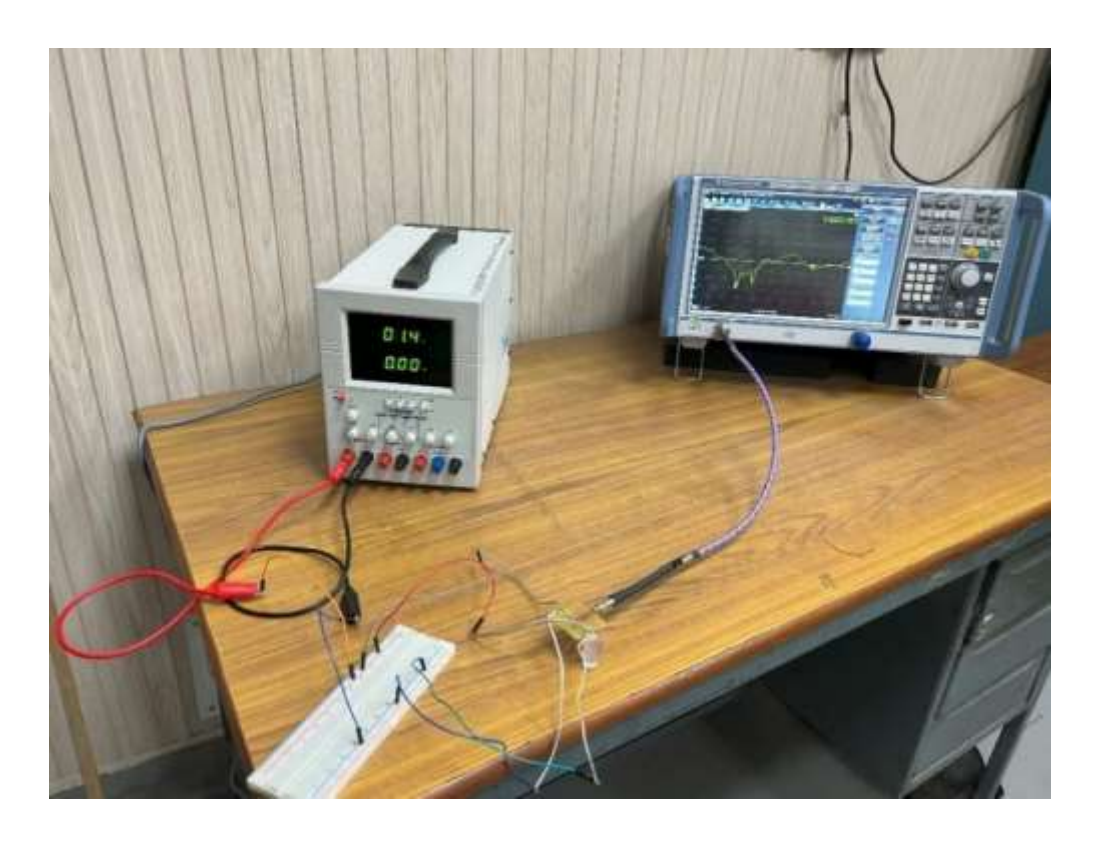


Fig.6.14. Snapshot of S parameter measurement at mode 3

### 6.5 Comparison of proposed gain enhanced HRA with existing structures

To explore the new contribution of the proposed HRA, a comparison is carried out with existing designs, which are listed in Table 6.3. Frequency and pattern reconfigurable antennas with a smaller number of diodes and multiple modes were realized in [110], [90], and [36] but they have not achieved multiband in a single operating state, and they are suffering from larger dimensions, limited beam tilting capacity, and narrow bandwidth. A higher number of frequency bands can be observed in [111], [112], and [36], but at the cost of a high number of PIN diodes and complex control structures, it is not attempted to enhance the gain of the reconfigurable antenna. A few designs,[104], [113], [114], and [115], [116], [117] were attempted to enhance the gain of the reconfigurable antennas but they were limited to either pattern, frequency or polarization reconfigurable only. The proposed HRA realizes only two PIN diodes, and better performance is achieved in terms of multiband frequency reconfiguration with pattern tilting capability and gain enhancement of 2-4 dBi with an FSS-based reflector

Table 6.3 Comparison of Proposed gain enhanced HRA with existing structures

Ref	Size of	Number	Number	Band	Structure	Reconfigurable	Multi	Gain
No.	antenna	of diodes	of Bands	Width	Complexit	property	Band	Enhancement
	( <b>mm</b> <sup>2</sup> )			(MHz)	y		(Yes/No)	(Yes/No)
[36]	31 × 27	8	6	410-1500	Very High	F/P	×	*
[90]	45 × 50	2	1	800	Very Low	F/P	×	*
[104]	97.5× 102	2	1	NG	Low	P	×	<b>√</b>
[110]	50 × 50	4	4	180-200	Low	F/P	×	×
[111]	30 × 20	4	5	410-1880	High	F/P	✓	×
[112]	46 × 32	12	5	230-1350	Very High	F/P	×	×
[113]	18.5× 18.5	8	3	10-140	High	P	<b>√</b>	<b>✓</b>
[114]	42.5×28.5	4	2	210-270	High	P	×	<b>√</b>
[115]	51×56	7	10	200-2500	High	F	<b>✓</b>	<b>✓</b>
[116]	113×113	1	2	2520	High	F	*	<b>✓</b>
[118]	30 × 30	3	6	400-500	Very Low	F/P	*	×
[119]	210 ×100	2	1	900	Low	P	×	<b>✓</b>
[120]	48 ×48	2	3	1230-2560	Low	Pol	✓	×
[121]	54×54	4	2	86-307	Low	F	*	<b>✓</b>
Prop	36 × 30	2	5	500-1800	Very low	F/P	✓	<b>✓</b>

# 6.6 The major contribution of proposed gain enhanced hybrid reconfigurable antenna

- Achieves multiband coverage of 5 G bands using two PIN diodes.
- ➤ In all the proposed modes, three different beams are obtained at a single frequency of operation: 6.5 GHz Wi-Fi 6E (5.925-7.125 GHz).
- ➤ It covers the complete band of the n78 band (3.3–3.8 GHz).
- ➤ The gain is enhanced by approximately 2-4 dBi with FSS placed below the radiating element at a distance without altering the resonant multiband and pattern tilting capability of the proposed structure without FSS.
- > The FSS and radiating element are fabricated on low-cost FR-4, so the cost of the proposed structure is very low.

### **6.7 Summary**

In this chapter, a multiband hybrid reconfigurable antenna is reported to have the capability of both frequency and pattern reconfiguration by utilizing two PIN diodes and enhancing the gain using an FSS-based reflector. The structure works in three modes, in each mode, it selects various frequencies with a radiation pattern tilt. Furthermore, it can be observed that the radiation efficiency of the proposed antenna is more than 85% in all three modes and that it can reconfigure the radiation pattern in the common frequency band of 6.5 GHz at three directions, namely 265°, 13°, and 337°. In all three modes, the realized gain is enhanced by the FSS-based reflector by nearly 2-4 dBi without affecting the other performance characteristics of the proposed HRA. The antenna supports 5G new radio applications in the n78 band (3.3 –3.8 GHz) and Wi-Fi 6E wireless standards (5.925 - 7.125 GHz), as well as 5.1 GHz and 5.3GHz for indoor WLAN applications. The current design has a limitation in that beam steering directions are limited.

#### **CHAPTER 7**

#### **Conclusion, Future Scope and Social Impact**

#### 7.1 Conclusion

The thesis reports the design and analysis of reconfigurable radiating structures with compact size, wideband, and multiband operations with a minimal number of RF switches, such as MADP-000907-14020P model PIN diode to enhance the system efficiency in next-generation wireless systems. The reported designs achieved frequency reconfiguration, frequency and pattern reconfiguration, and compound reconfiguration, ensuring optimal performance in dynamic 5G and Internet of Thing (IoT) environments.

The first two chapters discussed the introduction scope of research, reconfiguration techniques, and various types of reconfigurable antennas. By incorporating the PIN diode in the antenna's ground plane, a single-band frequency reconfigurable antenna with compact size and a V-shaped single, dual-band reconfigurable antenna are discussed based on the phase difference approach in the third chapter. These designs have a wideband of operation and suitable gain for 5G and Wi-Fi and Wi-Max applications. However, these designs are limited to frequency-reconfigurable antennae. The next chapter discusses a frequency and pattern reconfigurable antenna based on the Yagi-Uda principle by activating and deactivating the parasitic stubs. This design tilts the pattern omnidirectional to directional radiation, suitable for IoT close-range applications.

The suggested structure in the next chapter allows sub-6 GHz 5G, WLAN, and vehicle communications by offering tiltable radiation patterns with linear and circular polarization. It achieved dual band dual sense polarization in one of its operating states and improved its suitability for satellite communications. Additionally, the beam is tilted in this design independent of frequency for indoor WLAN applications. With an FSS-based reflector that enhances the gain by 2–4 dBi, a multiband hybrid antenna combines frequency and pattern reconfigurability across three operating modes, which is discussed in Chapter 6. This structure has an efficiency of over 85% and allows indoor WLAN, 5G, and Wi-Fi 6E applications.

The reported design results show a notable improvement in antenna reconfigurability, which can help in next-generation wireless standards. However, these limits to a few beam's steering directions and variation of ground length on the antenna performance.

### 7.2 Future Scope

### 7.2.1 Emerging Materials and Technologies

The reconfiguration from the proposed reconfigurable designs in this study was achieved by applying a PIN diode as a switch under the control of DC bias. At the same time, some switching techniques still need to be explored in this line of research.

The introduction of liquid metal in place of switch control has shown significant advancement, showcasing a promising solution for reconfigurable antenna design. Liquid metal can be effectively implemented in reconfigurable antenna using diverse metals like Liquid metal (LM) and eutectic gallium–indium (EGaIn; 75% gallium, 25% indium), these liquid metal highlights the characteristics of non-toxicity, good fluidity, and high conductivity (3.4 × 106 S/m) which makes them an ideal replacement for traditional mechanical switch control, ultimately providing better fluidity, flexibility and controllability without dealing with complex bias circuits. Materials like vanadium dioxide (VO<sub>2</sub>) and GST (Ge<sub>2</sub> Sb<sub>2</sub> Te<sub>2</sub>) enable reconfiguration via reversible transitions between states (e.g., insulating to conductive). Allow for adaptive behaviour in antennas under thermal or electrical stimuli. The graphene material offers excellent electrical, thermal, and mechanical properties and enables frequency reconfiguration via electrostatic biasing due to its tunable conductivity. Ferroelectric materials and BST (Barium Strontium Titanate) offer tunable permittivity for frequency reconfiguration and is effective in millimeter-wave applications. Further, advanced artificially engineered materials with different properties can enhance the antenna performance.

These technologies and materials drive the development of advanced reconfigurable antennas, enabling applications in 5G, IoT, satellite communications, and wearable devices.

### 7.2.2 Integration with AI and Machine learning for reconfigurable antenna design

The presented thesis addressed the challenges presented in the open literature with new designs and techniques. However, some new methods are further explored to ensure the efficient function of the wireless system.

The reconfigurable antenna design with integration of Artificial Intelligence and Machine learning models to optimize its parameters and adopt the real-time autonomous operation in the field of advanced wireless systems with different environmental conditions. Techniques like genetic algorithms, particle swarm optimization, and elementary search techniques optimize the antenna performance characteristics. The deep learning models can predict the antenna characteristics required for particular applications so that the number of iterations can be reduced in the simulations based on real-time control of antenna performance. The density of the user's reinforcement learning can be used to choose the optimal configuration dynamically by improving signal quality and network efficiency. The machine learning models precisely predict and analyze the real-time data in dense areas where several users can utilize the spectrum and facilitate the precise beam forming to support a more significant number of users, ensuring wide coverage with reduced interference.

AI-enabled self-healing mechanisms can monitor the performance of antenna hardware faults in real-time. ML models predict and optimize unit cell dimensions in metamaterial structures in reconfigurable antenna design by reducing the system complexity.

The difficulty is that integrating AI models with hardware necessitates a lot of processing power. Thus huge amounts of data is needed to train models for intricate multi-dimensional antenna designs.

### 7.3 Impact of Reconfigurable Antenna on Social Environment

This section discusses the impact of reconfigurable antennas on the social environment. Antennas are key components in any wireless communication system. Nowadays, most people around the globe use mobile phones for various activities in their daily lives. The smartphone consists of a more significant number of antennas to support multiple wireless standards, and these antennas can produce more radiation that will cause health issues for various living and non-living things. In industries, the size of different wireless devices also matters.

These challenges can be overcome by implementing multiple wireless standards in a single antenna, such as a reconfigurable antenna so that the radiation and size complexity will be reduced. The reconfigurable antenna can perform various activities from a single radiating structure. This consolidation minimizes the environmental impact associated with manufacturing and deploying multiple antennas. Additionally, their ability to dynamically adjust performance based on ecological conditions can optimize energy use in communication systems, contributing to more sustainable practices in technology deployment. However, privacy and security issues arise as more devices connect, making ethical considerations in technology deployment crucial.

Reconfigurable antennas provide smooth interaction between multiple devices and networks by adapting to varied frequencies and communication protocols. This flexibility makes better access to wireless services possible, especially in underserved areas. These antennas can improve connectivity in remote or rural areas by supporting several wireless standards, promoting digital inclusion, and reducing the digital divide. Reconfigurable antennas have a wide range of effects on social contexts, including social dynamics, economic growth, environmental sustainability, technical innovation, and connectedness. As these technologies develop, their pervasiveness in daily life will probably continue to profoundly influence social interactions and structures.

# References

- [1] Constantine A. Balanis, Antenna Theory: Analysis and Design. 2015.
- [2] V. Suryapaga and V. V. Khairnar, "Review on Multifunctional Pattern and Polarization Reconfigurable Antennas," *IEEE Access*, vol. 12, pp. 90218–90251, 2024, doi: 10.1109/ACCESS.2024.3420426.
- [3] "https://insidetowers.com/cell-tower-news-rockin-the-c-band/."
- [4] M. Zhang, G. Xu, and R. Gao, "Reconfigurable Antennas for Wireless Communication: Design Mechanism, State of the Art, Challenges, and Future Perspectives," *Int J Antennas Propag*, vol. 2024, no. 1, Jan. 2024, doi: 10.1155/2024/3046393.
- [5] S. Choudhury, Reconfigurable Antennas. in 2053-2563. IOP Publishing, 2023. doi: 10.1088/978-0-7503-5457-8.
- [6] K. Karthika and K. Kavitha, "Reconfigurable Antennas for Advanced Wireless Communications: A Review," 2021. doi: 10.1007/s11277-021-08555-4.
- [7] S. Ullah, S. Hayat, A. Umar, U. Ali, F. A. Tahir, and J. A. Flint, "Design, fabrication and measurement of triple band frequency reconfigurable antennas for portable wireless communications," *AEU International Journal of Electronics and Communications*, vol. 81, pp. 236–242, Nov. 2017, doi: 10.1016/j.aeue.2017.07.028.
- [8] T. Ali and R. C. Biradar, "A compact hexagonal slot dual band frequency reconfigurable antenna for WLAN applications," *Microw Opt Technol Lett*, vol. 59, no. 4, pp. 958–964, Apr. 2017, doi: 10.1002/mop.30443.
- [9] S. Ullah *et al.*, "Frequency reconfigurable antenna for portable wireless applications," *Computers, Materials and Continua*, vol. 68, no. 3, pp. 3015–3027, 2021, doi: 10.32604/cmc.2021.015549.
- [10] W. A. Awan *et al.*, "Design and realization of a frequency reconfigurable antenna with wide, dual, and single-band operations for compact sized wireless applications," *Electronics (Switzerland)*, vol. 10, no. 11, Jun. 2021, doi: 10.3390/electronics10111321.

- [11] N. Hussain *et al.*, "A compact flexible frequency reconfigurable antenna for heterogeneous applications," *IEEE Access*, vol. 8, pp. 173298–173307, 2020, doi: 10.1109/ACCESS.2020.3024859.
- [12] A. Boufrioua, "Frequency Reconfigurable Antenna Designs Using PIN Diode for Wireless Communication Applications," *Wirel Pers Commun*, vol. 110, no. 4, pp. 1879–1885, Feb. 2020, doi: 10.1007/s11277-019-06816-x.
- [13] I. Ahmad *et al.*, "Frequency reconfigurable antenna for multi standard wireless and mobile communication systems," *Computers, Materials and Continua*, vol. 68, no. 2, pp. 2563–2578, Apr. 2021, doi: 10.32604/cmc.2021.016813.
- [14] W. A. Awan *et al.*, "A miniaturized wideband and multi-band on-demand reconfigurable antenna for compact and portable devices," *AEU International Journal of Electronics and Communications*, vol. 122, Jul. 2020, doi: 10.1016/j.aeue.2020.153266.
- [15] G. Jin, C. Deng, J. Yang, Y. Xu, and S. Liao, "A new differentially-fed frequency reconfigurable antenna for WLAN and sub-6GHz 5G applications," *IEEE Access*, vol. 7, pp. 56539–56546, 2019, doi: 10.1109/ACCESS.2019.2901760.
- [16] H. R. D. Filgueiras, I. F. da Costa, S. A. Cerqueira, R. A. Santos, and J. R. Kelly, "Mechanically reconfigurable slotted-waveguide antenna array for 5G networks," in *2017 SBMO/IEEE MTT-S International Microwave and Optoelectronics Conference (IMOC)*, 2017, pp. 1–5. doi: 10.1109/IMOC.2017.8121105.
- [17] A. Raveendran, P. Mathur, and S. Raman, "Mechanically Frequency Reconfigurable Antenna and its Application as a Fluid Level Detector for Wireless Sensor Networks," in *2019 URSI Asia-Pacific Radio Science Conference (AP-RASC)*, 2019, pp. 1–4. doi: 10.23919/URSIAP-RASC.2019.8738663.
- [18] S. Gaya, A. Hamza, O. Sokunbi, S. I. M. Sheikh, and H. Attia, "Electronically Switchable Frequency and Pattern Reconfigurable Segmented Patch Antenna for Internet of Vehicles," *IEEE Internet Things J*, vol. 11, no. 10, pp. 17840–17851, May 2024, doi: 10.1109/JIOT.2024.3362906.
- [19] S. R. Isa *et al.*, "Reconfigurable pattern patch antenna for mid-band 5G: A review," *Computers, Materials and Continua*, vol. 70, no. 2, pp. 2699–2725, 2022, doi: 10.32604/cmc.2022.019769.
- [20] P. Arthur, M. S. Ellis, A. R. Ahmed, and J. J. Kponyo, "Design of pattern-reconfigurable circularly polarized unidirectional antenna based on quasi-radiator for ISM applications," *Heliyon*, vol. 8, no. 11, Nov. 2022, doi: 10.1016/j.heliyon.2022.e11721.

- [21] A. Boukarkar, S. Rachdi, M. Mohamed Amine, B. Sami, and A. Benziane Khalil, "A compact four states radiation-pattern reconfigurable monopole antenna for Sub-6 GHz IoT applications," *AEU-International Journal of Electronics and Communications*, vol. 158, Jan. 2023, doi: 10.1016/j.aeue.2022.154467.
- [22] J. You and Y. Dong, "Miniaturized Planar Pattern-Reconfigurable Antenna for Smart Wi-Fi Applications," *IEEE Antennas Wirel Propag Lett*, vol. 23, no. 1, pp. 109–113, Jan. 2024, doi: 10.1109/LAWP.2023.3318328.
- [23] J. You and Y. Dong, "Smart Wi-Fi Antenna With Reconfigurable Omnidirectional and Unidirectional Patterns," *IEEE Antennas Wirel Propag Lett*, vol. 23, no. 3, pp. 1010–1014, Mar. 2024, doi: 10.1109/LAWP.2023.3341869.
- [24] P. B. Nikam, J. Kumar, A. Baidya, and A. Ghosh, "Low-profile bandwidth and E-plane radiation pattern reconfigurable patch antenna for sub-6 GHz 5G applications," *AEU International Journal of Electronics and Communications*, vol. 157, Dec. 2022, doi: 10.1016/j.aeue.2022.154415.
- [25] W. Yuan, J. Huang, X. Zhang, K. Cui, W. Wu, and N. Yuan, "Wideband Pattern-Reconfigurable Antenna With Switchable Monopole and Vivaldi Modes," *IEEE Antennas Wirel Propag Lett*, 2022, doi: 10.1109/LAWP.2022.3207199.
- [26] Y. Liu and Y. Dong, "Pattern-Reconfigurable Planar Antenna Based on Vivaldi Structure," *IEEE Antennas Wirel Propag Lett*, vol. 23, no. 8, pp. 2516–2520, 2024, doi: 10.1109/LAWP.2024.3398370.
- [27] Z. Wang and Y. Dong, "Metamaterial-Based, Vertically Polarized, Miniaturized Beam-Steering Antenna for Reconfigurable Sub-6 GHz Applications," *IEEE Antennas Wirel Propag Lett*, vol. 21, no. 11, pp. 2239–2243, 2022, doi: 10.1109/LAWP.2022.3188548.
- [28] X. Zhang, K. Wei, Y. Li, and Z. Zhang, "A Polarization Reconfigurable Antenna for Satellite Communication in Foldable Smartphone," *IEEE Trans Antennas Propag*, vol. 71, no. 12, pp. 9938–9943, Dec. 2023, doi: 10.1109/TAP.2023.3314084.
- [29] H. Dong, Y. Xiao, S. Tan, J. Hu, and Z. Chen, "Dual-Broadband Circularly Polarized Reconfigurable Antenna Based on Asymmetric U-Slot Patch," *IEEE Antennas Wirel Propag Lett*, vol. 22, no. 12, pp. 3052–3056, 2023, doi: 10.1109/LAWP.2023.3309504.
- [30] B. Anantha, L. Merugu, and P. V.D. Somasekhar Rao, "A novel single feed frequency and polarization reconfigurable microstrip patch antenna," *AEU International Journal of Electronics and Communications*, vol. 72, pp. 8–16, Feb. 2017, doi: 10.1016/j.aeue.2016.11.012.

- [31] A. Bharathi and G. Ravi Shankar Reddy, "A novel dual-sense polarization reconfigurable dual-band microstrip antenna," *AEU International Journal of Electronics and Communications*, vol. 171, Nov. 2023, doi: 10.1016/j.aeue.2023.154926.
- [32] A. Bhattacharjee and S. Dwari, "Design of an Anisotropic Reconfigurable Reflective Polarization Converter for Realizing Circular Polarization-Reconfigurable Antenna," *IEEE Antennas Wirel Propag Lett*, vol. 21, no. 12, pp. 2392–2396, Dec. 2022, doi: 10.1109/LAWP.2022.3194347.
- [33] A. Panahi, X. L. Bao, K. Yang, O. O'Conchubhair, and M. J. Ammann, "A simple polarization reconfigurable printed monopole antenna," *IEEE Trans Antennas Propag*, vol. 63, no. 11, pp. 5129–5134, Nov. 2015, doi: 10.1109/TAP.2015.2474745.
- [34] Y. P. Selvam, L. Elumalai, M. G. N. Alsath, M. Kanagasabai, S. Subbaraj, and S. Kingsly, "Novel Frequency- And Pattern-Reconfigurable Rhombic Patch Antenna with Switchable Polarization," *IEEE Antennas Wirel Propag Lett*, vol. 16, 2017, doi: 10.1109/LAWP.2017.2660069.
- [35] S. Yao and S. V Georgakopoulos, "Origami Segmented Helical Antenna With Switchable Sense of Polarization," *IEEE Access*, vol. 6, pp. 4528–4536, 2018, doi: 10.1109/ACCESS.2017.2787724.
- [36] I. Ahmad *et al.*, "Design and Experimental Analysis of Multiband Compound Reconfigurable 5G Antenna for Sub-6 GHz Wireless Applications," *Wirel Commun Mob Comput*, vol. 2021, 2021, doi: 10.1155/2021/5588105.
- [37] M. Shaw and Y. K. Choukiker, "Reconfigurable polarization and pattern microstrip antenna for IRNSS band applications," *AEU International Journal of Electronics and Communications*, vol. 160, Feb. 2023, doi: 10.1016/j.aeue.2022.154501.
- [38] Y. Panneer Selvam *et al.*, "A Patch-Slot Antenna Array with Compound Reconfiguration," *IEEE Antennas Wirel Propag Lett*, vol. 17, no. 3, pp. 525–528, Mar. 2018, doi: 10.1109/LAWP.2018.2801124.
- [39] "https://www.macom.com/products/product-detail/MADP-000907-14020P."
- [40] S. K. Sharma and J.-C. S. Chieh, *Multifunctional antennas and arrays for wireless communication systems*.
- [41] J. Hu, X. Yang, L. Ge, Z. Guo, Z. C. Hao, and H. Wong, "A reconfigurable 1 × 4 circularly polarized patch array antenna with frequency, radiation pattern, and polarization agility," *IEEE Trans Antennas Propag*, vol. 69, no. 8, 2021, doi: 10.1109/TAP.2020.3048526.

- [42] M. Kaur, H. Shankar Singh, and M. Agarwal, "Design and development of low-profile hybrid reconfigurable antenna for 5G sub-6 GHz applications," *AEU International Journal of Electronics and Communications*, vol. 178, May 2024, doi: 10.1016/j.aeue.2024.155301.
- [43] M. Kaur, H. Shankar Singh, and M. Agarwal, "A compact two-state pattern reconfigurable antenna for 5G Sub-6 GHz cellular applications," *AEU International Journal of Electronics and Communications*, vol. 162, Apr. 2023, doi: 10.1016/j.aeue.2023.154577.
- [44] A. Bhattacharjee and S. Dwari, "A Monopole Antenna with Reconfigurable Circular Polarization and Pattern Tilting Ability in Two Switchable Wide Frequency Bands," *IEEE Antennas Wirel Propag Lett*, vol. 20, no. 9, pp. 1661–1665, Sep. 2021, doi: 10.1109/LAWP.2021.3092345.
- [45] G. R. Prasad *et al.*, "Concentric Ring Structured Reconfigurable Antenna using MEMS Switches for Wireless Communication Applications," *Wirel Pers Commun*, vol. 120, no. 1, pp. 587–608, Sep. 2021, doi: 10.1007/s11277-021-08480-6.
- [46] N. Narang, P. K. Shrivastava, A. Basu, and P. Singh, "A compact and reconfigurable C-band DGS-based power divider using RF MEMS capacitive switch," *Journal of Micromechanics and Microengineering*, vol. 34, no. 3, p. 35002, Feb. 2024, doi: 10.1088/1361-6439/ad2308.
- [47] S. Goel and N. Gupta, "Design, optimization and analysis of reconfigurable antenna using RF MEMS switch," *Microsystem Technologies*, vol. 26, no. 9, pp. 2829–2837, Sep. 2020, doi: 10.1007/s00542-020-04823-8.
- [48] Y. Chen *et al.*, "An L-Slot Frequency Reconfigurable Antenna Based on MEMS Technology," *Micromachines (Basel)*, vol. 14, no. 10, Oct. 2023, doi: 10.3390/mi14101945.
- [49] K. Kumar Naik and B. Venkata Sai Sailaja, "RF-MEMS Switch for Reconfigurable With Half-Moon Slots on Elliptical-Shaped Patch Antenna for 5G Applications," *IEEE Open Journal of Antennas and Propagation*, vol. 5, no. 3, pp. 673–685, 2024, doi: 10.1109/OJAP.2024.3384397.
- [50] Z. Ding, R. Jin, J. Geng, W. Zhu, and X. Liang, "Varactor Loaded Pattern Reconfigurable Patch Antenna With Shorting Pins," *IEEE Trans Antennas Propag*, vol. 67, no. 10, pp. 6267–6277, 2019, doi: 10.1109/TAP.2019.2920282.
- [51] V. M. Lad, K. V. Kulhalli, J. Kumar, and G. Patil, "Frequency-Tunable Multiband Reconfigurable Microstrip Patch Antenna for Wireless Application," *Wirel Pers Commun*, vol. 130, no. 2, pp. 1231–1242, May 2023, doi: 10.1007/s11277-023-10328-0.
- [52] N. Hussain *et al.*, "Dual-sense slot-based CP MIMO antenna with polarization bandwidth reconfigurability," *Sci Rep*, vol. 13, no. 1, p. 16132, 2023, doi: 10.1038/s41598-023-42569-1.

- [53] Q. H. Dang, N. Nguyen-Trong, C. Fumeaux, and S. J. Chen, "Tuning-Range Extension Strategies for Varactor-Based Frequency-Reconfigurable Antennas," *IEEE Open Journal of Antennas and Propagation*, vol. 4, pp. 1087–1094, 2023, doi: 10.1109/OJAP.2023.3329259.
- [54] S. Han, Z. Wang, and Y. Dong, "Miniaturized Circularly Polarized Reconfigurable Capacitance-Loaded Patch Antenna," *IEEE Antennas Wirel Propag Lett*, vol. 23, no. 4, pp. 1226–1230, 2024, doi: 10.1109/LAWP.2024.3349974.
- [55] S. N. M. Zainarry, N. Nguyen-Trong, and C. Fumeaux, "A Frequency- and Pattern-Reconfigurable Two-Element Array Antenna," *IEEE Antennas Wirel Propag Lett*, vol. 17, no. 4, pp. 617–620, Apr. 2018, doi: 10.1109/LAWP.2018.2806355.
- [56] S. K. Muthuvel, M. Shaw, and Y. K. Choukiker, "Concentric circular compound reconfigurable microstrip patch antenna for wireless applications," *AEU International Journal of Electronics and Communications*, vol. 141, Nov. 2021, doi: 10.1016/j.aeue.2021.153960.
- [57] J. F. Li, B. Wu, J. Q. Zhou, K. X. Guo, H. R. Zu, and T. Su, "Frequency and Pattern Reconfigurable Antenna Using Double Layer Petal Shaped Parasitic Structure," *IEEE Transactions on Circuits and Systems II: Express Briefs*, Apr. 2023, doi: 10.1109/TCSII.2023.3329659.
- [58] M. Wang *et al.*, "Miniaturization of Frequency-Reconfigurable Antenna Using Periodic Slow-Wave Structure," *IEEE Trans Antennas Propag*, vol. 69, no. 11, pp. 7889–7894, Nov. 2021, doi: 10.1109/TAP.2021.3076570.
- [59] L. Wang, Q. Li, Q. Fu, X. Ding, Y. Wang, and W. Zhu, "Optically Reconfigurable THz Metamaterial with Switchable Wideband Absorption and Transmission," 2023, doi: 10.3390/photonics.
- [60] H. H. Al-khaylani, T. A. Elwi, and A. A. Ibrahim, "Optically remote-controlled miniaturized 3D reconfigurable CRLH-printed MIMO antenna array for 5G applications," *Microw Opt Technol Lett*, vol. 65, no. 2, pp. 603–610, 2023, doi: https://doi.org/10.1002/mop.33504.
- [61] G. Jin, L. Li, W. Wang, and S. Liao, "A wideband polarization reconfigurable antenna based on optical switches and C-shaped radiator," *Microw Opt Technol Lett*, vol. 62, no. 6, pp. 2415–2422, 2020, doi: https://doi.org/10.1002/mop.32313.
- [62] A. Ali *et al.*, "Optically reconfigurable planar monopole antenna for cognitive radio application," *Microw Opt Technol Lett*, vol. 61, no. 4, pp. 1110–1115, 2019, doi: https://doi.org/10.1002/mop.31678.
- [63] M. Ciflik, S. C. Basaran, and O. Dandin, "Optically control tissue-independent reconfigurable antenna for body-centric communications at 2.4 GHz ISM band," AEU International Journal of

- *Electronics and Communications*, vol. 178, p. 155304, 2024, doi: https://doi.org/10.1016/j.aeue.2024.155304.
- [64] Y. Zhang, S. Lin, S. Yu, G. J. Liu, and A. Denisov, "Design and analysis of optically controlled pattern reconfigurable planar Yagi–Uda antenna," *IET Microwaves, Antennas & Propagation*, vol. 12, no. 13, pp. 2053–2059, 2018, doi: https://doi.org/10.1049/iet-map.2018.5204.
- [65] I. F. da Costa, A. Cerqueira S., D. H. Spadoti, L. G. da Silva, J. A. J. Ribeiro, and S. E. Barbin, "Optically Controlled Reconfigurable Antenna Array for mm-Wave Applications," *IEEE Antennas Wirel Propag Lett*, vol. 16, pp. 2142–2145, 2017, doi: 10.1109/LAWP.2017.2700284.
- [66] M. W. Nichols, A. Gonzalez, E. A. Alwan, and J. L. Volakis, "An Accordion-Folding Series-Fed Patch Array With Finite Thickness: A folding technique for CubeSat arrays," *IEEE Antennas Propag Mag*, vol. 65, no. 3, pp. 77–82, 2023, doi: 10.1109/MAP.2022.3229295.
- [67] C.-W. Luo, G. Zhao, Y.-C. Jiao, G.-T. Chen, and Y.-D. Yan, "Wideband 1 bit Reconfigurable Transmitarray Antenna Based on Polarization Rotation Element," *IEEE Antennas Wirel Propag Lett*, vol. 20, no. 5, pp. 798–802, 2021, doi: 10.1109/LAWP.2021.3063539.
- [68] Y. Damgaci and B. A. Cetiner, "A frequency reconfigurable antenna based on digital microfluidics," *Lab Chip*, vol. 13, no. 15, pp. 2883–2887, 2013, doi: 10.1039/C3LC50275A.
- [69] S. Lee, M. Lee, and S. Lim, "Frequency reconfigurable antenna actuated by three-storey tower kirigami," *Extreme Mech Lett*, vol. 39, p. 100833, 2020, doi: https://doi.org/10.1016/j.eml.2020.100833.
- [70] S. Yoo, H. Choo, and G. Byun, "Design of mechanically rotatable microstrip patch antennas using an asymmetric polariser for adaptive polarisation adjustment," *IET Microwaves, Antennas & Propagation*, vol. 13, no. 8, pp. 1122–1128, 2019, doi: https://doi.org/10.1049/iet-map.2018.5054.
- [71] X. Yang *et al.*, "A Mechanically Reconfigurable Reflectarray With Slotted Patches of Tunable Height," *IEEE Antennas Wirel Propag Lett*, vol. 17, no. 4, pp. 555–558, 2018, doi: 10.1109/LAWP.2018.2802701.
- [72] L. Song, W. Gao, and Y. Rahmat-Samii, "3-D Printed Microfluidics Channelizing Liquid Metal for Multipolarization Reconfigurable Extended E-Shaped Patch Antenna," *IEEE Trans Antennas Propag*, vol. 68, no. 10, pp. 6867–6878, 2020, doi: 10.1109/TAP.2020.2993079.
- [73] Y. J. Zhang, L. C. Wang, W. L. Song, M. Chen, and D. Fang, "Hexagon-Twist Frequency Reconfigurable Antennas via Multi-Material Printed Thermo-Responsive Origami Structures," *Front Mater*, vol. 7, Nov. 2020, doi: 10.3389/fmats.2020.600863.

- [74] D. Kim, K. Kim, H. Kim, M. Choi, and J. H. Na, "Design optimization of reconfigurable liquid crystal patch antenna," *Materials*, vol. 14, no. 4, pp. 1–12, Feb. 2021, doi: 10.3390/ma14040932.
- [75] Z. Jin, Y. Rong, J. D. Yu, and F. Wu, "Design of a Compound Reconfigurable Terahertz Antenna Based on Graphene," *Plasmonics*, vol. 19, no. 2, pp. 621–629, Apr. 2024, doi: 10.1007/s11468-023-02011-8.
- [76] M. Lee, H. Son, D. Lim, S. Lee, and S. Lim, "Liquid-metal-fluidically polarization reconfigurable microstrip patch antenna," *Microw Opt Technol Lett*, vol. 61, no. 10, pp. 2306–2314, 2019, doi: https://doi.org/10.1002/mop.31898.
- [77] A. Singh, I. Goode, and C. E. Saavedra, "A Multistate Frequency Reconfigurable Monopole Antenna Using Fluidic Channels," *IEEE Antennas Wirel Propag Lett*, vol. 18, no. 5, pp. 856–860, 2019, doi: 10.1109/LAWP.2019.2903781.
- [78] S. Dash, C. Psomas, and I. Krikidis, "Selection of metallic liquid in sub-6 GHz antenna design for 6G networks," *Sci Rep*, vol. 13, no. 1, p. 20551, 2023, doi: 10.1038/s41598-023-47870-7.
- [79] P. Tang, Q. Tao, S. Liu, J. Xiang, L. Zhong, and Y. Qin, "Reconfigurable Radiation Angle Continuous Deflection of All-Dielectric Phase-Change V-Shaped Antenna," *Nanomaterials*, vol. 12, no. 19, Oct. 2022, doi: 10.3390/nano12193305.
- [80] N. C. P. Mettu Goutham Reddy and S. S. Karthikeyan, "Investigation on tuning capabilities of self-diplexing antenna using different liquid dielectrics," *J Electromagn Waves Appl*, vol. 37, no. 10–12, pp. 1011–1022, 2023, doi: 10.1080/09205071.2023.2220091.
- [81] H. Liu, T. Yan, Z. Zhao, Z. Wang, and S. Fang, "Polarization-Reconfigurable Compact Wideband Slot Antenna by Using Liquid Metal," *IEEE Antennas Wirel Propag Lett*, vol. 21, no. 12, pp. 2327–2331, 2022, doi: 10.1109/LAWP.2022.3192529.
- [82] D. Connelly and J. Chisum, "VO antennas with metallic inclusions for low-loss reconfigurable cognitive radios," *Microw Opt Technol Lett*, vol. 63, no. 4, pp. 1257–1263, 2021, doi: https://doi.org/10.1002/mop.32729.
- [83] Z. Jin, Y. Rong, J. D. Yu, and F. Wu, "Design of a Compound Reconfigurable Terahertz Antenna Based on Graphene," *Plasmonics*, vol. 19, no. 2, pp. 621–629, Apr. 2024, doi: 10.1007/s11468-023-02011-8.
- [84] A. Kouki, F. Sboui, and L. Latrach, "Magnetically tuned SIW patch antenna based on nematic liquid crystal for 5G applications and satellite communication systems," *Int J Microw Wirel Technol*, vol. 15, no. 9, pp. 1610–1619, Nov. 2023, doi: 10.1017/S1759078723000302.

- [85] M. Geetha, K. Dhanalakshmi, V. Vetriselvi, S. Jayachandran, and I. A. Palani, "Frequency Response Characterization of Thin-Film Shape Memory Alloy Actuator for Reconfigurable Antenna," *J Electron Mater*, vol. 52, no. 8, pp. 5239–5248, Aug. 2023, doi: 10.1007/s11664-023-10485-9.
- [86] Y. Liu, Q. Wang, Y. Jia, and P. Zhu, "A Frequency- and Polarization-Reconfigurable Slot Antenna Using Liquid Metal," *IEEE Trans Antennas Propag*, vol. 68, no. 11, pp. 7630–7635, 2020, doi: 10.1109/TAP.2020.2993110.
- [87] N. O. Parchin, H. J. Basherlou, Y. I. A. Al-Yasir, A. M. Abdulkhaleq, and R. A. Abd-Alhameed, "Reconfigurable antennas: Switching techniques— a survey," Feb. 01, 2020, *MDPI AG*. doi: 10.3390/electronics9020336.
- [88] R. Alhamad, E. Almajali, and S. Mahmoud, "Electrical Reconfigurability in Modern 4G, 4G/5G and 5G Antennas: A Critical Review of Polarization and Frequency Reconfigurable Designs," *IEEE Access*, vol. 11, pp. 29215–29233, 2023, doi: 10.1109/ACCESS.2023.3260073.
- [89] "https://www.omnicalculator.com/math/hexagon."
- [90] A. Ghaffar *et al.*, "A flexible and pattern reconfigurable antenna with small dimensions and simple layout for wireless communication systems operating over 1.65–2.51 ghz," *Electronics* (*Switzerland*), vol. 10, no. 5, pp. 1–13, Mar. 2021, doi: 10.3390/electronics10050601.
- [91] L. Han, C. Wang, W. Zhang, R. Ma, and Q. Zeng, "Design of frequency- and pattern-reconfigurable wideband slot antenna," *Int J Antennas Propag*, vol. 2018, 2018, doi: 10.1155/2018/3678018.
- [92] D. Borakhade and S. Pokle, "Pentagon slot resonator frequency reconfigurable antenna for wideband reconfiguration," *AEU International Journal of Electronics and Communications*, vol. 69, Dec. 2015, doi: 10.1016/j.aeue.2015.06.012.
- [93] I. Ali Shah, S. Hayat, I. Khan, Imtiaz. Alam, S. Ullah, and A. Afridi, "A Compact, Tri-Band and 9-Shape Reconfigurable Antenna for WiFi, WiMAX and WLAN Applications," *International Journal of Wireless and Microwave Technologies*, vol. 6, no. 5, pp. 45–53, Sep. 2016, doi: 10.5815/ijwmt.2016.05.05.
- [94] A. Iqbal, S. Ullah, U. Naeem, A. Basir, and U. Ali, "Design, Fabrication and Measurement of a Compact, Frequency Reconfigurable, Modified T-shape Planar Antenna for Portable Applications," *Journal of Electrical Engineering and Technology*, vol. 12, pp. 1611–1618, Dec. 2017, doi: 10.5370/JEET.2017.12.4.1611.
- [95] M. Ganesh, N. S. Raghava, and T. Sabapathy, "Design a hexagonal shape frequency reconfigurable antenna for new C-band 5G applications," in 2022 IEEE International Conference on Electronics,

- Computing and Communication Technologies, CONECCT 2022, 2022. doi: 10.1109/CONECCT55679.2022.9865714.
- [96] D. Behera, D. Mishra, S. K. Behera, S. Pandav, A. Gorai, and S. K. Mohapatra, "A Frequency and Pattern Reconfigurable Planar Antenna for IoT Applications," in 2023 International Conference on Communication, Circuits, and Systems, IC3S 2023, Institute of Electrical and Electronics Engineers Inc., 2023. doi: 10.1109/IC3S57698.2023.10169816.
- [97] L. H. Trinh, T. N. Le, R. Staraj, F. Ferrero, and L. Lizzi, "A pattern-reconfigurable slot antenna for IoT network concentrators," *Electronics (Switzerland)*, vol. 6, no. 4, pp. 1–7, Dec. 2017, doi: 10.3390/electronics6040105.
- [98] Z. Wang, Y. Dong, and Y. Ning, "Frequency Reconfigurable SRR-Based Compact Antenna for IoT Application," in *Asia-Pacific Microwave Conference Proceedings, APMC*, Institute of Electrical and Electronics Engineers Inc., Dec. 2020, pp. 148–150. doi: 10.1109/APMC47863.2020.9331673.
- [99] W. A. Awan *et al.*, "Design and realization of a frequency reconfigurable antenna with wide, dual, and single-band operations for compact sized wireless applications," *Electronics (Switzerland)*, vol. 10, no. 11, Jun. 2021, doi: 10.3390/electronics10111321.
- [100] Z. Wang, S. Liu, and Y. Dong, "Compact Wideband Pattern Reconfigurable Antennas Inspired by End-Fire Structure for 5G Vehicular Communication," *IEEE Trans Veh Technol*, vol. 71, no. 5, pp. 4655–4664, May 2022, doi: 10.1109/TVT.2022.3152354.
- [101] P. Kumar, S. Dwari, R. K. Saini, and M. K. Mandal, "Dual-Band Dual-Sense Polarization Reconfigurable Circularly Polarized Antenna," *IEEE Antennas Wirel Propag Lett*, vol. 18, no. 1, pp. 64–68, Jan. 2019, doi: 10.1109/LAWP.2018.2880799.
- [102] K. Karthika and K. Kavitha, "Design and Development of Parasitic Elements Loaded Quadband Frequency and Pattern Reconfigurable Antenna," *International Journal of RF and Microwave Computer-Aided Engineering*, vol. 2023, 2023, doi: 10.1155/2023/4034241.
- [103] L. Ge, Y. Li, J. Wang, and C. Y. D. Sim, "A low-profile reconfigurable cavity-backed slot antenna with frequency, polarization, and radiation pattern agility," *IEEE Trans Antennas Propag*, vol. 65, no. 5, pp. 2182–2189, May 2017, doi: 10.1109/TAP.2017.2681432.
- [104] B. Barakali, K. L. Ford, and S. Khamas, "High-gain pattern reconfigurable micro-strip dipole antenna with a gain enhancing partially reflecting surface," *IET Microwaves, Antennas and Propagation*, vol. 12, no. 10, pp. 1679–1683, Aug. 2018, doi: 10.1049/iet-map.2018.0150.

- [105] D. Rodrigo, B. A. Cetiner, and L. Jofre, "Frequency, radiation pattern and polarization reconfigurable antenna using a parasitic pixel layer," *IEEE Trans Antennas Propag*, vol. 62, no. 6, pp. 3422–3427, 2014, doi: 10.1109/TAP.2014.2314464.
- [106] M. Ganesh, N. S. Raghava, T. Sabapathy, and Y. Sharma, "A compound reconfigurable electronically switched parasitic monopole antenna for sub 6 GHz wireless and vehicular applications," *AEU International Journal of Electronics and Communications*, vol. 179, May 2024, doi: 10.1016/j.aeue.2024.155335.
- [107] S. Zahertar, A. D. Yalcinkaya, and H. Torun, "Rectangular split-ring resonators with single-split and two-splits under different excitations at microwave frequencies," *AIP Adv*, vol. 5, no. 11, Nov. 2015, doi: 10.1063/1.4935910.
- [108] P. Kumar, T. Ali, and M. M. M. Pai, "Electromagnetic metamaterials: A new paradigm of antenna design," *IEEE Access*, vol. 9, pp. 18722–18751, 2021, doi: 10.1109/ACCESS.2021.3053100.
- [109] M. Pallavi, P. Kumar, T. Ali, and S. B. Shenoy, "A Review on Gain Enhancement Techniques for Vertically Polarized Mid-Air Collision Avoidance Antenna for Airborne Applications," 2021, Institute of Electrical and Electronics Engineers Inc. doi: 10.1109/ACCESS.2021.3059957.
- [110] Y. P. Selvam *et al.*, "A low-profile frequency- and pattern-reconfigurable antenna," *IEEE Antennas Wirel Propag Lett*, vol. 16, pp. 3047–3050, Oct. 2017, doi: 10.1109/LAWP.2017.2759960.
- [111] S. Ullah *et al.*, "A Compact Frequency and Radiation Reconfigurable Antenna for 5G and Multistandard Sub-6 GHz Wireless Applications," *Wirel Commun Mob Comput*, vol. 2022, 2022, doi: 10.1155/2022/4658082.
- [112] I. Ahmad *et al.*, "A pentaband compound reconfigurable antenna for 5g and multi-standard sub-6ghz wireless applications," *Electronics (Switzerland)*, vol. 10, no. 20, Oct. 2021, doi: 10.3390/electronics10202526.
- [113] K.Sumathi, S. Lavadiya, P. Z. Yin, J. Parmar, and S. K. Patel, "High gain multiband and frequency reconfigurable metamaterial superstrate microstrip patch antenna for C/X/Ku-band wireless network applications," *Wireless Networks*, vol. 27, no. 3, pp. 2131–2146, Apr. 2021, doi: 10.1007/s11276-021-02567-5.
- [114] B. Ashvanth, B. Partibane, M. G. N. Alsath, and R. Kalidoss, "Gain enhanced multipattern reconfigurable antenna for vehicular communications," *International Journal of RF and Microwave Computer-Aided Engineering*, vol. 30, no. 6, Jun. 2020, doi: 10.1002/mmce.22192.

- [115] R. Pandhare, M. Abegaonkar, and C. Dhote, "High gain frequency reconfigurable multifunctional antenna for modern wireless and mobile communication systems," *International Journal of RF and Microwave Computer-Aided Engineering*, vol. 32, Aug. 2022, doi: 10.1002/mmce.23385.
- [116] L. Sheng, L. Meng, Y. Lin, Y. Gong, X. Yang, and W. Cao, "A wideband frequency reconfigurable antenna with improved gain," *Microw Opt Technol Lett*, vol. 65, no. 3, pp. 915–920, Mar. 2023, doi: 10.1002/mop.33577.
- [117] K. Kandasamy, K. Kaliappan, S. Shanmugam, and A. Srinivasan, "Gain enhancement in octagonal shaped frequency reconfigurable antenna using metasurface superstrate," *Frequenz*, vol. 78, no. 5–6, pp. 241–252, Jun. 2024, doi: 10.1515/freq-2023-0269.
- [118] D. T. T. Tu, S. Cao, and H. Duong, "An open double ring antenna with multiple reconfigurable feature for 5G/IoT below 6GHz applications," *Bulletin of Electrical Engineering and Informatics*, vol. 11, no. 1, pp. 310–318, Feb. 2022, doi: 10.11591/eei.v11i1.3337.
- [119] K. Li, Y. M. Cai, Y. Yin, and W. Hu, "A Wideband E-plane Pattern Reconfigurable Antenna with Enhanced Gain," *International Journal of RF and Microwave Computer-Aided Engineering*, vol. 29, no. 2, Feb. 2019, doi: 10.1002/mmce.21530.
- [120] V. Rajavel and D. Ghoshal, "A miniaturized dual wide-band polarization reconfigurable antenna integrated with artificial magnetic conductor for next-generation wireless applications," *International Journal of Communication Systems*, 2024, doi: 10.1002/dac.5925.
- [121] K. Kandasamy, K. Kaliappan, S. Shanmugam, and A. Srinivasan, "Gain enhancement in octagonal shaped frequency reconfigurable antenna using metasurface superstrate," *Frequenz*, vol. 78, Aug. 2024, doi: 10.1515/freq-2023-0269.